The Characterization and Distribution of Magnesium Whitlockite Crystals in Human Articular Cartilage.

Colin Anthony Scotchford

Submitted in fulfilment of the requirements for the degree of Doctor of Philosophy in the Faculty of Science of the University of London.

Institute of Orthopaedics
University College London Medical School

July, 1993.

ProQuest Number: 10042923

All rights reserved

INFORMATION TO ALL USERS
The quality of this reproduction is dependent upon the quality of the copy submitted.

In the unlikely event that the author did not send a complete manuscript
and there are missing pages, these will be noted. Also, if material had to be removed,
a note will indicate the deletion.

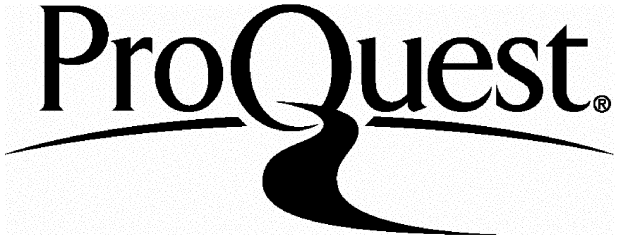

ProQuest 10042923

Published by ProQuest LLC(2016). Copyright of the Dissertation is held by the Author.

All rights reserved.
This work is protected against unauthorized copying under Title 17, United States Code.
Microform Edition © ProQuest LLC.

ProQuest LLC
789 East Eisenhower Parkway
P.O. Box 1346
Ann Arbor, MI 48106-1346

"All true wisdom is only to be found far from the dwellings of men, in the great solitudes; and it can only be obtained through suffering. Suffering and privation are the only things that can open the mind of man to that which is hidden from his fellows."

Caribou Eskimo Igjugarjuk.

ACKNOWLEDGEMENTS

This thesis is dedicated to my parents.

I would like to thank Professor Yousuf Ali for his support and advice during this study, providing me with opportunity to work for a Ph.D. and enthusiastically introducing me to the world of calcification.

Mike Kayser has provided me with excellent training in electron microscopic and histological techniques, photographic and darkroom skills. I am also grateful for his assistance producing the micrograph figures.

I am indebted to Dr Jean Pringle of the Institute of Orthopaedics, Department of Morbid Anatomy and the theatre staff of Edgware General Hospital for the invaluable supply of cartilage specimens.

I would also like to thank the staff of the Department of Morbid Anatomy (Institute of Orthopaedics), Dr Steve Greenwald (Royal London Hospital), Dr Chris Buckley and Martin Vickers (Birkbeck College) for the processing of tissue for wax histology, instruction and advice on the use of the Joyce Loebl Magiscan image analysis system, STXM and SFXM imaging and x-ray diffraction analyses respectively and Dr Adele Boskey for providing me with the basics of x-ray diffraction techniques.

My colleagues within the Institute have provided much help and some entertainment over the last three years. In particular I would like to thank Paul Unwin for discussion of computing and statistical matters, Caroline Clifford for initial assistance with cartilage digestion and grammatical precision in proof reading, Dr David Lee for helpful comments arising from proof reading and Dr. Gordon Blunn for assistance with scanning electron microscopy.

I also gratefully acknowledge Philips Electron Optics for the loan of equipment and use of SEM facilities and JEOL UK for the use of SEM faciities.

Finally I would like to thank the Arthritis and Rheumatism Council for funding this work.

ABSTRACT

The occurrence of crystals (previously termed 'cuboid crystals' 50-500nmsize range) not apparent by light microscopy, in human articular cartilage has been confirmed by transmission electron microscopy of tissue prepared by various techniques, including anhydrous and cryo processing. Earlier reports of such crystal deposition had been limited to osteoarthritic and elderly femoral head articular cartilage. In this study crystals have been reported in articular cartilage across an age range from five to ninety two years in normal and osteoarthritic tissue from a variety of joint sites.

The distribution of crystal deposition within articular cartilage was described both qualitatively and quantitatively; normal femoral head tissue was investigated in most detail. Over 90 % of crystals were commonly deposited within the first 50μm below the articular surface; crystals appeared either in a band parallel to the surface or in a pericellular distribution. In deeper zones crystal deposition was restricted to pericellular distribution, and areas of chondrocyte necrosis. Quantitative analysis of crystal deposition distribution in articular cartilage at sites around the femoral head revealed a significantly greater deposition in the superior (zenith) region than the inferior (infrafoveal) region.

Elemental analysis of crystals confirmed a calcium, phosphorus and magnesium content. It also demonstrated no variation in the mean calcium to phosphorus ratio with crystal size, specimen age, or between normal and osteoarthritic specimens. A crystal isolation technique involving collagenase digestion, centrifugation and sodium hypochlorite treatment was developed, enabling crystal characterization by electron and x-ray diffraction. Crystals were identified as magnesium whitlockite; the first report of this mineral in articular cartilage.

The mode of formation and role of these crystals remain unknown, although histological and histochemical investigations revealed a consistent association with intramatrical lipid, containing a phospholipid component. The results of this study are most tenable with a concept of opportunistic crystal deposition.

Contents

List of Figures and Tables

GENERAL INTRODUCTION

Articular cartilage is a specialised connective tissue essential to the normal function of synovial joints. It is located on the articular ends of bones where it performs three main functions (Kempson 1979): to reduce potentially damaging stresses applied to the subchondral bone (Swanson *et al.* 1971, Freeman *et al.*1975), to prevent abrasion between the articulating bone extremities and to provide low friction bearing surfaces which do not themselves suffer from severe abrasive wear (Weightman and Kempson 1979, Swanson 1979).

The tissue consists of a relatively small number of chondrocytes distributed throughout an abundant extracellular matrix; the composition and molecular structure of the matrix determines the material properties and many biological functions of cartilage. As cartilage is essentially avascular, lacks a lymphatic system and is not innervated, the matrix controls passage of metabolites and nutrients to and from cells and helps regulate metabolic activities (McKibben and Maroudas 1979). It also protects chondrocytes from mechanical injury (Poole *et al.* 1987) and the transmission of mechanical, electrical and chemical signals through the matrix influences chondrocyte function (Sah *et al.* 1989).

Failure of articular cartilage as a load-bearing material is attributable to the cumulative modification of individual molecular components or their composite form (Bader *et al.* 1992). A change in matrix components may produce a loss of functional integrity, frequently expressed as an erosion in the cartilage layer. Such erosion is generally observed as fibrillation and stripping of the cartilage (Sokoloff 1983). In advanced disease stages this may expose the underlying bone; such osteoarthritic states are characterised by severely inhibited joint articulation, swelling and accompanying pain. These symptoms are a final stage in osteoarthritic disease. The initiating factors are unknown, but may include changes in load distribution and tissue compliance (Bullough *et al.* 1973, Armstrong *et al.* 1977), traumatic injury to joint tissues (Jackson 1968), molecular changes in the extracellular matrix (ECM) structure or turnover (Maroudas 1976) and the deposition of crystals within the matrix (Dieppe and Calvert 1982).

A variety of crystals have been recorded in articular cartilage including monosodium urate (MSU), calcium pyrophosphate dihydrate (CPPD) and basic calcium phosphates (BCP) (Schumacher 1988). Calcium crystal deposition is more common in older persons. The degenerative and destructive arthropathies associated with them will predictably become increasingly common as our population ages. (McCarty 1988). The mechanisms of these depositions remain unclear, as does their precise relationship with chronic arthritic disease. BCP crystals have been less detectable than MSU or CPPD but are capable of inducing pathological changes in joint tissues. Amongst the BCP crystals, the cuboid crystals described by Ali (1985) and Stockwell (1990) in OA and elderly articular cartilage remain poorly studied. These crystals require further characterization and investigation as to their role in articular cartilage physiology or pathology.

CARTILAGE COMPOSITION AND STRUCTURE

Articular cartilage is one of a group of dense connective tissues, comprising hyaline, yellow elastic and white fibrocartilage. The cartilages characteristically consist of a relatively small number of chondrocytes distributed throughout an abundant ECM, and have a water content of between 70 and 80% (Stockwell 1979). The main variation between types is in the composition of the ECM which, in turn, dictates the functional properties of the tissues. Hyaline cartilage comprises the foetal skeleton, epiphyseal growth plate and articular cartilage.

Adult articular cartilage consists of chondrocytes, occupying only 10% of the total volume of the tissue (Stockwell 1971), which, with the exception of the superficial zone, are located within a morphologically distinct pericellular "basket", the lacuna. This unit has been termed the chondron (Poole *et al.*1987). Chondrocytes are dispersed throughout the ECM, the main components of which are collagens and proteoglycans. Other minor structural components include those which facilitate cell-matrix interactions. Articular cartilage may be divided into four zones for descriptive purposes: the superficial, intermediate, deep and calcified zones. The zones are differentiated on the basis of chondrocyte morphology, collagen fibre orientation and proteoglycan concentration (Meachim and Stockwell 1979). Brief descriptions of the structural components of articular cartilage are given here.

Chondrocytes

Chondrocytes arise from the condensation of mesenchymal cells in the foetal skeleton (Thorogood and Hinchliffe 1975). Chondrocyte morphology is variable, the cells appear as discs flattened parallel to the surface in the superficial zone whilst being oval or rounded in deeper zones. Where more than one chondrocyte is present within one lacuna adjacent surfaces appear flattened. Such multiple occurrences of cells are assumed to be derived from a single chondrocyte by mitosis. Chondrocyte nuclei are either elongated or rounded, according to cell shape, and frequently show shallow undulations (Ghadially 1983). A characteristic condensation of heterochromatin is separated from the nuclear membrane by the nuclear fibrous laminin (Oryschak *et al.* 1974). Nuclei are typically surrounded by dense rough endoplasmic reticulum (RER) which is most highly developed in the intermediate and deep zones (Ghadially 1983). The cisternae of the RER show variable dilation in healthy chondrocytes (Stockwell and Meachim 1979). Intermediate filaments are typically abundant in the cytoplasm becoming more frequent with age; this has been considered a sign of cytoplasmic degeneration (Ghadially 1983), but other workers consider them to be regular constituents of viable, healthy cells (Schenk *et al.* 1986). Chondrocytes typically show cytoplasmic processes extending into the pericellular matrix (Ghadially *et al.* 1965, Weiss *et al.* 1968).

Collagens

Collagen is the major structural component of the organic matrix, the interstitial fibrils having great tensile strength. To date, fourteen species of collagen molecule have been identified

within tissues. Of these, five have been located in human articular cartilage: collagen types II, VI, IX, X, and XI. Although the collagen types have different structural and functional properties the basic molecular structure remains similar. For a detailed review of molecular structure see Prockop and Williams (1982). The molecule is composed of three polypeptide α-chains, each of which is coiled into a left handed helix with approximately three amino acids per turn. The helical chains are twisted around each other into a right handed triple helix, to form a rigid structure. Collagen types vary in their precise amino acid sequence although all contain large amounts of glycine, proline and hydroxyproline which are essential to the structure and stability of the collagen molecule (For reviews see Grant *et al.* 1988, Mayne 1989).

Type II collagen comprises approximately 85% of the total collagen content of human articular cartilage (Grant *et al.* 1988) forming the basis of the fibrillar meshwork throughout the interterritorial matrix (Duance *et al.* 1982, Muller-Glauser *et al.* 1986). The monomers are organised, to facilitate maximum electrostatic and hydrophobic interaction of the amino acids projecting from the molecules into a quarter stagger arrangement, giving the characteristic 67nm periodicity when viewed under the electron microscope (Hulmes *et al.* 1973, Cunningham *et al.* 1976, Chapman and Hulmes 1984). The precise longitudinal displacement is slightly less than a quarter of the length of the molecule, leaving a "hole region" between the end of one monomer and the beginning of the next. In fibril cross section it appears the monomers aggregate in a quasi-hexagonal lattice arrangement (Bornstein and Sage 1980).

Type VI collagen has been localised to the pericellular capsule of the matrix, and also more sparsely throughout the fibrillar collagen network (Poole *et al.* 1984, 1988, Ayad *et al.* 1984). This collagen molecule may exist as a monomer but is frequently found as aggregated di or tetramers bonded by disulphide bridges (Jander *et al.* 1984, Von der Mark *et al.* 1984) and possibly stabilized by interaction with hyaluronan (Kielty *et al.* 1992). Roles suggested for collagen type VI include regulation of fibril diameter, protection against compressive loading and as a component in cell substratum interactions.

Type IX collagen may also be defined as a proteoglycan, comprising three α-chains with a 70% incidence of a single chondroitin sulphate glycosaminoglycan on the α2 chain (Huber *et al.* 1986, Muller Glauser *et al.* 1986). It accounts for up to 5% of collagen extractable from mammalian cartilage by pepsin digestion (Ayad *et al.* 1982). Type IX collagen has been localized in the pericellular capsule (Duance *et al.* 1982) and also in a periodic manner covalently bound to type II collagen on the surface of fibrils (Eyre *et al.* 1987). It has been suggested that the molecule may play a role in restricting fibril diameter (Wotton *et al.* 1988).

Type X collagen contains three chains arranged in the typical collagenous triple helical structure (Schmid and Linsenmayer 1984), although it is approximately half the size of the type II collagen molecule (Schmid and Linsenmayer 1983). Type X collagen occurs transiently in cartilages that undergo endochondral bone formation and is not present in those that do not (Linsenmayer *et al.* 1988); it is known to be synthesized by growth plate hypertrophic chondrocytes (Kwan *et al.* 1986). The molecule becomes associated with

preexisting collagen fibrils, an interaction which is stabilised by covalent bonding (Chen *et al.* 1992). This occurs prior to hydroxyapatite accumulation (Schmid and Linsenmayer 1985) but does persist in calcified cartilage (Kwan *et al.* 1986; Schmid *et al.* 1990). The precise function of type X collagen remains undetermined, although current concepts suggest a role in influencing the site and subsequent spread of initial mineral formation (Poole and Pidoux 1989).

Collagen type XI was first reported as a constituent of human cartilage by Burgeson and Hollister (1979). It accounts for 8-10% of collagen in most cartilages (Grant *et al.* 1988). Collagen type XI has been located to the pericellular capsule (Ricard Blum *et al.* 1982, Evans *et al.* 1983) and also in the same fibrils as type II collagen (Vaughan *et al.* 1988). Mayne (1989) suggested it may be positioned in the centre of the fibrils, with a role of incorporating type II collagen. Smith *et al.* (1985) suggested it may have a role in fibril diameter regulation and be situated on the fibril surface.

Collagen fibrils are organised into a three-dimensional architecture. A model of this structure, in which collagen fibrils arose from the deep layer radially to the subchondral bone, arched through the intermediate zone to run tangentially in the superficial zone, was originally proposed by Beninghoff (1925). More recent work, using transmission and scanning electron microscopy, has broadly supported this basic precept. Broom (1986) has proposed a model in which the radially arranged fibrils are deflected sideways in a small scale alternating manner to interact with their nearest neighbour, forming a radially orientated meshwork; the fibrils become tangential in the superficial zone providing resistance to tensile stresses. Work by Clark (1990) and Jeffrey *et al.* (1991) suggests that fibrils are arranged in sheets with a radial orientation in the deep zone running continuously through the intermediate zone to lie tangentially in the superficial zone overlapping their neighbours. This structure is covered by a fine fibrillar layer. The sheets or leaves vary in form, orientation, and packing density depending on site.

Proteoglycans

The other major component of cartilage matrix, is a viscoelastic gel composed primarily of the aggregating proteoglycan, aggrecan. A proteoglycan may be defined as any macromolecule that has a core protein containing at least one covalently bound glycosaminoglycan chain (Hascall and Kimura 1982). A glycosaminoglycan is a heteropolymer consisting of repeating disaccharide sequences containing hexosamine and hexuronic acid or hexose (Carney and Muir 1988).

Cartilage proteoglycan aggregates contain four major glycosaminoglycans: chondroitin-4-sulphate, chondroitin-6-sulphate, keratan sulphate and hyaluronan (Carney and Muir 1988). Together these make up 18% of the dry weight of femoral head articular cartilage (Stockwell 1979). Also the smaller O- and N-linked oligosaccharides are present. The glycosaminoglycans, with the exception of hyaluronan, are covalently linked to a core protein via O-glycosidic bonds to form proteoglycan monomers (Bray *et al.* 1967). Core protein may

be divided into three regions: the hyaluronan binding region, (HABR), a keratan sulphate-rich region, and a chondroitin sulphate-rich region (Heinegard and Hascall, 1974). Hyaluronan comprises less than 6% of the total cartilage glycosaminoglycan (Elliot and Gardner 1979), but it is essential in the formation of proteoglycan aggregates (Hascall and Heinegard 1974).

Proteoglycan monomers interact with hyaluronan via the HABR to form aggregates (Hardingham and Muir, 1974). The linkage, thought not to be covalently bound (Carney and Muir 1988), is stabilised by a glycoprotein, link protein. which is thought to make the bond irreversable under normal physiological conditions (Hardingham 1979).

Aggrecan composition varies with age, site and depth within cartilage. Proteoglycan aggregates are larger in the newborn, there being a marked decrease in the proportion of aggregated monomers to single monomers with age (Buckwalter and Roughly 1987). The composition of monomers is also variable; the ratio of chondroitin-4-sulphate to chondroitin-6 -sulphate decreases during the first 25 years of life (Murata and Bjelle 1979). Keratan sulphate concentration increases with age (Bayliss and Ali 1981, Inerot and Heinegard 1983, Roughley and White 1980). At 20 years the ratio of chondroitin sulphate to keratan sulphate may be 85% to 15%; with age the percentage of keratan sulphate may rise to 30%. Variations in both aggrecan compostion and concentration in different zones of adult articular cartilage are also apparent. The highest concentration of chondroitin sulphate occurs in the mid-zone, whereas keratan sulphate increases progressively through the cartilage depth, producing a combined distribution of proteoglycan which is greatest in the mid-zone and least near the articular surface (Stockwell and Scott 1967, Bayliss *et al.* 1983, Ratcliffe *et al.* 1984).

Proteoglycan aggregates are sufficiently large to be easily immobilised within cartilage by topographical entanglement with the collagen network (Muir 1979). There is also evidence to suggest direct interaction between proteoglycans and collagen (Orford and Gardner 1984). Immobilisation of aggrecans in the cartilage matrix confers on the tissue a high negative charge density due to carboxylate and sulphate ester groups. The negative charge is balanced by cations which are held in the cartilage, generating an osmotic pressure of several atmospheres (Maroudas 1979) which is responsible for almost all of the swelling pressure of the tissue (Myers *et al.* 1984). This pressure is balanced by the tensile stress induced in the collagen network. During compressive loading fluid is lost from cartilage due to a pressure gradient; this has the effect of increasing proteoglycan concentration and hence swelling pressure until an equilibrium is reached between swelling pressure and applied load. Hence the proteoglycan component controls the fluid content of cartilage during compression.

Proteoglycans also exclude other macromolecules from their molecular environment. This creates a water compartment only part of which is available to other matrix macromolecules, increasing macromolecule concentration. This may increase reaction rates and all concentration dependent interactions (Hardingham and Fosang 1992). It has been shown that this effect prevents molecules larger than haemoglobin entering cartilage (Maroudas 1979), and influences the formation and thermal stability of collagen fibrils. The

fibril- proteoglycan system provides the cartilage with a porous structure (Mow *et al.* 1984), providing resistance to fluid motion through cartilage and hence resistance to compressive loading (Armstrong and Mow 1982).

Minor Matrix Components

Other minor matrix components include those associated with chondrocyte-matrix attachment. The glycoproteins fibronectin and chondronectin have been implicated in such a role (Weiss and Reddi 1981, Hewitt *et al.* 1982, Brown and Jones 1992). Interaction between collagens and glycosaminoglycans of the ECM and chondrocyte membranes directly, via integrins such as anchorin CII and CD44 respectively, have also been described (Mollenhauer *et al.* 1984, Culty *et al.* 1990).

CALCIFICATION

Mineral Phases

Calcium phosphates are capable of forming a number of mineral phases dependent upon the physical and chemical conditions of the mineralising system. The phases relevant to the work discussed in this thesis are outlined in table I, in order of decreasing acidity, decreasing solubility and increasing thermodynamic stability.

Table I. Calcium Phosphate Compounds (After Neuman 1980).

Formula	Name	Molar Ca/P	Abbreviation
$Ca(HPO_4).2H_2O$	Dicalcium phosphate dihydrate	1.0	DCPD
$Ca_4H(PO_4)_3$	Octocalcium phosphate	1.33	OCP
$Ca_9(PO_4)_6$ (var.)	Amorphous calcium phosphate	1.3-1.5	ACP
$Ca_3(PO_4)_2$	Tri-calcium phosphate	1.5	TCP
$Ca_5(PO_4)_3OH$	Hydroxyapatite	1.66	HAP

The mineral component of mature bone is generally considered to be a poorly crystalline nonstoichiomtrical hydroxyapatite which becomes more crystalline and approaches ideal stoichiometry with time after deposition (Glimcher 1984). The individual crystallites have been measured at 4 to 6 nm using line broadening analysis (Carlstrom and Glas 1959). The formation, remineralisation and dissolution of bone are very complicated processes due, in part, to the presence of multiple calcium phosphate phases that may be involved in the reactions. Investigation of these processes has taken two courses, *in vitro* and synthetic chemical modelling, and direct observation of initial bone mineral formation; these are reviewed by Eanes (1985) and Bonar *et al.* (1985). HAP cannot form *de novo* from constituent ions in solution due to its unit cell complexity. Model studies have revealed the

possible importance of nonapatitic mineral phases such as ACP, OCP and DCPD as transient intermediates to apatite *in vivo.* The lifetime of precursors may be extremely short and therefore such phases are not easily detected by physical means even in the earliest stages of mineralization (Eanes 1985). ACP has been detected as the initial precipitation in kinetic studies (Termine and Eanes 1972, Posner and Betts 1975). It was suggested that this may go on to nucleate OCP which was capable of providing a template for HAP formation (Feenstra and de Bruyn 1979). This would account for the plate-like habit of bone mineral crystals observed by TEM (Landis *et al.* 1977, Jackson *et al.* 1978, Weiner and Price 1986).

DCPD is the only phase for which there is direct evidence for its role as a precursor to HAP in biological systems (Roufosse *et al.* 1979). There is no direct evidence for OCP as a precursor; this may be because it is very hard to distinguish one from the other on diffuse x-ray diffraction patterns (Eanes 1985). Eanes cites the similarity between the radial proliferation of crystals about matrix vesicle loci (Bernard 1969, Jones and Boyde 1983) and crystal masses occurring in synthetic systems in which OCP is a transient intermediate (Eanes and Meyer 1977) as evidence for a precursor role for OCP. From detailed analyses of embryonic chick bone, Glimcher and colleagues have been unable to produce evidence in support of a precursor phase to HAP formation. Bonar *et al.* (1985) suggest their earlier observation of DCPD (Rouffose *et al.* 1979) may have been artefactual. In view of their more recent work, they suggest that bone mineral is a poorly crystalline hydroxyapatite with extensive disorder, with incorporation of impurities especially HPO_4^{2-}, some of which is present in a configuration similar to DCPD but in an apatitic lattice, and of very small crystallite size. During maturation crystallinity improves, crystal size increases, disorder decreases and most impurity levels decrease. Alternatively, Driessens and Verbeeck (1986) proposed a composition based on data from chemical analyses of bone mineral. They suggested that bone mineral is a combination of three phases; a sodium and carbonate containing apatite phase and magnesium whitlockite, a magnesium substituted calcium phosphate, present from the beginning of mineralization together with OCP. The HAP and whitlockite phases are deposited proportional to total mineral deposition as bone develops, whilst OCP is transformed slowly to a heavily carbonated defective apatite. A magnesium whitlockite phase has been detected in young bone (Cheng and Pritzker 1983, Lee *et al.* 1984).

Mechanisms of Calcification

It has been very difficult to explain biological calcification by a universal mechanism, there being appreciable differences between, for example, calcification of the epiphyseal growth plate and lamella bone formation. Despite this diversity, any mechanism of normal calcification must consist of several sequential steps: first soluble calcium and phosphate ion concentrations must be complexed to produce an insoluble solid, secondly, growth must occur to produce apatite crystals, thirdly there must be an increase in crystal numbers to saturate the matrix of the tissue and finally a reorganisation of the mineralised matrix may be required to produce a stable, organised and structurally sound calcified tissue(Posner 1969).

It has been shown that serum and its ultrafiltrate are metastable with respect to calcium and phosphate (Howell *et al.* 1968, Cheng *et al.* 1988), requiring a two phase mechanism of nucleation and proliferation for tissue mineralization. Crystal nucleation has been proposed by both homogenous and heterogenous means. Homogenous nucleation requires the calcium x phosphate ion product to be increased locally up to the level required for direct precipitation of the first solid calcium phosphate phase. Robison (1923) proposed that this could be achieved by alkaline phosphatase, an enzyme invariably present at calcification sites, hydrolysing phosphate esters to raise the local inorganic phosphate concentration. Subsequent work, showing a distribution of alkaline phosphatase beyond calcifying tissues, and micropuncture studies, showing a lack of elevated calcium x phosphate ion product, weakened support for this mechanism (Howell *et al.* 1968). Alkaline phosphatase has also been implicated in mineral formation by other mechanisms including the local destruction of mineral growth inhibitors, action as an inorganic phosphate transporter, action as a calcium ion binding protein and action as a calcium ion pump in cell or matrix vesicle membranes. These roles have been reviewed by Wuthier and Register (1985).

It has been suggested that mitochondria may be involved in the initiation of mineral formation in epiphyseal growth plate. These organelles demonstrate the ability to concentrate calcium ions, accumulating granules composed of calcium and phosphate (Lehninger 1970). It has been speculated from electron microscopic observations of normal and rachitic rat growth plates (Brighton and Hunt 1978) that calcium ions are released from mitochondria to the surrounding matrix and participate in crystal nucleation. The mechanism of release is unknown, although Brighton and Hunt suggest a reduction in oxygen tension in the hypertrophic zone may be important. (Brighton and Hunt 1978).

A mechanism involving extracellular organelles has attracted greater attention. Much of this work has been carried out using epiphyseal growth plate cartilage, the primary centre of calcification providing the mechanism for long bone growth. The sequential stages of the processes involved co-occur, separated spatially within the tissue into a series of zones, as outlined in Fig. I.

Matrix vesicles, identified independently by Bonnucci (1967) and Anderson (1967) in epiphyseal growth plate and in bone by Bernard and Pease (1969) are distinct membrane-invested extracellular particles approximately 100nm in diameter, which are considered to be sites of initial calcification. Much evidence has been provided to support this role. They occur in the tissue matrix with a distribution corresponding to that of crystal formation (Ali *et al.* 1970, Anderson *et al.* 1970, Ali 1976). In the longitudinal septa of the upper hypertrophic zone the first apatite crystals may be observed in close apposition to the inner leaflet of the matrix vesicle membrane (Anderson 1976). With increasing support for this role, the origin, composition and mode of action of matrix vesicles has attracted much attention .

Matrix vesicles are thought to be derived from the chondrocyte plasma membrane via cell processes (Ali 1983). Evidence to support this is derived from electron microscopic observation and biochemical analyses; enzymes and phospholipids identified in matrix

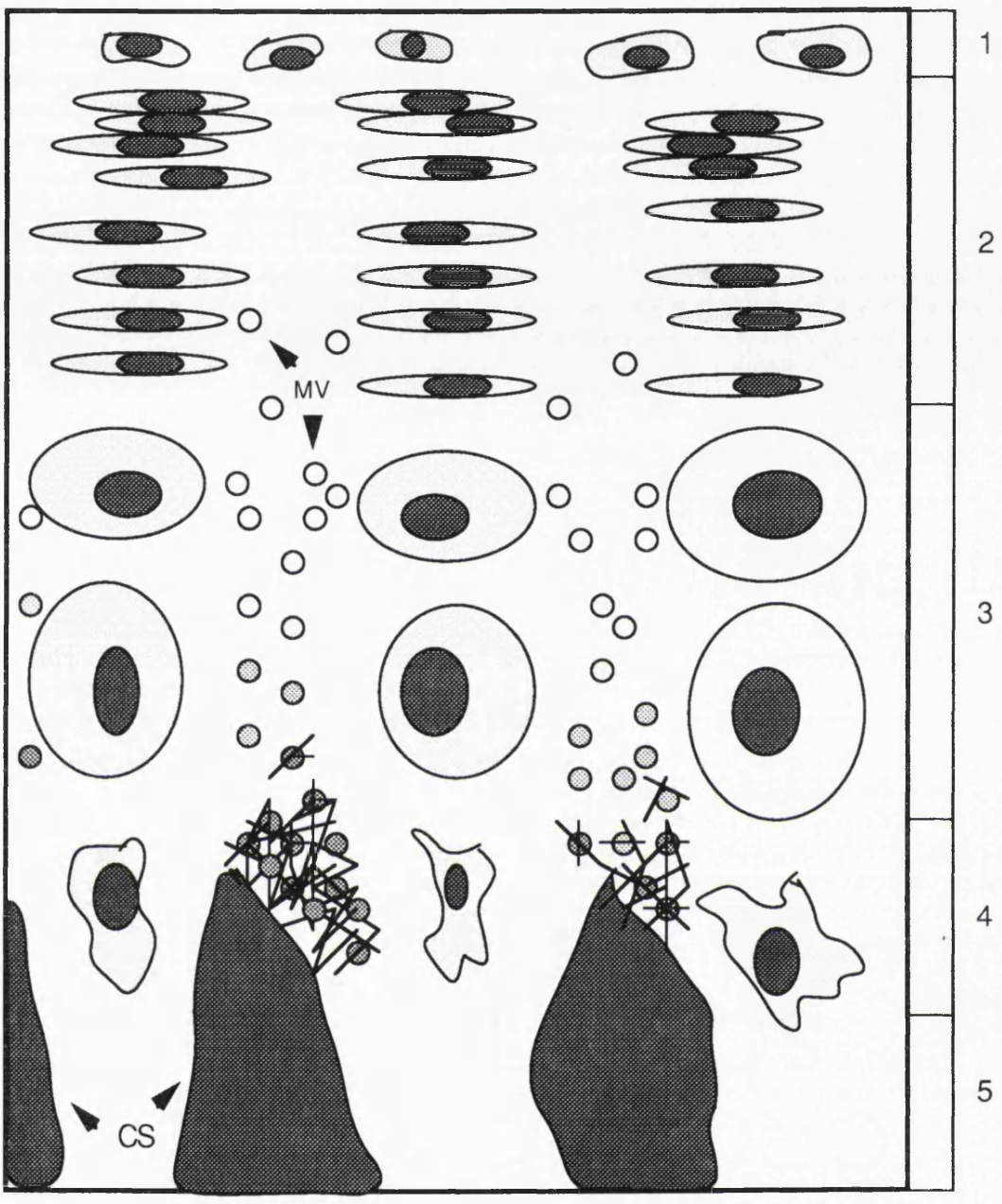

Fig. 1. Schematic representation of epiphyseal cartilage showing columns of chondrocytes separated by longitudinal septa. The growth plate is divided into (1) the reserve zone of resting cells, (2) the proliferative zone, (3) the hypertrophic zone of mature cells, (4) the degenerative zone which coincides with (5) the calcified septum region. Matrix vesicles (MV) produced by cell processes in the lower proliferative zone begin to display initial mineral deposition in the upper hypertrophic zone, with mineral extending outside vesicles by the lower hypertrophic zone, forming nodules which coalesce to form calcified septa (CS).

vesicles are common to the plasma membrane. These include 5'-AMPase, a wide specificity phosphatase capable of hydrolysing phosphate esters including pyrophosphate and nucleotide phosphates (Ali *et al.* 1970) phosphotidylserine, phosphotidylinositol, cholesterol and sphingomyelin (Peress *et al.* 1974). Alkaline phosphatase is a major constituent of matrix vesicles. Indeed, matrix vesicle alkaline phosphatse accounts for over 80% of alkaline phosphatase activity in epiphyseal tissue (Ali *et al.* 1970, Ali 1976); this has been localized on the outside of the matrix vesicle membrane with nucleotide phosphatases and pyrophosphatase (Matsuzawa and Anderson 1971). Active neutral metalloproteinases capable of degrading proteoglycans have been identified in the matrix vesicle sap (Dean *et al.* 1992).

Matrix vesicles are thought to concentrate calcium and phosphate to enable initial mineral formation. The proposed process involves alkaline phosphatase increasing the level of inorganic phosphate by hydrolysis of appropriate phosphate containing substrates (Ali *et al.* 1970). An alternative source of inorganic phosphate has been suggested in the mineralization inhibitor pyrophosphate acting as a substrate for alkaline phosphatase or related pyrophosphatase (Ali *et al.* 1970, Anderson and Reynolds 1973). Ali and colleagues (1973,1976) demonstrated that matrix vesicles can actively transport calcium, accumulating concentrations up to twenty five times greater than in adjacent chondrocytes (Wuthier 1977). This may be achieved by a combination of calcium binding phospholipids and proteins, and annexins situated in the membrane acting as ion channels (Genge *et al.* 1992). Following initial formation, growing crystals protrude through the matrix vesicle membrane, a process that may be assisted by matrix vesicle derived proteinases and lipases. Liberated crystals are available to seed rapid proliferation of apatite by epitaxial growth, which may then spread to the collagen fibrils.

Whilst matrix vesicles have been observed in many normal and pathologically mineralising tissues (Kim and Huang1972, Sayegh *et al.* 1974, Dmitrovsky *et al.* 1978) , this mineral nucleation mechanism does not fit the accumulated data relating to lamella bone mineralization. The majority of bone mineral is located within the collagen fibrils; calculations of the exact amount vary between 69 and 90% (Neuman 1980 ,Bonar *et al.* 1985a, Landis *et al.* 1986). The c-axis of the hydroxyapatite crystals within the fibrils is aligned to the collagen fibril axis, indicating that collagen fibril structure may exert an influence over crystal nucleation (Weiner 1986). With the proposal of a staggered array model for collagen fibril organisation, based on electron microscopic data, the gap region was recognised as a possible initial location for mineral (Weiner 1986). A theory for initial mineral formation implicating the type I collagen matrix as a nucleating substrate has been supported by workers including Glimcher (1976) and Solomons and Neuman (1960).

Electron microscopy has shown that initial calcium phosphate crystals in bone are deposited in the hole zone regions (Glimcher1976, 1985). These observations were confirmed using X-ray and neutron diffraction techniques (White *et al.* 1977, Berthet Colominas 1979) which suggested that the initial mineral does not uniformly fill the gap

region. In a model that best fits the data, mineralisation would start at the N-terminal side of the gap region and progress to the C-terminal whilst simultaneously increasing in thickness. At full maturation the mineral phase may become continuous via pores within the fibril connecting the gap regions (Neuman 1980).

Control of collagen mineralization is thought to be mediated by promotors of crystal nucleation or growth. Variations in fibril thickness and intermolecular packing of molecules in the fibrils make type II collagen a less favourable site for initial mineral formation. The type I collagen of bone appears unique in that the pore size of bone collagen is around 0.6nm (Neuman 1980) which is large enough to accommodate diffusion of phosphate anions (0.4nm). Most collagens have a pore size around 0.3nm (Neuman 1980). Determination of pore sizes appears to involve specific collagen fibril crosslink formation (Mechanic *et al.* 1985). The presence of "helper" molecules to enhance crystal initiation, located in the gap region, has been suggested. Alternatively inhibitors of calcification in other collagens may be active. Potential mediators are outlined below.

Other possible crystal nucleators or nucleation enhancers include phospholipids, acidic calcium phospholipid phosphate complexes, proteolipids and non collagenous matrix proteins. Initial suggestions of the involvement of lipids in the process of calcification were prompted by the observations of the accumulation of sudan black B, a lipid staining dye at the mineralizing front of epiphyseal growth plate (Irving 1963). Shapiro (1970) and Wuthier (1968) characterized phospholipids associated with calcifying cartilage and bone.

The acidic phospholipids, phosphatidylserine and phosphatidylinositol, are thought to be the most important in relation to calcification (Boskey 1989). These phospholipids, located in the membranes of cells, cellular organelles, cell debris and matrix vesicles, are important determinants of membrane fluidity; they may be instrumental in matrix vesicle generation and function, as alkaline phosphatase has been shown to be bound to the cell membrane via phosphatidylinositol (Low and Zilversmit 1980). Probably more significant is the ability of these phospholipids to form acidic calcium phospholipid phosphate complexes with the ability to nucleate mineral formation. Recent work (Boskey and Dick 1991) has shown that phosphatidylserine is also able to inhibit HAP growth *in vitro*, suggesting these phospholipids may have multiple effects on HAP formation *in situ*. Such complexes in mineralized mammalian tissue were first identified in compact bone (Boskey and Posner 1976) and have subsequently only been located in calcified or calcifiable tissues associated with sites of early mineral deposition (Boskey 1989). The association of phospholipids with collagen fibrils in dentin and enamel, demonstrated by specific staining, suggests that matrix phospholipids are involved in matrix-nucleated mineral formation (Goldberg and Septier 1985). Lipid and type I collagen associations have been noted in other mineralizing tissues (Lelous *et al.* 1982, Ennever *et al.* 1984).

The complexed acidic phospholipids were found to be associated with proteolipids in calcified tissues. (Boyan -Salyers and Boskey 1981, Boyan and Boskey 1984). From studies using a bacterial model of membrane-mediated calcification it has been suggested that the

protein portion of the proteolipid organises the lipid structure (Boggs *et al.* 1977) which in turn facilitates complexed acidic phospholipid formation on the membrane surface (Boyan *et al.* 1986).

The non collagenous proteins osteocalcin (bone GLA protein), osteopontin and osteonectin have been proposed roles in calcification. The role of these proteins in mineralization is unclear, though they have been implicated in both promotion and inhibition of crystal nucleation and growth. All have been shown to inhibit hydroxyapatite growth by apparently binding at lattice growth sites (Romberg *et al.*1986, Boskey *et al.* 1992). It has been proposed that osteonectin- collagen complexes play a role in crystal nucleation in bone (Termine *et al.* 1981, Glimcher 1989).Ultrastructural immunolocalisation has demonstrated osteonectin and osteocalcin to be associated with collagen fibrils (Bianco *et al.* 1984) and osteocalcin and osteopontin in the calcifying matrices of both cartilage and bone from chicken epiphyseal growth plate (McKee *et al.* 1989).

Non mineralising tissues and fluids contain powerful circulating inhibitors of calcification; inhibitors characterised in plasma and urine include citrate, magnesium and albumin. Albumin has been shown to be a mediator of hydroxyapatite growth inhibition (Garnett and Dieppe 1990). Salivary inhibitors of calcium phosphate formation include proline rich peptides (Oppenheim *et al.* 1971) and the acidic peptide stratherin (Schlesinger and Hay 1977). A recognised inhibitor of hydroxyapatite formation present in body fluids including joint fluid is inorganic pyrophosphate (Fleisch and Neuman 1961, Meyer 1984) and ATP has been reported to have similar properties (Blumenthal *et al.* 1975). Removal of such factors has been postulated to be part of mineralization processes. Hydrolysis of these inhibitors from tissue sites, mediated by alkaline phosphatase, pyrophosphatase or ATPase, all present in matrix vesicles, may facilitate crystal formation. Inhibition of crystal formation by integral matrix components also appears likely. Aggregating proteoglycans have been shown to inhibit hydroxyapatite formation *in vitro* (Chen *et al.* 1984, Chen and Boskey1985, 1986). *In vivo*, cleavage of proteoglycans at the mineralising front of growth cartilage (Buckwalter 1983, Campo and Romano 1986) may make them less effective inhibitors of crystal formation. It is possible that such changes may be mediated by matrix vesicles which have recently been shown to contain metalloproteinases capable of degrading proteoglycans (Dean *et al.* 1992).

It is becoming clear that none of the mechanisms outlined solely accounts for mineralization of cartilage and bone. It is more likely that the correct interaction of the above factors at the appropriate site leads to the selective deposition of specific structural and morphological mineral phases (Addadi and Weiner 1985). Moreover individual factors may be important at different times in the step by step sequence of the mineralization process (Ali 1992).

OSTEOARTHRITIS

The breakdown of the highly integrated articular cartilage structure is manifest in degenerative arthritis. Osteoarthritis (OA) is a progressively destructive disease of articular

cartilage characterised by local erosion, fibrillation, osteophyte formation and bone remodelling (Howell 1984).

OA has traditionally been considered a wear and tear condition, occurring predominantly in weight bearing joints. This concept has become largely discounted due to a number of observations including studies of groups prone to excessive joint use demonstrating no increase in OA incidence (Purnanen *et al.* 1975, Radin *et al.* 1972, Brodelius 1961), the low incidence of the disease in certain ethnic groups, suggesting it is not simply related to aging (Byers 1975), and the observations that cartilage fibrillation may remain non progressive or become progressive (Byers 1970).

Morphological and biochemical evidence that changes in OA differ from changes with aging (Ali and Bayliss 1974, Muir 1977, Bayliss and Ali 1978), plus an association with crystal deposition (McCarty 1962, Dieppe *et al.* 1976), joint congruity (Bullough *et al.* 1973) and altered cartilage and subchondral bone compliance (Armstrong *et al.* 1977, Radin and Rose 1986), called for a reassessment of the disease. The view of OA has become modified with the premise that, in some cases an active metabolic abnormality of articular cartilage, possibly precipitated by aetiological factors described above, resulting in cartilage destruction, is gaining supportive evidence. The normal equlibria between enzymes including metalloproteases, serine protease and collagenases and their inhibitors have been shown to be disturbed in osteoarthritic tissue and uninhibited enzyme may be active in ECM degradation (Dean *et al.* 1987, Yamada *et al.* 1987, Ehrlich 1978). Breakdown of the collagen network has been suggested as an initiating factor in OA, followed by swelling of cartilage and unravelling of proteoglycans with eventual loss to the synovial fluid (Maroudas 1976). As a result of proteoglycan loss, tissue would become less able to support compressive loading, causing an abnormally large deformation under normal loading conditions (Armstrong and Mow 1982). The majority of load would be supported by collagen fibrils, subjecting them, as well as chondrocytes, to unusually high stresses, which may lead to further tissue deterioration. Abnormal synthesis and deposition of minor cartilage collagens has also been suggested to contribute to this process (Muir 1986).

Crystal deposition disease has been considered a subset of OA. Such categorisation has been challenged (Dieppe and Watt 1985). OA has been shown to be only slightly more common in joints with CPPD crystal deposition than in those without (Ellman *et al.* 1981, Wilkins *et al.* 1983). Although joint inflammation is common in OA and HAP crystals have been shown to induce an inflammatory response, albeit a mild one (Mandel 1976), Dieppe and colleagues (reviewed in Dieppe and Watt 1985) were unable to show a convincing association between HAP in synovial fluid and OA joint inflammation. A tendency to more severe disease in OA patients with HAP deposition than those without has been reported (Halverson and McCarty 1979, Schumacher *et al.* 1979). However evidence exists for a specific pattern of arthritis in some patients with CPPD and HAP crystal deposition (McCarty *et al.* 1981, Resnik and Niwayama 1981, Dieppe *et al.* 1982) and CPPD crystal deposition

disease can be distinguished from OA by the age of the presenting patients (Pritzker 1980) and histological differences between the two conditions (Ishikawa *et al.* 1989).

Crystal deposition has been reported to be secondary to local tissue alteration or damage (Wilkins *et al.* 1983, Doherty *et al.* 1982). Hence it has been suggested that alteration of cartilage matrix components, for example OA changes, may precede and predispose the tissue to crystal deposition. Crystal presence may modify the underlying disease, contributing to accelerated destructive changes by a variety of secondary mechanisms (Dieppe and Dohety 1982, Dieppe and Watt 1985). This hypothesis involves a feedback loop and is outlined in Fig. II. Set apart from this, the rapidly progressive, destructive diseases associated with CPPD and HAP (McCarty *et al.* 1981, Resnik and Niwayama 1981, Dieppe *et al.* 1982) may still qualify as specific subsets of OA.

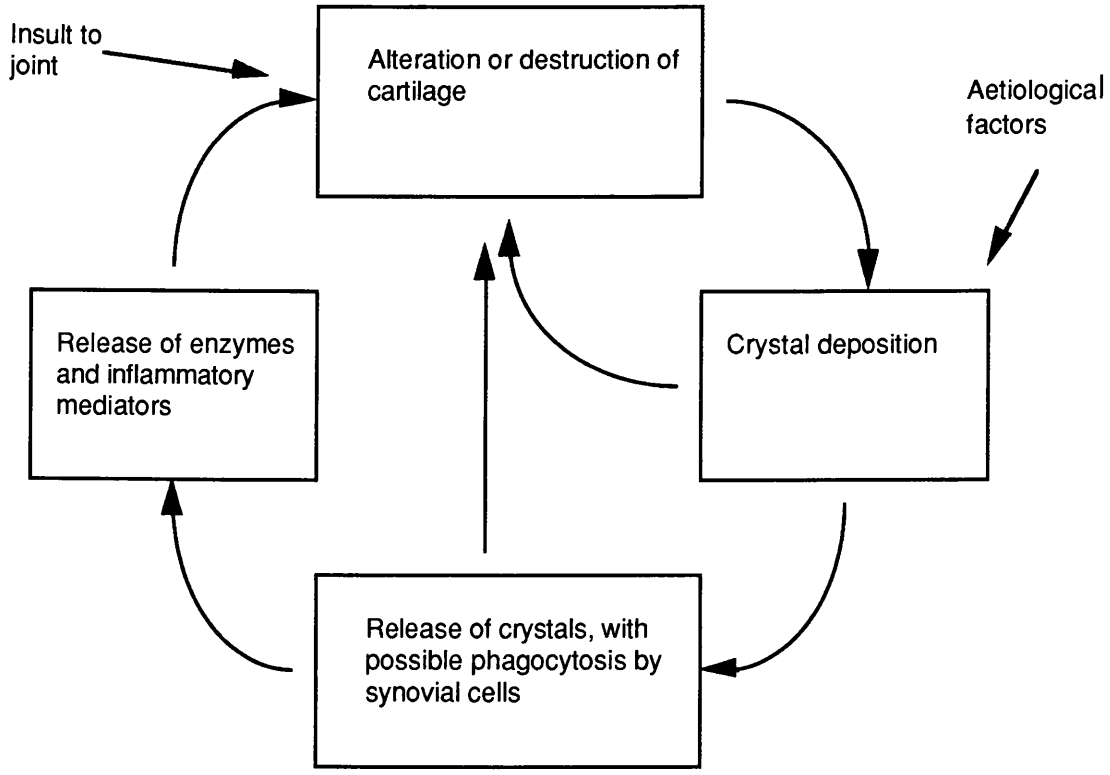

Fig. 2. Crystal deposition as an amplification loop in chronic arthritis. Such mechanisms have been proposed for both CPPD and BCP crystal deposition (After McCarty *et al.* 1981 and Dieppe and Calvert 1983).

CRYSTAL DEPOSITION DISEASE

A crystal deposition disease may be defined as a pathological condition associated with the presence of crystals which then contribute to tissue damage (Dieppe and Calvert 1983). Depositions are widespread in the body, as calculi, or within tissues, at sites including lungs, arterial walls, kidneys, gall bladders, dental plaques, heart valves, lymph nodes, and joints and associated tissues. Crystals deposited at these sites vary; apatite distribution is widespread whilst other crystals including CPPD, monosodium urate (MSU), struvite cholesterol ester and

whitlockite have a more specific distribution with respect to tissue type (Gatter and McCarty 1967).

Three main mineral types are recognised in articular crystal deposition disease (Schumacher 1988). Crystals have long been associated with inflammatory joint disease; supporting evidence was provided in the1960s when MSU crystals were shown to be associated with gout (McCarty and Hollander 1961). Soon after, the first calcium salt to be implicated in joint disease was CPPD (McCarty *et al.* 1962). More recently a variety of crystals has been detected in human articular and periarticular tissue. Of these,the basic calcium phosphates (BCP), including, hydroxyapatite (Dieppe *et al.* 1976) carbonated apatites (McCarty *et al.* 1983), and octocalcium phosphate (Faure *et al.* 1980, 1982, McCarty *et al.* 1983), have been assigned a role in crystal arthropathy (Dieppe *et al.* 1976, Schumacher *et al.* 1983, Schumacher *et al.* 1981, Ohira and Ishikawa 1987). Other crystals reported are summarised by Dieppe *et al.* (1983). Separate pathologies have been characterised for these three groups;however the co-occurrence of two or three of these crystal types within the same joint has been reported. For a review see Dieppe *et al.* (1988).

Pathology of Crystal Deposition Disease

The response to the deposition of crystals in articular tissues may take one of three forms; these may be isolated or sequential, the time course, severity and relative incidence of response being dependent upon the crystal type deposited. First the crystals discussed can, in some cases, exist without causing overt disease; many cases of chondrocalcinosis are asymptomatic (Dieppe and Calvert 1983). Secondly crystals may induce an acute inflammatory response, or thirdly, a chronic destructive arthropathy (Dieppe and Calvert 1983).

Deposition of crystals.

MSU crystals, precipitated due to hyperuricaemia, appear predominanlty in connective tissue. Articular connective tissue, typically the synovium, may be the first site of crystallisation of MSU (Schumacher 1988). In association with articular cartilage MSU crystals have been observed diffusely coating the surface or depositied within the tissue (Schumacher 1988, Hayes *et al.* 1992).

CPPD crystal deposition has many similarities with MSU crystals, but differs in that deposition occurs only in joints, bursae and periarticular structures. Fibrocartilage is the most common tissue site with the most common articular cartilage site being the knee. CPPD crystal deposition in cartilage is commonly observed in a perilacunar distribution (Pritzker *et al.* 1988, Schumacher 1988), with tophus-like deposits becoming most prominent in the mid zone and adjacent to chondrocytes (Schumacher 1988, Pritzker *et al.* 1988) or throughout the cartilage depth (Ohira and Ishikawa 1987, Hayes *et al.* 1992). In advanced chronic disease crystals may be grossly visible opening onto or coating cartilage surfaces. This may be due to the erosion of superficial cartilage. Cartilage matrix adjacent to deposits may appear normal or show fibrillation (Mitrovic 1983). The association of chondrocyte cloning and necrosis with CPPD

deposition has been frequently described (Schumacher 1988). CPPD deposition has rarely been observed within cells, such reports being associated with phagocytosis (Mitrovic 1983).

The deposition of CPPD, chondrocalcinosis, has been associated with a number of metabolic, local and familial predispositions. Clinical studies have demonstrated hypothyroidism, hyperparathyroidism, haemochromatosis, hypophosphatasia, hypomagnesaemia, gout and steroid therapy to be associated with CPPD deposition (McCarty *et al.* 1974, Pritchard and Jessop 1977, Ellman *et al.* 1980, Alexander *et al.* 1982). However such predispositions are only found in a minority of patients with chondrocalcinosis. Local joint abnormalities including joint laxity and meniscectomy have also been identified as predisposing factors to CPPD deposition (Jackson 1968, Doherty *et al.* 1982). Familial pyrophosphate arthropathies have been reported in a number of countries including Slovakia (Zitnan and Sitaj 1976). The most common aetiologic association of CPPD is with aging. By the age of 80 years CPPD crystal deposits can be found in the articular cartilage or intervertebral discs in approximately 25 % of the population (Pritzker 1980, Wilkins *et al.* 1983, Gordon *et al.* 1984) These surveys did not show any obvious relationship between chondrocalcinosis and associated joint disease.

BCP crystal deposition takes place at two main sites associated with synovial joints; periarticular tendon (McCarty and Gatter 1966) and intra-articular cartilage (Dieppe *et al.* 1976, Ali and Griffiths 1981a,b, Ali1985). Tendon calcification is common in the shoulder in association with the rotator cuff and the hip. In articular cartilage apatite crystals tend to be deposited in smaller amounts than in tendon, as described by Ali (1985); crystals demonstrated a pericellular distribution (Howell 1982, Ali 1985) , associated with an extension of the calcified zone. Small cuboid crystals were also been described in OA cartilage, with fine apatite crystals coating the cartilage surface (Ali 1985). Ohira and Ishikawa (1987) observed apatite deposition close to abnormal chondrocytes and areas of degenerate collagen and amorphous material.

Acute crystal deposition disease.

Acute inflammation due to MSU crystal deposition, gout, is characterised by sudden onset, generally considered to be brought about by crystals shedding from a deposit in the synovium into the joint space; such an event could be triggered by mechanical disruption or partial dissolution of crystals. Acute gout attacks are characteristically short compared to CPPD and BCP crystal induced inflammation (Dieppe and Calvert 1983).

The acute inflammatory state associated with chondrocalcinosis has been termed 'pseudogout' (McCarty *et al.* 1962). It is however slower in onset, less severe and takes longer to resolve than gout. Attacks are associated with joint effusions containing crystals. Radiological evidence linking CPPD crystal shedding and the onset of acute pseudogout has been reported (Doherty and Dieppe 1981).

Although much periarticular apatite deposition is asymptomatic there is one well defined acute inflammatory syndrome associated with it, acute calcific periarthritis (Fam *et*

*al.*1979). This condition commonly affects the shoulder. An attack is thought to be brought about due to the release of a preformed deposit, as radiological evidence has shown that deposits disappear coinciding with the onset of attacks. For a review of calcifying tendinitis of the shoulder see Faure and Daculsi (1983). Microcrystal nodules have been reported in the synovial fluid from cases of acute synovitis (Schumacher *et al.* 1979) .

Chronic crystal deposition disease.

MSU tophi in synovium may generate a chronic inflammatory response characterized by a rim of inflammatory cells and fibrosis (Schumacher 1988). Large deposits in joints may extend into cartilage and associated inflammatory tissue may form a pannus on the articular surface. Extension of tophi into the subchondral bone may result in resorption of trabeculae leaving a lesion in the subchondral plate. Such deposition leads to a characteristic destructive arthropathy of which the most common site is the metatarso-phalangeal joint (Dieppe and Calvert 1983).

Chronic disease is the main clinical condition relating to chondrocalcinosis and the knees, wrists and hands are the most commonly affected sites. Pathologically there may be severe joint destruction with bone damage (Richards and Hamilton 1974), features which have much in common with OA. The details of the association between chronic CPPD deposition disease and OA are not clear. One hypothesis to explain the relationship described by Dieppe and Calvert (1983) has been cited above and outlined in Fig. II. However in a number of patients with CPPD, a distinctive pattern of OA has been recognised which includes unusual articular and intra-articular distribution, prominant subchondral cyst formation and severe destructive bone changes (Resnik and Niwayama 1981, Dieppe *et al.* 1982).

BCP crystals have been reported in synovial fluid of approximately 30 % of OA patients in a number of studies using transmission electron microscopy and an apatite-specific diphosphonate binding assay (Dieppe *et al.* 1976, Halverson and McCarty 1979, Schumacher *et al.* 1981, Ohira and Ishikawa 1987). Several patterns of arthritis have been associated with BCP crystals including primary arthritis, polyarticular arthritis, and Milwaukee shoulder syndrome (Halverson and McCarty 1988). The deposition of BCP crystals in articular cartilage may be a secondary event due to other changes in cartilage metabolism or structure. Their presence however may induce further damage to the tissue by mechanisms similar to those outlined in Fig. II. Support for such a relationship may be drawn from a number of studies. The severity of knee joint degeneration has been correlated with HAP concentration in synovial fluid (Halverson and McCarty 1979, Paul *et al.* 1983) and a rapidly progressive, destructive disease of the shoulder associated with HAP deposition has been described (McCarty *et al.* 1981, Dieppe *et al.* 1984); many features were common in all reported cases, and the presence of activated collagenase and synovial proliferation in response to HAP crystal presence has been reported (McCarty *et al.* 1981, Halverson *et al.* 1984).

Mechanisms of Crystal Deposition Disease

The manifestation of a crystal deposition disease requires two aspects; firstly a mechanism by which crystals are deposited and secondly a mechanism or mechanisms by which crystals cause clinically overt problems.

Pathological Mineral Formation.

Pathological mineral deposition is generally considered to be mediated by a combination of three factors: First, an increase in local ionic concentrations to levels of supersaturation with respect to the appropriate ions is a necessary precursor to crystal nucleation. Secondly, matrix modifications resulting in the appearance of specific mineralization promotors, and thirdly, matrix modifications which result in the removal or modification of inhibitors of mineral formation and growth (Anderson 1988).

Pathological BCP crystal deposition shows basic similarities with normal calcification mechanisms; the initial mineral phase is associated with extracellular vesicle membranes, with subseqent calcification resulting in a highly insoluble mineral deposit (Anderson 1988). Several workers have identified such processes occurring in the formation of pathological HAP deposits in cartilage. Increased formation of extracellular matrix vesicles away from the tidemark, with increased alkaline phosphatase activity associated with excess apatite deposition, has been demonstrated in OA articular cartilage (Ali 1977, Anderson 1980, Ali and Griffith 1981a, Howell 1982, Rees and Ali 1988). Ohira and Ishikawa (1987), however, failed to find any evidence of matrix vesicles in calcification of femoral head articular cartilage. BCP crystals may form in cartilage with a modified matrix due to removal of inhibitors or addition of promotors of calcification. The reduced size of aggrecan in OA (Buckwalter and Rosenberg 1988), combined with loss of other inhibitors, may predispose matrix to BCP crystal deposition. Lipid accumulation has been reported at sites of HAP deposition (Irving 1963, Ohira *et al.* 1988). Dirksen (1969) and Wuthier (1975) reported an increase in acidic phospholipid at sites of HAP deposition. Calcium-acidic phospholipid complexes were associated with all HAP deposits studied by Boskey and Bullough (1984). Elevations in local calcium and inorganic phosphate ion concentrations have been associated with pathological BCP crystal deposition (Sokoloff 1983). These may include increases in association with chondrocyte death (Farber 1981), which, in addition, may provide membrane fragments on which HAP formation can occur (Matthews *et al.* 1978). Enzymes released at cell death may also upset the balance between promotors and inhibitors of calcification (Boskey and Bullough 1984).

Boskey and Bullough (1984) found HAP deposition to be more widespread across a range of articular tissues; CPPD deposition was observed in intervertebral disc and articular cartilage only. They suggested that tissues are predisposed to HAP deposition as mechanisms for promoting and controlling the deposition are already present in the tissues.

In contrast with HAP deposition, matrix vesicles have not been observed at the site of CPPD deposition (Pritzker *et al.* 1988, Schumacher 1988, Bjelle and Sundstrom 1975).

Cartilage is not normally supersaturated with respect to CPPD (Hearn and Russell 1980). To enable CPPD deposition calcium ions or inorganic pyrophosphate may be elevated due to altered metabolism. Pyrophosphate production has been shown to be increased in OA (Caswell *et al.* 1983). The current concensus supports the hypothesis that CPPD deposition is related to an imbalance between nucleoside triphosphate pyrophosphohydrolase (NTPPPase) and alkaline phosphatase, as an increase in NTPPPase without a concommitant increase in alkaline phosphatase activity may lead to excessive formation of pyrophosphate in the territorial matrix (Tenenbaum *et al.* 1981, Muniz *et al.* 1984, Ryan *et al.* 1985,). The observation that CPPD crystals form first at the edge of the territorial matrix would support this hypothesis (Ali *et al.* 1983, Pritzker 1986).

Factors other than excess pyrophosphate are required for CPPD crystal formation. *In vitro* studies have shown that CPPD forms within a narrow range of ambient ionic concentrations of calcium, inorganic pyrophosphate, magnesium, sodium and inorganic phosphate and that introduction or alteration of matrix macromolecules in such a system can prevent crystal formation (Pritzker *et al.* 1985). Promotors and inhibitors of CPPD deposition are therefore likely be important *in vivo* also. A number of matrix components have been suggested to play a role in CPPD deposition. Magnesium ions have been shown to hinder CPPD precipitation *in vitro* (Hearn & Russell 1980). Local modifications in proteoglycan distribution in association with CPPD deposition have been indicated (Ishikawa *et al.* 1989, Schumacher 1988). An association between early CPPD deposition and degenerating collagen fibrils has been shown close to hypertrophic type chondrocytes; such chondrocytes were not observed in cases of crystal free OA (Ishikawa *et al.* 1989). Lipid has been demonstrated histologically within CPPD tophi-like deposits and in degenerated matrix containing CPPD crystals (Ohira *et al.* 1988). TEM observation of similar areas demonstrated lipid in surrounding chondrocytes and as small droplets in the matrix.

Whilst calcium salts appear to be deposited at the site of primary abnormality, MSU crystal deposition is more likely due to secondary factors at the deposition site due to the systemic nature of the underlying condition. The specific distribution of MSU crystals in articular cartilage observed by Hayes and colleagues (1992) suggests the importance of local matrix factors influencing deposition. Lipids and mucopolysaccharides have been reported in the matrix of MSU tophi in early studies (Schumacher 1988) although it was not determined whether these were present prior to crystal deposition. Alteration in major matrix components, such as collagen and glycosaminoglycans in association with tophi, has also been reported (Schumacher 1988). More recently serum albumin has been shown to bind in a specific manner with MSU crystals (Perl-Treves and Addadi 1988). This has led to the suggestion of a crystal nucleation mechanism for MSU crystals *in vivo*.

Conditions for CPPD and HAP deposition appear to be mutually exclusive, and the capacity for heterogenous crystal seeding seems limited (McGill and Dieppe 1991).Therefore, in cases where mixed crystal deposition has been observed, it has been suggested that metachronous nucleation must occur (Pritzker *et al.* 1985).

Mechanisms of Disease.

The contribution of crystals to disease mechanisms in articular tissues is multifaceted. Effects may be biologically or mechanically mediated, involving inflammation and/or tissue destruction. Biochemical effects may be mediated through crystal contact with cells or phagocytosis and appear to be related to the size, shape and surface chemistry of the crystals involved. Initial cell:crystal interaction occurs at the plasma membrane. This has been shown to be important, causing cell lysis or altering cellular metabolism, inducing mitogenesis and the secretion of inflammatory mediators or degradative enzymes(Terkeltaub and Ginsberg 1988, Cheung and McCarty 1988). Cellular response to crystals is modulated by crystal structure, plasma membrane constituents and crystal surface coatings.

BCP and CPPD crystals have been shown to stimulate the growth of a variety of cells including human skin fibroblasts and canine synovial fibroblasts in culture (Cheung *et al.* 1984, Cheung *et al.* 1986). Stimulation required contact between cells and mineral (Bowen-Pope and Rubin 1983), and may reflect the synovial cell proliferation in calcium containing crystal deposition disease (Schumacher 1988). Evidence has been produced to suggest that the external stimulus of BCP crystals is transferred to generate a mitogenic response via a signal transduction mechanism (Mitchell *et al.* 1989). Although this appears to be the main transduction pathway, Cheung and McCarty (1988) suggest that the increase in cellular calcium ion concentration due to phagocytosed crystal dissolution is required for the full mitogenic response observed in cells. Recently similar effects have been demonstrated with chondrocytes (Cheung *et al.* 1983, Mitchell *et al.* 1992). Crystals may also stimulate mitogenesis indirectly; Di Giovine and colleagues (1987) demonstrated the ability of MSU-induced interleukin-1 to stimulate synovial cell proliferation *in vitro*.

Both cellular and humoral mechanisms may be involved in mediating an inflammatory response to crystals and different crystals activate different pathways. There appears to be a relationship between crystal structure and the intensity of inflammation. Weight for weight, MSU was shown to be more reactive than CPPD, HAP, and brushite in that order. An important factor in the inflammatory potential of a crystal is surface roughness and the presence of exposed charged groups, smooth crystals being inactive (Mandel 1976). The mechanisms of crystal-induced inflammation are complex and multifactorial; it is likely that different crystal types invoke different mechanisms to variable degrees.

MSU and CPPD crystals are avid binders of protein, especially IgG (Kozin and McCarty 1977). The Fc fragment of the adsorbed molecules remains functionally available (Kozin and McCarty 1980). Immunoglobulin coatings modify the crystal surface characteristics, possibly enhancing interactions with cell membranes, and activation of cell-free inflammatory mechanisms. The activation of the complement system by immune complexes containing MSU and CPPD is important in crystal-induced inflammation (Ginsberg *et al.* 1979). Several workers (Hasselbacher 1979a, Giclas *et al.* 1979) have shown that MSU crystals can bind with C1 *in vitro* and activate the classical complement pathway in the absence of IgG. Inflammatory

crystals have also been shown capable of activating the alternative pathway of the complement system (Doherty *et al.* 1983, Hasselbacher 1979b) in a manner suggested to be independent of immunoglobulin. It appears that free crystals may activate both classical and alternative pathways, whilst crystals with bound IgG predominate, activating the classical pathway through Fc binding. BCP crystals have a relatively low complement activating potential (Hasselbacher 1982).

The activation of Hageman factor by MSU crystals has been demonstrated (Ginsberg *et al.*1980). Hageman factor was split into two by MSU crystals, producing one bound and one free fragment. This process may activate the kinin system leading to the formation of potent vasodilators and the vascular permeability and pain apparent in the early stages of acute gout (Ginsberg *et al.*1980).

Neutrophils play a central role in crystal-induced inflammation (Phelps and McCarty 1966). Crystal phagocytosis by neutrophils is associated with secretion of a number of chemotactic factors, capable of inducing neutrophil influx in rabbit joints (Spillberg and Mandel 1982). Such factors have also been detected in human gouty fluids (Phelps *et al.* 1981). Other cells with crystal phagocytic ability and a potential role in the inflammatory response *in vitro* include macrophages, monocytes, fibroblasts and synovial lining cells (Evans *et al.* 1984ab, Owens *et al.* 1986). Synoviocytes have been shown to release vasoactive prostaglandins, and monocytes exposed to urate crystals released prostaglandin E2 (PGE2), lysosomal enzymes, interleukin-1 (IL-1) and tumour necrosis factor-α (TNFα) (Malawista *et al.* 1985, DiGiovine *et al.* 1987). Such factors may mediate early vasodilation, vascular permeability and pain in acute gout. It is believed that crystals are phagocytosed, initially by synoviocytes (Schumacher *et al.* 1974) via crystal bound IgG-cell membrane interactions. The protein coat of the crystal is then stripped within a phagolysosome, causing lysis due to crystal membrane interactions, leading to cell rupture and release of crystals. This mechanism is consistent with *in vivo* sequences observed for MSU, CPPD and HAP crystals (Schumacher 1977).

Concensus favours crystal release into the joint space as the most likely trigger for acute inflammation, with attacks being terminated by either removal of crystals by phagocytosis or the activation of inhibitory mechanisms, as crystals can still be found in synovial fluid after an attack of gout or pseudogout has been terminated (Dieppe and Calvert 1983). Changes in the protein coat of crystals with time, such as the addition of fibrin, fibronectin and apolipoprotein B-containing lipoproteins, may be important in terminating acute attacks (Carsons *et al.* 1980, Terkeltaub *et al.* 1984).

The chronic destructive arthropathies associated with the presence of crystals in joints appear to be mediated by a number of mechanisms. These include mechanical effects related to the physical properties of the crystals and the products of crystal-stimulated changes in chondrocyte metabolism.

The presence of crystals in the cartilage matrix alone may have deleterious effects on the tissue, altering the cartilage compliance. This may be envisaged to act in two ways: first,

reducing the load spreading ability of the cartilage transmitting excess forces to the bone below locally (Dieppe and Calvert 1983), and secondly, the difference in physical properties between cartilage matrix and crystals may lead to fractures at crystal-cartilage boundaries (Dieppe and Calvert 1983). Calcium phosphate crystals have also been described buried in the surface of articular cartilage (Ali 1985). Such hard sharp crystals on the cartilage surface may abrade the cartilage surface.

BCP and CPPD crystals incubated with cells from human and canine synovial membranes have been found to stimulate release of proteases including collagenase, and PGE2 (Borkowf *et al.* 1986). The activated collagenase may contribute to damaging cartilage matrix and PGE2 has the potential to activate bone resorption. Chondrocytes have been shown to respond similarly (Cheung *et al.* 1983, Mitchell *et al.* 1992). BCP crystals showed specificity in stimulation of activated collagenase. Endocytosis of BCP and CPPD crystals by canine and rabbit synovial fibroblasts was shown to be associated with the genesis of PGE2 (McCarty and Cheung 1985, Rothenberg 1987). McCarty and colleagues (1981) have described patients with severely damaged joints where their synovial fluid contained hydroxyapatite crystals and high levels of activated collagenase, suggesting similar systems may operate *in vivo*. Dieppe and colleagues (1988) however were unable to show an increase in activated collagenase in some synovial fluids with HAP present. The presence of such factors is considered important in association with the mediation and progression of joint degeneration.

'CUBOID CRYSTAL' REVIEW

As a consequence of the above, investigation of the microcrystals described in human arthritic articular cartilage by Ali and Griffiths (1981a,b) was considered important. Reasons for selecting the 'cuboid' (type II) crystals were twofold. First, their anomalous shape was hard to reconcile with the apatite habit. Secondly, and more importantly, they had potential for a pathological role. These crystals were observed in diseased tissue, with increased numbers of matrix vesicles and raised alkaline phosphatase activity (Ali 1985). Hence it was suggested that they may be associated with a calcification abnormality involved in the arthritic process; this was envisaged in a number of ways (Ali 1985). It was suggested that the presence of cuboid crystals in the surface zone may put stress on the the ECM leading to its eventual degeneration. Any crystals shed on to the surface of the cartilage may act as an abrasive, and lead to degeneration of the articular cartilage contact areas. Shedding of crystals may also invoke an inflammatory response, with the adhesion of complement, fibronectin or antibodies to crystal surfaces. An ensuing invasion of phagocytic cells releasing cytokines and enzymes with the potential to leave the articular cartilage susceptible to rapid degeneration under stress may be envisaged. There was also speculation that under certain conditions there may be an association between cuboid crystal deposition and calcium pyrophosphate dihydrate depostion (Ali 1985, Rees *et al* 1986).

Initial reports were limited to brief characterisation of the crystals. Using x-ray microanalysis (XRMA) an apatite-like Ca/P ratio was attributed to them. It was suggested,

however, that the crystals appeared, from their shape, more like whitlockite, an anhydrous tricalcium phosphate containing magnesium. The crystals, observed in arthritic specimens, were either "totally absent or rarely present" (Ali and Griffiths, 1981a,b) in normal articular cartilage specimens and were too small to be viewed by light microscopy or radiography. An artifactual origin was ruled out by their occurrence in sections obtained by cryoultramicrotomy. Their distribution was described as being just below the surface of the cartilage and forming a band in the surface zone, or occuring in the pericellular matrix, surrounding chondrocytes (Ali and Griffiths, 1981a,b).

Similar bodies, referred to as calcified bodies, occurring in association with "intramatrical lipidic debris", were observed by Ghadially and Lalonde (1981) within human semilunar cartilage. These bodies demonstrated similar morphological features and distribution with respect to chondrocytes, but had a lower Ca/P ratio; however the authors advised this figure be treated with caution. Magnesium was also detected within these calcific bodies and a morphological distinction was drawn between cuboid and spheroid bodies, though no difference in elemental composition was detected between the two. In 1983 magnesium was reported in cuboid crystals in human arthritic articular cartilage (Ali and Griffiths 1983), increasing speculation that they may be whitlockite.

The observation of these crystals in elderly normal cartilage was confirmed by Marante *et al* (1983). The Ca/P ratios were suggestive of apatite, supporting previous observations (Ali and Griffiths 1981a,b, 1983). Spherical variants of the cuboid crystals in articular cartilage were described by Marante *et al.* (1983) and Rees *et al.* (1986), the latter using a technique of microincineration to view the crystals three dimensionally in the scanning electron microscope. There was one report of cuboid crystals and calcium pyrophosphate dihydrate deposition in close proximity within one femoral head specimen (Ali, personal communication).

Rees *et al* (1986), using a microincineration technique, reported the crystals to vary in size between 50 and 650nm in any one dimension. XRMA results suggested that larger crystals(>250nm) had a lower Ca/P ratio than the smaller counterparts, which was still close to that expected for hydroxyapatite. Rees *et al.* (1986) suggested two distinct populations of crystal formed under different conditions and speculated that, under certain conditions, some of the crystals may have a role in the deposition of calcium pyrophosphate dihydrate.

Stockwell (1990) quantified the distribution of crystals in elderly human normal femoral head articular cartilage; the pericellular distribution and specificity to the surface zone was confirmed.

Little evidence to determine the mode of formation of these crystals has been produced. Suggestions as to the mode of formation may be divided between those where a chondrocytic role is attributed and those where crystal deposition is not due primarily to chondrocyte activity. Ali (1985) reports an association with matrix vesicles and suggests a mechanism of crystal formation similar to that of epiphyseal cartilage. Ghadially and Lalonde suggest crystals are formed in or on matrical lipidic debris (50-600nm) which is not consistent

with the "special" matrix vesicles description. They suggest these bodies are derived from shedding of cell processes by chondrocytes and *in situ* necrosis of chondrocytes as speculated by earlier workers (Barnett *et al.* 1963, Ghadially *et al.* 1965, Stockwell 1979). Marante *et al.* (1983) noted the distribution of crystals corresponds to the sites of extracellular lipid observed in aging articular cartilage. Stockwell (1990) suggests that high deposition of crystals in areas of cell debris, or changes in the matrix induced by cell death may be factors responsible. The lack of increased crystal deposition near chondrocytes is cited to detract from the matrix vesicle theory of cuboid deposition. Stockwell (1990) suggests the presence of matrix vesicle-like structures, reduced proteoglycan concentrations in the matrix and that an extra articular source of calcium and phosphate ions may be necessary for the deposition of cuboidal crystals.

The aims of this thesis are to establish ,(1) the occurrence of these crystals in fresh normal human articular cartilage, (2) the spatial distribution of these crystals within articular cartilage, (3) their occurrence in cartilage from various joint sites and other species, (4) the development of an isolation technique to enable (5) the identification of the crystal mineral phase and (6) to identify factors that contribute to the formation of the crystals. This will be achieved by applying electron microscopy and related techniques to fresh human normal and osteoarthritic articular cartilage.

CHAPTER 1
CRYSTAL DISTRIBUTION

Introduction.

Continued refinement of analytical techniques has, in recent years, permitted observation of smaller and smaller mineral deposits within joint tissues. This has led to a great deal of confusion in the interpretation of the observation of crystal deposition, particularly basic calcium phosphates, in relation to arthritic disease. More rigorous reporting and characterization of such deposition may shed light on this problem. A clear starting point for this is quantification of crystal deposition in tissue samples correlated with precise location and state of tissue from which specimens were taken.

The work to date involving 'cuboid' crystals has been mainly qualitative. Most reports have been from OA or elderly specimens with little correlation between crystal deposition and precise sampling site (Ali and Griffiths 1981a,b, 1983, Marante *et al.* 1983, Ali 1985) . Stockwell (1990) provided a detailed image analysis-based quantitative study of deposition in femoral head articular cartilage with careful correlation between sample site and crystal deposition data, but the samples were restricted to a small number of elderly individuals. Further, although the mineral phase of these calcium phosphate crystals has been subject to speculation, identification has not been made.

Quantitative analysis of such small objects with the observed non homogenous distribution requires a number of factors to be taken into consideration. First, pure random sampling has a tendency to produce erroneous results; better results are achievable with a stratified systematic sampling method (Aherne and Dunnill 1982). Secondly, as ultrathin sections have finite thickness, areas may be overestimated or underestimated due to factors such as the Holmes effect (Aherne and Dunnill 1982), the apparent area of an object being contributed to by its size within the volume of the section, rather than the area exposed at the section surface; also truncation phenomena may occur due to poor contrast of section components (Hunziker *et al.* 1989). Some authors consider that these two effects tend to cancel themselves out for intracellular organelles in TEM sections (Weibel *et al.* 1969, Eisenburg *et al.* 1974). Thirdly, counting discrete objects in histological sections presents further problems as sections will contain whole objects and parts of objects. Techniques have been developed to overcome these problems; however the population characteristics of the microcrystals under investigation fail to satisfy the requirements of any of these methods fully, for example, they are not ellipsoid and have a large size range. (Aherne and Dunnill 1982).

In this investigation absolute counts are not strictly required. By applying strict sampling and analytical protocol to all samples variations between specimens will be real although absolute estimations of crystal area or number may be biased.

To produce as full a picture as possible of crystal distribution in articular cartilage, a qualitative grading index was devised to enable broad comparisons of crystal distribution at different sample sites. A preliminary semi-quantitative study was made to establish general variations in deposition within femoral head articular cartilage, a site where regular specimen availability makes identification of variations in deposition with age and disease possible, and define the areas and criteria for a detailed quantitative study.

Reports of 'cuboid' crystal distribution to date all relate to tissue that has been processed for TEM using aqueous solvents. These are known to cause translocation of diffusable ions such as calcium and phosphorus (Morgan *et al.* 1975), dissolution and reprecipitation of mineral salts (Boothroyd 1964, Thorogood and Craig Gray 1975, Landis *et al.* 1977) and mineral phase transformations (Landis and Glimcher 1978). Brushite formation has been detected in sections of noncalcified tissue prepared in phosphate-buffered formalin (Cheng and Pritzker 1983), and during cryopreparation of cartilage, an amorphous calcium phosphate type mineral has been reported to appear randomly in connective tissue matrix (Landis and Glimcher 1982), which was not observed when cryo-preservation was carried out in ethylene glycol (Morris *et al.* 1983). To establish the authenticity of the 'cuboid' crystals, adjacent samples from the same specimen were processed by standard resin processing, cryo-processing, and anhydrous processing with organic solvents as described by Landis and colleagues (1977).

This chapter attempts to establish the presence of the crystals and describe their distribution qualitatively and quantitatively within femoral head articular cartilage and at other joint sites in health and osteoarthritis. Subsequent chapters aim to identify the mineral phase or phases of this crystal deposition and finally look in greater detail at the crystal-ECM component relationships as a means of gaining insight into the origin of 'cuboid' crystal deposition and the consequences for articular cartilage.

Materials and Methods.

This general methods section describes in detail the tissue processing schedules that were used for studies reported in this and later chapters. Whilst reference will be made to this section in subsequent chapters, specific methods and techniques will be described in the chapter where they are appropriate.

Specimen Details.

Articular cartilage specimens were taken from a total of 70 patients (Table 1.1). The majority of specimens were either, normal femoral head articular cartilage resected due to tumour located distant to sampled cartilage, or fracture of femoral neck. or osteoarthritic articular cartilage from the same site. Cartilage was taken from other joint sites when available, due to amputation or resection for tumour. A selection of patient details (those used for quantitative analysis) is provided in appendix I. Specimens of bovine, porcine and lapine articular cartilage were also examined.

In all cases full depth blocks of articular cartilage, plus subchondral bone, were taken from sample sites. Specimens were generally obtained within 20 minutes of resection. Normal femoral head articular cartilage samples were taken from the superior, inferior and, in a number of cases, anterior and posterior aspects. Samples from OA femoral heads were taken from three areas; immediately adjacent to the eburnated bone (type IV) (Ali and Bayliss 1974) , any remaining full depth cartilage and peripheral osteophyte. At other joint sites samples were taken from weight bearing regions of the cartilage. Specimens were divided for wax embedding and freezing for

histology, and resin embedding and freezing for electron microscopy. All tissue remained undecalcified.

Histology.

Wax processing and histology.

Tissue samples were fixed in 10% formal saline for a minimum of 48 hours. Samples were processed in a Reichert automatic tissue processor before embedding in wax.

Histologically serial sections were cut, at 7μm thickness, on a Leitz base sledge microtome and were stained with Ehrlich's haematoxylin and eosin (Bancroft and Stevens 1990). Histological processing and some staining were carried out by the Department of Morbid Anatomy, Institute of Orthopaedics RNOH.

Cryo-processing and histology.

Full depth tissue samples were orientated in 'cryo-m-bed' cryomountant (TAAB Laboratories, Aldermaston, UK.) on 15mm diameter cork discs, plunge-frozen in liquid nitrogen and stored at -70^{o} C. Samples were brought to -20^{o}C and 10μm sections were cut on a Bright cryostat and collected onto subbed slides (Pappas 1971). Sections were rinsed briefly in distilled water, stained with alizarin red solution (McGee-Russell 1958) and dehydrated in 100% acetone, followed by infiltration with an acetone/xylol (1:1), xylene sequence, prior to mounting in DPX.

All sections were photographed using an Olympus BH2 photomicroscope.

Transmission Electron Microscopy.

Standard resin processing.

Tissue samples were subdivided to full depth blocks approximately 1mm in the remaining two dimensions. A small amount of subchondral bone was left attached to minimise tissue distortion during processing (Ghadially 1983) and facilitate easy tissue orientation. The tissue blocks were fixed for 2-4 hours in 1.5% glutaraldehyde (Agar scientific, Stansted, UK) in 0.085 M sodium cacodylate buffer (pH 7.4) (Merck, Poole, UK). Specimens were then washed in three changes of 0.085M sodium cacodylate buffer containing 0.2M sucrose (pH7.4) (wash buffer). The tissue blocks were then divided and half the blocks underwent secondary fixation with 1% osmium tetroxide (Agar Scientific, Stansted, UK) in 0.085 M sodium cacodylate for 90 minutes at room temperature. Buffer washing was repeated and all tissue blocks were dehydrated through a graded alcohol series as outlined below:

70% methanol	2 x 5 minutes
90% methanol	2 x 5 minutes
96 % methanol	2 x 5 minutes
Absolute Ethanol	3 x 10 minutes.

Specimens were transferred to propylene oxide (Agar Scientific, Stansted, UK) for 30 minutes prior to infiltration with a 1:1 propylene oxide:araldite CY212 resin (Agar Scientific, Stansted, UK) mixture for 1 hour, followed by infiltration in neat CY212 resin under vacuum (150mbarr)

overnight, and embedding in fresh resin at 60°C for 48 hours. CY212 resin was mixed according to the manufacturer's instructions with the omission of methyl phthalate (plasticiser).

Anhydrous processing.

The processing schedule was modified from that described by Landis *et al* (1977). Full depth articular cartilage blocks measuring approximately 1mm in the remaining 2 dimensions were placed in vials containing 100% ethylene glycol within 20 minutes of resection. The vials were maintained under vacuum in a vacuum dessicator, with continuous agitation at 4°C for 24 hours. The cartilage blocks were brought to atmospheric pressure and transferred to Cellosolve (monomethyl ether of ethylene glycol: Merck) for 2x12 hours at 4°C prior to infiltration with a 1:1 propylene oxide/araldite CY212 resin mixture for 24 hours. Infiltration was completed in neat CY212 resin under vacuum overnight and embedded in fresh resin at 60°C for 48 hours.

Semi-thin (500nm) and ultra thin (70-100nm) sections were cut using a Reichert Ultracut E ultramicrotome (Leica, Milton Keynes, UK). Semi-thin sections were cut with glass knives, dried onto glass slides and stained either with Humphrey's stain (Humphrey and Pittman 1974) or toluidine blue (Richardson *et al.* 1960) to orientate the tissue. Sections were photographed using an Olympus BH 2 photomicroscope.

Ultrathin sections were cut with diatome diamond knives (Leica, Milton Keynes, UK) and floated onto 0.085M sodium cacodylate buffer prior to collection onto G200 HS copper grids (TAAB Laboratories, Aldermaston, UK). Where necessary the grids were precoated with 0.45% piolform (Agar Scientific, Stansted, UK) in chloroform (Merck, Poole, UK). If required, ultrathin sections were stained on drops of aqueous saturated uranyl acetate (Agar Scientific, Stansted, UK) (Watson 1958) for 10 minutes at room temperature followed by lead citrate (Reynolds 1963) for 5 minutes at room temperature in the presence of sodium hydroxide pellets (Merck, Poole, UK).

TEM cryo-processing.

Full depth tissue blocks were taken, as described for resin processing , and fixed in 0.2% glutaraldehyde / 4% paraformaldehyde in 0.085M sodium cacodylate buffer (pH 7.4) for a minimum of 4 hours. Freshly fixed tissue was washed in 0.085M sdium cacodylate buffer for 2x 10 minutes then transferred to an aqueous 2.3M sucrose solution. After complete infiltration with sucrose solution (indicated by tissue sinking and becoming translucent), tissue blocks were trimmed to approximately 0.5 mm cubes, including the articular surface, oriented in a drop of sucrose on a Reichert cryomounting pin and plunge-frozen in liquid nitrogen. Sections were cut on a Reichert Ultracut E ultramicrotome fitted with a Reichert FC4 E cryo-attachment, using a Diatome diamond cryo-knife. Sections were collected onto piolform coated nickel G200 HS grids (TAAB Laboratories, Aldermaston, UK) and floated section side down on 0.085M wash buffer. Sections were stained on drops of 2% neutral uranyl acetate for 5 minutes, washed on distilled water and stained for a further five minutes with saturated aqueous uranyl acetate. Grids were then

placed on drops of 1% methylcellulose containing 0.3% saturated aqueous uranyl acetate (Griffiths *et al.* 1984, Tokuyasu 1986).

All ultrathin sections were examined and photographed using a Philips CM12 transmission electron microscope operating at 80kV, with the exception of cryosections which were examined at 120kV.

Preliminary Quantitation.

100nm sections were oriented on G200 HS copper grids with the articular surface oriented along one of the grid axes. Sections were observed at 8,800 X magnification and the number of crystals in each grid square (quadrat, 13,225μm^2) recorded along a transect one grid square wide, from the articular surface to the calcified zone.

Five transects, perpendicular to the articular surface, from the surface to 2 grid squares depth were subdivided and the number of crystals present in each quadrat (7.4x10.2μm) recorded for each specimen. Quadrat size was determined by the apparent size of the plate field marker on the large screen of the TEM at 8,800x magnification).

Quantitative Analysis.

Femoral heads, resected due to total hip replacement, or amputation for fracture of the femoral neck, or distal femoral tumour, were obtained from 12 patients within 20 minutes of resection. The patients (4 male, 8 female) ranged in age from 10 to 89 years.Samples were taken from superior and inferior regions of the femoral head, processed for TEM and embedded in araldite CY212 resin as described above. A stratified systematic random sampling procedure was employed. Three of six resin embedded blocks were selected at random and two non serial, 100nm sections were examined unstained using a Philips CM12 transmission electron microscope operating at 80kV. In total 45 areas each consisting of five fields were recorded in a defined systematic manner for each sample region (Fig. 1.1). The number of areas to be sampled from each region was established from the preliminary study using criteria outlined by Aherne and Dunnill (1982) (Appendix II). Fields were photographed at 10000x magnification. The study area comprised a band delineated by the articular surface and a parallel line 50μm below this. An 18.2μm^2 area of each micrograph was systematically examined using a Joyce Loebl Magiscan image analyser to record the number of crystals, the area of each crystal profile and the total crystal profile area. The image analyser was calibrated before each session using a micrograph of a carbon diffraction grating replica (1200 lines/mm, Agar Scientific, Stansted, UK) photographed in the same TEM at 10000x magnification. The task list set up to process the images, measure and record data is given in appendix III. In total, over 2,500 negatives were analysed. The Mann-Whitney U test was employed as a test for significance ($P<0.05$) unless otherwise stated.

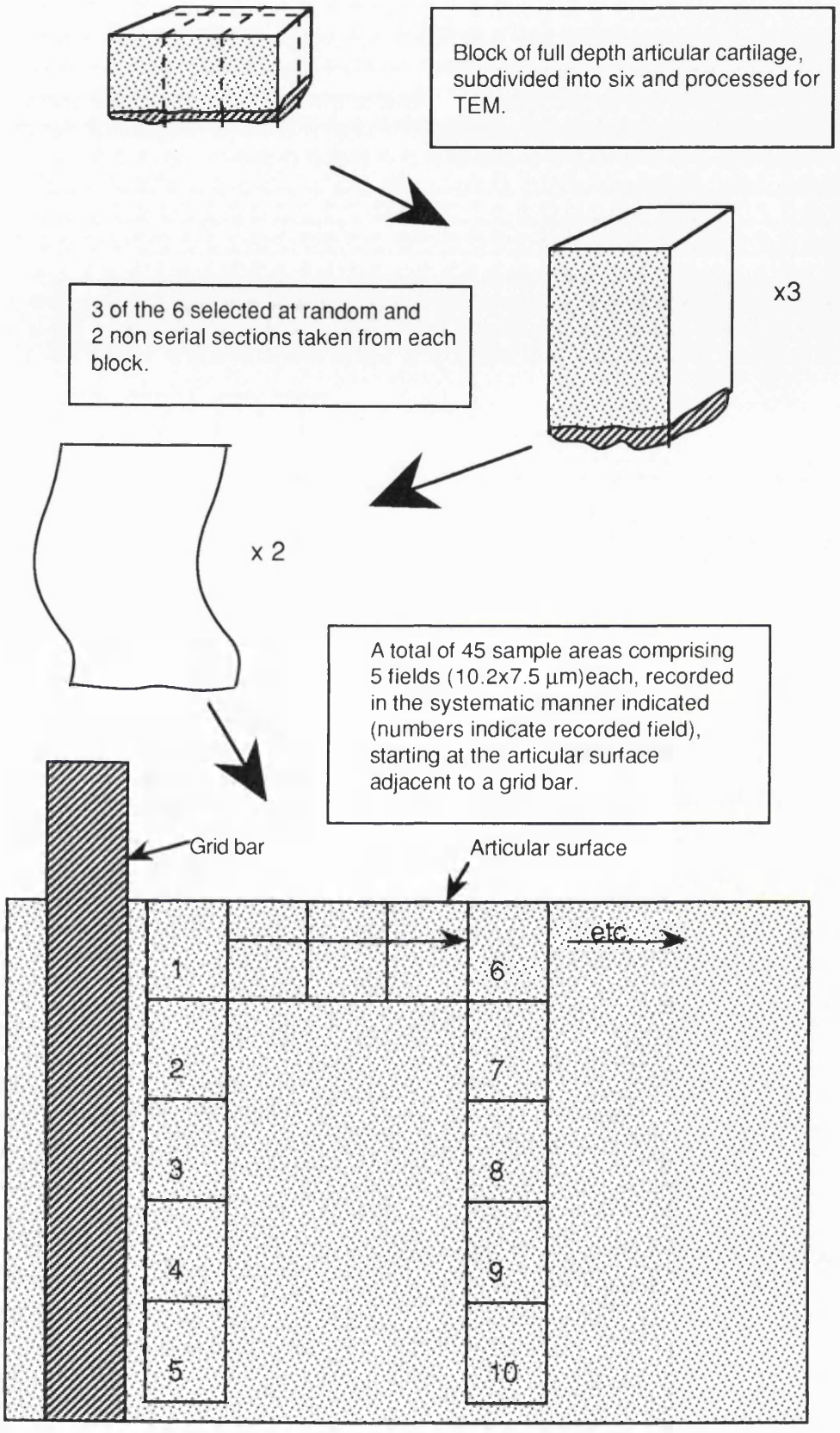

Fig. 1.1. Schematic representation of the stratified, systematic, random sampling procedure followed for quantitative analysis of crystal distribution.

Results.

In the description of the results, 'crystals' is used to refer to those described previously as 'cuboid' crystals (Ali and Griffiths 1981a,b, 1983, Ali 1985, Rees *et al.* 1986). Other crystal types described will be clearly distinguished.

Demonstration of Crystals in Articular Cartilage.

Femoral head articular cartilage was classified as either type I or type II (Ali and Bayliss 1974) from normal femoral heads (Fig. 1.2a) or type IV from OA femoral heads (Fig. 1.2b). Light microscopic observation of normal femoral head articular cartilage samples stained with H&E demonstrated well organised tissue with flattened chondrocytes in the superficial zone below a non fibrillated articular surface, evenly spaced rounded chondrocytes in the deeper tissue and no indication of crystal deposition in the matrix (Fig. 1.3a). Samples from OA femoral heads demonstrated variously tissue fibrillation, chondrocyte clusters and a loss of basophilic staining and, in some cases, fibro-cartilaginous tissue at the surface, but no evidence of crystal deposition (Fig. 1.3b). Further, it was not possible to demonstrate the presence of these crystals in the ECM of frozen normal articular cartilage sections stained with the alizarin red stain for calcium although the calcified zone cartilage and suchondral bone produced a clear positive result (Fig. 1.4).

In unstained ultrathin sections of articular cartilage examined by TEM, the crystals were seen in sharp contrast to the surrounding tissue due to their high electron density relative to the unstained organic matrix (Fig. 1.5). The crystals appeared stable under the electron beam, although evidence of sublimation was apparent at high magnification for extended periods. Crystals exhibited frequently a rhomboid to square shape in section, suggesting a cuboid morphology when projected to three dimensions (Fig. 1.5). They ranged in size from 50 to 500nm along any one axis. No evidence of a limiting membrane was observed surrounding crystals. Other angular shapes, consistent with sectioning a cube, were also observed, as were ovoid type crystals, of similar size and electron density to the cuboid crystals. A substantial loss of crystals from resin sections cut on to distilled water was observed. It was possible to achieve a negligible loss by cutting sections onto 0.085M sodium cacodylate buffer. A similar loss of crystals was frequently observed in sections stained with uranyl acetate and lead citrate.

Crystals were observed in articular cartilage samples processed for TEM by all techniques. Cryo-processed normal femoral head articular cartilage demonstrated distinct , recognisable crystals in the ECM, although ultrastructural preservation of cells was poor (Fig. 1.5c). Articular cartilage samples from normal and OA femoral head, femoral condyle and tibial plateau sites were prepared anhydrously. Ultrastructural detail in such samples was less well preserved than with standard resin processing (Fig. 1.6). Crystals in cartilage processed anhydrously (Fig. 1.6a,c) exhibited the same characteristic morphology, a similar size range and density of crystal deposition to adjacent tissue from the same specimen processed for TEM by the standard method (Fig. 1.6b,d), though there was much variation between specimens. The distribution of crystals with respect to depth within the tissue and proximity to chondrocytes was also similar for adjacent cartilage blocks processed by these two methods.

Crystals were observed in OA and normal articular cartilage from a number of joint sites, across an age range from 5 to 92 years. The density and extent of deposition was extremely variable and is described in detail below.

Qualitative Distribution of Crystals in Normal Articular Cartilage.

In normal femoral head articular cartilage crystal deposition was greatest in the superficial zone. Crystals were present either in a band running parallel to the articular surface and starting within 5μm of the surface (Fig. 1.7), or in close proximity to chondrocytes, and occasionally in dense clusters (Fig. 1.7). A band of crystals was identified in many specimens of variable density and depth, frequently with a degree of patchiness. The depth of the band in some specimens was limited to the extreme superficial articular cartilage ECM between the articular surface and the most superficial chondrocytes, a region frequently observed to contain characteristic granular intramatrical lipidic debris, including membranous structures. Other specimens demonstrated a deepening of the band, encompassing initial superficial zone chondrocytes. Such differences between specimens appeared to be related to specimen age. Older specimens had deeper bands of crystal deposition. Crystals were commonly observed deposited pericellularly to chondrocytes, apparently associated with intramatrical lipidic debris (Fig. 1.8). In many cases the crystal distribution was biased with greater numbers adjacent to the articular surface aspect of the cells when viewed in sagittal section. A degree of polarity toward the ends of the cells was apparent in this orientation.However tangential sections of such chondrocytes revealed a more even pericellular distribution of crystals in the plane of the cell (Fig. 1.9). Tangential sections also revealed the extent of the band of crystal deposition described above, extending broadly in the ECM immediately below the surface (Fig. 1.9c). Crystals were frequently observed within chondrocyte territorial matrix often in close proximity to the plasma membrane (Fig. 1.8b,d); however crystals were never observed within living chondrocytes. The observation of crystals within dead or degenerate cell outlines and within focal areas of intramatrical lipidic debris, was made in a number of specimens of both normal and OA origins (Fig. 1.10). These areas were identified as advanced stages of *in situ* necrosis of chondrocytes, due to shape, size and composition of the debris. Dense focal areas of crystal depostion were also observed in the absence of obvious matrix debris; such areas were of similar size and shape to superficial zone chondrocytes (Fig. 1.8c).

In deeper zones crystals were rarely observed. Crystal deposition when encountered was, in the main, perilacunar, amongst areas of lipidic debris (Fig. 1.11a); very few crystals were encountered in the interterritorial ECM. In three specimens crystals were observed in close proximity to hypertrophic chondrocytes and initial spherulites of apatite crystallite deposition (Fig. 1.11b).

Despite occasional focal densities and dense banding of crystals in the superficial zone matrix there was no evidence of structural disruption of collagen fibril orientation by crystals in normal articular cartilage, nor was there any evidence of chondrocyte degeneration induced by crystal deposition. Superficial zone chondrocytes, within areas of crystal deposition,

demonstrated nuclei with smooth contours and marginal condensates of heterochromatin bounded by a nuclear fibrous lamina. Mitochondria generally showed good integrity and lipid droplets, glycogen granules and intermediate filaments were observed in variable concentrations. In situ necrosis of chondrocytes was observed in many samples. Such observations were infrequent and occurred throughout the cartilage depth. There was no evidence to suggest necrosis was associated with crystal deposition.

Qualitative Distribution of Crystals in OA Articular Cartilage.

The distribution of crystal deposition in OA femoral head articular cartilage was less predictable than for normal tissue, being dependent upon the degree of tissue degeneration and further complicated in a number of specimens by the presence of apparent fibro-cartilage at the surface (Fig. 1.11c). In specimens with extensive deep fibrillation, acellular regions and chondrocyte clusters, crystals were limited to scattered patches pericellular in distribution with occasional isolated observations. It proved difficult to obtain femoral head cartilage in early stages of degeneration but a number of such specimens were examined, being supplemented by articular cartilage from other joint sites, with slight fibrillation and some chondrocyte clusters. In such specimens the distribution was similar to that described for normal femoral head articular cartilage with one noticeable difference being an increase in pericellular crystal deposition below the superficial zone. This increase was accompanied by a more extensive deposition of pericellular matrix debris (Fig. 1.12).

Variation in Crystal Deposition with Joint Site.

Crystals were observed in articular cartilage from all sites sampled (Table 1.1). The distribution in all cases was similar to that described for normal femoral head articular cartilage, however the density of deposition showed much variability with no site reaching the highest densities observed in normal femoral head tissue. A five point qualitative grading scale was devised (criteria for grading are listed in Table 1.3) to compare crystal deposition in tissues from different sites. In the knee, whilst articular cartilage from both the femoral condyle (grade 2) and the tibial plateau had crystals present, deposition in tibial plateau tissue was very sparse (grade 1) (Fig. 1.13a,b). A small number of specimens from several smaller joints were examined. Crystal deposition density in cartilage from the proximal ulna and radial head was similar to that in femoral condyle samples (grade 2 to 3) (Fig. 1.13c,d). In samples from the remaining sites deposition was sparser than this (grade 2) with the least dense observed in a sample of phalangeal cartilage (grade 1) (Fig. 1.13e,f). No crystals were observed in peripheral osteophyte from OA femoral heads or epiphyseal growth cartilage.

Crystal Deposition in Other Species.

Clearly defined 'cuboid' crystals were not observed in non-human articular cartilage, although similar deposits were apparent in specimens from two out of the three species examined (Table 1.2). Unstained sections of porcine femoral head articular cartilage from 20 week old animals

demonstrated ovoid, intensely electron dense bodies of approximately 200nm diameter with crystalline characteristcs associated with lipidic and membranous structures in superficial cartilage (Fig. 1.14). The distribution of these bodies was similar to that of 'cuboid' crystals in young human superior femoral head articular cartilage. The chondrocytes and matrix showed good preservation with no evidence of degenerative changes. In 20 month old lapine femoral head articular cartilage membranous structures with less clearly defined ovoid, electron dense areas among them were observed in the superficial zone (Fig. 1.14). Their distribution in the matrix was between a densely packed band of collagen fibrils at the articular surface and the chondrocytes closest to this. In both cases the electron dense bodies were of a similar size, density and distribution to 'cuboid' crystals found in the superficial zone of human articular cartilage. Articular cartilage from the metacarpal of 18 month old steers was also examined for the presence of such electron densities though none was identified, the superficial zone matrix being clear of such matrix debris.

Preliminary Semi-Quantitative Analysis of Crystal Distribution.

All semi-quantitative analysis of crystal distribution was performed on normal femoral head articular cartilage. Examination of samples of cartilage from different areas of the same femoral heads revealed variation in crystal deposition density indicated by the qualitative grading system described above. There was a consistently greater level of deposition in cartilage from the superior region than inferior region samples (Table 1.3). Cartilage from anterior and posterior regions had similar crystal deposition, being close to those observed in the superior region (Table 1.3).

For statistical analysis, to establish any age-related trends in crystal deposition, specimens were divided into three groups. These were, 'juvenile to young adult' (10-25 years), 'adult' (40-55 years) and 'elderly' (75 to 90 years). Groupings were dictated to an extent by specimen availability, with the consequence that the 40-55 year group was very small.

Preliminary quantitation of crystal distribution within full depth articular cartilage suggested that, in all cases, over 90% of crystal deposition was restricted to the first 115 μm below the articular surface in both superior and inferior regions (Fig. 1.15). Crystal deposition below this, though sparse and sporadic, was greater in samples from older specimens (Fig. 1.15). The number of crystals within this first quadrat was consistently less in the inferior region than the superior region, though this difference was smaller in samples from older specimens (Fig. 1.15).

Closer investigation of the first 200μm depth of superficial zone articular cartilage recognised a peak of crystal deposition within the first 50μm depth into the cartilage in which over 90% of crystals in all samples examined were located (Fig. 1.16). The distribution with respect to sample site and specimen age remained as described for the full depth cartilage study.

Quantitative Analysis of Crystal Distribution.

No abnormality of cartilage was observed at a gross or light microscopic level in specimens used for this study. All specimens had intact superficial zone cartilage with a non-fibrillated articular

surface. Surface roughening at the electron microscopic level was observed in some inferior region specimens, this was not considered to be degenerative. The sharp contrast of crystals with the unstained matrix facilitated simple automated selection of crystal profiles for analysis. The characteristic electron density, morphology and size range allowed for any contaminant or artifact to be removed from the analysis at an optional editing step in the procedure. Crystal profile areas ranged from 0.0001μm^2 to 0.6μm^2 and the area ranges were similar in all patients. Samples from both sites of all patients contained crystals but there was great variation in crystal numbers and area densities between sites and patients (Fig. 1.17, Table 1.4). The area density of crystals for an entire sample site ranged from 0.008% to 0.39%; within the crystal band itself this rose to a maximum of 1.02%. The highest density recorded for a single unit area (18.2μm^2) was 6%.

Crystal profile area.

In all samples the crystal area profile frequency distributions were skewed to the lower end of the range. For statistical comparisons log transformations of these data enabled parametric analysis (Fig. 1.18). In superior region samples a significant correlation ($r = 0.7$: $P<0.05$) between mean crystal area and age was observed (Fig.1.18) with crystal areas ranging from 0.0001μm^2 to 0.6μm^2. Crystal areas in inferior region samples ranged from 0.0001μm^2 to 0.4μm^2. No correlation with age was observed (Fig. 1.18).

Crystal numbers and Area Density (% area of section occupied by crystal profiles).

In the superior samples great variation between patients was observed in both variables ranging from 38 (crystal number) or 0.02% (area density) to 1202 or 0.39% (Table 1.4); this variation did not appear to be age related. Inferior samples also demonstrated great variation in both parameters ranging from 2 or 0.008% to 541 or 0.11%. The area density in the 10-25 year age group for inferior samples was significantly lower than the two older inferior region groups ($U=2$). In this region there appeared to be a trend for an increase in crystal number and area density with age. There were, however, significant differences in area density between the superior and inferior regions in each of the 3 age groups (Table 1.4).

Distribution of crystals with depth in cartilage.

The banding of crystals below the articular surface as described above was confirmed quantitatively by subdividing the data for crystal number and area density into five sampling layers, each 10μm in depth and parallel to the articular surface. In the superior samples this band was well defined extending from the surface to between 20 and 30μm depth (Fig. 1.19). Crystal area densities ranged from 1.02% within the band to 0% below this. This trend became less apparent with increasing age; in the oldest group area densities ranged from 0.59% to 0.02%. The inferior region samples demonstrated low crystal numbers throughout the depth profile in the younger specimens, the maximum area density being 0.04%. There was a slight increase in crystal area density with age throughout the depth profile, to a maximum of 0.45% (Fig. 1.19).

Crystal density and profile area relationships.

By considering each of the five sampling layers from each sampling area as individual units it was possible to produce scatterplots relating the number of crystals in each unit to the area of that unit occupied by crystal profile (Fig. 1.20). The number of points for each plot was 225 multiplied by the number of specimens in each age group. Plots with few points registered indicated a high proportion of low or zero values. The relationship between crystal number and crystal profile area was approximately linear across the age range in both superior and inferior regions. There was however a trend for an increase in the gradient of this relationship with age, this being more apparent in the superior region than the inferior (Fig. 1.20).

Fig. 1.2

Fig. 1.2. Normal (a) and OA (b) femoral heads demonstrating some of the articular cartilage types (type II, type IV; Ali and Bayliss 1974) used in this study. Femoral head specimens provided the majority of samples for this study. The areas of the femoral head from which articular cartilage was taken for comparative quantitative analysis are indicated in the diagram of the proximal femur (c).

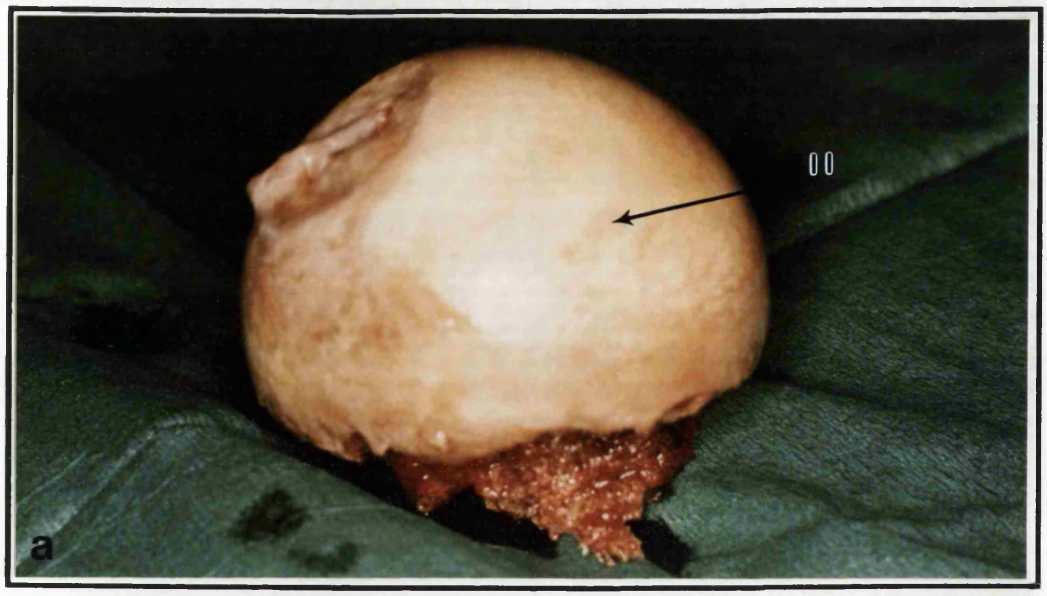
OD
a

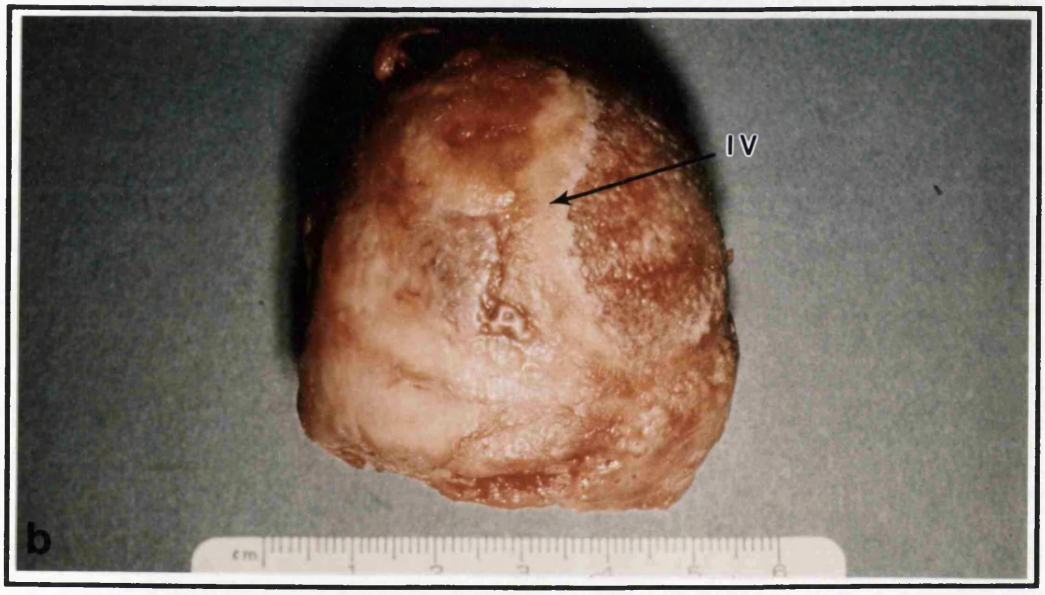
IV
b

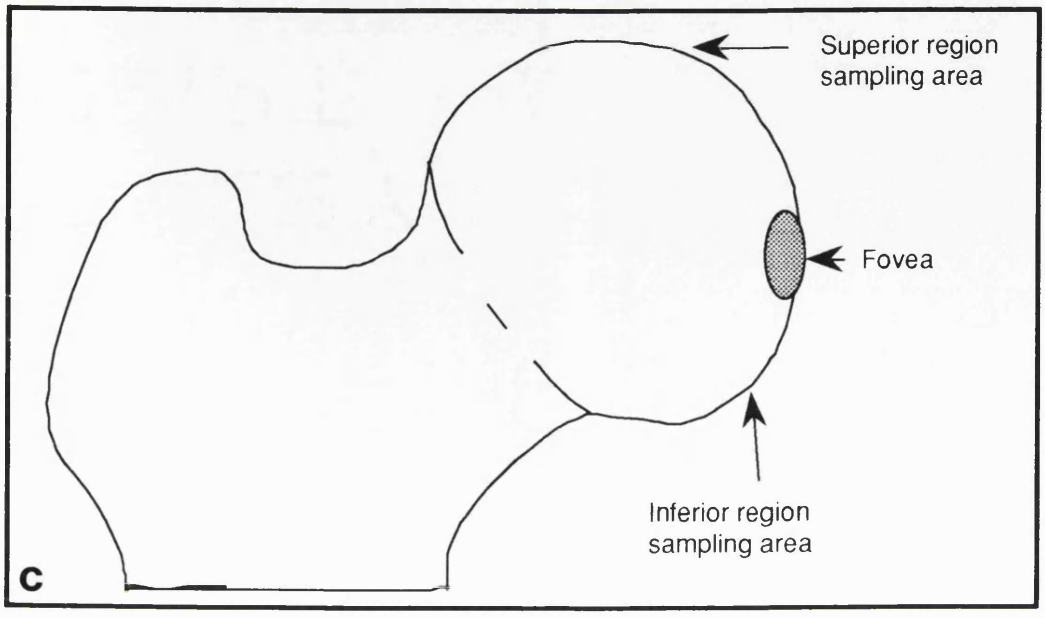
Superior region
sampling area
Fovea
Inferior region
sampling area
c

Fig. 1.3

Fig. 1.3a. Normal full depth femoral head articular cartilage (DT 89 years) stained with Ehrlichs haematoxylin and eosin. The articular surfaces appear smooth below which flattened superficial zone chondrocytes are present, in the tissue below this chondrocytes appear rounded. No evidence of crystal deposition is apparent in the matrix .

Fig. 1.3b. Full depth OA femoral head articular cartilage (AT 79 years) stained with Ehrlichs haematoxylin and eosin. The articular surface appears fibrillated (F) and chondrocytes appear clumped (C). No evidence of crystal deposition is apparent in the matrix .

a

b

Fig. 1.4

Fig. 1.4a. Normal femoral head superificial zone articular cartilage (DT 89 years) stained with the Alizarin Red stain for calcium. No positive stain for calcium is observed in this area.

Fig. 1.4b. Electron micrograph of superficial zone articular cartilage taken from an adjacent site to that shown in (a); crystals are clearly present in the ECM. Unstained section.

Fig. 1.4c. Full depth articular cartilage section, from which the detail shown in (a) is taken, stained with the Alizarin Red stain for calcium; the positive stain for calcium is clear in the subchondral bone (B).

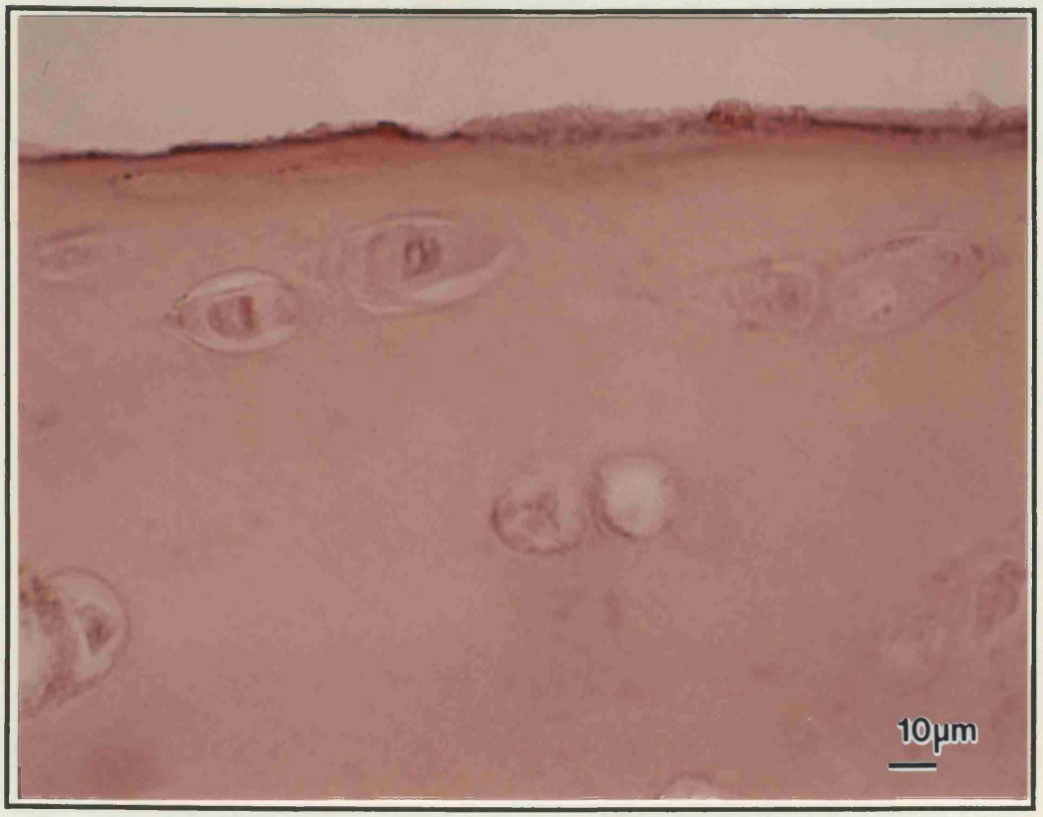

a

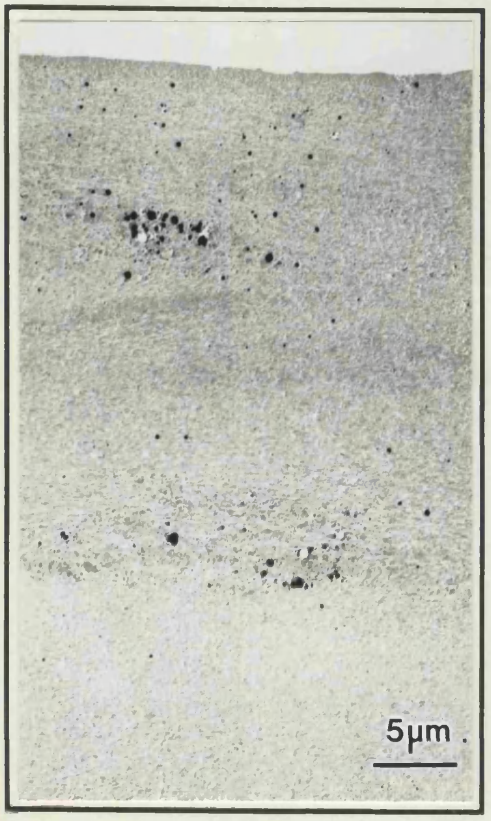

b

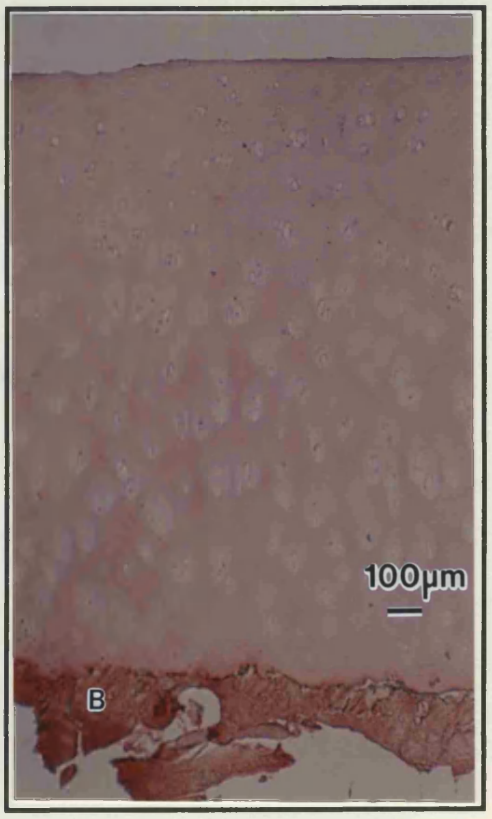

c

Fig.1.5

Fig. 1.5a. Typical morphology of a 'cuboid' crystal in femoral head articular cartilage matrix (JO 26 years). Section stained with uranyl acetate and lead citrate.

Fig. 1.5b. Distribution of crystals in superficial zone articular cartilage matrix (YA 16 years). Section stained with uranyl acetate and lead citrate.

Fig. 1,5c. Electron micrograph of an articular cartilage cryo-section, demonstrating a crystal in the ECM (KM 43 years). Section stained with uranyl acetate.

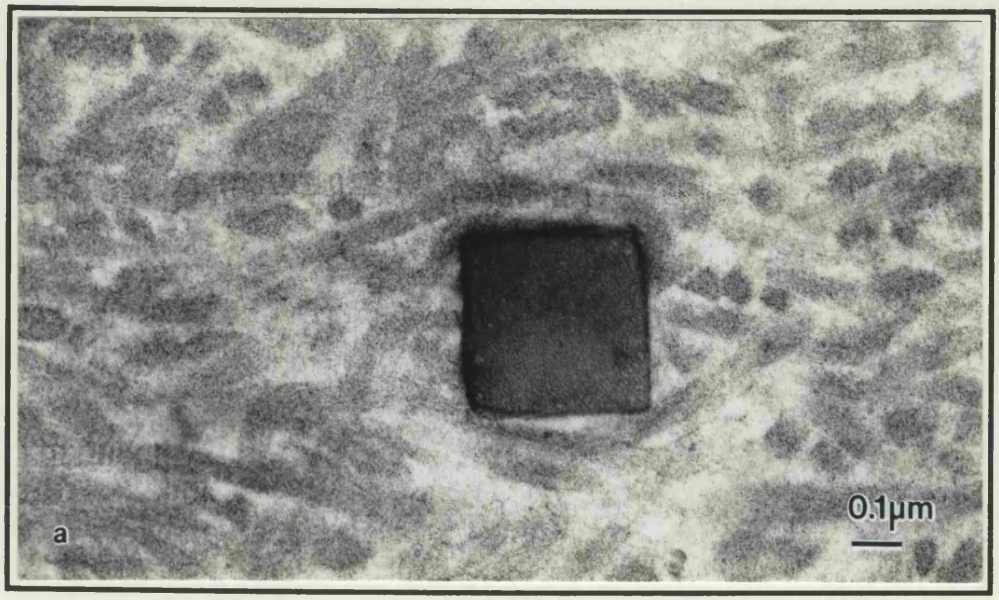
a
0.1μm

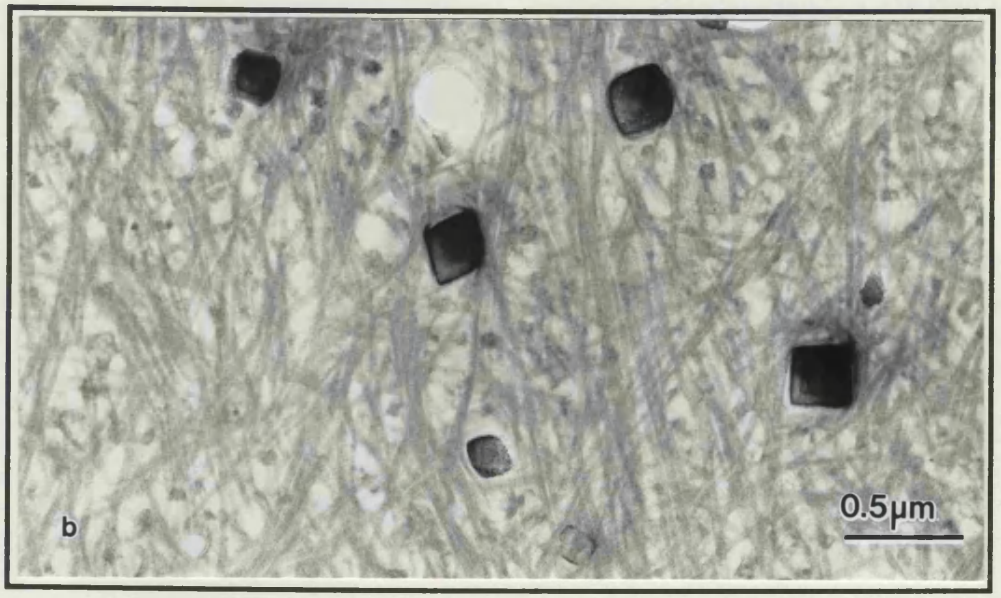
b
0.5μm

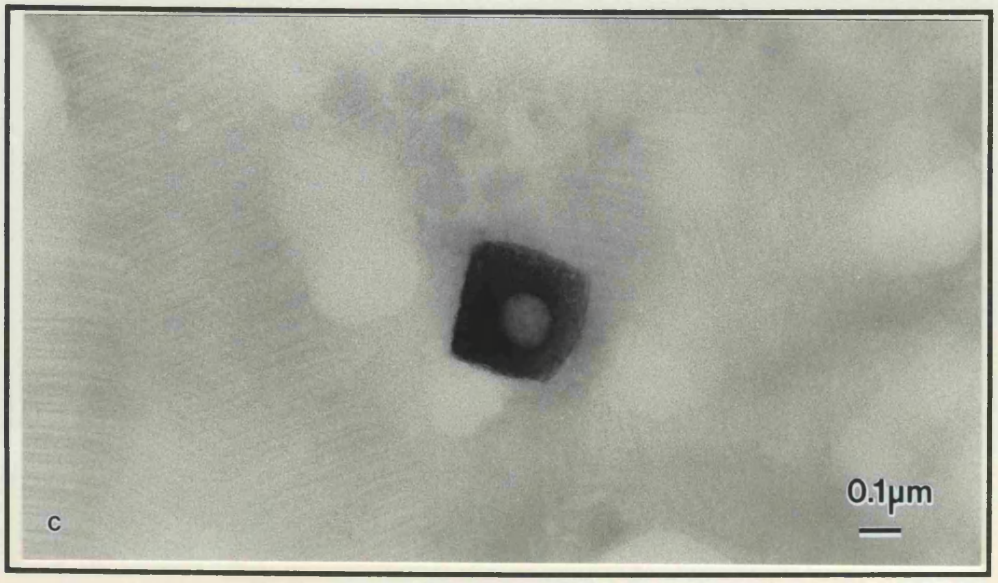
c
0.1μm

Fig. 1.6

Fig. 1.6a. Superficial zone of femoral head articular cartilage, processed using the anhydrous technique and observed unstained (JY 55 years). Crystals are distributed both as a band below the articular surface (A) and pericellularly. Unstained section.

Fig. 1.6b. Superficial zone of tissue adjacent to that of (a), but processed using the standard TEM protocol and observed unstained (JY 55 years). Crystals show a similar distribution to that observed in (a). Unstained section.

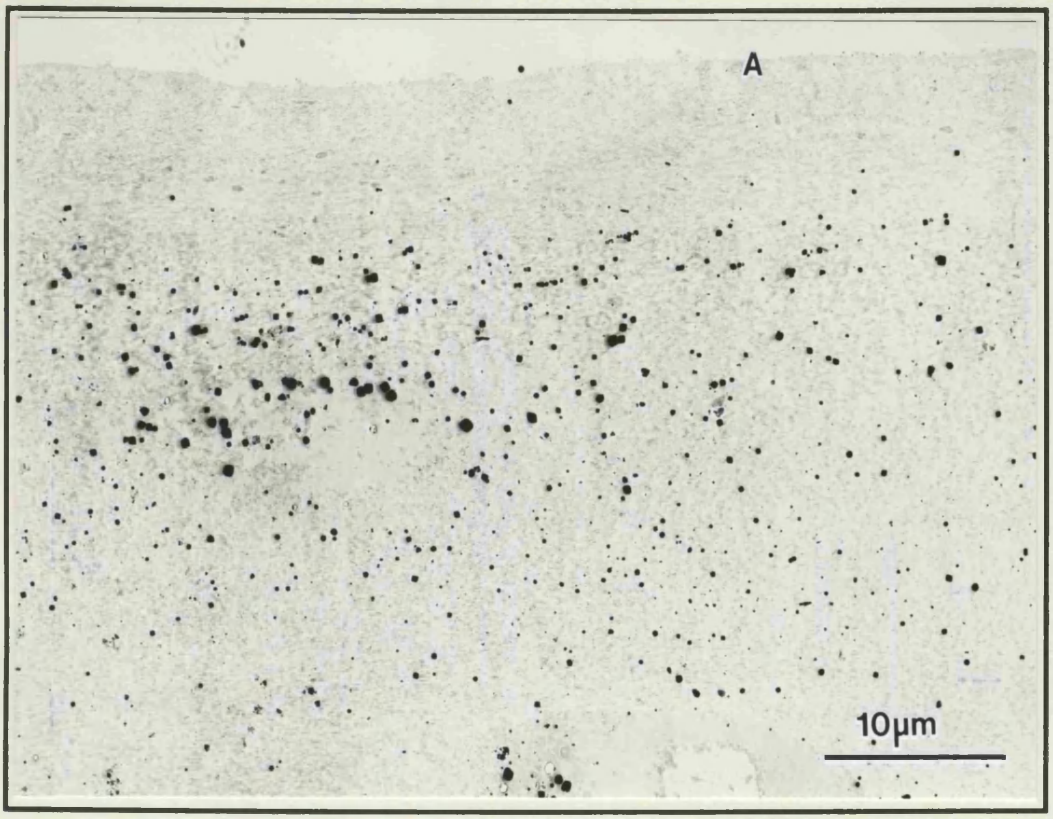

a

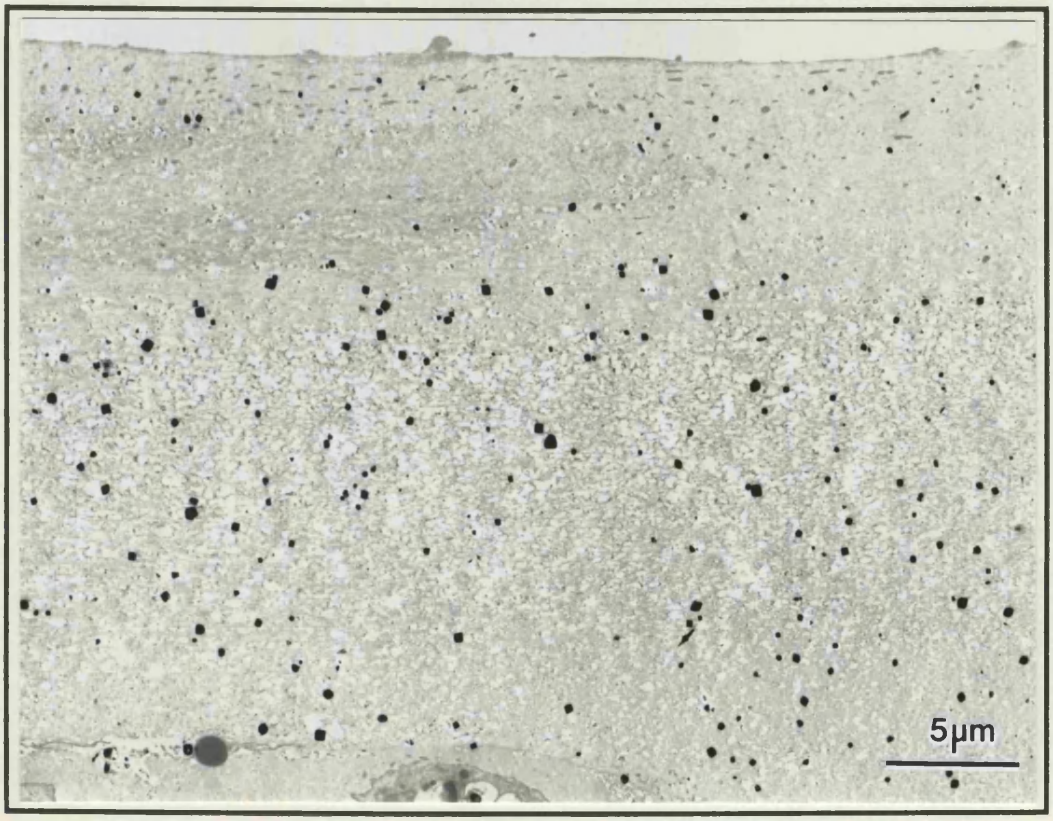

b

Fig. 1.6

Fig. 1.6c. Electron micrograph demonstrating the pericellular distribution of crystals in the superficial zone of articular cartilage, processed using the anhydrous technique (JY 55 years). Note the poor cellular preservation (C) compared to (d). Unstained section.

Fig. 1.6d. Electron micrograph demonstrating the pericellular distribution of crystals in the superficial zone of tissue adjacent to that of (c), but processed using the standard TEM protocol (JY 55 years). Note improved cellular preservation (C) and the similarity in crystal morphology and size range. Unstained section.

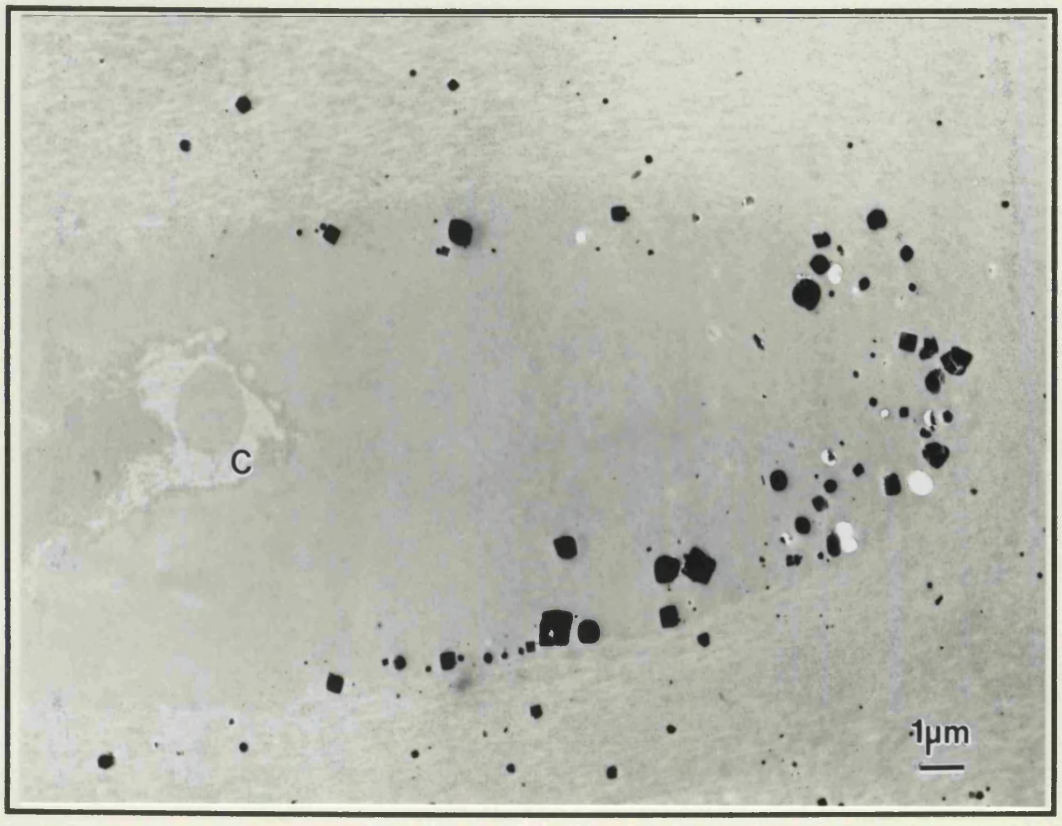

c

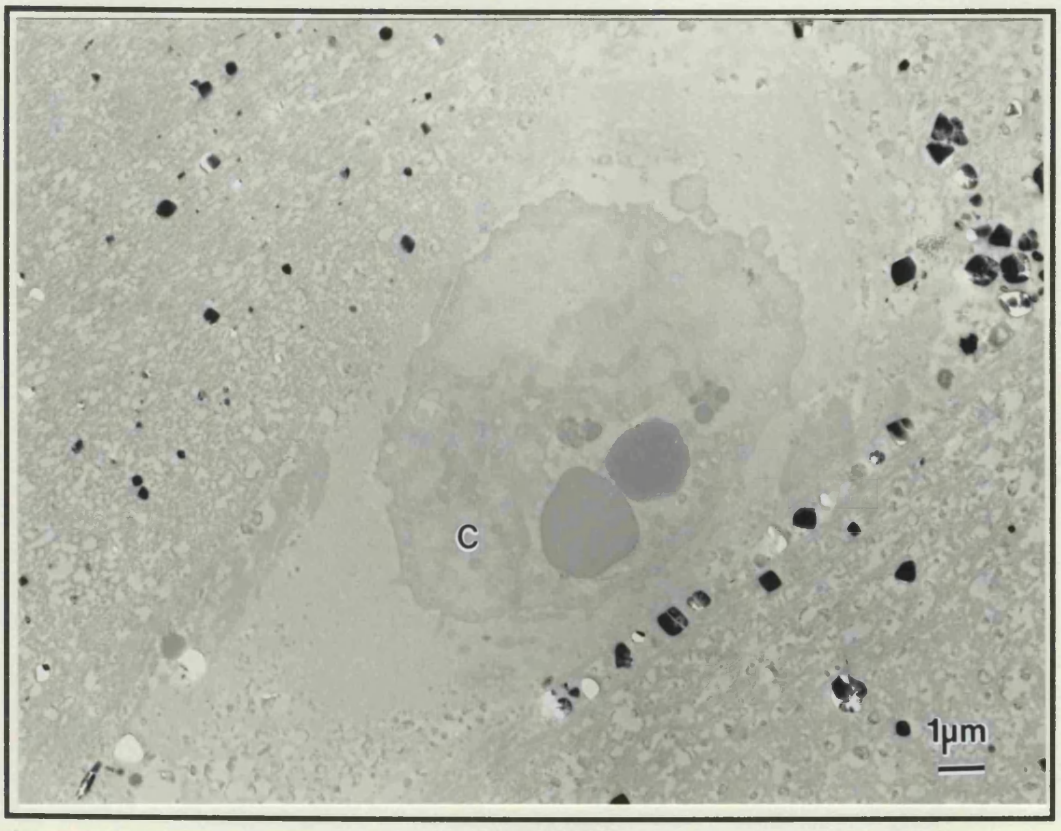

d

Fig. 1.7

Fig. 1.7a. Superficial zone of normal articular cartilage from the superior region of the femoral head, demonstrating a band of crystals below and parallel to the articular surface, crystals pericellular to chondrocytes and crystal deposition within necrotic chondrocyte debris (N) (KM 43 years). Note smooth articular surface (A). Unstained section.

Fig. 1.7b. Superficial zone of normal articular cartilage from the inferior region of the femoral head described in (a), demonstrating lesser crystal deposition than that observed in the superior region sample (a), (KM 43 years). Note smooth articular surface (A). Unstained section.

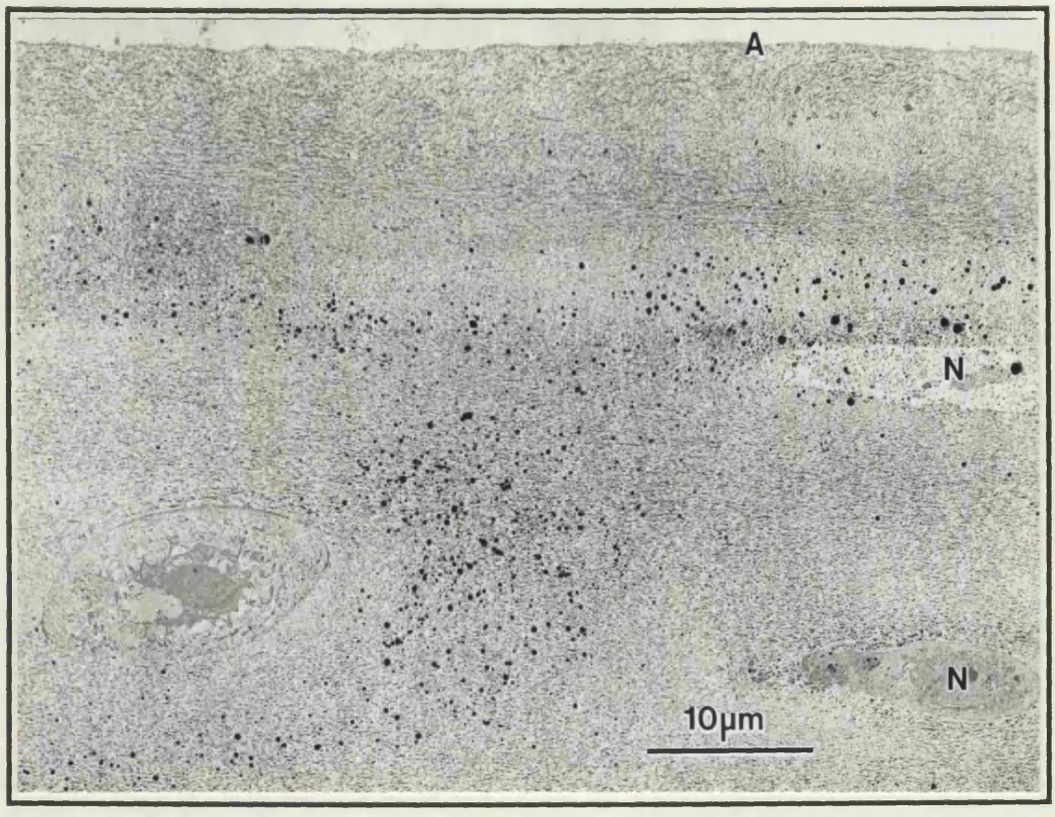

a

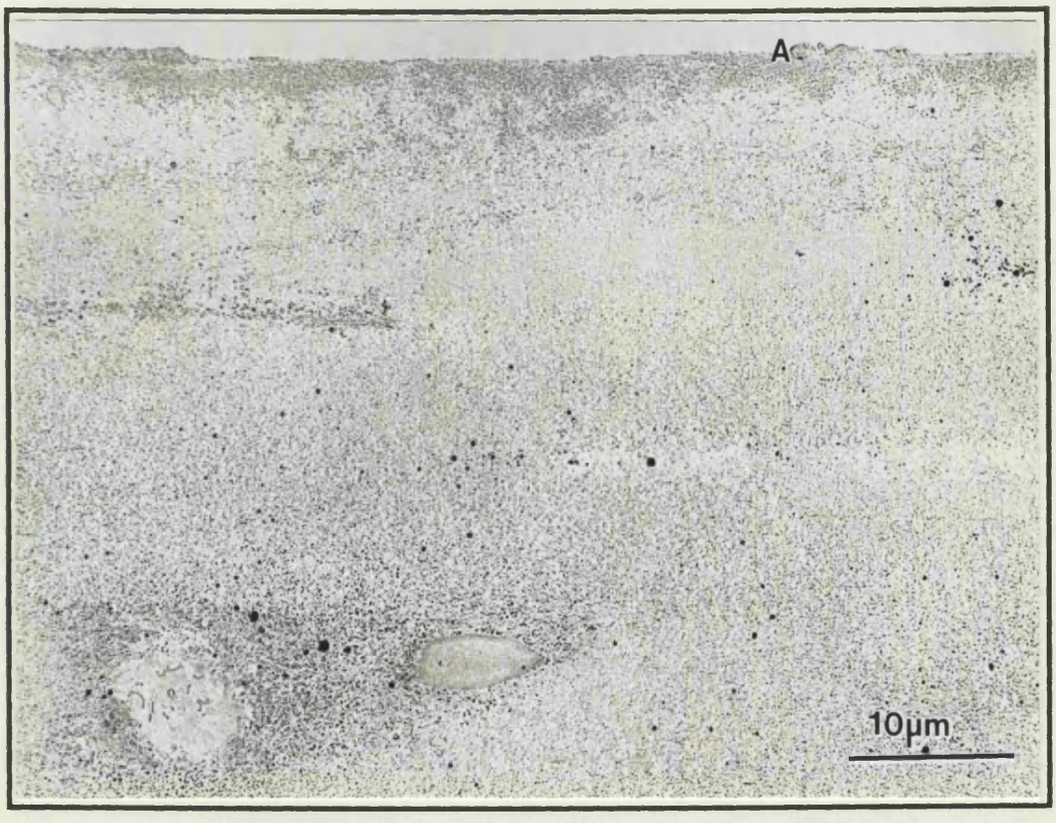

b

Fig. 1.8

Fig. 1.8a. Pericellular distribution of crystals in superficial zone, normal femoral head articular cartilage (JY 55 years). Unstained section.

Fig. 1.8b. Crystal (C) in the territorial matrix (T) of of a superficial zone chondrocyte of femoral condyle articular cartilage, within close proximity to cell processes (P) (PH 20 years). Section stained with uranyl acetate and lead citrate.

Fig. 1.8c. A defined clump of large crystals in superficial zone of normal femoral head articular cartilage, with a size and outline consistent with that of superficial zone chondrocytes (MS 84 years) (Arrow points to articular surface) Unstained section.

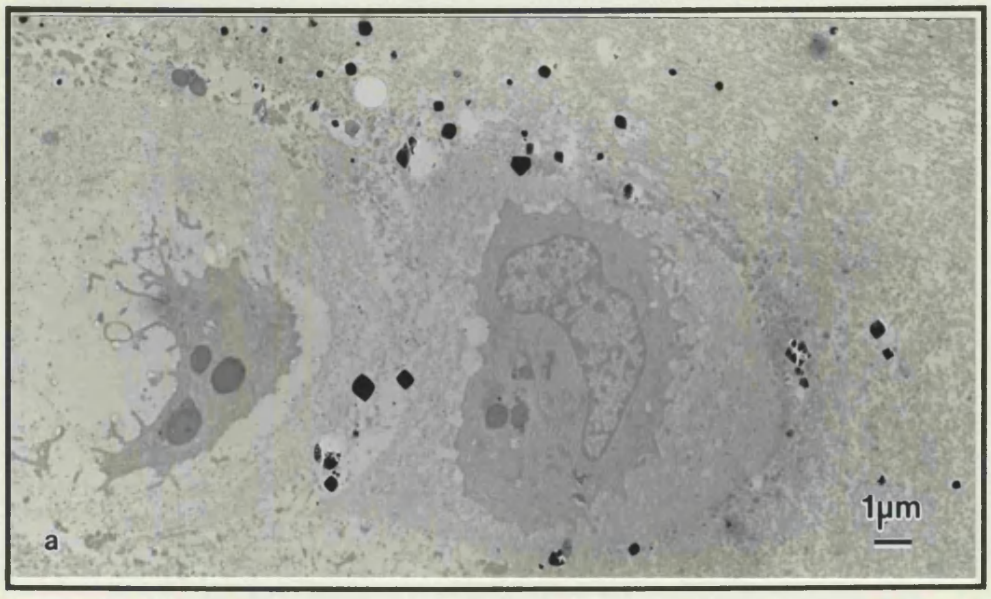
1µm
a

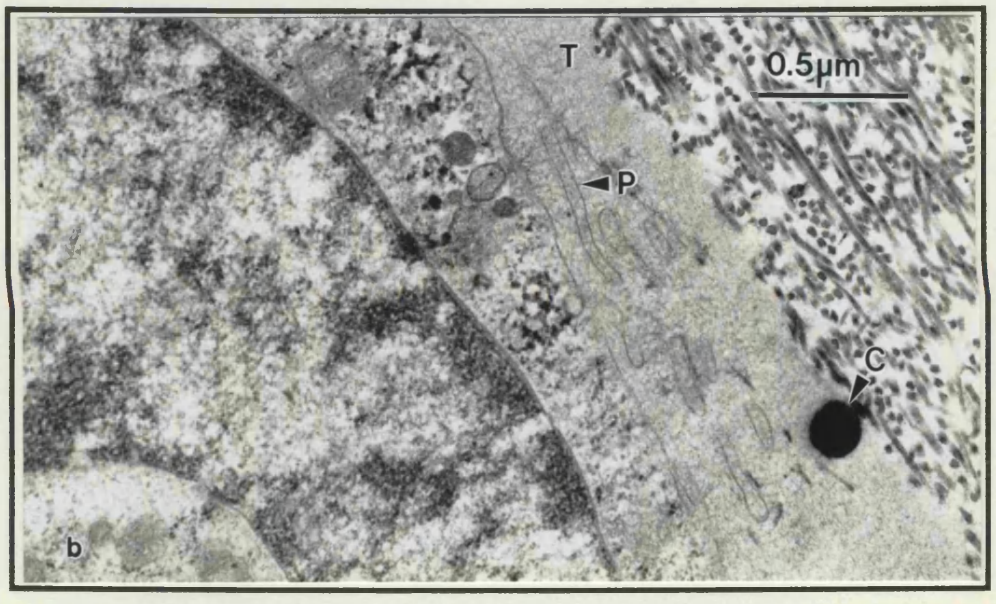
T
0.5µm
P
C
b

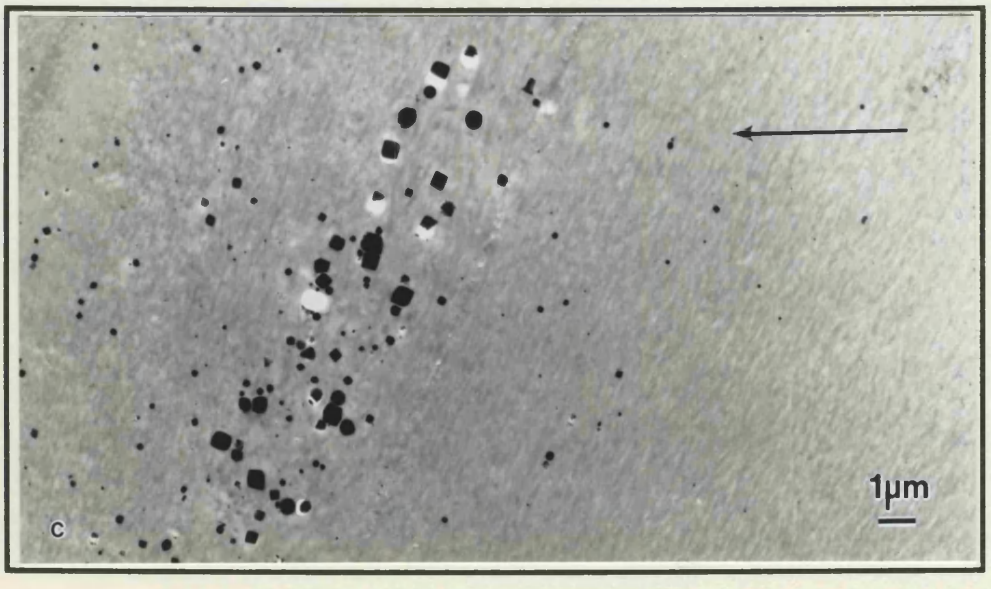
1µm
c

Fig. 1.8

Fig. 1.8d. Crystal (C) in close proximity to a superficial zone chondrocyte plasma membrane (M) and a cell process (P). A crystal is also present amongst pericellular membranous debris (D) (YA 16 years; Femoral head articular cartilage). Section stained with uranyl acetate and lead citrate.

Fig. 1.8e. Crystal deposition amongst intramatrical lipidic debris in the superficial zone of slightly fibrillated metatarsal articular cartilage. Note the range of crystal size exhibited (61 years). Unstained section.

Fig. 1.8f. Crystal deposition limited to a discrete region of pericellular intramatrical lipidic debris (D) within the superficial zone of normal articular cartilage (IB 19 years; distal ulna). Unstained section.

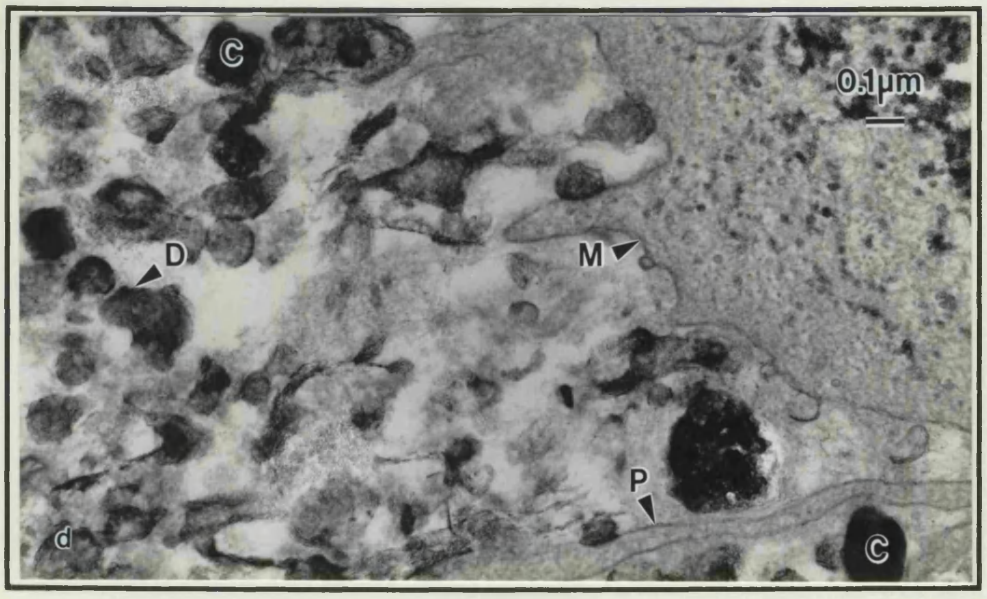
C
0.1μm
D
M
P
d
C

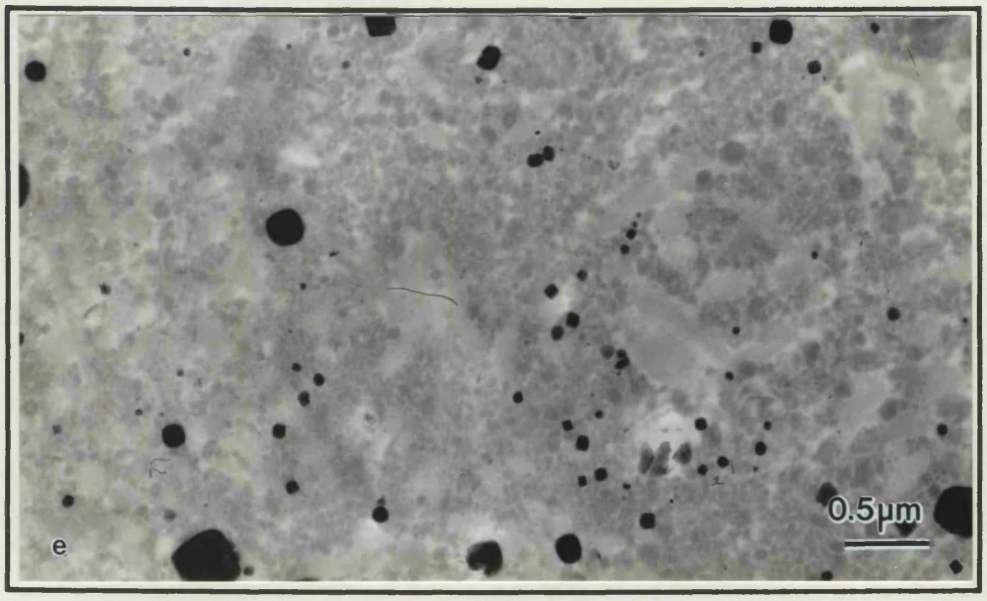
0.5μm
e

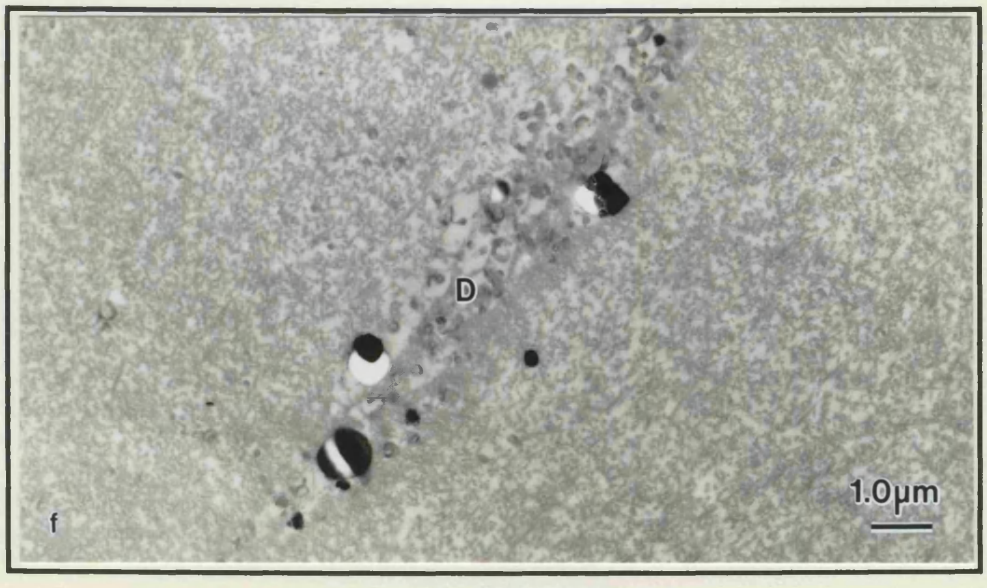
D
1.0μm
f

Fig. 1.9

Fig. 1.9a. Superficial zone chondrocyte in sagittal section, showing typical flattened appearance with apical crystal deposition (C) amongst lipidic debris (D) (YA 16 years; femoral head articular cartilage). Section stained with uranyl acetate and lead citrate.

Fig. 1.9b. Superficial zone chondrocyte from the same specimen as (a), in tangential section, showing discoid morphology and pericellular distribution of lipidic debris (D) with crystal deposition (C) (YA 16 years; femoral head articular cartilage). Section stained with uranyl acetate and lead citrate.

Fig. 1.9c. Tangential section of articular cartilage ECM taken immediately below the articular surface, demonstrating the band of crystal deposition present in this plane (YA 16 years; femoral head articular cartilage). Section stained with uranyl acetate and lead citrate.


C
D
1μm
a

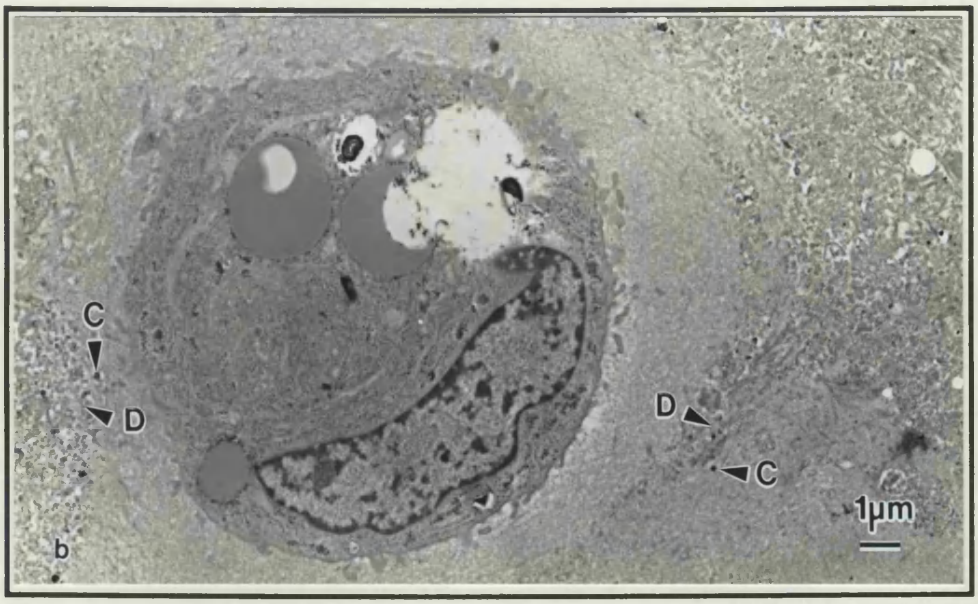
C
D
D
C
1μm
b

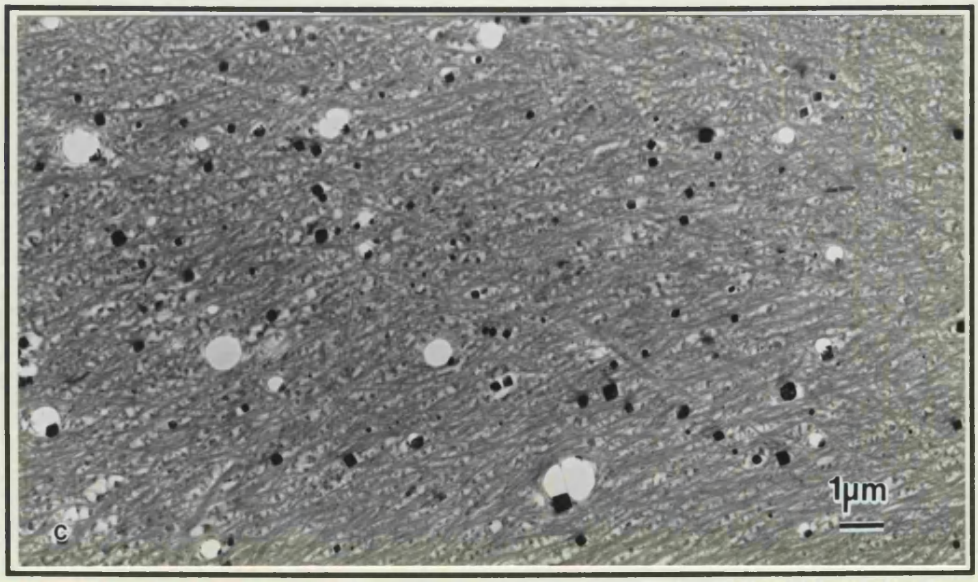
1μm
c

Fig. 1.10

Fig. 1.10a. Necrotic chondrocyte debris (D) in the intermediate zone of normal femoral head articular cartilage. Crystals (C) are apparent amongst the chondrocyte debris, whilst the surrounding ECM is free from such deposition (KM 43 years). Unstained section.

Fig. 1.10b. A necrotic chondrocyte (N) from the superficial zone of fibrillated, femoral head articular cartilage. Crystals (C) are present within or immediately adjacent to the cell outline (IP 46 years). Section stained with uranyl acetate and lead citrate.

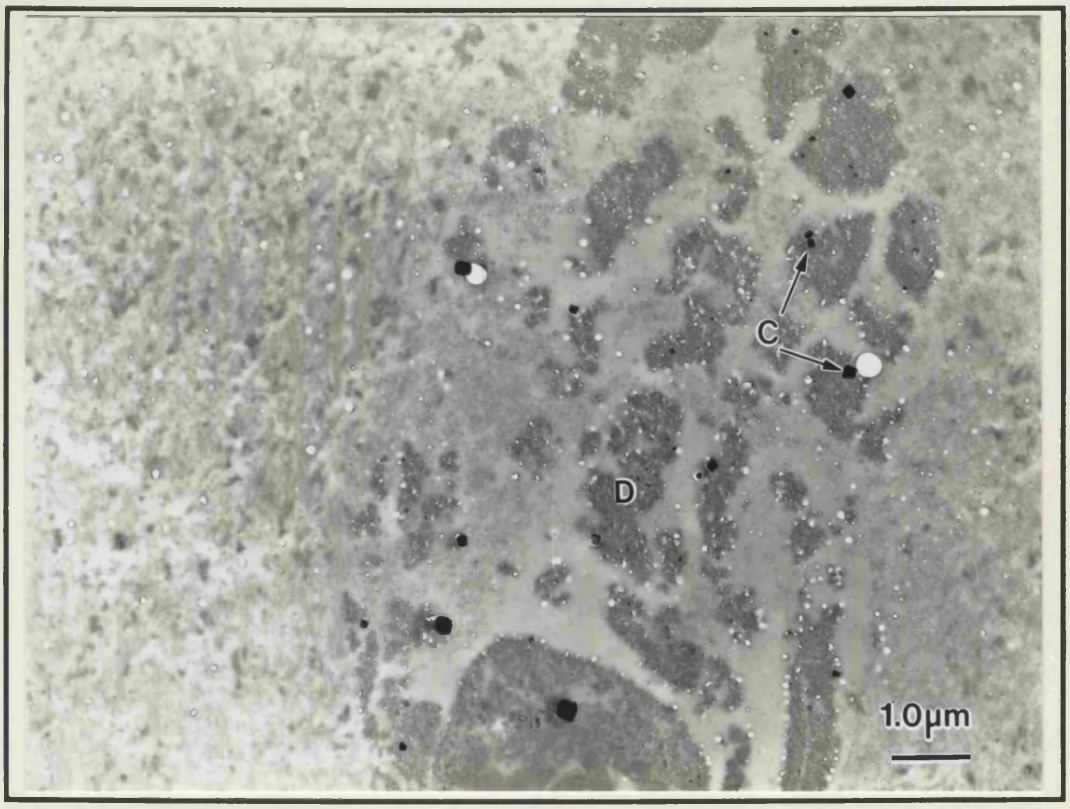

a

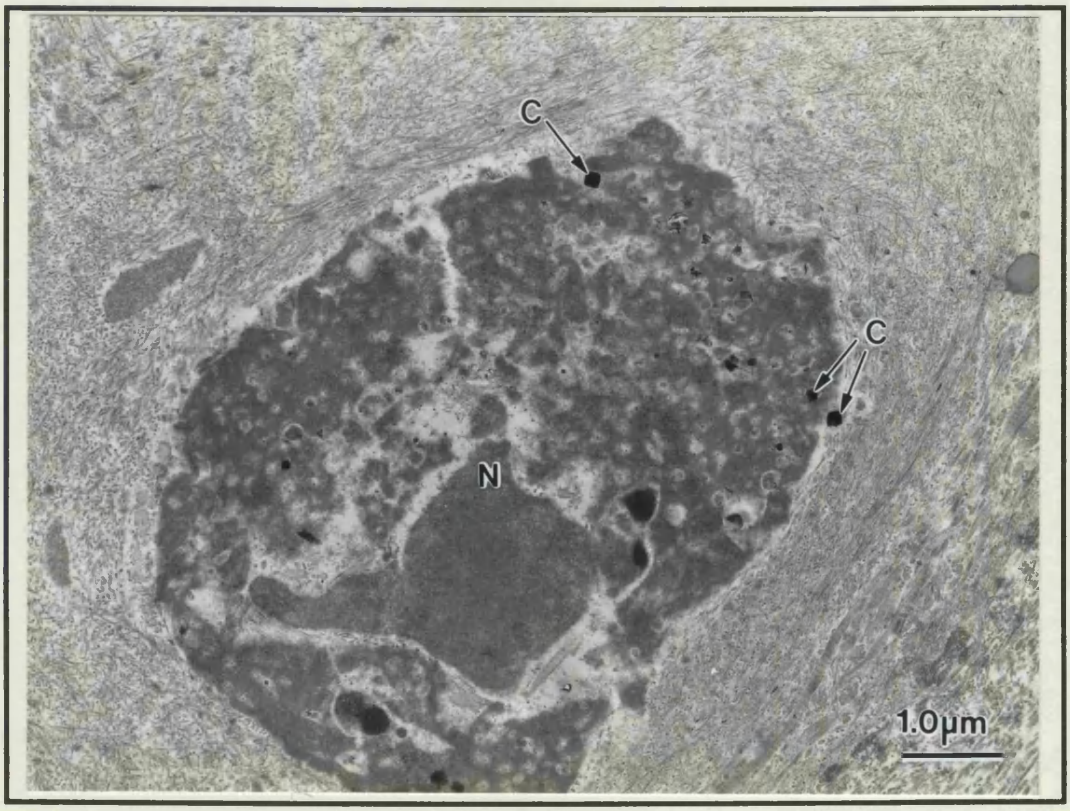

b

Fig. 1.11

Fig. 1.11a. Perilacunar lipidic debris (D) in the mid zone of femoral head, articular cartilage. Crystal deposition (C) is present amongst the debris (SS 84 years). Unstained section.

Fig. 1.11b. Cuboid crystal depostion (C) amongst hypertrophic chondrocyte debris (H); in close proximity to initial apatitic mineral nodules (A) associated with the articular cartilage calcification front (62 years; femoral head articular cartilage). Unstained section.

Fig. 1.11c. The most superficial tissue from fibrillated articular cartilage taken from an OA femoral head specimen. Fibrous tissue (F) is seen above articular cartilage ECM (A); crystals (C) are present within this ECM, although no crystals are present above the junction (arrow) of these matrices(EB 70 years). Unstained section.

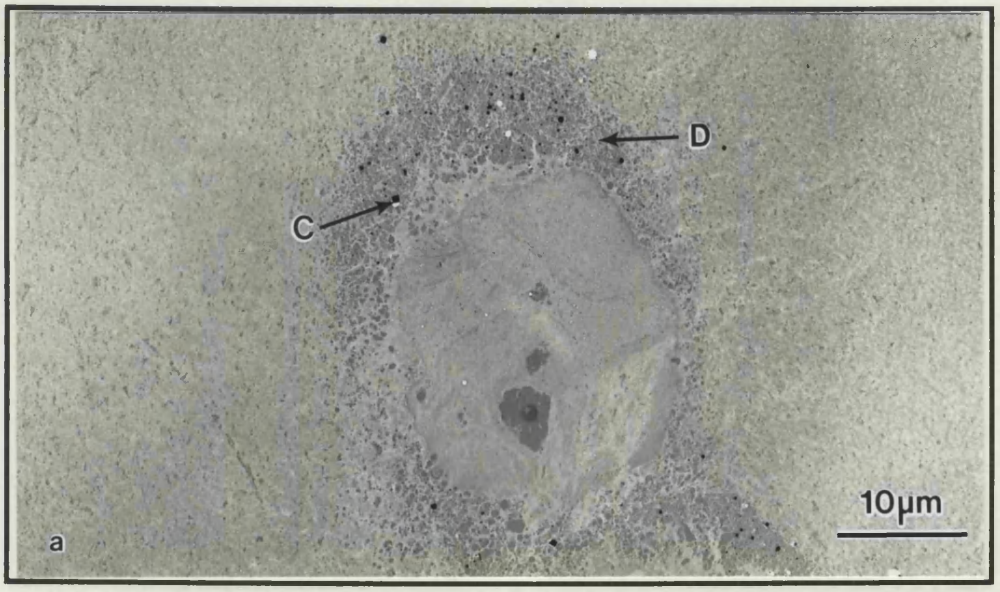
D
C
10µm
a

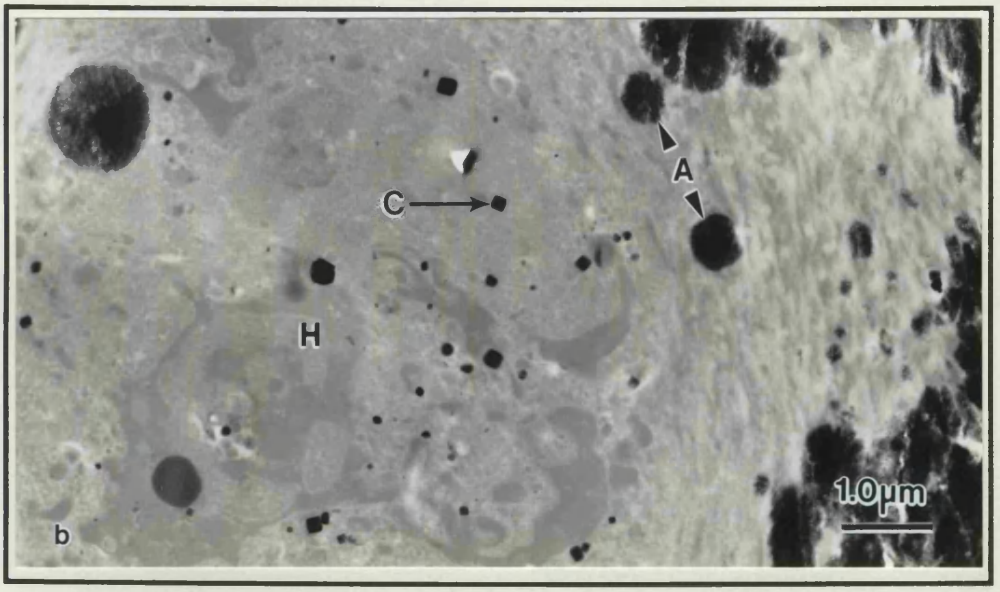
A
C
H
1.0µm
b


C
F
A
1µm
c

Fig. 1.12

Fig. 1.12a. Normal articular cartilage stained with toluidine blue, showing a smooth articular surface and individual or paired chondrocytes distributed within the ECM (VB 17 years; metatarsal).

Fig. 1.12b. Chondrocytes from the intermediate zone of normal metatarsal articular cartilage showing a pericellular ECM with very little intramatrical lipidic debris (D) and no pericellular crystal deposition (C) (VB 17 years). Section stained with uranyl acetate and lead citrate.

Fig. 1.12c. Articular cartilage stained with Humphrey's stain, showing a fibrillated surface and clusters of chondrocytes (arrow) within the ECM (61 years; metatarsal).

Fig. 1.12d. A chondrocyte from the intermediate zone of fibrillated articular cartilage demonstrating abundant pericellular intramatrical lipidic debris (D) containing crystal deposition (C) (61 years; metatarsal). Unstained section.

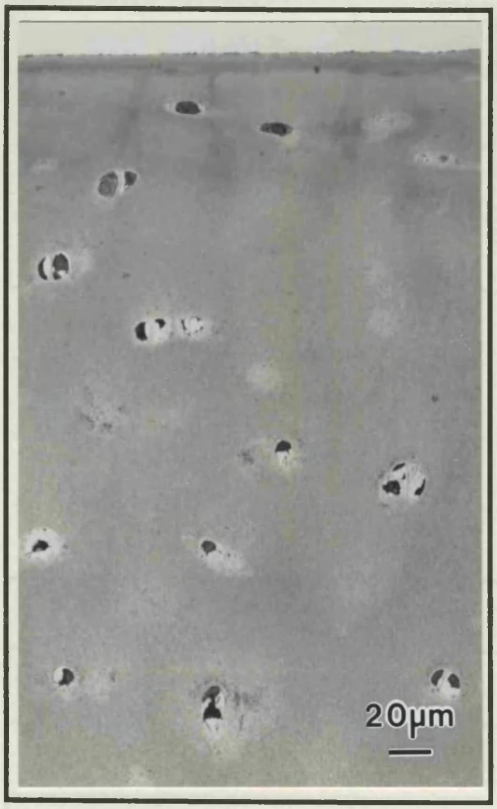

a

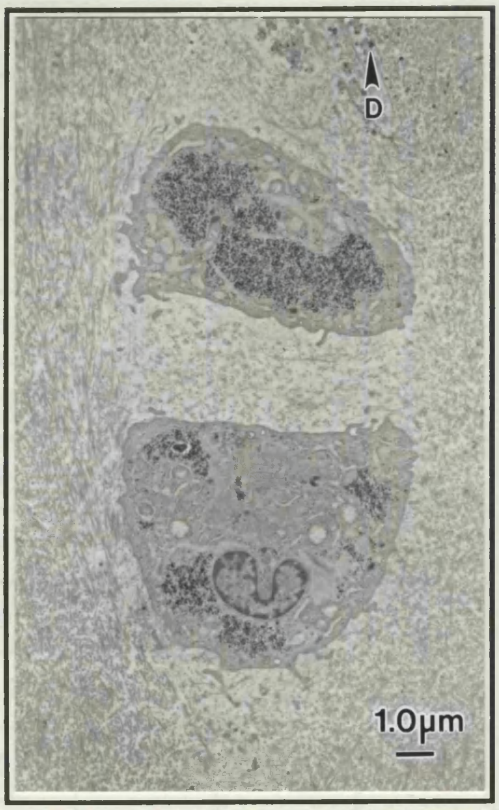

b

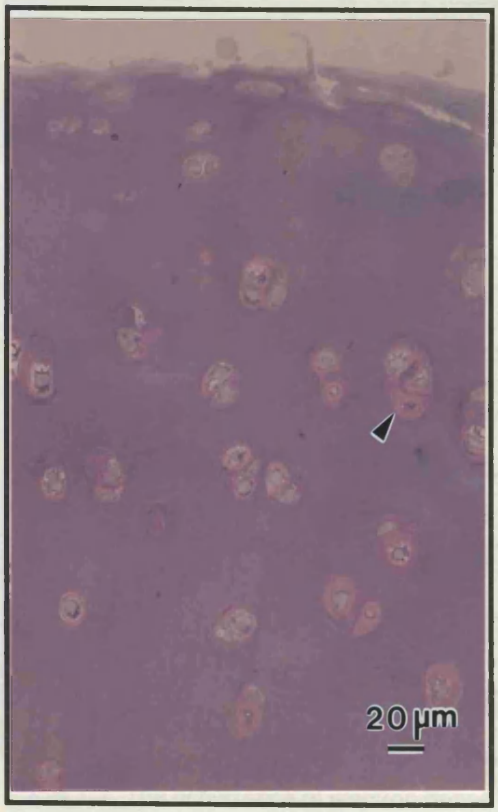

c

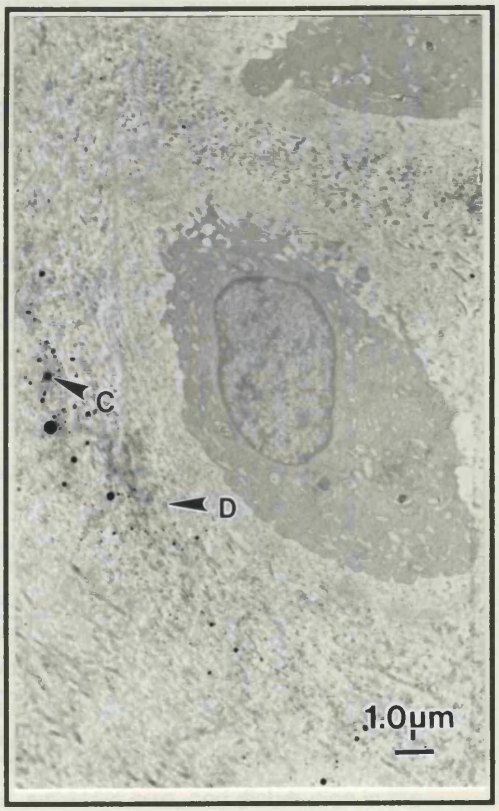

d

Sample site	Sample no.	Age range	Sex ratio:M/F	Crystals present	Crystals not observed
Femoral Head (Normal)	34	10 - 93	14/20	34	-
Femoral Head (OA)	26	46 - 83	8/18	26	-
F. H.* Peripheral Osteophyte	5	53 - 73	3/2	-	5
Femoral Condyle	3	5 - 20	2/1	3	-
Tibial Plateau	2	19 - 20	2/0	2	-
Radial Head	1	19	1/0	1	-
Proximal Ulna	1	19	1/0	1	-
Distal Radius	1	19	1/0	1	-
1st Metatarsal	2	17 - 61	1/1	2	-
Carpal	1	19	1/0	1	-
2nd Metacarpal	2	19 - 62	2/0	2	-
Lunate	2	19 - 62	2/0	2	-
Phalanges	1	17	0/1	1	-
Epiphyseal Growth Plate	1	9	1/0	-	1

*Femoral Head

Table 1.1. The range of sample sites from which full depth articular cartilage specimens were taken for this study. The number of specimens obtained from each site listed are given with the age ranges and male to female ratios for each case. The extent of 'cuboid' crystal deposition across this range is indicated on a simple presence/ not observed basis as determined by TEM As a part of the sampling procedure specimens were taken from what was considered to be weight bearing regions of each sample site where appropriate.

Species and sample site	Age	Observation
Porcine Femoral Head	20 wks.	Electron dense bodies associated with matrix debris similar in distribution to 'cuboid' crystals.
Lapine Femoral Head	20mths.	Small elctron dense bodies associated with matrix debris similar in distribution to cuboid crystals.
Bovine Metacarpal	18mths.	No electron dense bodies comparable to 'cuboid' crystals observed.

Table 1.2. The occurrence of electron dense bodies, similar in size, and distribution in the matrix, to 'cuboid' crystals described in human articular cartilage, in the superfical zone of articular cartilage from species other than human.

Fig. 1.13

Fig. 1.13a. Femoral condyle articular cartilage stained with toluidine blue (LM), with crystal deposition in the superficial zone ECM demonstrated by TEM (EM); (PH 20 years). Section stained with uranyl acetate and lead citrate.

Fig. 1.13b. Tibial plateau articular cartilage stained with toluidine blue (LM), with crystal deposition in the superficial zone ECM demonstrated by TEM (EM); (TD 19 years). Unstained section.

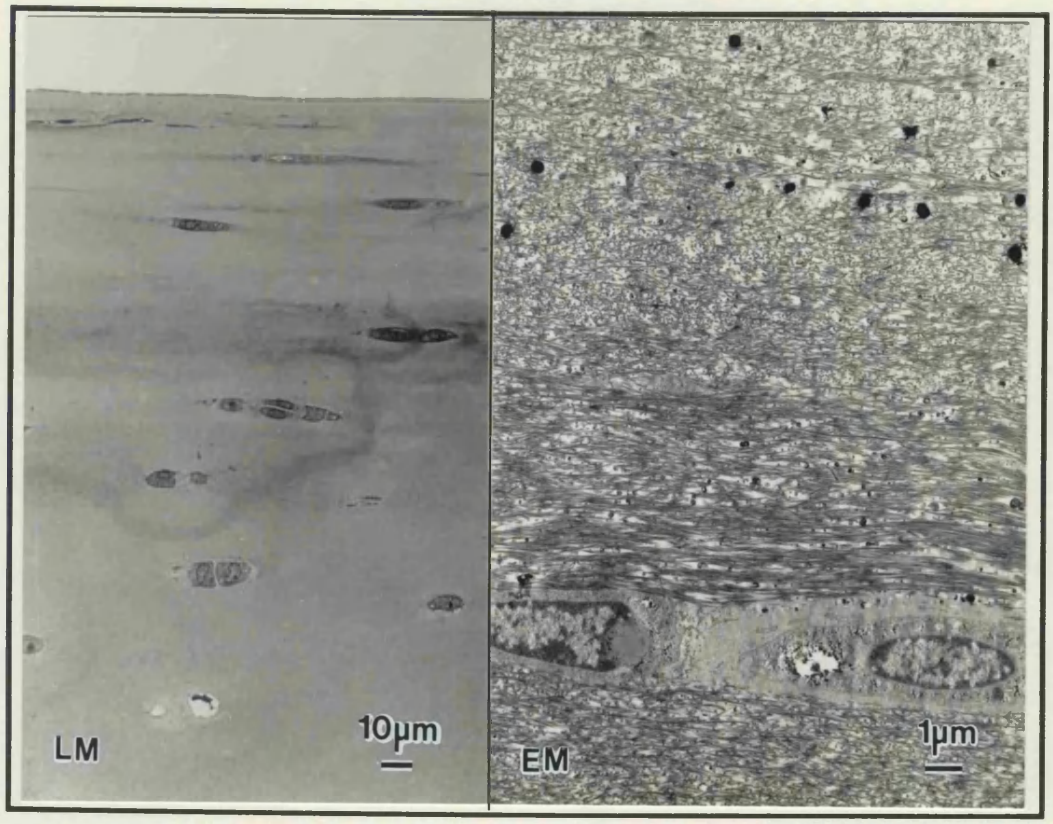

a

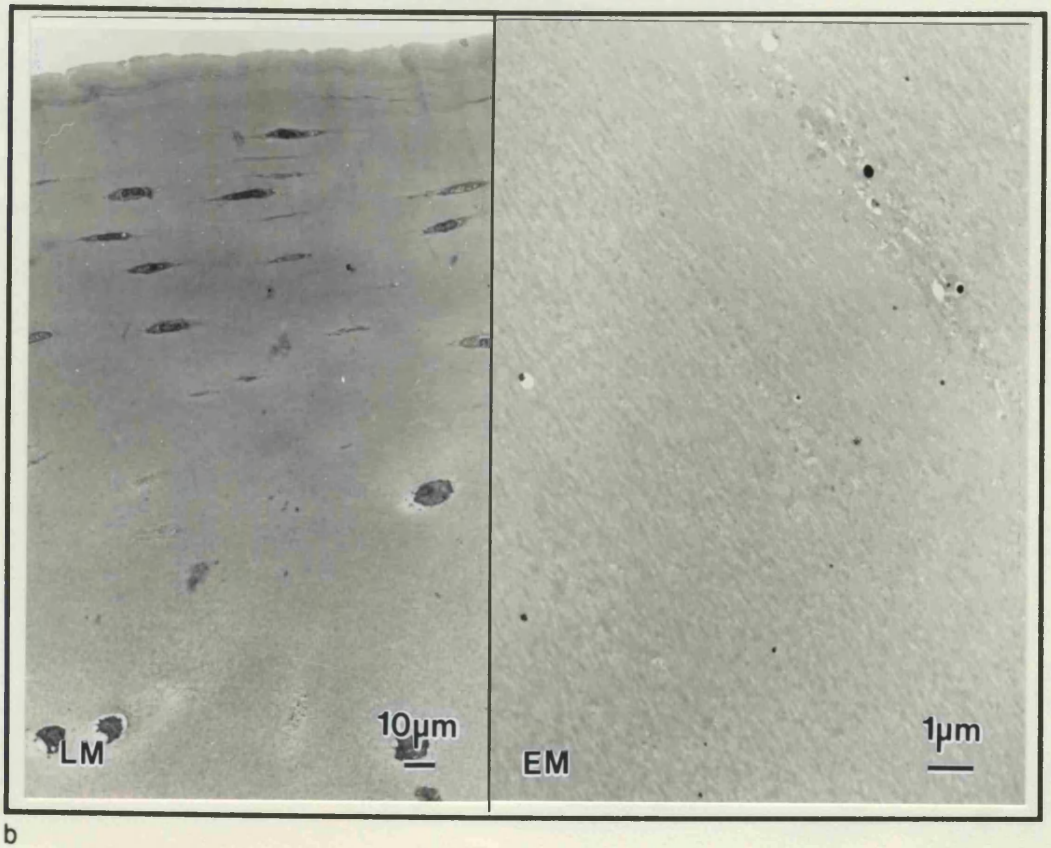

b

Fig. 1.13

Fig. 1.13c. Radial head articular cartilage stained with toluidine blue (LM), with crystal deposition in the superficial zone ECM demonstrated by TEM (EM); (IB 19 years). Unstained section.

Fig. 1.13d. Proximal ulna articular cartilage stained with toluidine blue (LM), with crystal deposition in the superficial zone ECM demonstrated by TEM (EM); (IB 19 years). Unstained section.

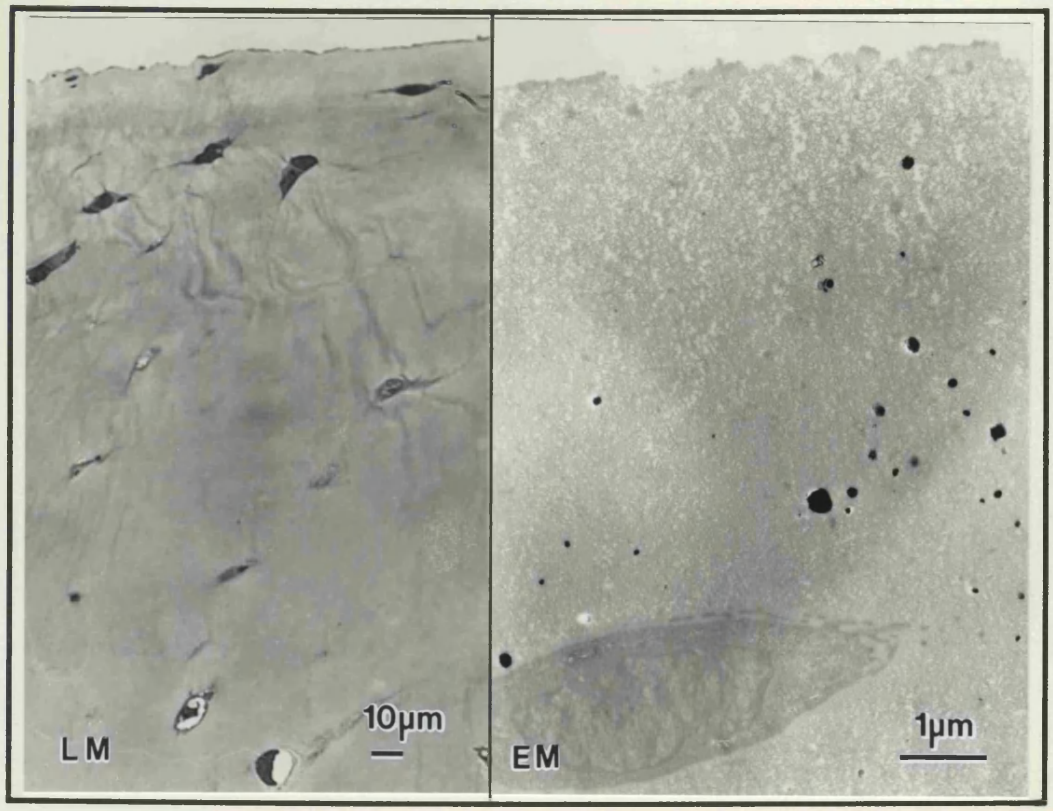

c

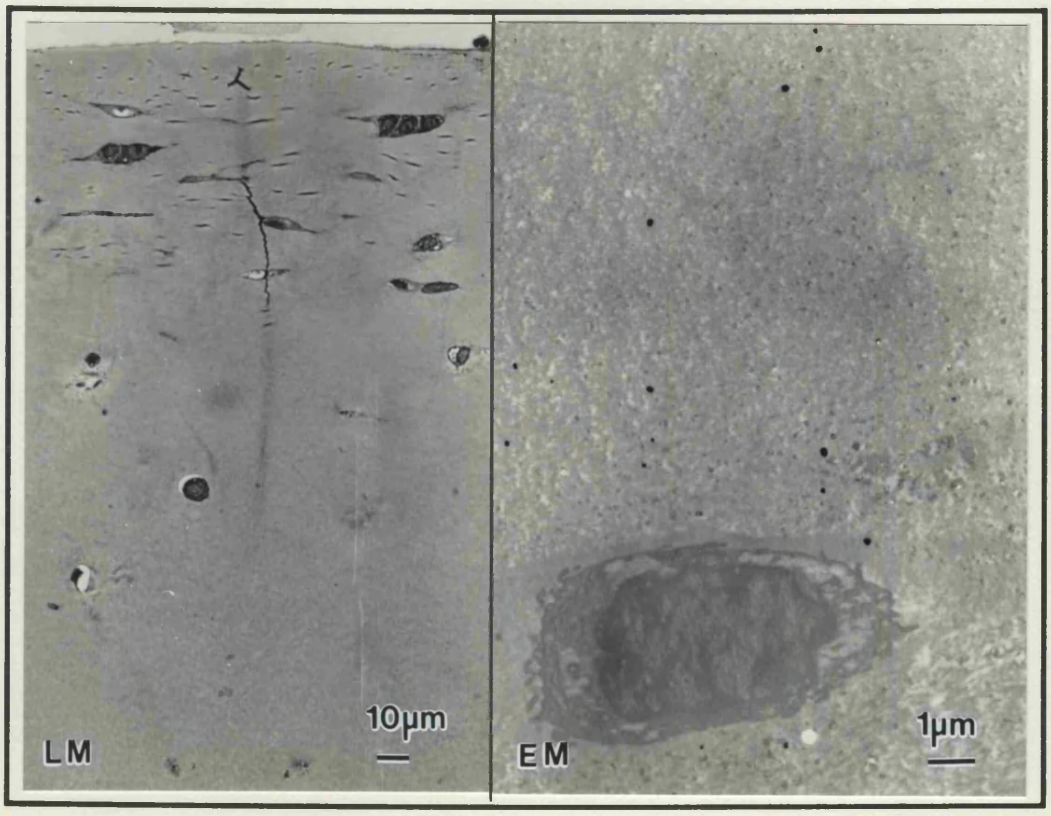

d

Fig. 1.13

Fig. 1.13e. Metacarpal articular cartilage stained with toluidine blue (LM), with crystal deposition in the superficial zone ECM demonstrated by TEM (EM); (IB 19 years). Unstained section.

Fig. 1.13f. Phalangeal articular cartilage stained with toluidine blue (LM), with crystal deposition in the superficial zone ECM demonstrated by TEM (EM); (VB 17 years). Unstained section.

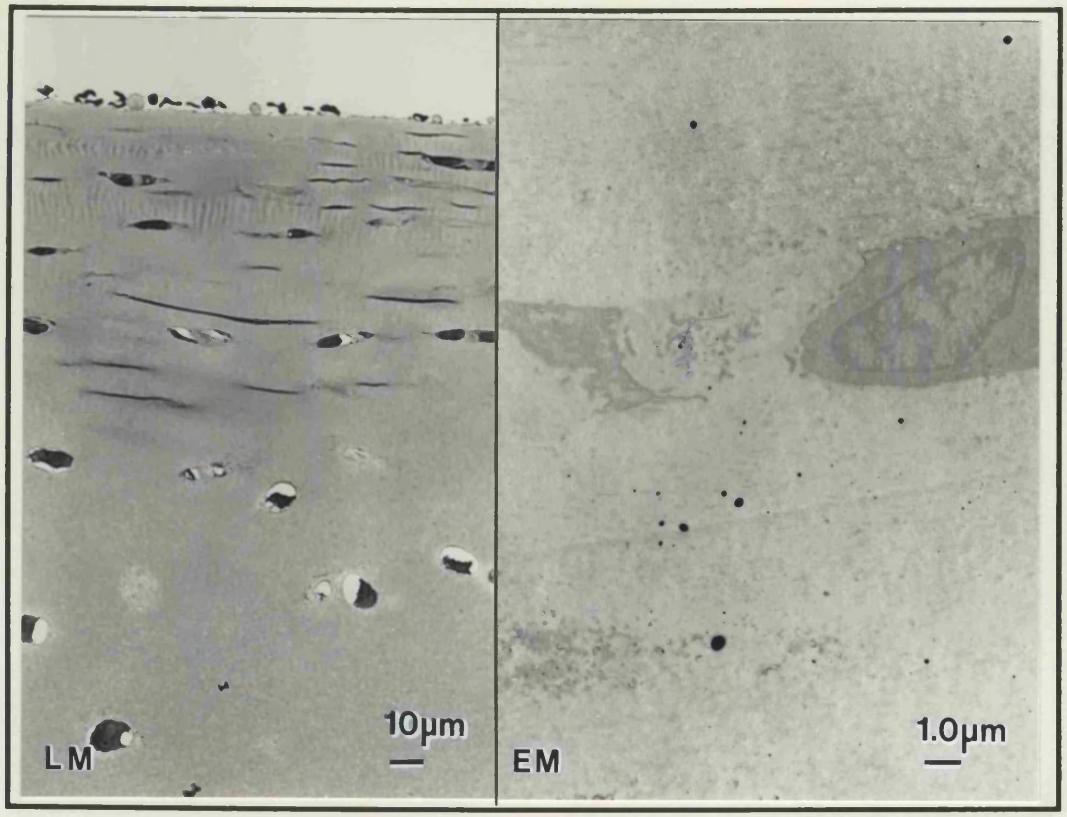

e

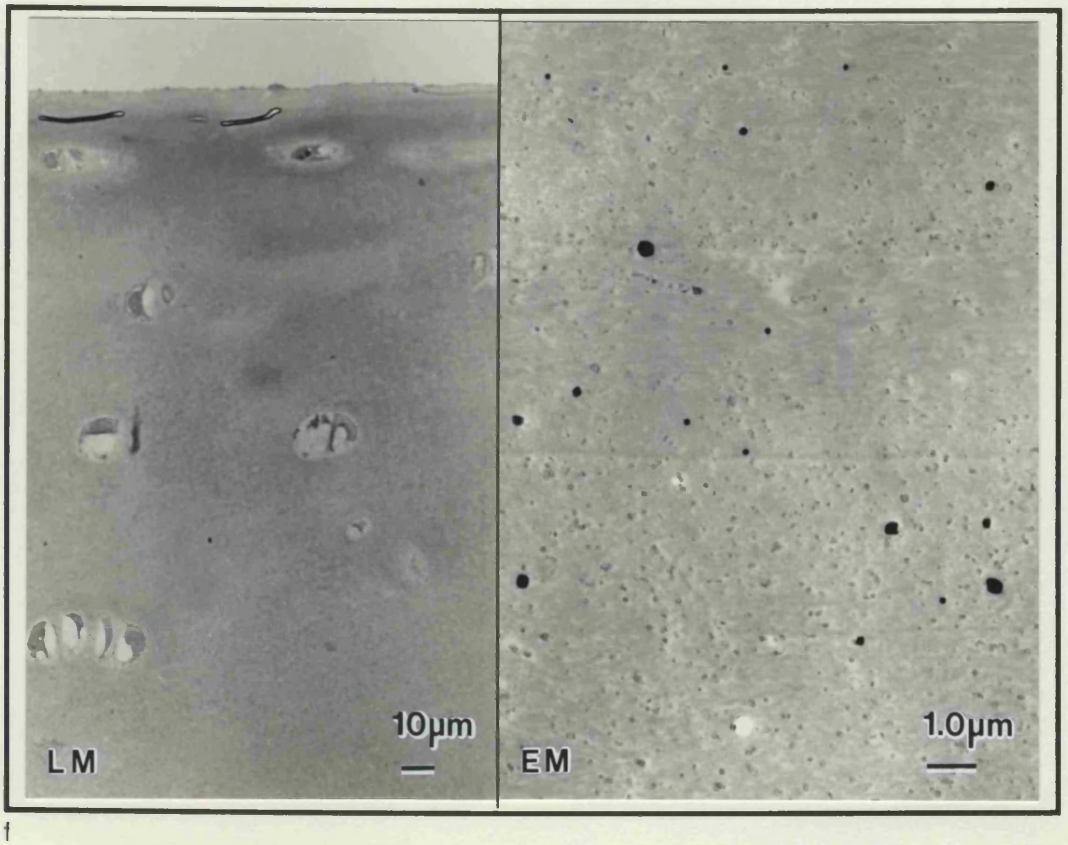

f

Fig. 1.14

Fig. 1.14a Porcine articular cartilage: superficial zone ECM, showing intramatrical lipidic debris (D) and mineral deposition (M) (20 weeks, femoral head).

Fig. 1.14b. Mineral deposition (M) amongst lipidic debris (D) in the ECM of porcine, femoral head, articular cartilage (20 weeks, femoral head).

Fig. 1.14c. Lapine articular cartilage: superficial zone ECM, showing intramatrical lipidic debris (D) (20 months, femoral head).

Fig. 1.14d. Mineral deposition (M) in close proximity to superficial zone, lapine chondrocyte (C) (20 months, femoral head).

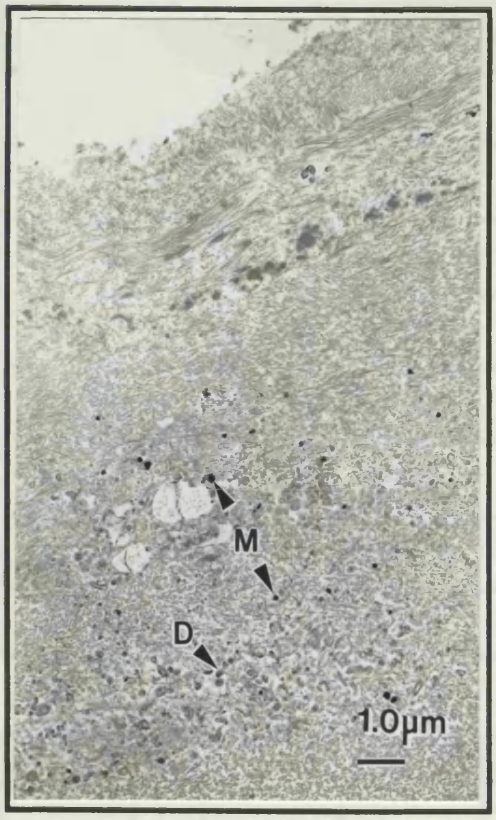

a

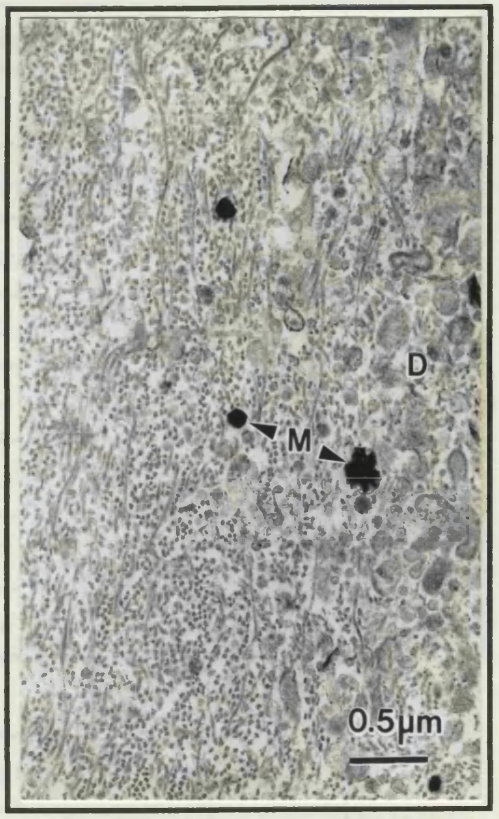

b

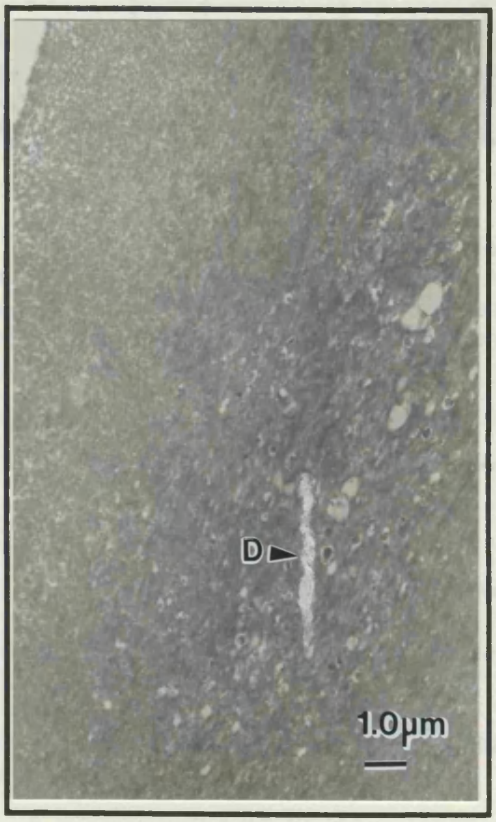

c

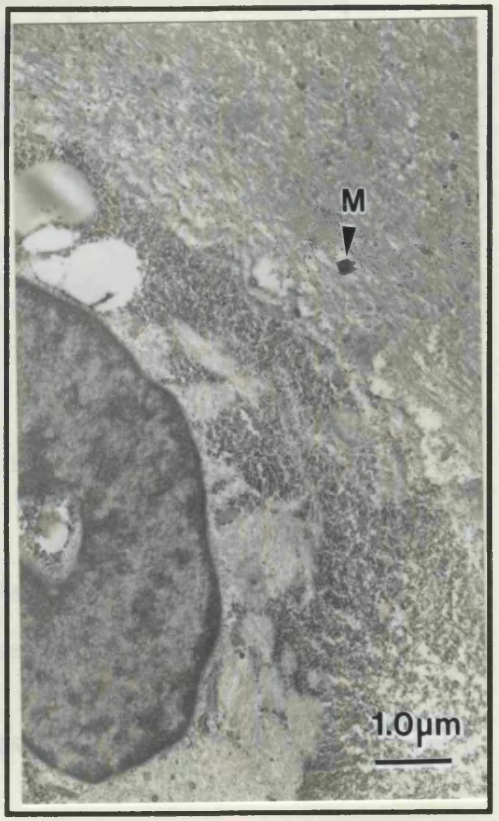

d

Patient	Sex	Age	resection for	Superior	Anterior	Posterior	Inferior
MC	F	12	Tumour	4	3	3	0
YA	M	16	Tumour	4	3	3	1
YH	F	20	Tumour	3	4	3	1
TB	F	23	Tumour	3	2	2	1
KM	M	43	Tumour	4	2	3	2
RH	M	47	Tumour	2	-	-	-
CL	M	81	Fracture	3	3	3	1
MS	F	84	Fracture	4	3	3	1

Patient	Sex	Age	resection for	Sloping zone	FD Cartilage	Osteophyte
MB	M	53	OA	-	2	0
CB	F	68	OA	1	1	0
GM	M	72	OA	0	2	0
RL	F	73	OA	0	1	0

Table 1.3. Distribution of crystal deposition density in normal and OA femoral head articular cartilage indicated by a qualitative grading *. Normal femoral head cartilage was sampled from superior, anterior, posterior and inferior regions: OA femoral head cartilage was sampled from the 'sloping zone' adjacent to the eburnated region, original full depth cartilage and peripheral osteophyte.

*Criteria for qualitative grading of crystal deposition density:

0. Crystals not observed.

1. At least one crystal observed, searching necessary.

2. Crystals present in a diffuse distribution, no apparent pattern, regular encounters, extensive searchnig not necessary.

3. Crystal present in localised groupings, generally pericellular to chondrocytes plus a diffuse intermittent band.

4. Crystals effectively form a continuous band, running parallel with and immediately below the articular surface; local patchiness may be observed in the band at higher magnifications.

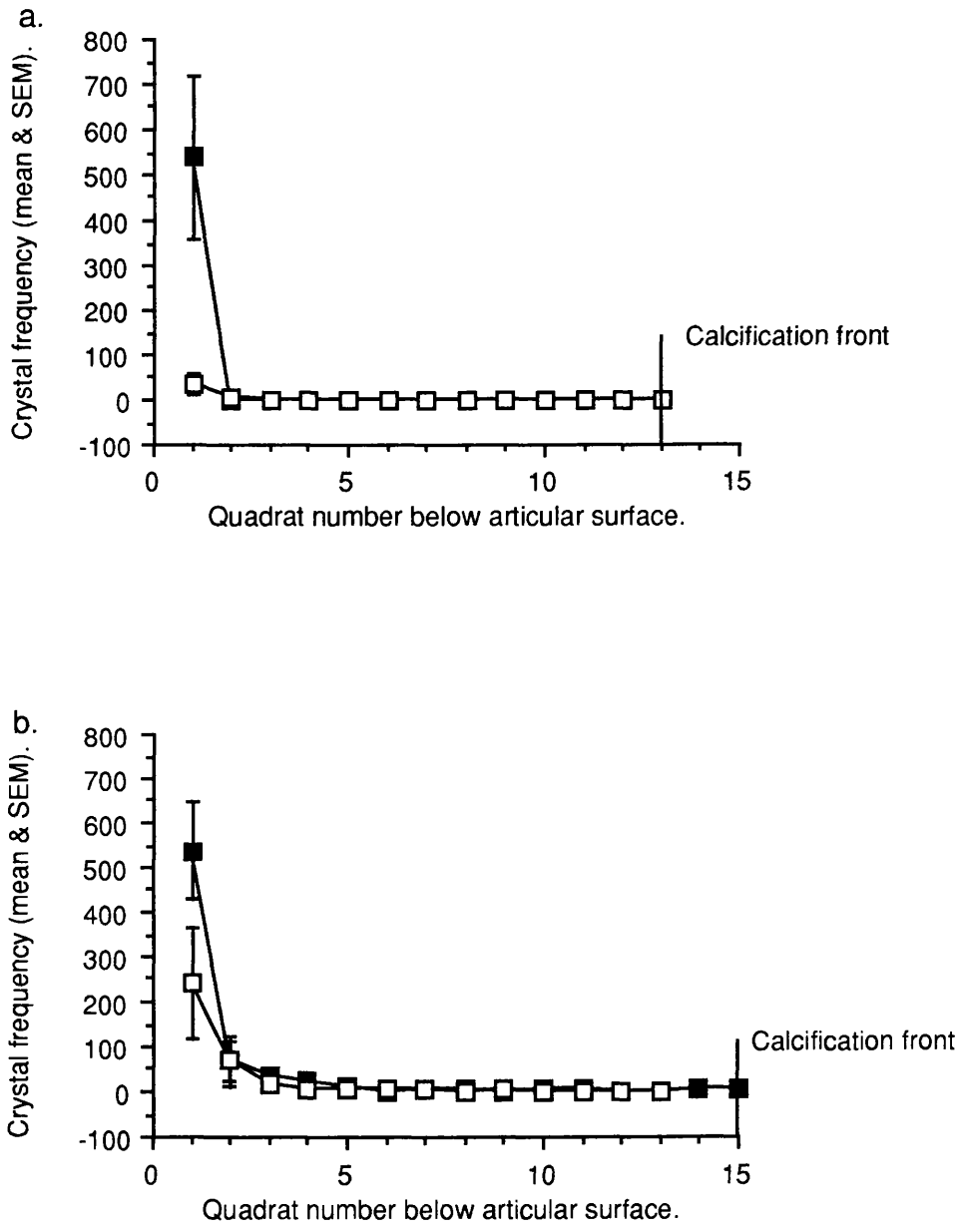

Fig. 1.15. Profiles of crystal distribution throughout the full depth of, superior region (■) and inferior region (□) femoral head articular cartilage from (a) 10-25 year and (b) 75-90 year specimens. The sampling quadrat dimensions were 115μm x 115μm: n=3 for both groups.

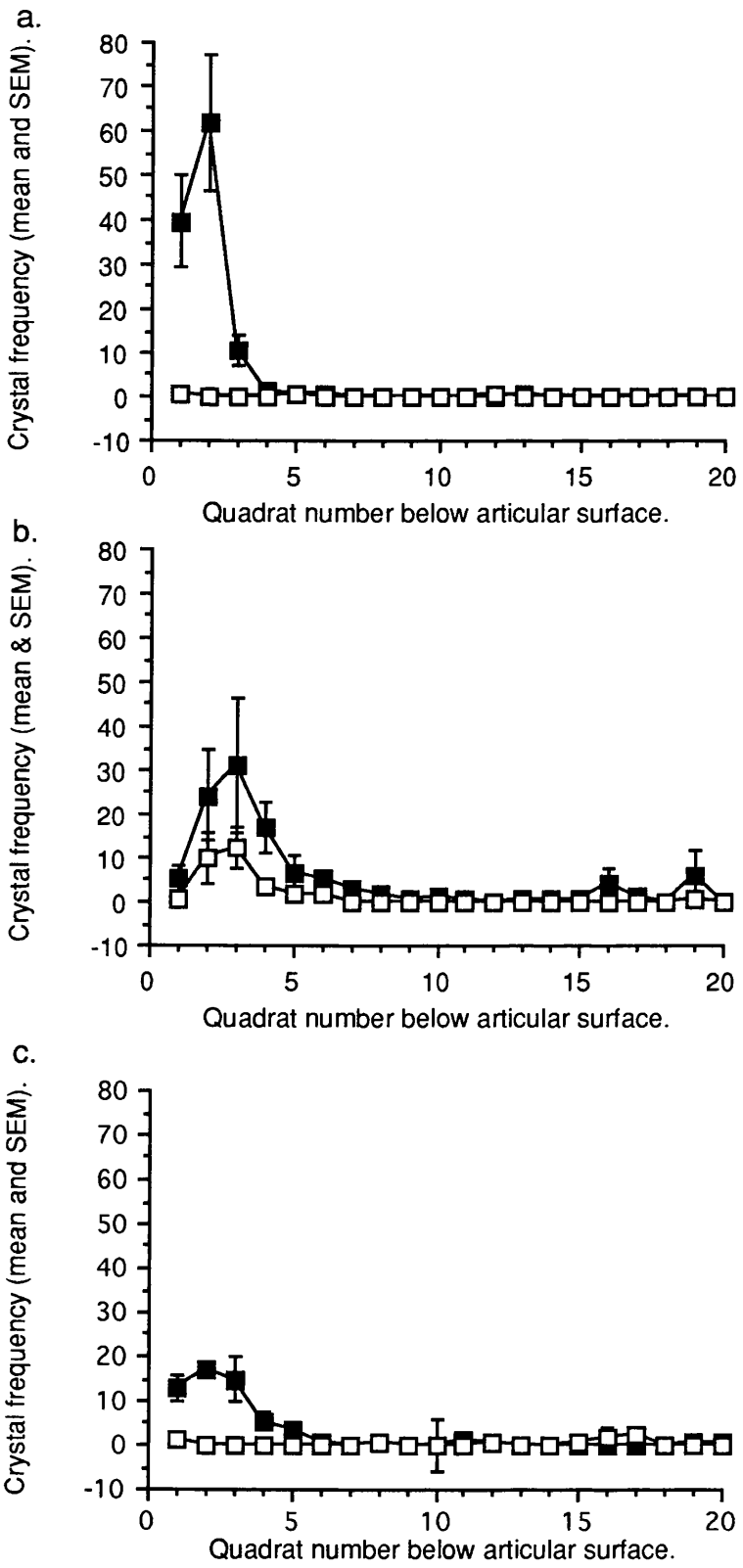

Fig. 1.16. Semi quantitative depth profile of crystal distribution in the superficial zone, superior region (■) and inferior region (□) femoral head articular cartilage for 3 specimens; (a) 16 years, (b) 43 years, (c) 81 years. The sampling quadrat dimensions were10.2μm x 7.4μm, with the long axis perpendicular to the articular surface.

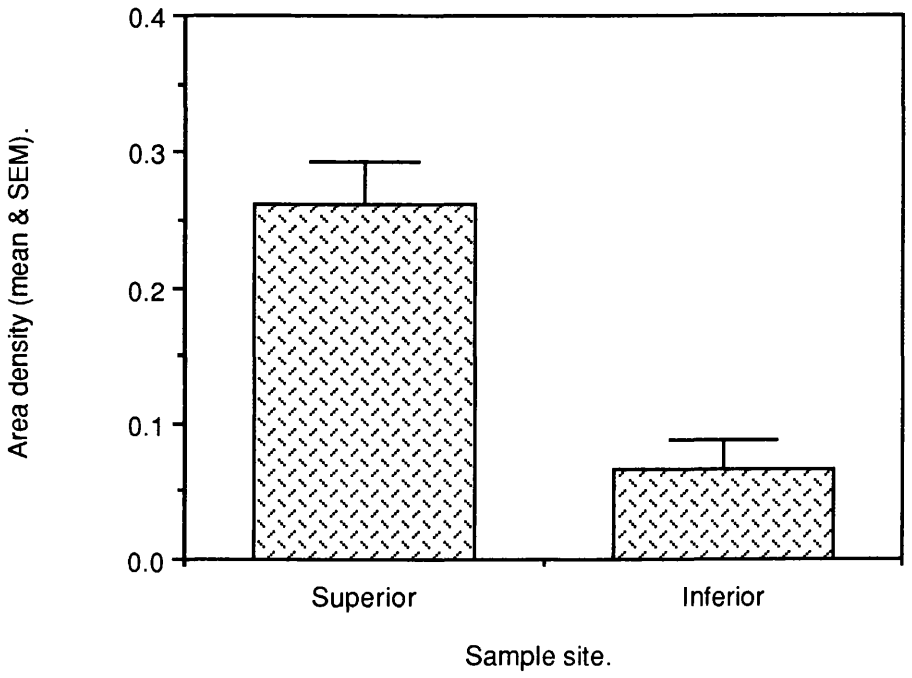

Fig. 1.17. Area density (percentage area of section occupied by crystal profiles) of crystals in superficial zone articular cartilage (to 50μm depth) from different femoral head sites; values are means (SEM). The observed difference between superior and inferior region sites was highly significant (P<0.001: Student's t-test, t=5.71; n=12).

Table 1.4. Mean number and area density (percentage area of section occupied by crystal profiles) of crystals in different regions of superficial zone femoral head articular cartilage with age. Values are means (SEM).

	10-25 years	40-55 years	75-90 years
Superior			
Crystal number	644 (475.1)[a]	885 (202.23)[c]	524.6 (155.2)[e]
Area density	0.186 (0.134)[b]	0.335 (0.007)[d]	0.308 (0.075)[f]
Inferior			
Crystal number	17.6 (13.54)[a]	336 (289.2)[c]	203.6 (155.03)[e]
Area density	0.012 (0.01)[b]	0.085 (0.35)[d]	0.116 (0.107)[f]

[a] U=0; [b] U=0; [c] U=0; [d] U=0; [f] U=0; significant difference (p<0.05). [e] U=2 no significant difference.

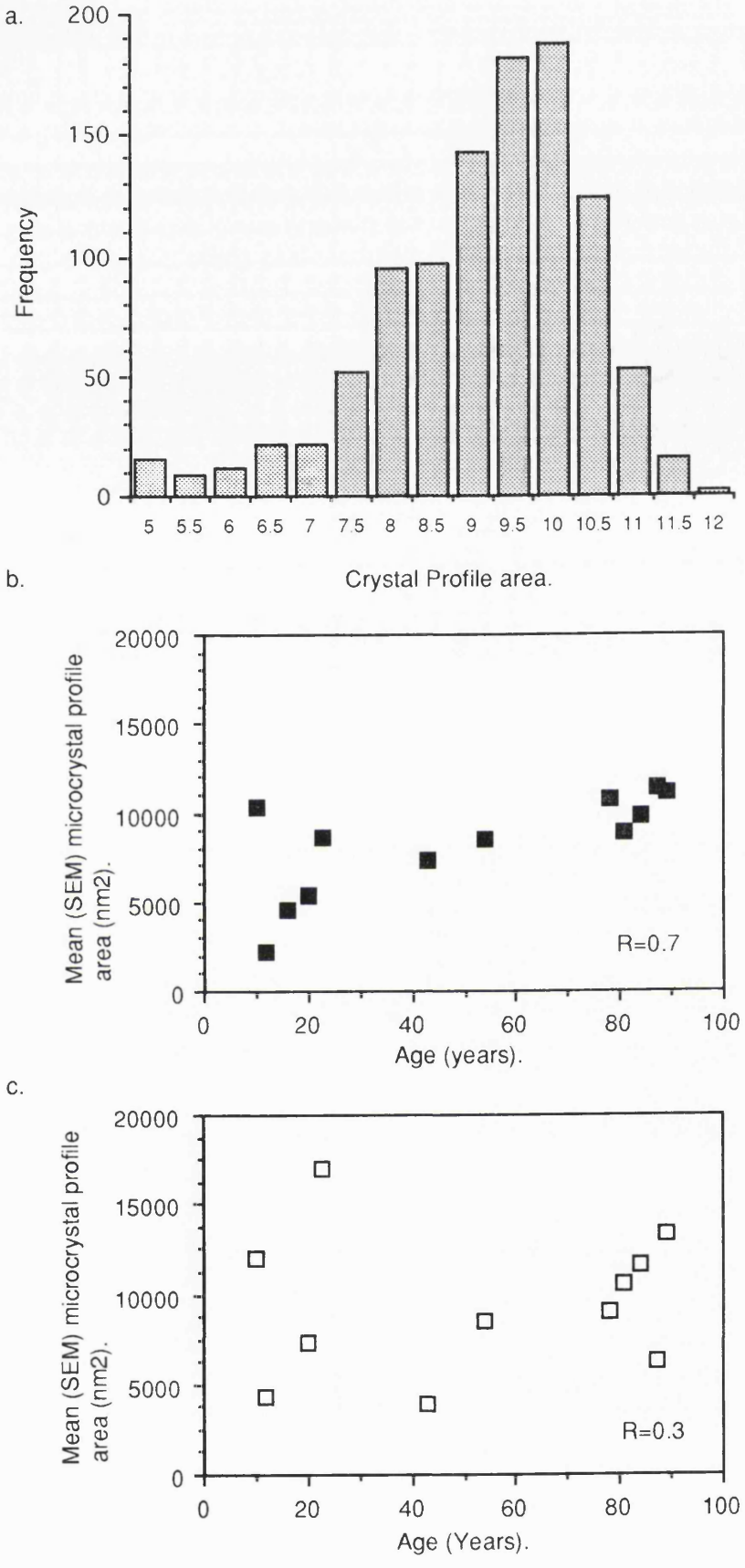

Fig. 1.18. Crystal profile area (size) distribution: (a) typical crystal profile area (log (n) nm^2) distribution (Superior region, KM 43 years); (b) crystal profile area distribution with age in superior region and (c) inferior region femoral head articular cartilage (Values are means, SEM values are too close to mean values to register on this scale).

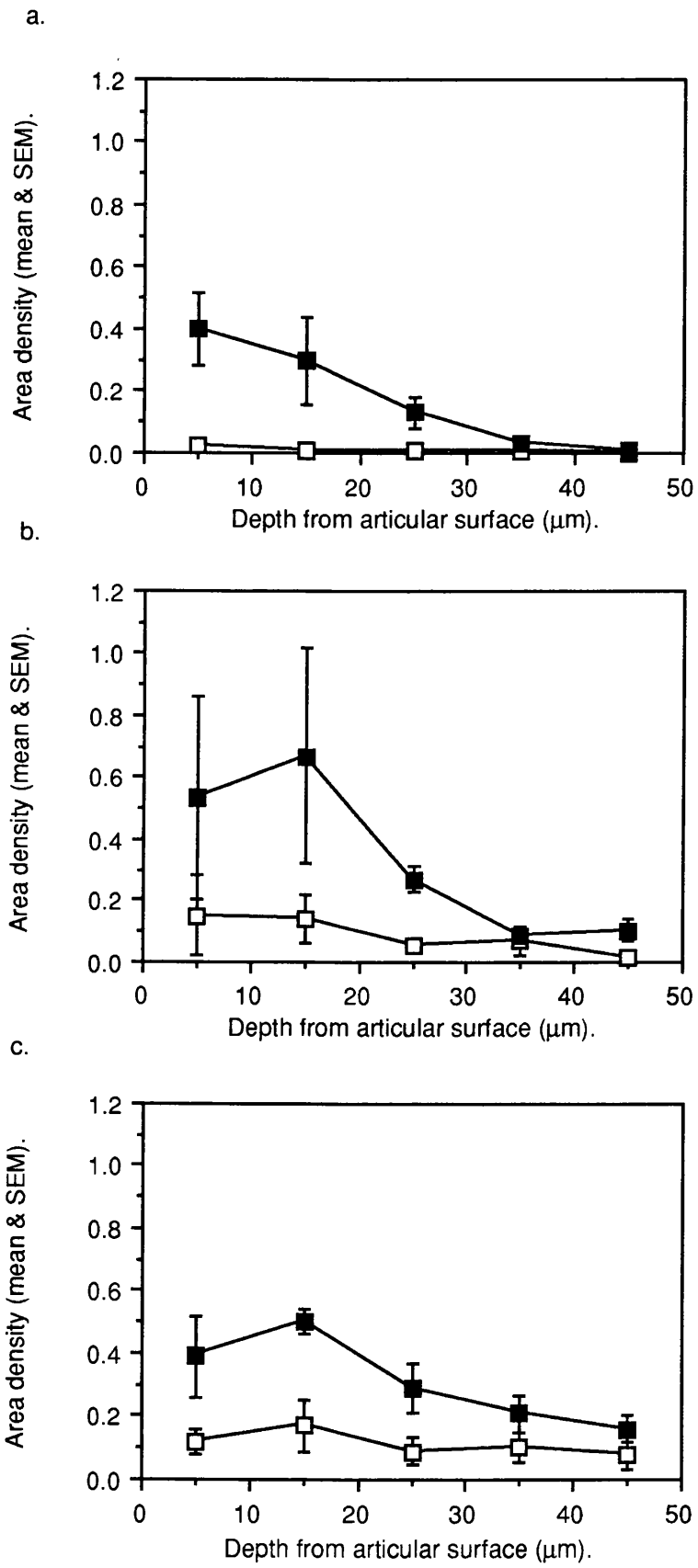

Fig. 1.19. Depth profile of crystal area density in the superficial zone, superior region (■) and inferior region (□), femoral head articular cartilage for three age groups; (a) 10 to 25 years, (b) 40 to 55 years, (c) 75 to 90 years.

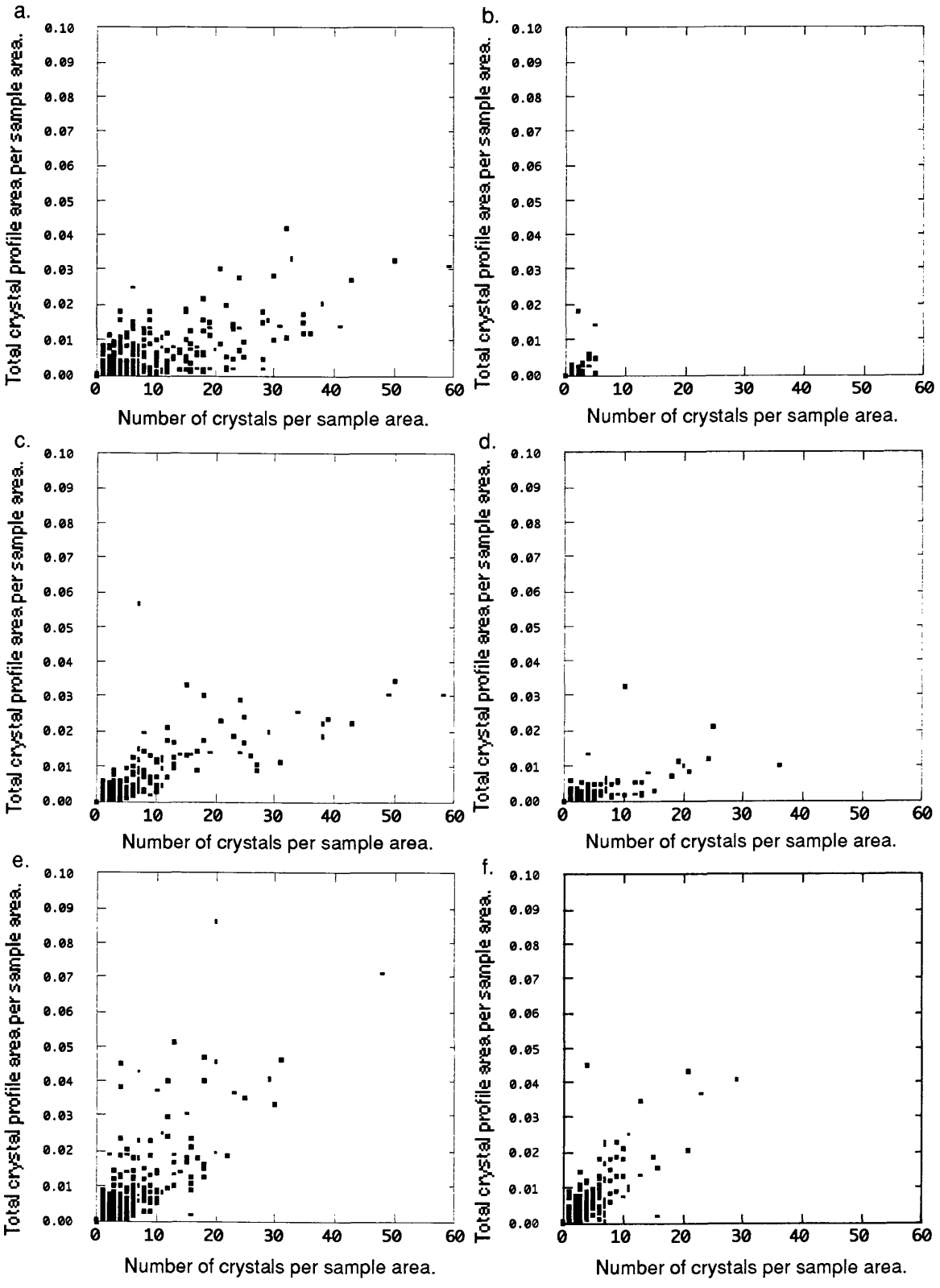

Fig. 1.20. Scatterplots demonstrating the relationship between the number of crystals and the total area (μm^2) occupied by crystal profiles in each sample area ($18.2\mu m^2$) in the superficial zone of articular cartilage from superior and inferior regions of the femoral head for three age groups; (a.) superior, (b.) inferior, 10-25 years; (c.) superior, (d.) inferior, 40-55 years; (e.) superior, (f.) inferior, 75-90 years.

Discussion.

The occurrence of crystals in standard, anhydrous and cryo-processed sections removes any doubt that their presence in articular cartilage is a processing artefact. Detailed investigation suggests that the structural organisation of mineral phases of cartilage and bone processed by the anhydrous method closely represents the state of the mineral phase in vivo (Landis and Glimcher 1978). Another source of artefact may be the time between removal of the specimen and processing. Efforts were made to minimise this possibility, and hence artefactual mineral formation is considered negligible on a number of counts. First, specimens were obtained quickly from theatre and, in cases of amputation, joints opened immediately prior to cartilage sampling. Secondly, ultrastructural preservation was excellent in many samples, as indicated by mitochondrial integrity, a sensitive indicator of tissue preservation (Ghadially 1983). Thirdly, as articular cartilage is an avascular tissue, oxygen and nutrients must diffuse over relatively great distances to reach chondrocytes (Stockwell and Meachim 1979). From experimental measurements, oxygen tensions in articular cartilage are proposed to be at most one third of that found in the spaces between capillaries in soft tissues (Stockwell and Meachim 1979), hence autolytic and physical degenerative changes may be deemed to have a relatively slow onset. Changes in temperature, (Font *et al.* 1982), and oxygen tension, (Brighton and Heppenstall 1971), within the tissue are two physical factors which may be deemed important in relation to artefactual mineral formation. As the standard resin processing technique for TEM described here appears to be a true representation of crystal deposition it's use may be favoured for the superior degree of ultrastructural preservation achievable.

Lack of evidence of crystal deposition at LM level is presumably attributable to the small crystal size. The failure to detect the presence of calcium using the alizarin red S stain would be most easily explained by the relatively diffuse deposition of these small crystals being beyond the sensitiviy of the stain, particularly as the calcified cartilage and subchondral bone within the same section elicit an intense positive result.

The ease of observation of crystals in unstained sections cut onto sodium cacodylate buffer was reduced in stained sections, not only due to the enhanced matrix electron density, but also due to crystal dissolution and drop out, attributable to uranyl acetate staining. This may be due to the slightly acidic aqueous uranyl acetate stain. Staining of sections with uranyl acetate and lead citrate however has been shown to remove early calcium phosphate mineral deposition from thin sections, with uranium and lead binding to remaining organic components at such sites (Arsenault and Hunziker 1988). The interpretation of associations between crystals and organic components should therefore be treated with caution. Such effects may explain the electron dense lamina reported around crystals, suggested by Marante *et al.* (1983) to be a membrane.

The rhomboid to square shape of the crystals observed in section agrees with the descriptions of crystals in OA and elderly articular cartilage (Ali and Griffiths 1981a,b, 1983, Ali 1985, Stockwell 1990). The smaller irregularly angled crystals presumably being glancing sections of the more familiar crystal shape. The observation of ovoid crystals amongst the cuboid deposition corresponds with observations of Rees *et al.* (1986) in articular cartilage; the crystals

appear similar to those described in semi lunar cartilage by Ghadially and Lalonde (1981). The cuboid and ovoid shapes of these crystals are hard to correlate with the apatite mineral phase even though both morphological forms described bear a strong resemblance to crystals observed using TEM by Pritzker and Luk (1976) from a pulmonary nodule and Faure *et al.* (1980) from subcutaneous calcification in scleroderma; both were identified as apatite. It is interesting to note that Faure and colleagues compared the crystals with similar shaped crystals from renal and dental calculi, sites which commonly host magnesium whitlockite deposition; a mineral more easily reconciled with the crystal shapes observed in this study. That these crystals are not CPPD is suggested by their relative stability in the electron beam, CPPD crystals are prone to sublimation producing a characteristic foamy appearance (Omar *et al.* 1979, Mitrovic 1983, Ishikawa *et al.* 1989), and small relatively uniform size, despite a pericellular distribution similar to that of early CPPD deposition (Ali *et al.* 1983) .

It has been suggested that the deposition of cuboid crystals is related to aging of normal cartilage or osteoarthritis (Ali and Griffiths1981a,b, 1983, Ali 1985, Marante *et al.* 1983, Stockwell,1990). Many of the articular cartilage specimens examined in this study were considered to be functionally normal, yet crystals were present in all cases, eighteen of which were under twenty five years. Indeed the youngest was five and a sixteen year old specimen had the second highest crystal area density of the samples analysed quantitatively. It is acknowledged that the specimens were taken from patients with osteosarcoma or possible osteoporotic conditions (frequently associated with fracture of the femoral neck), both of which may alter cartilage metabolism (Roberts *et al.* 1986) , allowing for the possibility of an increase in calcium ion concentrations. Serum calcium levels, however, were found to be within the normal range in the cases where data was available (Appendix I). Serum calcium and phosphate concentrations in osteoporosis are typically within the normal range, although there is a tendency towards the upper limit (Aitkin 1982). Stockwell (1990) suggests the comparative immobility of elderly patients may dispose patients to increased serum calcium and phosphorus concentrations through accelerated bone resorption. One may equally surmise that this is unlikely to be true in the younger patients of this study. As it is known that the ionic concentrations of calcium and phosphate in cartilage are normally supersaturated (Maroudas 1979), it is considered that this study is investigating processes attributable to normal articular cartilage and hence these crystals would appear to be a constituent of femoral head articular cartilage.

The unpredictability of the observation of crystal deposition observation in OA femoral head articular cartilage is most probably a consequence of tissue loss and regeneration. The superior region of the femoral head is most frequently affected by cartilage loss in OA and, in the cartilage adjacent to this, the superficial zone is frequently lost (Bullough and Vigorita,1984), hence the sites of most abundant crystal deposition within femoral head articular cartilage are not available for examination in these specimens. Crystals observed in specimens in such advanced stages of OA degeneration presumably correspond to the perilacunar crystal deposition described in deeper zones of cartilage showing less severe evidence of osteoarthritic

degeneration. The situation is further complicated by the presence of cartilaginous tissue probably of regenerative origin (Ali and Bayliss 1974) at the tissue surface.

The association of crystals with intramatrical lipidic debris, whether this be pericellular in the superficial zone, in deeper layers, in association with chondrocytes which have undergone in situ necrosis or in the region of crystal banding, agrees with previous observations. Ali (1985) describes crystals in association with matrix vesicles just below the articular surface. Terms such as vesicular components, intramatrical lipidic debris and cell debris may be more appropriate for describing the material associated with crystal deposition in this study (Rees *et al.* 1986, Ghadially and Lalonde 1981, Stockwell 1990). The association between intramatrical lipidic debris and the deposition should be interpreted with care, as demonstrated by Hunziker *et al.* (1989). The need for caution is due to the problems posed by overprojection and truncation phenomena, as the structures in question lie within the same dimensional range as section thickness. The authors concede that to overcome this problem many technical problems must be solved. The mean size of crystals in this study is approximately a factor of ten larger than the initial apatite crystallites discussed by Hunziker *et al.* (1989), making it possible to estimate their location within the space of the section with more confidence. It seems reasonable to correlate the distribution of lipidic debris and crystal deposition as related matrix components. Intramatrical lipidic debris is common in the matrix of rabbit (Barnett *et al.* 1963) and human (Ghadially *et al.* 1965) articular cartilage. In both porcine and lapine articular cartilage the distribution of crystal-like electron densities was very sparse and restricted within a band of lipidic debris consistent with that described by Ghadially (1983). In situ necrosis of chondrocytes and shedding of cell processes are thought to be the source of this debris (Ghadially 1983). Such an origin would be consistent with the observed distribution of debris and crystals in this study. Ghadially (1983) suggests that the lipidic debris produced in such a way finds its way to the surface and is discharged into the synovial fluid.

Deposition of crystals as a band below the articular surface supports the findings of Stockwell (1990), that the majority of crystal deposition occurred in the first 50μm of the articular cartilage depth. The presence of the crystal band appearing within this region may be considered in relation to the three dimensional collagen architecture of articular cartilage proposed independently by Clark (1990) and Jeffery *et al.* (1991). From the deep to the superficial zones collagen is organised in a layered or leaf-like manner. The orientation changes from radial in the intermediate zone to become tangential to the surface in the superficial zone (Jeffery *et al.* 1991). At the articular surface the tangential fibres are covered by a dense separate layer of small fibrils (Clark 1990). If this is considered in the context of the vertical migration of intramatrical lipidic debris a situation may be envisaged where such debris is slowed or trapped by the dense tangential layers of the collagen fibrils, resulting in a dense band of lipidic debris immediately below the surface. A second factor, which may indeed exert greater influence on the migration of debris, is the proteoglycan component of the matrix. Due to the high hydrophilicity of, and large volume occupied by, this matrix component (Maroudas 1979), a role in determining the migration of hydrophobic lipid debris to the proteoglycan poor, superficial zone may be anticipated. The resulting proximity of the lipidic debris to the articular surface may expose them to an extra articular

source of calcium and phosphate ions and enhance mineral deposition, as suggested by Stockwell (1990). Resistance to the movement of larger matrix components through superficial zone cartilage has been noted previously. Maroudas and Bullough (1968) and Brown and Jones (1992) have reported reductions in the permeability of articular cartilage to proteins migrating in the same direction through the superficial zone.

The cartilage sites in which crystals were not observed, epiphyseal growth cartilage, peripheral osteophyte and fibrocartilaginous overgrowth in OA specimens, are similar in that they are all relatively young tissues in a state of flux and rapid growth.

Increase in mean microcrystal profile area with age in the superior region is an interesting phenomenon and appears to be due to an increased proportion of microcrystals approaching the observed upper end of the crystal area profile range. The area profile range is similar from patient to patient irrespective of age. The lack of a trend in the inferior region may be due to much lower numbers of microcrystals present in some specimens providing an unrepresentative sample of the population. The increase in gradient observed in the relationship between the number of crystals and the total area occupied by crystal profiles per unit area (18.2μm^2), whilst undoubtedly being related to the increase in mean crystal profile area with age, may also be associated with the clumping of large crystals observed more frequently in older specimens, crystals in younger tissues being more diffusely distributed through the ECM. Such clumping may be part of a pericellular crystal deposition associated with a chondrocyte out of the plane of section, however, from the size and shape of such depositions, and the observation of crystals in areas of chondrocyte necrosis, it is more likely to mark the former location of necrotic cells. The finding that lipidic debris increases during aging (Barnett *et al.* 1963), and that *in situ* necrosis is a major source of such debris (Ghadially 1983), would be consistent with these results.

The small sample size and large variability in crystal number and area density between patients precludes any definite associations between crystal deposition, patient age and cartilage site. However it is possible to describe trends and from these to suggest further factors influencing the formation and distribution of these crystals.

The results for crystal profile number and for crystal area density show a similar pattern. It is, however, difficult to estimate the absolute number of objects within an area or volume of tissue for a number of reasons (Aherne and Dunnill 1982). These relate to the fact that sections will contain whole crystals and segments of crystals. A number of methods have been developed to overcome problems arising from this, but these have limitations on their use. For the purpose of comparison, estimates of area density (the percentage area of crystal profiles in the plane of the tissue section) are both simpler to obtain and more reliable.

The most striking result of this study is the difference in crystal deposition between the superior and inferior regions of articular cartilage coupled with the trend for this difference to lessen with increasing specimen age. This may explain the lack of such a difference recorded by Stockwell (1990) whose study was restricted to elderly femoral fracture patients.

One factor known to exert a major influence on articular cartilage is mechanical loading (Sah *et al.* 1989, Van Campen and Van de Stadt 1987). It has been suggested that mechanical

stress is involved in the regulation of chondrocyte metabolism (Stockwell,1987). The femoral head is part of one of the most heavily loaded joints in the body (Bullough *et al*. 1973, Paul 1976). The distribution of weight bearing stresses around this joint correspond to the observed differences in crystal loading between the superior and inferior surfaces (Bullough *et al.*1973, Afoke *et al.* 1987). Whilst crystals were present in cartilage from other joint sites, the density of such deposition was always less than in the superior region femoral head as determined by the qualitative grading system. This was most noticeable in specimens from the smallest, most peripheral joint sites which are normally subject to lesser loading stresses (Paul 1976). The only previous recorded observation of calcified bodies similar to cuboid crystals at cartilage sites other than the femoral head was in the meniscus of the knee joint (Ghadially and Lalonde 1981), also a load bearing joint (Paul 1976). The maximum strain during compressive loading of articular cartilage is exerted in the superficial zone (O'Connor *et al* . 1988). Any response of articular cartilage to mechanical load or strain may be attributable to changes in chondrocyte metabolism, which may implicate the chondrocyte with an indirect role in crystal formation. For example lipidic debris has been shown to increase during ageing (Barnett *et al.* 1963) and, in situations of cartilage injury the occurrence of *in situ* necrosis is elevated (Ghadially *et al.* 1971); it may be feasible therefore to suggest an increase in lipidic debris in relation to greater load bearing stresses via detachment of cell process tips or *in situ* necrosis.

The observation of crystal deposition in association with pericellular intramatrical lipidic debris is suggestive of an opportunistic mineralisation process rather than a specific system. It has been suggested that cellular debris and lipid in the matrix may be involved in the mineral formation process in hydroxyapatite deposition within osteoarthritic articular cartilage (Ali 1985, Ohira and Ishikawa 1987) and CPPD crystal deposition disease (Ohira *et al.* 1988). The evidence presented would support the co-occurrence of intramatrical lipidic debris (matrix vesicle like structures of low specificity) and an extra-articular source of calcium and phosphate ions as favourable conditions for cuboid crystal deposition. However the cuboid crystals demonstrate a greater ubiquity in relation to cartilage age and a more specific distribution than was previously apparent. A further factor, mechanical load, is suggested for crystal formation, with this and the collagenous architectural arrangement of the matrix contributing to their observed distribution.

CHAPTER 2
ELEMENTAL ANALYSIS OF CRYSTALS

Introduction

Crystals containing calcium and phosphorus, deposited in articular tissues may exhibit a variety of forms, primarily calcium phosphates and calcium pyrophosphate dihydrate. The calcium phosphates form a series of mineral phases, precipitation of a particular phase depending upon ambient physical and chemical conditions; the stability of these phases may be modified by the incorporation of impurities such as carbonate, fluoride and magnesium. The most biologically relevent of these have been described in the general introduction. CPPD (McCarty *et al.* 1962), HAP (Ali 1985, Ohira and Ishikawa 1987), carbonated apatites (McCarty *et al.* 1983) and OCP (Faure *et al.* 1980, McCarty *et al.* 1983) have been reported in articular tissues using a variety of techniques including x-ray diffraction, infra red spectroscopy and electron probe x-ray microanalysis.

The use of electron probe x-ray microanalysis (XRMA) has been applied to the study of biological mineral formation in both pathological and physiological contexts (Ali 1977, Faure *et al.* 1982, Landis 1979). The technique is suited to such study due to its extreme sensitivity and ability to correlate elemental composition with ultrastructural location. Experience has shown that care must be taken in the interpretation of such results as slight alterations in mineral phase or translocation of calcium and phosphate due to sample preparation are easily detected and may lead to misinterpretation of processes (Morgan *et al.* 1975 Thorogood and Craig Gray 1975, Landis 1979). A number of acceptable preparation techniques for use with XRMA have been characterized (Ali and Wisby 1975, Landis and Glimcher 1978, Landis *et al.* 1977, Ozawa and Yamamoto 1983). Calcium phosphate mineral phases may be suggested by the characteristic Ca/P ratio determined for the mineral (Landis 1979, Ali 1985). This method is not absolute as different minerals may possess the same Ca/P ratio, whilst one mineral phase may occur with variable Ca/P ratios (Winard *et al.* 1965, Nancollas *et al.* 1989). Furthermore any change in mineral phase over very small distances due to epitaxial growth or mineral sandwiching may remain undetected and be averaged. For confirmation of mineral phases this method is best used in conjunction with electron or x-ray diffraction. Larger volumes of mineral sample are, however, required for such techniques.

XRMA has been applied to the study of cuboid crystals by a number of workers (Ali and Griffiths 1981, 1983, Rees *et al.* 1986). The crystals were found to be predominantly calcium phosphate, although the Ca/P ratio is significantly lower than that for HAP. The presence of magnesium has been suggested (Ali and Griffiths, 1983), although this has not been clearly established. The calcified bodies described by Ghadially and Lalonde (1981) in human meniscus were reported to have a Ca/P ratio lower than that expected for hydroxyapatite; however they advised this figure be treated with caution. They also detected magnesium within the crystals. Rees et al (1986) described a trend for a reduction in Ca/P ratio with a increase in crystal size starting around 2.1 for crystals less than 250nm and decreasing to 1.56 for the largest crystals analysed. It was suggested that the crystals may be undergoing a maturation process or act as potential seed crystals for the growth of other crystals, such as CPPD. It is assumed that a system of epitaxial growth or a phase transformation was envisaged.

Epitaxial growth of one calcium phosphate phase on another may occur where there is suitable crystal lattice matching. Due to the dominance of the crystal architecture by phosphate groupings , there are common features between the mineral phases in the calcium phosphate series; a structural plane of OCP or DCPD can be essentially identical to a comparable plane of HAP thus allowing the possibility of sandwich mixtures or surface compounds (Neuman 1980). HAP growth has been demonstrated on DCPD (Nancollas *et al.* 1989) and DCPD on OCP (Heughebaert *et al.* 1986). Using high resolution TEM the overgrowth of OCP on apatite has been demonstrated (Nelson *et al.* 1986). Brown *et al.* (1979) suggested that OCP and HAP can occur as intracrystalline interlayered mixtures. Such a system or the *in situ* transition of OCP to apatite (Eanes 1985) may explain the plate-like morphology of bone crystallites observed by TEM (Landis *et al.* 1977, Jackson *et al.* 1978, Weiner and Price 1986) and 3D microtomography (Landis *et al.* 1992) which is not consistent with the hexagonal symmetry of HAP. The concept of phase transformations of mineral phases is not without precedent in biological mineralisation. The phase transformations of the calcium phosphate series as proposed for bone mineral maturation are outlined in the introduction and evidence of such events in bone formation cited.

A further possibility for variation in calcium phosphate mineral phases within the same crystal deposit has been described when a calcium phosphate phase exposed to a solution more acid than that in which it was precipitated, may become covered by a surface coating of a more acidic calcium phosphate appropriate to the current pH; this may complicate the apparent solubility behaviour of the initial mineral phase, hence one calcium phosphate phase may be stabilised by a boundary phase coating it (Nancollas 1982). Similar processes may be involved in the heterotopic calcifications described by Faure *et al.* (1982) from shoulder tendon sheath calcifications. The systems described above may confuse XRMA Ca/P ratios and should be considered when interpretting results.

Scanning transmission (STXM), and scanning fluorescence (SFXM) x-ray microscopy were used firstly to confirm the distribution of the crystals in the cartilage on the basis of elemental signals, and secondly to evaluate the application of these newly developed techniques to biological calcification research, an area to which they seemed well suited due to convenient x-ray absorption characteristics of calcium (Buckley *et al.* 1992).

This study aims to look for evidence suggestive of the 'cuboid' crystal mineral phase and identify any changes in calcium to phosphorus ratio, possibly indicative of a mineral phase change, with crystal morphology, size, specimen age, joint site and clinical condition of tissue of origin. Whilst this information is important in the characterisation of these crystals, it is also necessary before attempts may be made to isolate crystals for diffraction analyses, as such studies necessitate a larger sample volume, probably from more than one specimen. Such analyses would only be meaningful therefore with an homogenous mineral phase.

Materials and Methods

Specimens.

Articular cartilage samples were taken as described in chapter one. The samples used in the comparative analyses were all taken from normal and OA femoral heads, with the exception of one of the anhydrous/ normal comparison samples which was from the femoral condyle. XRMA was used on all the specimens decribed in chapter one to confirm the calcium phosphate nature of the mineral although the number of crystals analysed in this screening process was not enough to justify statistical analysis. Samples of porcine and lapine femoral head articular cartilage were also analysed.

Tissue samples were processed using the standard resin protocol for TEM, as described in chapter one, although secondary fixation with 1% osmium tetroxide was omitted as interaction of the osmium Mα peak (1.91keV) and the phosphorus Kα peak (2.01keV) may be expected to produce spurious calcium to phosphorus ratios. Adjacent samples from three of the specimens were processed using the anhydrous processing technique described in chapter one. Four known synthetic calcium phosphate samples were also fixed and processed using the standard resin protocol; these were hydroxyapatite ($Ca_5(PO_4)_3OH$), tricalcium phosphate ($Ca_3(PO_4)_2$), calcium pyrophosphate dihydrate ($Ca_2P_2O_7$) and magnesium whitlockite ($Ca_{18}Mg_2H_2(PO_4)_{14}$). The hydroxyapatite and tricalcium phosphate standards were provided by Dr. C. Klein and were well characterised by X-ray diffraction (Klein *et al.* 1988); synthetic magnesium whitlockite was provided by Dr P Shellis (Bristol) and the calcium pyrophosphate dihydrate was from commercially available stock (Sigma, Poole, UK). Small powdered samples of each known calcium phosphate were processed in Eppendorf tubes, with centrifugation between each stage. On transfer to the embedding resin the preparation was heated to 60°C for 10mins to reduce the viscosity of the resin prior to centrifugation and polymerisation.

100nm sections were cut from all tissue, and known calcium phosphate, blocks as described in chapter one. Sections were cut onto 0.085M sodium cacodylate buffer and collected on piolform coated G200 HS copper grids.

Electron probe x-ray microanalysis.

Unstained sections were examined using a Philips CM12 transmission electron microscope with an EDAX PV9800 XRMA system. Spectra were recorded at 100 kV (operation at maximum available kV has been recommended to obtain maximum peak to background ratios (Joy and Maher 1977) for 200 live seconds with a tilt angle of 20°, giving a total 'take off' angle of 40°. The electron probe size was selected to encompass individual crystals and was never greater than 200nm diameter, a 70nm 'top hat' condenser aperture was used to minimise the background effect of x-rays generated higher in the column from reaching the specimen area. Calcium to phosphorus ratios were calculated using the quantitative analysis of thin sections software package (EDAX PV9800) based on the ratio model (Russ1974). The synthetic hydroxyapatite sample was used as the calcium phosphate standard for these analyses (Klein *et al.* 1988). The

unpaired Student's t-test and one way analysis of variance were used to compare crystal groups where appropriate.

Elemental maps were produced using the external beam image deflection (EBID) unit (on loan from Philips Analytical, UK) with the SEM software package (EDAX 9800) under the same operating parameters as described above. Defined areas of 100nm sections were scanned with a 20nm diameter probe across a 256x200 point matrix, with a dwell time of 1 second per point. Maps were produced for calcium, phosphorus and magnesium from each section scanned.

Scanning Transmission and Scanning Fluorescence X-ray Microscopy

CY212 resin embedded articular cartilage sections were cut at 100nm thickness for STXM and 5μm for SFXM. Sections were attached to silicon nitride windows for examination using both techniques. STXM and SFXM examination was performed by Dr C Buckley at the National Synchrotron Light Source, Brookhaven, USA (Buckley *et al.* 1992).

Images are formed in the STXM by raster scanning the specimen across a 50nm x-ray probe, and detecting the transmitted x-rays at every pixel. Calcium imaging by STXM is achieved by utilizing the rapid change in mass absorption coefficient with change in x-ray energy. A transmission image is taken at 350.6eV where the absorption of x-rays by calcium is relatively low. The energy of the radiation is changed 351.6eV at which the absorption by calcium is higher (at an absorption edge) and a second image is taken. A signal which is proportional to the amount of calcium per unit area is formed by subtracting the logs of the two images. The elemental map can then be displayed via a suitable colour map or grey scale.

The SFXM employs a 10x10μm x-ray probe which is formed by collimation of a polychromatic or monochromatic source. The specimen is raster scanned across the probe and fluoresced radiation generated by the sample is detected by a lithium drifted silicon diode. The detector produces pulses with heights that are proportional to the energy of the incident radiation; the various pulse heights can be grouped into channels representing the characteristic radiation of a number of elements. The counts in a particular channel can then be displayed at each pixel to form an elemental map via a colour map or grey scale.

Results.

Typically, the crystals examined produced spectra comprising two major peaks with a low background. The major peaks were identified as corresponding to calcium (Kα at 3.69keV) and phosphorus (Kα at 2.01keV). A small magnesium peak (Kα 1.25keV) was identified when a spectrum from adjacent matrix was subtracted from a crystal spectrum (Fig. 2.1). This procedure removed interference due to arsenic (Lα 1.28keV) , attributable to the sodium cacodylate buffer used during processing and section collection. Similar peaks for calcium and phosphorus were observed in spectra from the known synthetic hydroxyapatite sample, calcified cartilage, subchondral bone and tricalcium phosphate, but the synthetic magnesium whitlockite sample was the only one to demonstrate an accompanying small magnesium peak. Representative areas of sample sections from which spectra were generated are shown in Fig.2.2. The presence of magnesium in the crystals was clearly demonstrated by the discrete co-localisation of calcium,

magnesium and phosphorus mapped across areas of crystal-laden articular cartilage ECM, from samples that had been processed using the anhydrous technique and cut onto distilled water (Fig. 2.3). A peak at 1.74 keV, identified as silicon Kα, was occasionally detected; this was often in association with very small crystals. Similar peaks were also detected in the matrix adjacent to such crystals, in the absence of calcium. Crystals from other joint sites screened using XRMA generated spectra with similar characteristics notably the magnesium peak and characterisitc relative peak heights for calcium and phosphorus.

Of the two articular cartilage samples probed for XRMA which had been divided and processed by normal and anhydrous techniques, no significant difference in the mean calcium to phosphorus ratio of crystals from the two groups was observed (Fig. 2.5). No significant difference was observed between mean calcium to phosphorus ratios of crystals from the same block in sections cut onto 0.085M sodium cacodylate buffer or distilled water (Fig. 2.5); it was also noted that crystal drop out in sections cut onto buffer was negligible.

From a calibration curve relating calcium to phosphorus ratios determined by XRMA and calcium to phosphorus molar ratios for the known calcium phosphate samples (Fig 2.4), a calcium to phosphorus molar ratio can be determined for an unknown from its XRMA ratio. It was seen from the calibration curve that the XRMA technique,using the semi-quantitative ratio model to determine calcium to phosphorus ratios, provided a ratio very close to that of the molar ratio.

The mean calcium to phosphorus molar ratio of 'cuboid' crystals ranged from 1.32 to1.47, these values were close to those recorded for synthetic tricalcium phosphate, but were significantly lower than those recorded for bone mineral (Fig. 2.4). The calcium to phosphorus ratios used below for statistical analyses are XRMA derived ratios.

No significant difference in mean calcium to phosphorus ratio was recorded between crystals with apparent spheroid and cuboid morphologies (Fig. 2.6). There was no significant change in the mean calcium to phosphorus ratio of crystals, with respect to an increase in crystal size, crystals being grouped into five100nm size bands for this comparison (Fig. 2.7).

The mean calcium to phosphorus ratio of crystals from specimens ranging in age from ten to eighty nine years, both normal and OA, were compared using a one way analysis of variance. No significant difference in mean calcium to phosphorus ratio between groups was detected (Fig. 2.8).

The STXM technique proved successful at mapping the crystal in ultra thin sections via their calcium signal. The technique had a lower resolution than the XRMA elemental mapping, but was a useful confirmatory technique for crystal distribution at lower magnifications (800-1600x) (Fig. 2.9). Results from the SFXM were of lower resolution still, due to increased section thickness and larger probe size, although it was possible to map full depth cartilage sections indicating the presence of a band of calcium immediately below the articular surface; this was interpretted as further confirmation of a subsurface crystal band (Fig. 2.9).

The electron densities present in porcine and lapine femoral head articular cartilage, described in chapter one as having crystalline characteristics, were analysed for their calcium and phosphorus content. Calcium and phosphorus were detected, although the signals were not

always strong. In cases where clear spectra with low backgrounds were recorded, the calcium to phosphorus molar ratio was around 1.52 for lapine cartilage crystals and 1. 39 for porcine cartilage crystals (Fig. 2.10).

Fig. 2.1

Fig. 2.1a. Detail of an XRMA spectrum generated by the sintered hydroxyapatite standard after the subtraction of a spectrum generated by an adjacent area of resin.

Fig. 2.1b. Detail of an XRMA spectrum generated by an area in the calcified zone of articular cartilage close to the subchondral bone interface, after the subtraction of a spectrum generated by a crystal free area of matrix. (JO 26 years femoral head).

Fig. 2.1c. Detail of an XRMA spectrum generated by the magnesium whitlockite standard after the subtraction of a spectrum generated by an adjacent area of resin; note the presence and relative height of the magnesium Kα peak.

Fig. 2.1d. Detail of an XRMA spectrum generated by a 'cuboid' crystal after the subtraction of a spectrum generated by an adjacent, crystal free area of matrix; a magnesium Kα peak with a similar height relative to the calcium Kα and phosphorus Kα peaks, as seen in 2.1c is present (MS 84 years, femoral head).

Fig. 2.1e. Expanded section of 2.1d, with a computer generated, arsenic Lα peak (dotted line) overlying the spectrum, showing a lack of fit with the original spectral peak.

Fig. 2.1f. Expanded section of 2.1d, with a computer generated, magnesium Kα peak (dotted line) overlying the spectrum, showing a good fit with the spectral peak.

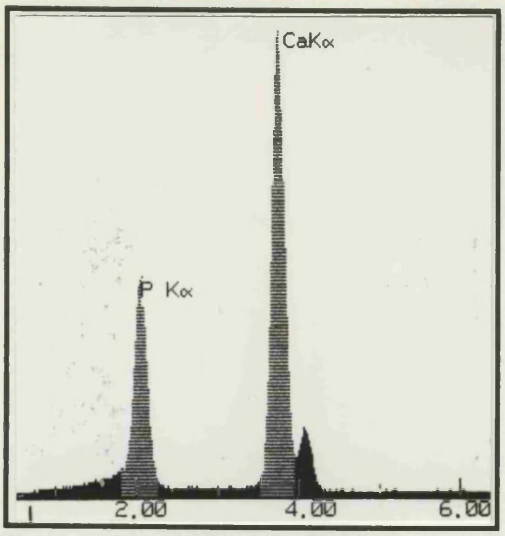
CaKα
P Kα
2.00
4.00
6.00

a

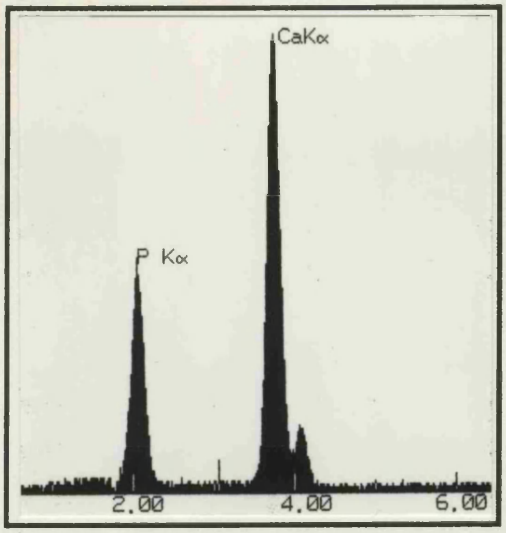
CaKα
P Kα
2.00
4.00
6.00

b

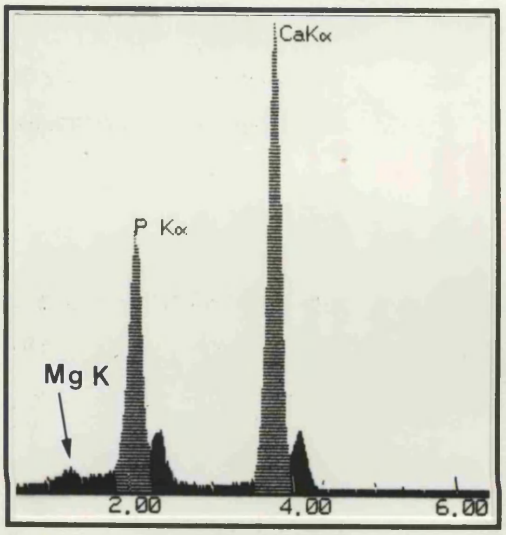
CaKα
P Kα
Mg K
2.00
4.00
6.00

c

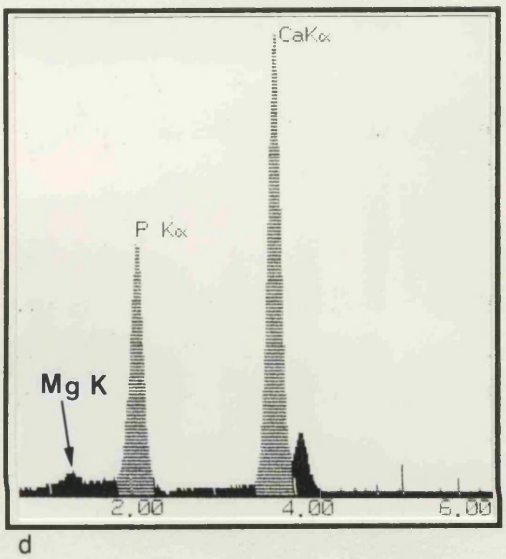
CaKα
P Kα
Mg K
2.00
4.00
6.00

d

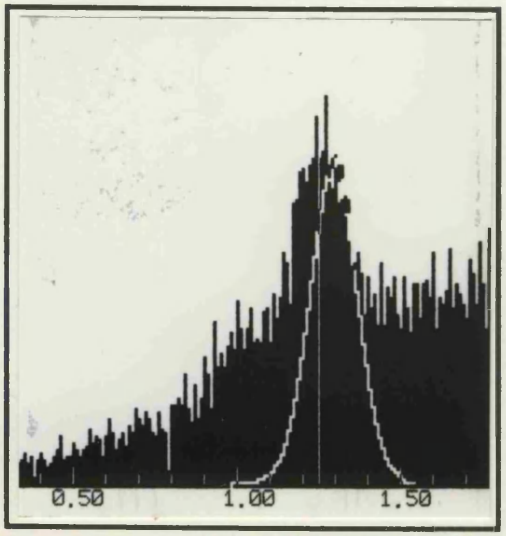
0.50
1.00
1.50

e

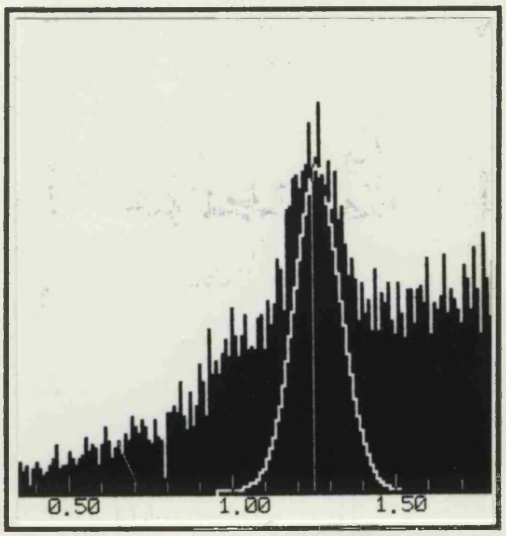
0.50
1.00
1.50

f

Fig. 2.2

Fig. 2.2a. Sintered hydroxyapatite standard in an ultrathin resin section, used for XRMA.

Fig. 2.2b. An area of the calcified zone of femoral head articular cartilage, close to the subchondral bone interface, used for XRMA. (JO 26 years).

Fig. 2.2c. Magnesium whitlockite standard in an ultrathin resin section, used for XRMA.

Fig. 2.2d. Cuboid crystals in the ECM of femoral head articular cartilage, used for XRMA; an area of crystal that has been probed for analysis previously is indicated (arrow), (MS 84 years).

a

b

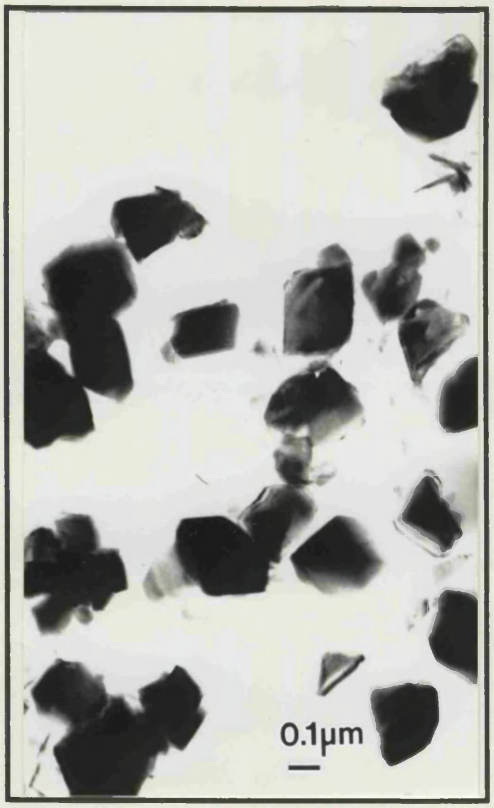

c

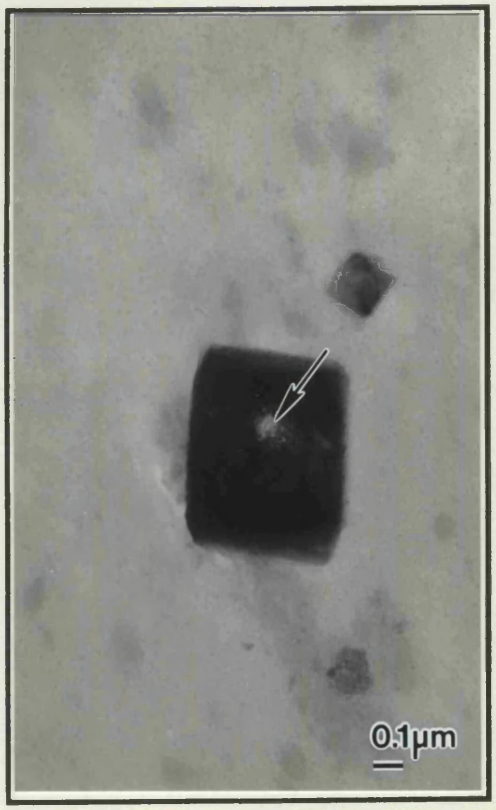

d

Fig. 2.3

Fig. 2.3a. Calcium map of an area of femoral head articular cartilage containing crystals. The specimen was prepared using the anhydrous technique (JY 55 years).

Fig. 2.3b. Magnesium map of the area shown in 2.3a.

Fig. 2.3c. Phosphorus map of the area shown in 2.3a.

Fig. 2.3d. Electron micrograph of the area shown in 2.3a Crystal damage caused by extended exposure to the electron beam is indicated (arrows).

a

b

c

d

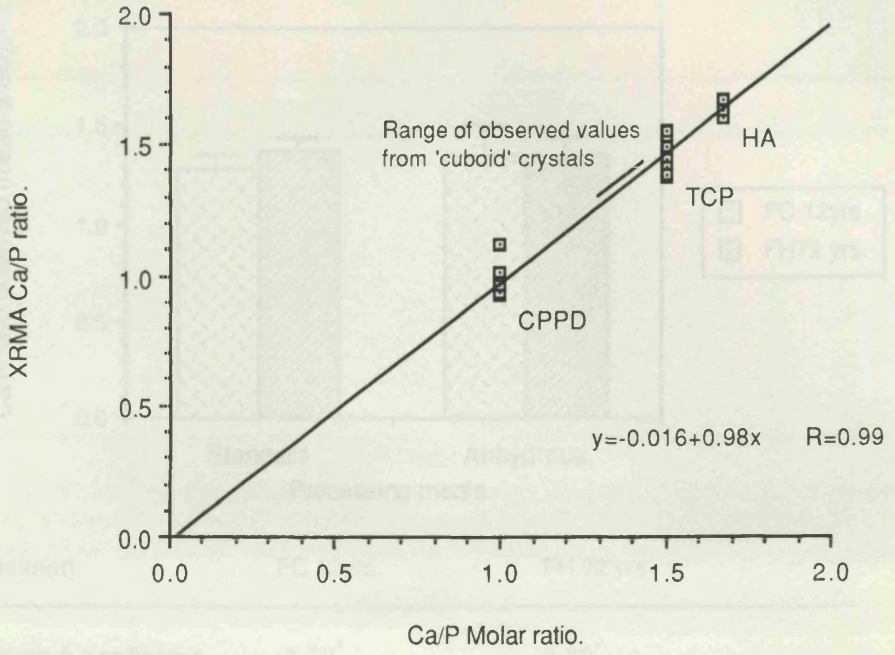

Fig. 2.4. Known calcium phosphate minerals used for XRMA. The calibration curve shows the calcium to phosphorus ratios observed using XRMA, plotted against the molar ratio for each known mineral. Synthetic hydroxyapatite was used for calibration of the system. Calcium to phosphorus ratios from the known mineral phases plus subchondral bone and cartilage from the calcified zone are shown below.

Calcium phosphate standard	Ca/P ratio (XRMA)
Calcium pyrophosphate dihydrate (CPPD).	0.97±0.06*
Tricalcium phosphate (TCP).	1.45±0.06*
Hydroxyapatite (HA).	1.63±0.03*
Subchondral bone.	1.62±0.02*
Calcified cartilage.	1.58±0.05*

*n=10.

(CPPD): Sigma UK.
(TCP): Klein *et al.* 1988.
(HA) : Klein *et al.* 1988.

a.

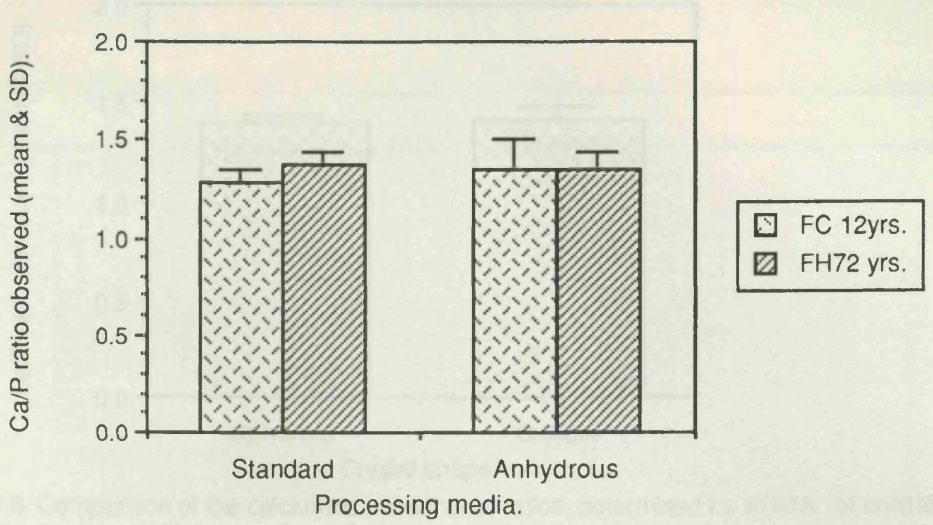

Specimen.	FC 12yrs.	FH 72 yrs.
t statistic & significance.	-1.52*	0.62*

n=10: values are considered significantly different if P<0.05: **difference significant, *difference not significant.

b.

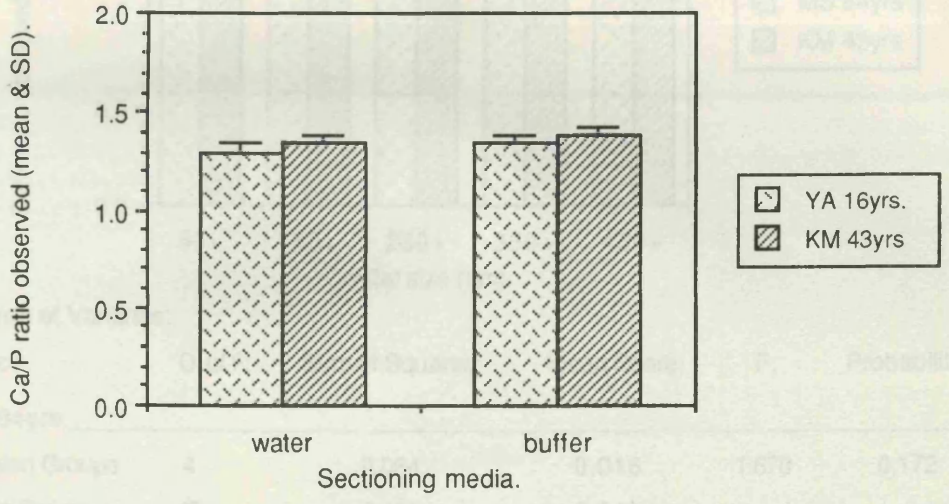

Specimen.	YA 16yrs.	KM 43yrs.
t statistic & significance	-1.61*	-1.79*

n=10: values are considered significantly different if P<0.05: **difference significant, *difference not significant.

Fig. 2.5. Comparison of the calcium to phosphorus ratios, determined by XRMA, of crystals in articular cartilage samples exposed to different preparation media: (a). variation between samples processed by the standard method for resin embedding and that using anhydrous solvents, (b). variation between sections cut onto distilled water (pH 7.3) and 0.085M sodium cacodylate buffer (pH7.4). t values were derived using an unpaired Student's t-test.

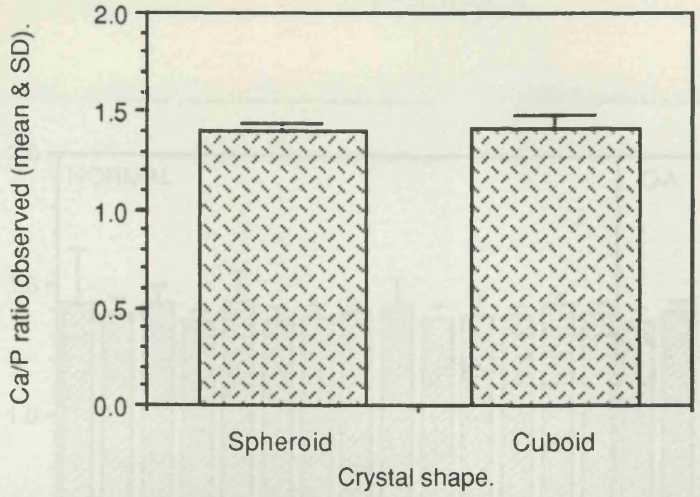

Fig. 2.6. Comparison of the calcium to phosphorus ratios, determined by XRMA, of crystals in articular cartilage (MS 84 years), exhibiting apparent spheroid and cuboid morphologies. No significant difference in Ca/P ratio was observed between these two groups (Unpaired Student t-test, t=-0.38: p<0.05: n=10).

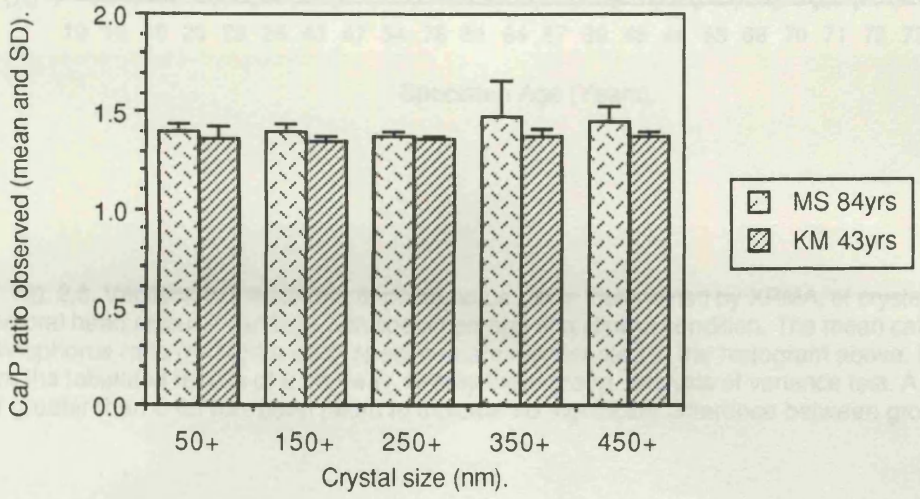

Analysis of Variance:

Source	D. of F:	Sum of Squares:	Mean Sqare:	F:	Probability:
MS 84yrs.					
Between Groups	4	0.064	0.016	1.678	0.172
Within Groups	45	0.431	0.010		
Total	49	0.495			
KM 43yrs.					
Between Groups	4	0.008	0.002	1.387	0.253
Within Groups	45	0.064	0.001		
Total	49	0.072			

Fig. 2.7. Comparison of the calcium to phosphorus ratios, determined by XRMA, of crystals in articular cartilage, with variation in crystal size. The significance of variation in Ca/P ratios was determined using one way, five group analysis of variance tests; p-values of greater than 0.05 are taken to indicate no significant difference between groups.

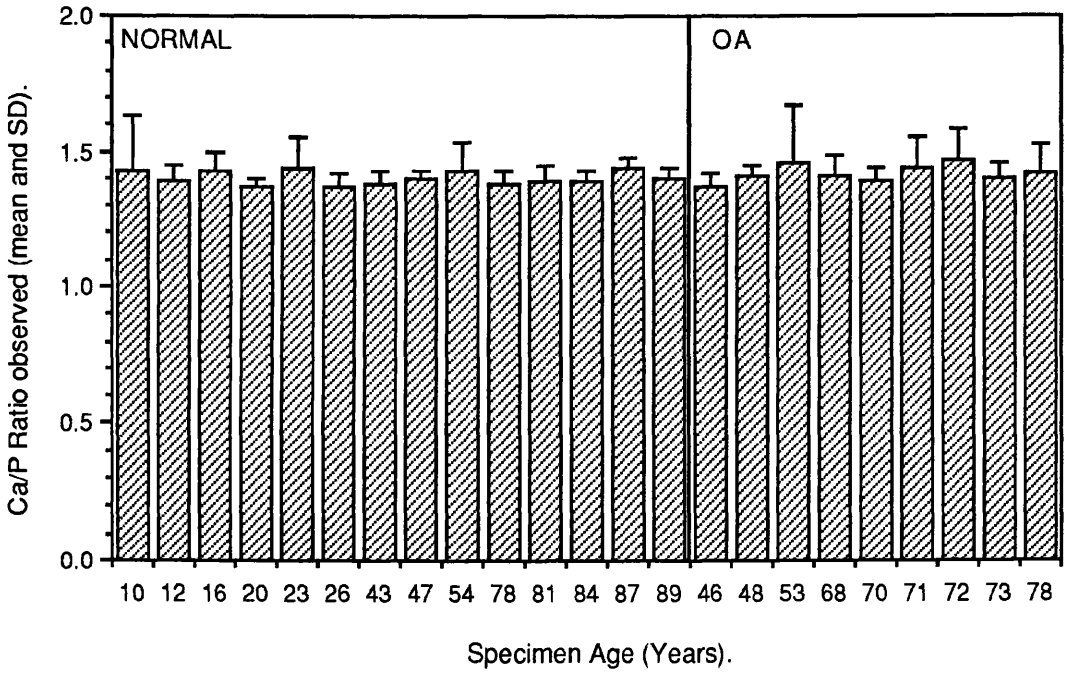

Fig. 2.8. Variation in the calcium to phosphorus ratios, determined by XRMA, of crystals in femoral head articular cartilage with specimen age and clinical condition. The mean calcium to phosphorus ratio (n=10) for each specimen are represented in the histogram above. Below are the tabulated results of a one way, twenty three group, analysis of variance test. A p-value of greater than 0.05 has been taken to indicate no significant difference between groups.

Source:	D. of F:	Sum of Squares:	Mean Square:	F:	P.
Between groups	22	0.216	0.010	1.282	0.186
Within groups	207	1.584	0.008		
Total	229	1.8			

Fig. 2.9

Fig. 2.9a. STXM calcium map of the area shown in 2.9b: white areas represent the highest calcium concentration, with no signal detected in black areas. The distribution of calcium indicated here fits closely with the crystal distribution shown in 2.9b.

Fig. 2.9b. Crystals in the superficial zone of femoral head articular cartilage, immediately below the articular surface (A), (KM 43 years). Unstained section.

Fig. 2.9c. SFXM calcium map of full depth femoral head articular cartilage (minus the calcified zone): white areas represent the highest calcium concentration, with no signal detected in black areas. The calcium concentration distribution corresponds to the distribution of crystals described in chapter 1.

Fig. 2.9d. Light micrograph of the region mapped in 2.9c, (YA 16 years). Section stained with toluidine blue.

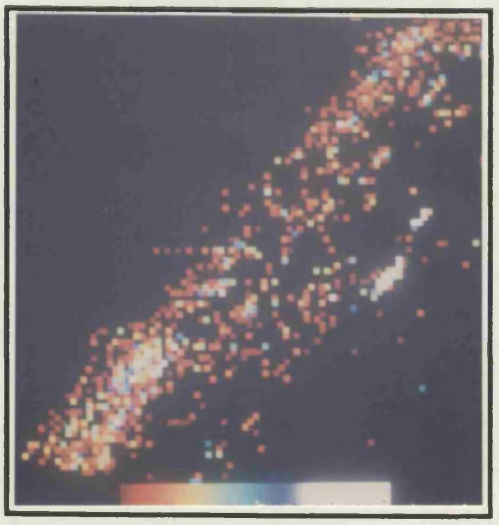

a

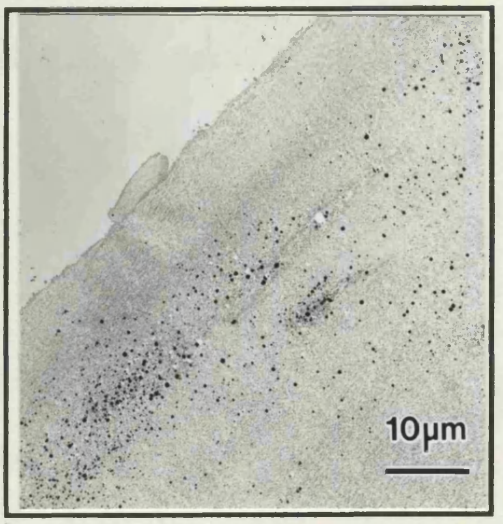

b

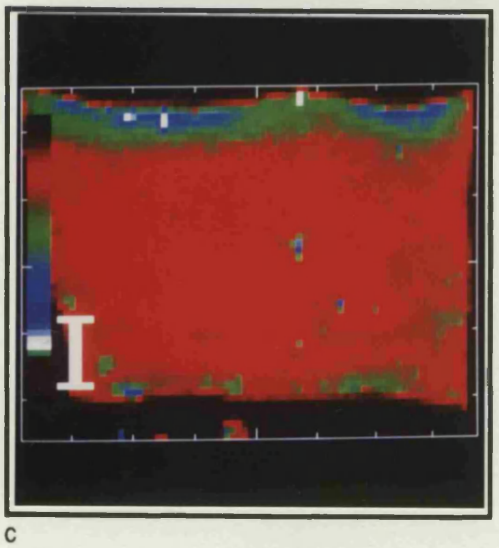

c

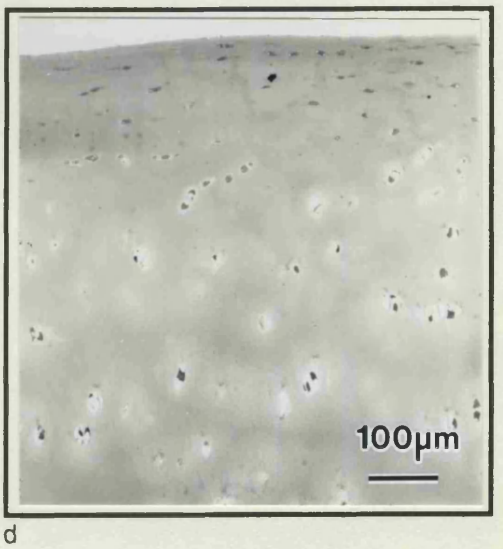

d

Fig. 2.10

Fig. 2.10a. Detail of an XRMA spectrum generated from a mineral deposit in the superficial zone of lapine femoral head articular cartilage, indicating strong calcium and phosphorus components (20 months).

Fig. 2.10b. Detail of an XRMA spectrum generated from a mineral deposit in the superficial zone of porcine femoral head articular cartilage, indicating strong calcium and phosphorus components (20 weeks).

Fig. 2.10c. Mineral deposits in the superficial zone of lapine femoral head articular cartilage (20 months).

Fig. 2.10d. Mineral deposits in the superficial zone of porcine femoral head articular cartilage (20 weeks).

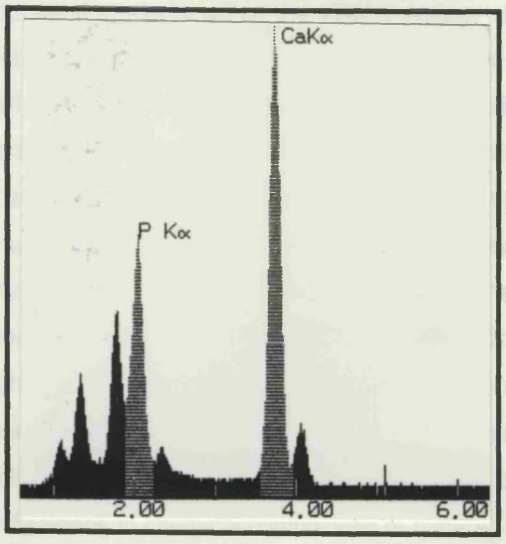

a

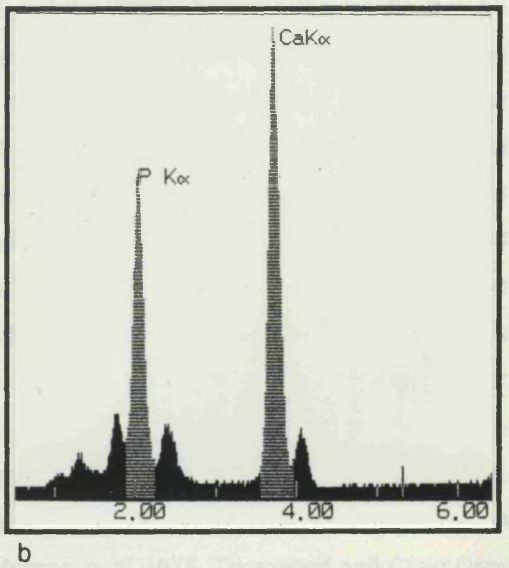

b

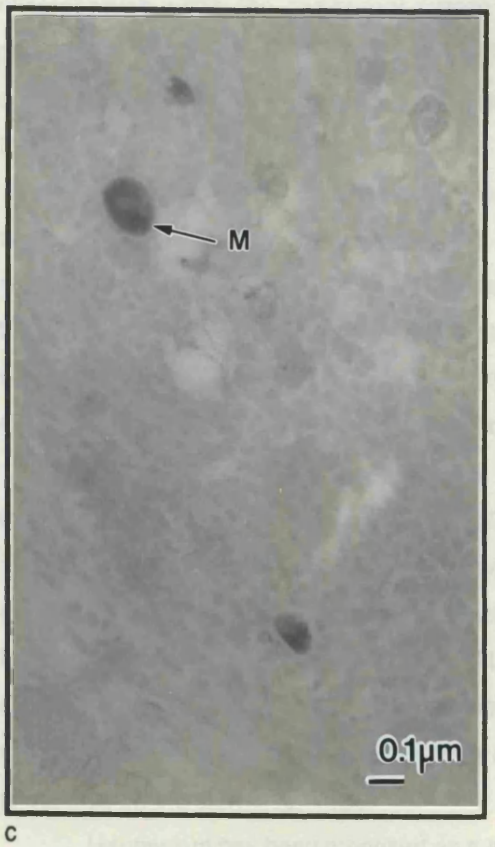

c

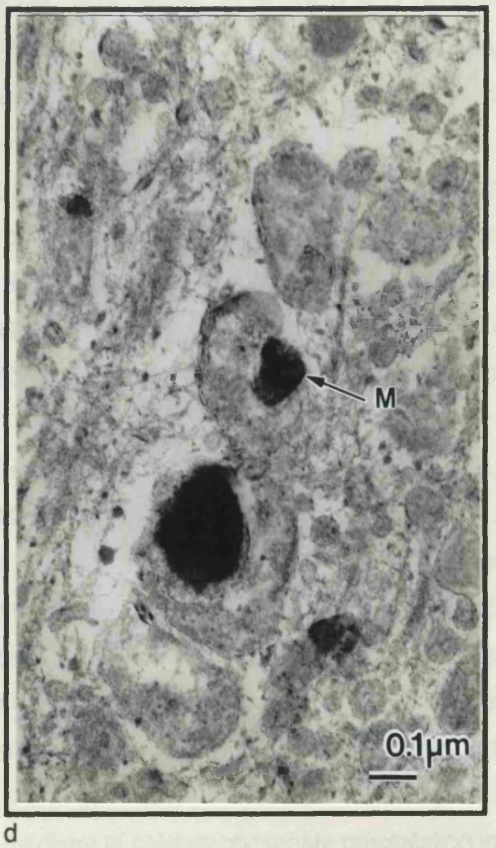

d

Discussion

Much attention has been focussed on mineral phase transformations due to tissue preparation for TEM in relation to XRMA (Morgan *et al.* 1975, Thorogood and Craig Gray 1975, Landis 1979, Ozawa and Yamamoto 1983, Ali and Wisby 1975), hence it was initially important to establish potential artefacts within the XRMA system used and the degree to which the results may be interpretted. Heavy metal stains were omitted from specimen preparation due to their reported effects on calcium phosphate mineral (Nanci *et al.* 1983, Ozawa and Yamamoto 1983, Arsenault and Hunziker 1988). To determine the extent of transformation within crystals due to standard tissue processing methods, comparisons with crystals from anhydrously processed tissue were made; no significant difference was observed between the two groups. As all knowns and standards were processed in an identical manner to the tissues it was reasoned that any changes that did occur may be considered uniform. The close correlation observed between calcium to phosphorus ratios determined by XRMA and molar ratios for the known mineral phases used for the calibration curve suggests negligible transformation of mineral phases. The calcium to phosphorus ratios obtained for subchondral bone further support the validity of this method. Alterations in chemical composition of mineral due to translocation of diffusable ions, dissolution and reprecipitation and mineral phase changes (Morgan *et al.* 1975, Thorogood and Craig Gray 1975, Landis *et al.* 1977) may be more important in the initial stages of mineral formation where mineral may exist in a relatively unstable form at physiological pH, with a high surface area to volume ratio. Such sites include embryonic bone formation (Rouffose *et al.* 1979), initial mineralization within the epiphyseal growth plate (Ali 1976, Morris *et al.* 1983) and mineral granules deposited within mitochondria (Ali and Wisby 1975). On the basis of the above, comparisons of the various crystal groups were made using tissue processed by the standard technique.

Despite the lack of significant difference in Ca/P ratio between crystals cut onto water and those cut onto buffer there was a noticeable 'drop out' of crystals from sections cut on water not seen in those cut onto buffer. It was noted that the pH of distilled water varied over the course of the study and, considering that distilled water has been shown to remove crystals form thin sections of enamel (Bishop and Warshawsky 1982), buffer was used throughout the study to standardise conditions and prevent crystal 'dropout'.

Calcium and phosphorus were the dominant peaks in a very consistent spectrum, supporting earlier studies (Ali and Griffiths 1981, 1983, Marante *et al.* 1983, Rees *et al.* 1986). The identification of magnesium associated with the crystals confirmed reports by Ali and Griffiths (1983) and Rees *et al.* (1986) and is consistent with the analysis of the calcified bodies from human meniscus described by Ghadially and Lalonde (1981). Magnesium has been reported as a common contaminant in XRMA studies (Warley and Gupta 1992); however contamination can be ruled out here as it is invariably present in crystal spectra and co-localises with calcium and phosporus on the elemental maps.

Magnesium has been proposed as a major mediator of calcium phosphate precipitation in biological systems, selectively stabilizing the more acid precursor phases (Nancollas et al 1989).

The relatively high concentration of magnesium ions in blood serum (approximately 1mM) is thought to be a major component which prevents the precipitation of HAP in vivo (Nancollas 1982). In model systems magnesium ions have been reported to stabilize calcium phosphate precursor phases of HAP such as a TCP-like phase (Nancollas 1982), ACP (Boskey and Posner 1974) and OCP (Brown et al 1962) and have also been characterised as a stabilizing impurity in ß-tricalcium orthophosphate (Schroeder et al 1977). That this stabilization is variable has been shown by Salimi *et al.* (1985), who demonstrated that magnesium retarded HAP crystallisation, to a much greater extent than that of OCP. Evidence for inhibition of biological HAP formation by magnesium has been presented by LeGeros (1974) and Cheng and Pritzker (1983) . In the presence of 3mM magnesium, the calcium salt magnesium whitlockite was formed at medium Ca/P ratios ($0.1<Ca/P<1.0$: at $[Ca^{++}][Pi] = 10mM^2$), brushite and HA were formed at ratios below and above this respectively (Cheng and Pritzker 1983). Magnesium may be located on the surface of bone apatite crystallites (Neuman and Mulryan 1971) and recent reports (LeGeros and LeGeros 1984, Okazaki *et al.* 1986) suggest it may be incorporated to a limited extent in the apatite crystals, although the substitution of magnesium for calcium is strongly discriminated against; the presence of magnesium contributes to the chemical instability of HAP. Santos and Gonzalez-Diaz (1980) reported apatites from urinary calculi containing magnesium and suggested that magnesium occupies calcium sites at the apatite crystal surface as due to size differences they cannot substitute into the apatitic lattice. This would be expected to inhibit further crystal growth.

The calcium to phosphorus ratio range is consistent with the molar ratio expected for magnesium whitlockite and ratios recorded in biological depositions (LeGeros *et al.* 1988, Sakae *et al.* 1989), although it does not rule out an apatitic nature for the crystals as calcium-deficient apatites have been described and synthesized. Low Ca/P ratios of apatites precipited under physiological conditions are widely believed to result from structural calcium deficiencies (Berry 1967). Such nonstoichiometric compounds retain HAP structure (as indicated by X-ray diffraction); carbonate-substituted HAP with distorted structure (Blumenthal *et al.* 1975a) and changed lattice parameters (LeGeros *et al.* 1968) has similar diffraction patterns. HAP structure is therefore thought to remain intact over a range of conditions and disorders (Blumenthal *et al.* 1981) . Winard *et al.* (1965) proposed a model by which calcium deficient HAP may exist with a Ca/P ratio from 1.33 to 1.67. This concept was supported by work from Rothwell *et al.* (1980) using ^{31}P NMR analysis. Nancollas *et al.* (1989) have shown, in seeded growth experiments, the formation of nonstoichiometric apatite with a Ca/P ratio varying from 1.49 to 1.65 dependent on pH. Another explanation for HAP with low Ca/P ratios may be interlayering of OCP and HA (Brown 1966). Blumenthal *et al.* (1981) conclude that generally pathologically immature or newly forming bone mineral contains the most calcium deficient apatite.

Silicon has been implicated in the initiation of mineral deposition within the tibiae of young mice and rats (Carlisle 1970), associated with low calcium concentrations near the mineralising front, diminishing as mineral was deposited. Wergedal and Baylink (1974) detected very low levels of silicon in such areas but these were constant, showing no spatial variation with respect to regions of mineral formation. Whilst silicon was detected more frequently in association

with very small crystals, it was also detected in the absence of calcium in the ECM adjacent to such crystals. Silicon is also a potential contaminant of XRMA studies from a variety of sources (Warley and Gupta 1992), although due to the irregular and fluctuating appearance of a signal for silicon it is more likely attributable to contamination.

The range of mean calcium to phosphorus ratios observed may be attributable to a number of factors. First, dissolution due to tissue preparation which, for the reasons discussed above, is considered to be a minor potential source of variation. Secondly, contributions to the phosphorus detected may come from ECM components. Organically bound phosphorus has been identified in reconstituted, demineralised and highly purified collagens (Glimcher *et al.* 1964, Koutsoukos and Nancollas 1986). However XRMA of ECM adjacent to the matrix consistently failed to detect calcium or phosphorus and probes were placed entirely on crystal profiles to generate spectra, omitting contributions from the ECM. A further source of error may arise from the ratio determination method as the background or continuum to be subtracted prior to calculation of calcium to phosphorus ratios was defined manually and hence open to operator bias. Attempts to minimise such variation were made by comparing the background defined during each session against a reference spectrum. Whilst the latter consideration may have affected the ratios across the entire study, in cases where the mean calcium to phosphorus ratios of crystal groups were to be compared, calculation of calcium to phosphorus ratios was performed at the same sitting to negate any variation due to background stripping .

The lack of variation in calcium to phosphorus ratio with crystal morphology agrees with previous observations of calcified bodies in human meniscus (Ghadially and Lalonde 1981) and crystals in human articular cartilage (Rees *et al.* 1986). Faure *et al.* (1982) demonstrated the presence of morphologically distinct microcrystals identified as carbonated apatite with a Ca/P ratio close to that expected for HAP within the same area of pathological calcification as a poorly crystalline material with values around 1.45. The lack of variation with crystal size contradicts the findings of Rees *et al.* (1986) whose results suggested that there was an inverse relationship between crystal size and calcium to phosphorus ratio. The present study is considered more reliable as it is larger and uses thin section samples. Therefore, there is little chance of bias in the results due to variation in the volume of the crystal below the probed crystal surface contributing to the observed spectrum, or the associated problems of emitted x-rays travelling variable distances through the specimen to the detector. Also the TEM probe size is smaller and hence can exclude contributions from the surrounding matrix. The lack of variation in calcium to phosphorus ratio with respect to age from both normal and OA tissue suggests that the crystals are in a stable state and not functioning as intermediaries in a mineral maturation process. From these studies it is not possible to rule out the presence of a fine coating of other mineral at the surface, or epitaxy or mineral phase sandwiching, but no evidence of such processes was apparent.

The relatively new techniques of STXM and SFXM proved to be complimentary to the use of elemental mapping by XRMA , which has superior resolution and sensitivity at higher magnifications and the ability to map any element with an atomic number greater than eleven. The

STXM and SFXM techniques were most useful at lower magnifications, imaging crystal distribution via their calcium signal with respect to full depth cartilage.

Whilst the crystalline bodies described in lapine and porcine articular cartilage in chapter one proved to be a calcium phosphate-type deposit differences between the species were identified. The more distinct crystals from porcine cartilage had a Ca/P ratio within the range of those found in human tissue, whilst the ratio of those from the lapine cartilage were notably higher. Such high ratios may be due to the high backgrounds on these spectra but also it has been reported that rabbits have a predisposition to the deposition of hydroxyapatite crystals in articular cartilage (Yosipovitch and Glimcher 1972).

XRMA is only capable of providing information about elemental composition and is not able to differentiate between two compounds with the same elemental ratios, for example monetite and CPPD both have a Ca/P ratio of 1. However morphological characteristics such as crystalline shape, crystalline size and the behaviour of crystals within the electron microscope (CPPD crystals produce a characteristic frothy appearance as they sublimate under the electron beam (Omar *et al.* 1979, Mitrovic 1983), may give some indication of mineral phase differences. Considering the Ca/P ratio, morphology and size range and characteristic stability under the electron beam it seems most probable that the crystals consist of a homogenous calcium phosphate mineral phase, possibly magnesium whitlockite. The above would justify attempts to isolate and concentrate the crystals for the purpose of electron and x-ray diffraction analyses to determine their mineral phase.

CHAPTER 3
IDENTIFICATION OF CRYSTAL MINERAL PHASE

Introduction

The application of physical methods capable of providing information about mineral phase structure to understanding the role of crystals in biological deposition can provide useful information in two ways. Firstly by understanding the nature of the crystalline deposit and secondly by understanding the processes of crystal growth (Shah 1983). Of interest in this study are the identification of crystal structure and determination of crystallographic parameters, from which information relating to the conditions and mode of crystal formation may be obtained. X-ray powder diffraction is the most reliable technique for detecting and identifying crystalline phases in mineral deposits (Hukins 1989). Electron diffraction has been used to investigate small crystals (Mann 1986).

Single crystal electron diffraction allows mineral phase analysis of crystals at discrete sites in an ultrastructurally relevant manner, which is unattainable with x-ray diffraction techniques. Knowledge of the orientation of the crystal with respect to the crystallographic axes is necessary to record accurate d-spacings (a measurement of spacings between individual crystal planes, a set of all possible spacings of a crystal being characteristic of that crystal) from the diffraction pattern generated, with slight tilting of crystals from a specified plane leading to potential confusion between crystals with similar diffraction patterns. Impurities incorporated into the host lattice, for example F^-, Cl^-, CO_3^{2-}, accommodated substitutionally in the hydroxyapatite lattice (Driessens 1980, LeGeros and LeGeros 1984), alter the lattice parameters of the crystals by small amounts (Shah 1983, LeGeros and LeGeros 1984), increasing the requirement for precise orientation of single crystals. From the previous chapter and earlier studies (Ali 1985, Rees *et al.* 1986), it is suggested that the mineral phase of the 'cuboid' crystals may be an apatite associated with magnesium, or magnesium whitlockite. The diffraction patterns of hydroxyapatite and whitlockite are similar (Hukins 1989), and whitlockite exists in a solid solution series in which small, variable amounts of magnesium substitute for calcium in the crystal lattice (Rowles 1968, Calvo and Gopal 1975). This substitution causes slight changes in the crystallographic lattice axes (Rowles 1968, LeGeros and LeGeros 1984) which are reflected in altered d values in the diffraction pattern. To avoid errors in interpretation of electron diffraction data, a technique was developed for crystal isolation. This enabled diffraction patterns to be generated from a dense mass of crystals present in many orientations, which allowed measurement of a complete series of diffraction rings, minimising potential errors. This was not possible from cartilage sections as crystals were too diffusely distributed. Such isolation also enabled x-ray diffraction analysis.

In consideration of a crystal isolation protocol it was important that the organic phase was removed under conditions that least affected the mineral phase. The possibilities for artefactual transformations have already been discussed. Isolation protocols involving harsh treatments such as ethylenediamine extraction (Williams and Irvine 1954) and autoclaving (Robinson 1952) are prone to unreliable results, with apatitic recrystallization and amorphous to crystalline phase transformations (Termine and Posner 1967). Crystallites of bone mineral have been successfully isolated by Termine and colleagues (1973) and more recently by Weiner and Price (1986). The initial stage of these protocols required milling of specimens in lyophilised, frozen form or grinding

with a mortar and pestle. Considering the differences in tissue characteristics between bone and articular cartilage and the relative abundances of the respective crystals, such treatments were considered inappropriate. A more compatible starting point for crystal isolation was considered to be the protocol used by Ali *et al.* (1970) for the isolation of matrix vesicles from epiphyseal cartilage. This involved collagenase digestion of cartilage to digest the matrix components and release crystals, the digest was then centrifuged at successively higher speeds to spin down particles of increasingly smaller mass. Adaption of this technique was attempted to produce crystal rich pellets. It was anticipated that further treatments may be required to remove organic debris from crystal rich fractions. The use of mild detergents or sodium hypochlorite (Boyde and Jones 1970, Weiner and Price 1986) to remove organic debris from crystal preparations was investigated. Evidence is presented to show that the crystals are unlikely to have been severely altered by the isolation protocol developed.

Materials and Methods

Specimen Details and Crystal Isolation.

Normal and OA femoral heads from the groups of patients described in chapter one were collected within twenty minutes of resection. A small full depth sample of articular cartilage was taken from the superior region of each femoral head for TEM processing then the femoral head was stored at -70°C.

Femoral heads were brought to ambient temperature and the superficial and intermediate zone articular cartilage pared away carefully, under aseptic conditions, to avoid inclusion of calcified zone cartilage or subchondral bone. The condition of cartilage sampled included types I, II, III and IV (Ali and Bayliss 1974), although, types I and II were favoured, when available. The excised cartilage was weighed, minced with a scalpel in 5ml per 0.5g of 50mM *N*-tris-(hydroxymethyl)-2-aminoethane sulphonic acid (TES) buffer, pH 7.4 (Merck, Poole, UK), containing 0.25M sucrose (Merck, Poole, UK) and 1000u/ml Sigma type 1 *Clostridium* collagenase (Sigma, Poole, UK). 10 µl of gentamycin (80g/2ml; Roussel, Uxbridge, UK) were added to the digest which was then incubated at 37°C on a roller mixer for varying times from 4 to 24 hours. On removal from incubation,digests were left to stand for 5 minutes to allow large particulate debris to settle. The supernatant was removed and pellet fractions plus the final supernatant were collected from varying sequential centrifugation regimes, using polyallomer centrifuge tubes in a Beckman L4 ultracentrifuge fitted with a type 65 rotor. The forces used for centrifugation ranged from 200 x g to 60,000 x g.

Pellet fractions and the final supernatant fraction were processed for TEM using the standard processing technique without osmium tetroxide fixation outlined in chapter one. Samples of supernatant were mixed with molten agar (Lab M, Bury, UK.) at approximately 50°C, the mixture allowed to gel and processing proceeded as for the pellets. 100nm sections, cut as described in chapter one were mounted on G 200 HS copper grids with the base of the pellet orientated parallel to one of the grid bar axes and the number of crystals per grid square (13,225μm^2) were counted in a transect from the base of the pellet to the surface. As the

centrifugation regimes were refined, the crystal distribution was averaged over five such transects to detect changes in crystal distribution related to less severe alterations in centrifugation regimes.

To further concentrate crystals within the crystal rich pellet fractions and/or remove organic debris, pellets were subjected to a number of further treatments.

i) Pellets were resuspended in 0.085M sodium cacodylate buffer (pH 7.4) and centrifuged at 35,000 x g for 15 minutes.

ii) Pellets were resuspended in 0.085M sodium cacodylate buffer (pH 7.4) containing 0.01% vv Triton X100 (Fisons, Loughborough, UK) and centrifuged at 35,000 x g for 15 minutes.

iii) Pellets were resuspended in 0.085M sodium cacodylate buffer (pH 7.4) and centrifuged at 35,000 x g for 15 minutes. The resulting pellets were ultrasonicated in 2.6% sodium hypochlorite solution (Merck, Poole, UK.) for 15 minutes and centrifuged at 35,000 x g for 15 minutes. The supernatant was removed and remaining pellets were washed in 0.085M sodium cacodylate buffer (pH 7.4) followed by absolute ethanol with centrifugation as outlined in Fig 3.6.

X-ray Microanalysis.

XRMA was carried out using TEM as described in chapter two. 100nm sections were cut from crystal rich pellets embedded for TEM; isolated precipitates were either incorporated into blocks of molten agar, processed for TEM and sectioned at 100nm thickness or scattered directly onto piolform coated grids for observation and analysis.

Selected Area Electron Diffraction.

100nm sections of crystal rich pellets, processed for TEM and cut as described in chapter one, were mounted on piolform coated copper grids and examined using a Philips CM12 TEM operating at 100kV. Areas with densely packed crystals were selected and diffraction patterns were obtained at a camera length of 2.05m with a spot size of 2μm and an 80nm selected area aperture. The TEM was calibrated in the diffraction mode using a thallous chloride standard (Agar Scientific, Stansted, UK), before d-spacings of experimental patterns were measured. Where diffraction rings were incomplete 10 sets of d-spacings were measured and mean values were taken for comparison with the Joint Committee on Powder Diffraction Standards (JCPDS, Pennsylvania, USA) standard diffraction files.

X-ray Powder Diffraction.

Samples of crystals isolated from articular cartilage removed from a number of femoral heads were pooled to provide sufficient sample for analysis. Data was collected on a Siemens D500 powder diffractometer employing a theta/2 theta Bragg-Brentano geometry with scintillation counter detector. The source radiation was copper $K\alpha_{1/2}$ at 40kV,30mA and inelastic scatter was reduced using a post sample graphite monochromator. The system was controlled by a Microvax 3100 mini computer. Due to their small size, samples were mounted on a flat, single crystal of silicon to reduce background noise and rotated in the x-ray beam to minimise preferred

orientation effects. The samples were scanned from 5° to 50° 2 theta, stepping at 0.05° and counting for approximately 40 or 50 seconds per point. The long count time was necessary due to small sample sizes. The resultant diffraction spectra were compared with JCPDS standard diffraction files for mineral phase identification, then indexed using the Siemens Diffrac 5000 Lattice Parameter Refinement software system to derive lattice constants and unit cell volumes for the samples.

Scanning Electron Microscopy.

Crystals isolated from femoral head articular cartilage and selected known calcium phosphate mineral phases were mounted on aluminium or polished carbon stubs with double sided adhesive tape (Agar Scientific, Stansted, UK.), coated with a 20nm layer of gold in a Polaron E5100 sputter coater fitted with a Polaron E5500 film thickness detector and examined and photographed in either, a JEOL 35C, a JEOL JSM 6300 (courtesy JEOL UK) or a Philips XL 20 (courtesy Philips Analytical UK) scanning electron microscope (SEM) at 7, 20 or 30kV. Samples of synthetic magnesium whitlockite (Dr. P Shellis, Bristol, UK) and ß-tricalcium phosphate (Dr R LeGeros, New York, USA) were prepared and observed as above.

Results

Crystal Isolation.

In the following description of the isolation protocol development, the first pellet is that produced by the lowest centrifugal force and the base of each pellet is the surface that was in contact with the centrifuge tube.

Samples of full depth articular cartilage were removed from femoral heads prior to storage at -70°C and on thawing before tissue mincing and digestion for TEM processing. Ultrathin sections from these samples were compared to observe differences in crystal deposition, attributable to freezing; samples were assessed qualitatively for changes in crystal size, shape, distribution and deposition density. No differences were observed in any of these, although damage to cellular ultrastructure was noted (data not shown). The initial isolation parameters used, derived from the protocols for chondrocyte and matrix vesicle isolation, proved favourable, although, as anticipated, modification was required. A 24 hour incubation period proved necessary to digest the majority of minced cartilage. The remaining macroscopic particles of poorly digested tissue quickly sedimented on standing. The initial centrifugation protocol subjected the supernatant to 8,750 x g for 20 minutes to produce a pellet, then the subsequent supernatant was centrifuged at 60,000 x g for 1 hour to produce a second pellet. The remaining supernatant was also collected. Crystals were observed in the upper half of the first pellet and the lower half of the second pellet, scattered diffusely in both, with an apparently higher density in the first pellet. No crystals were observed in the processed samples of supernatant. The base of the first pellet appeared to be composed of relatively large particulate debris some of which was recognisable as particulate cartilage with *in situ* crystal deposition. The debris amongst isolated

crystals and in the second pellet appeared to be of membranous or lipidic nature, becoming finer in the second pellet.

On the basis of the above, a third centrifugation step was introduced at 35,000 x g for 30 minutes to produce three pellets. The majority of crystals were observed in the first two pellets with the greatest density, though still very diffuse, appearing towards the top of the first pellet. No crystals were observed in the third pellet.The appearance and distribution of the organic debris remained as described above, but spread across three pellets. As a further modification, the 8,750 x g and 35,000 x g steps were maintained and a brief initial fraction was taken at 200 x g for 10 minutes, in an attempt to remove the particulate debris from the pellet with the greatest crystal deposition. The distribution of crystals observed in pellets under this schedule is shown in figure 3.1a. Most of the crystals in the first pellet were associated with recognisable cartilage debris and much of this pellet consisted of large particulate debris. As can be seen from the figure, most of the crystals were spread diffusely through the second pellet or in the lower half of the third, the crystals in this pellet being restricted to the lower end of the size range apparent in cartilage. The debris in the second pellet appeared to be mainly lipidic and membranous; in the third pellet debris was finer and small fibrillar components were observed.

In an attempt to concentrate the diffuse distribution within the 8,750 x g and 35,000 x g pellets, treatments (i) and (ii), described above, were applied to them. Re-suspension of the pellet followed by centrifugation alone (i), appeared to produce a denser crystal band at the base of the pellet. The addition of the detergent Triton X100 to this treatment (ii) appeared only to reduce the size of the individual components of the organic debris, without reducing the volume of the pellets. An alternative approach of increasing the number of centrifugation steps within a narrower overall range was applied. It was anticipated that the organic debris associated with each pellet would be reduced proportional to crystal deposition in the crystal rich pellets. The re-suspension and centrifugation of treatment (i) was applied to each pellet . The distribution of crystals within this series of pellets is outlined in figure 3.1b. It can be seen that the vast majority of crystals were deposited in the 2,250 x g and 4,750 x g pellets and the deposition was at the base of each pellet. The size range of crystals varied between the pellets; in the 2,250 x g pellet, crystals at the pellet base ranged from 50-800nm in any one dimension, with 50-300nm crystals plus the occasional erratic around 800nm observed throughout the depth of the pellet. In the second pellet crystals ranged from 50-500nm at the base, with a range of 50-100nm amongst debris, with isolated crystals up to 200nm. The third pellet contained crystals with a size range from 200-450nm at the base of the pellet with crystals scattered throughout the pellet ranging from 50-100nm a small proportion of which measured up to 150nm. In the final pellet a small precipitate of crystals around 100nm was observed at the base of the pellet, interspersed with a few apatite-like 'needles', whilst 30-50nm crystals remained throughout the pellet. Organic debris still accounted for the majority of the volume of both pellets.

To establish a standard isolation protocol, it was decided to take one pellet at 4,750 x g after discarding the 200 x g pellet, followed by a 19,500 x g pellet, with the associated superatant being discarded. This protocol is shown schematically in figure 3.2. and the typical distribution of

crystals within the series of pellets from this regime is shown in figure 3.1c. This protocol produced one crystal rich pellet in which the crystals formed a dense plug at the base of the pellet with the bulk of the crystals being weighted at the pellet's centre (Fig.3.3). The majority of crystals in this pellet ranged in size from 50-500nm in any one dimension with the largest crystal measured at 610nm. The second pellet contained crystals with a reduced size range of 50-200nm, this being reduced to 30 to 50nm at the top of the pellet. Although the crystal plug of the 4,750 x g pellet was still associated with a large component of organic debris, it proved to be adequate for selected area, electron diffraction studies. Initial attempts to generate x-ray diffraction patterns from such pellets were, however, unsuccessful. The organic component generated a very high background with a broad hump in the spectrum between five and twenty, two theta degrees obscuring any signal from the mineral phase. It was decided to apply treatment (iii) to the 4,750 x g pellet and to the second pellet collected at 19,500 x g to maximise the crystal yield. The resultant pellet from this treatment appeared as a fine white powder on the wall of the centrifuge tube. Under TEM and SEM this appeared to consist primarily of clumps of crystals with a shape and size range consistent with those observed in cartilage sections (Figs. 3.4, 3.5a). The crystal clumps tended to be associated with residual organic debris and amorphous debris, probably shavings of tissue culture plastic incorporated into the digest when the tissue was minced.

The crystals isolated from articular cartilage and observed by SEM exhibited morphologies approximating cuboidal or ovoid (Fig. 3.5a). The size range and shape of many of these crystals exhibited strong similarities to those of synthetic magnesium whitlockite observed under the same conditions (Fig. 3.5b).

No change in crystal morphology was identified between crystals in articular cartilage ECM (Fig. 3.3d.) and either those in the crystal rich pellets (Fig. 3.3c.) or those having been completely isolated (Fig. 3.4). Similarly there was no significant difference in the calcium to phosphorus ratios of crystals in cartilage and those in crystal rich pellets (Table 3.1) or crystals in cartilage and isolated crystals (Table 3.2).

Selected Area Electron Diffraction

Electron diffraction patterns generated from individual crystals within the articular cartilage matrix exhibited ordered reproducible patterns (Fig. 3.6). The area of densely packed crystals at the base of the 4,750 x g pellet generated diffraction patterns that, whilst not having complete rings, contained arcs or rings of closely spaced spots which permitted measurement of d-spacings (Fig. 3.7a). The mean d-spacings for crystal rich pellets from two isolation runs are listed in Table 3.3 and compared to those given in the JCPDS standard file 13. 404 for magnesium whitlockite. This file provided the closest match of any of the calcium phosphate standard files. It can be seen from the table that there is close correlation between diffraction rings with a relative intensity greater than 30% in the standard file and those of the measured patterns. Electron diffraction patterns were also generated from an area at the subchondral bone calcified cartilage interface, to act as a control for the processing and diffraction technique (Fig. 3.7b). The d-spacings were

measured and compared with the JCPDS standard file 9.432 and a precise match was observed (Table 3. 3).

X-ray Powder Diffraction

The total crystal yield from cartilage removed from four femoral heads was pooled for analysis by x-ray powder diffraction, as previous attempts with smaller samples had proved unsuccessful. This pooled sample generated a distinct diffraction spectrum, which was only partially affected by a high background between two and twenty four, two theta degrees, attributed to amorphous material (Fig. 3.8). The spectrum was compared with JCPDS calcium phosphate standard files and was shown to match that of magnesium whitlockite (Fig. 3.8a). As a control trabecular bone chips from resected femoral heads were subjected to the same isolation procedure used for crystals and the resultant mineral analysed by XRMA and x-ray powder diffraction. The isolated mineral had a mean calcium to phosphorus ratio of 1.67(n=10,SD=0.08) and the x-ray diffraction spectrum generated indicated no mineral phase change (Fig.3.8d).

The lattice constants and unit cell volume for the magnesium whitlockite crystals isolated from cartilage are given in Table 3.4. Values of standards and those reported in the literature are given for comparison.

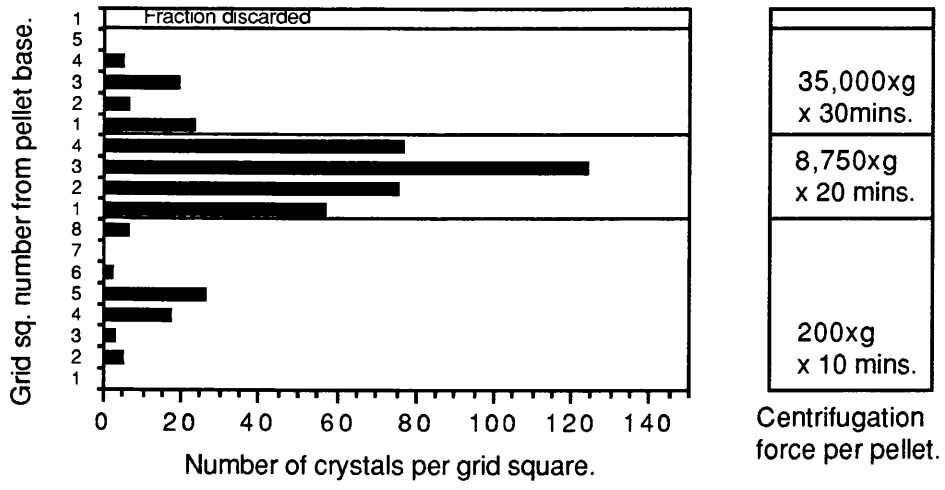

a.

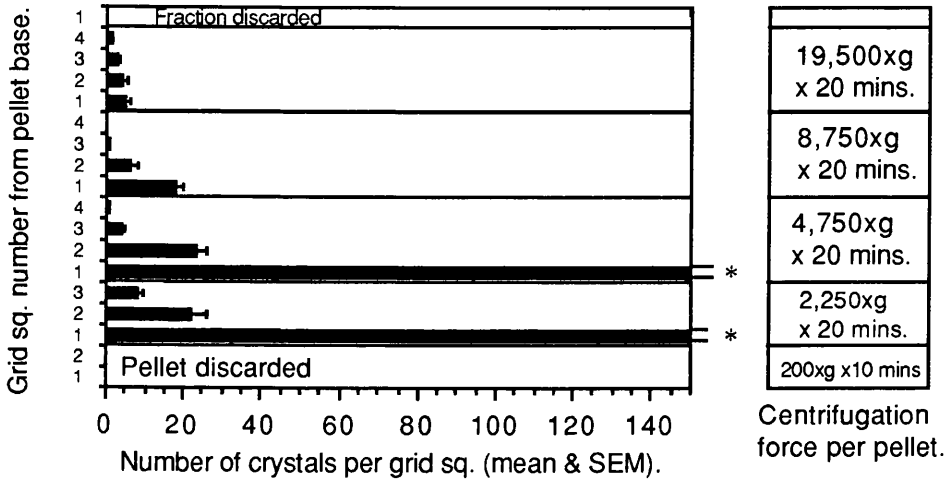

b.

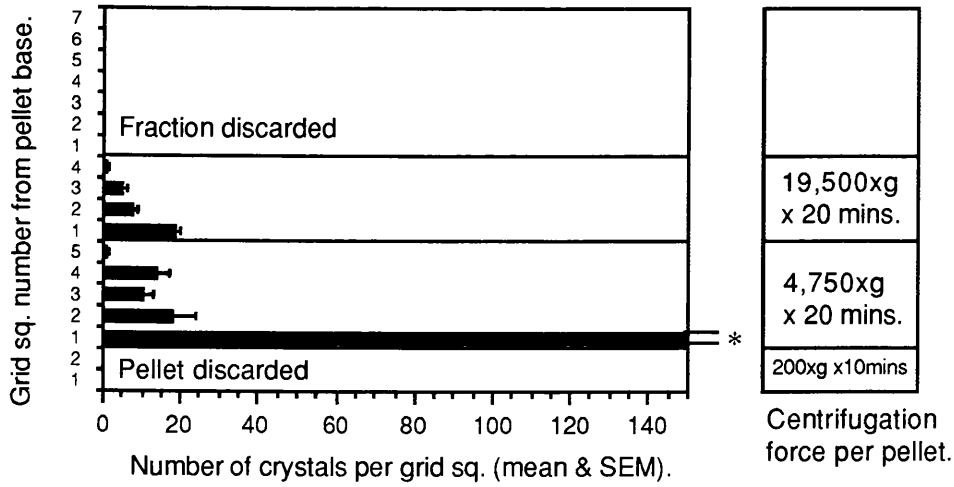

c. * Crystals packed closely covering between 30 & 100 % of the grid sq. (13,225μm^2).

Fig. 3.1. Distribution of crystals in sequential, fractions under different centrifugation regimes: a. pellets collected and examined after each spin, b. 200xg pellet discarded to remove large debris, then sequential pellet fractions resuspended and spun at 35,000xg for 30 mins. prior to examination, c. protocol similar to b., but only two crystal rich pellet fractions were collected.

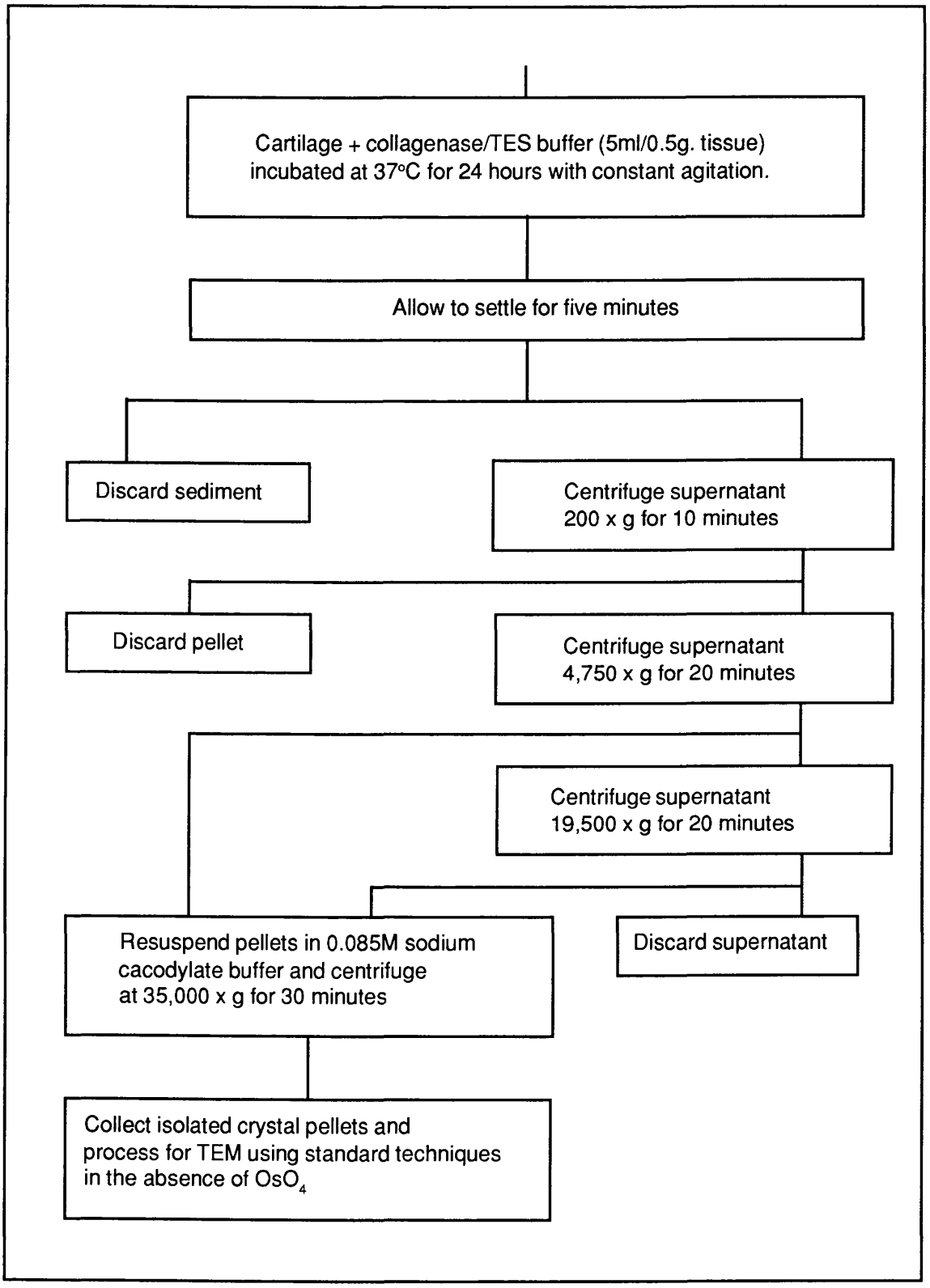

Fig. 3.2. Schematic representation of the final protocol adopted for the production of crystal rich pellets from articular cartilage, for analysis using selected area electron diffraction.

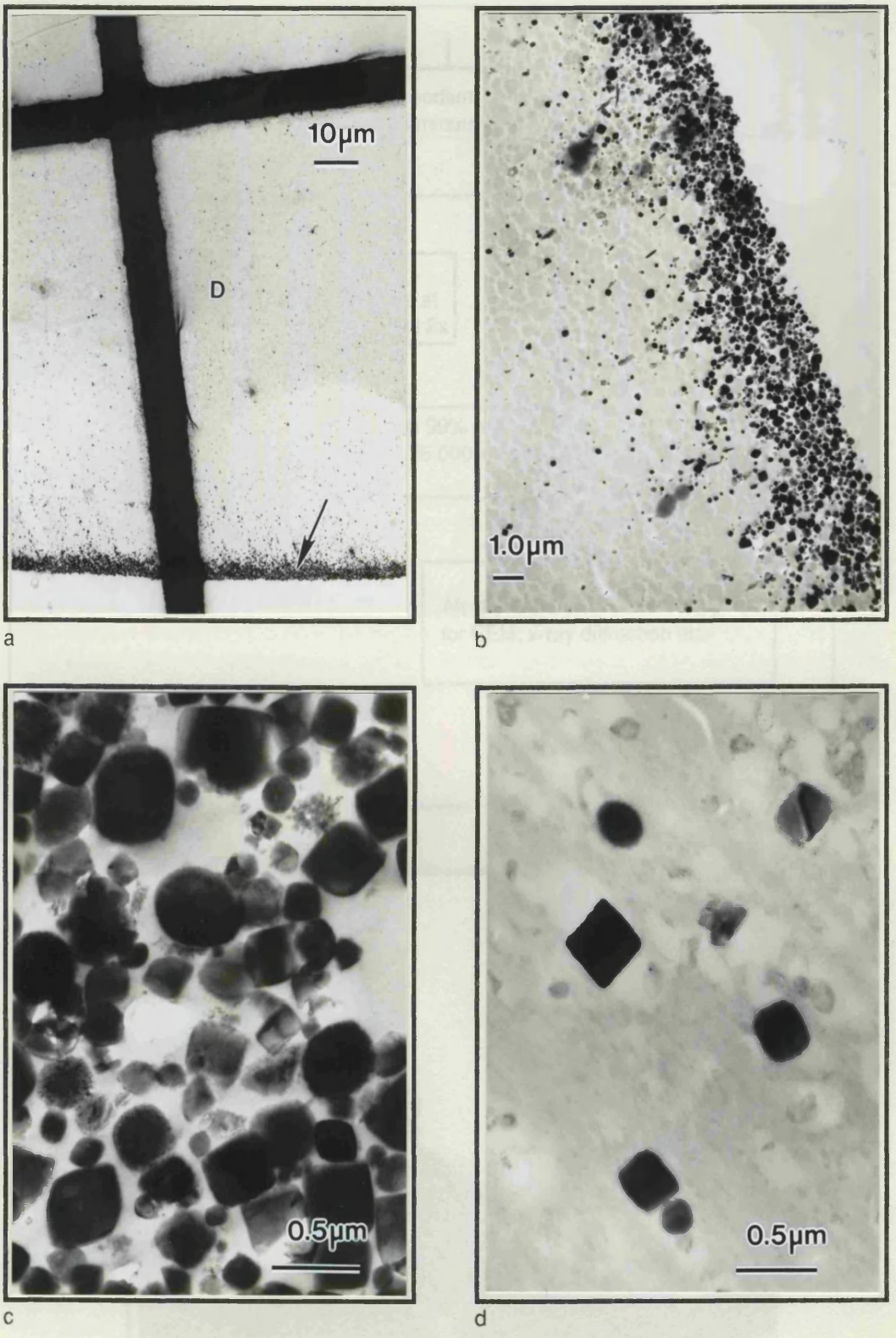

Fig. 3.3. Comparison of the morphology of crystals in femoral head articular cartilage ECM with those in a crystal rich pellet collected from articular cartilage digests from the same femoral head: (a) TS through pellet, showing a dense band of crystals at the base (arrow), below organic debris (D); (b) crystals at the base of a crystal rich pellet; (c) detail of the morphology of isolated crystals, for comparison with (d) crystals in articular cartilage ECM.

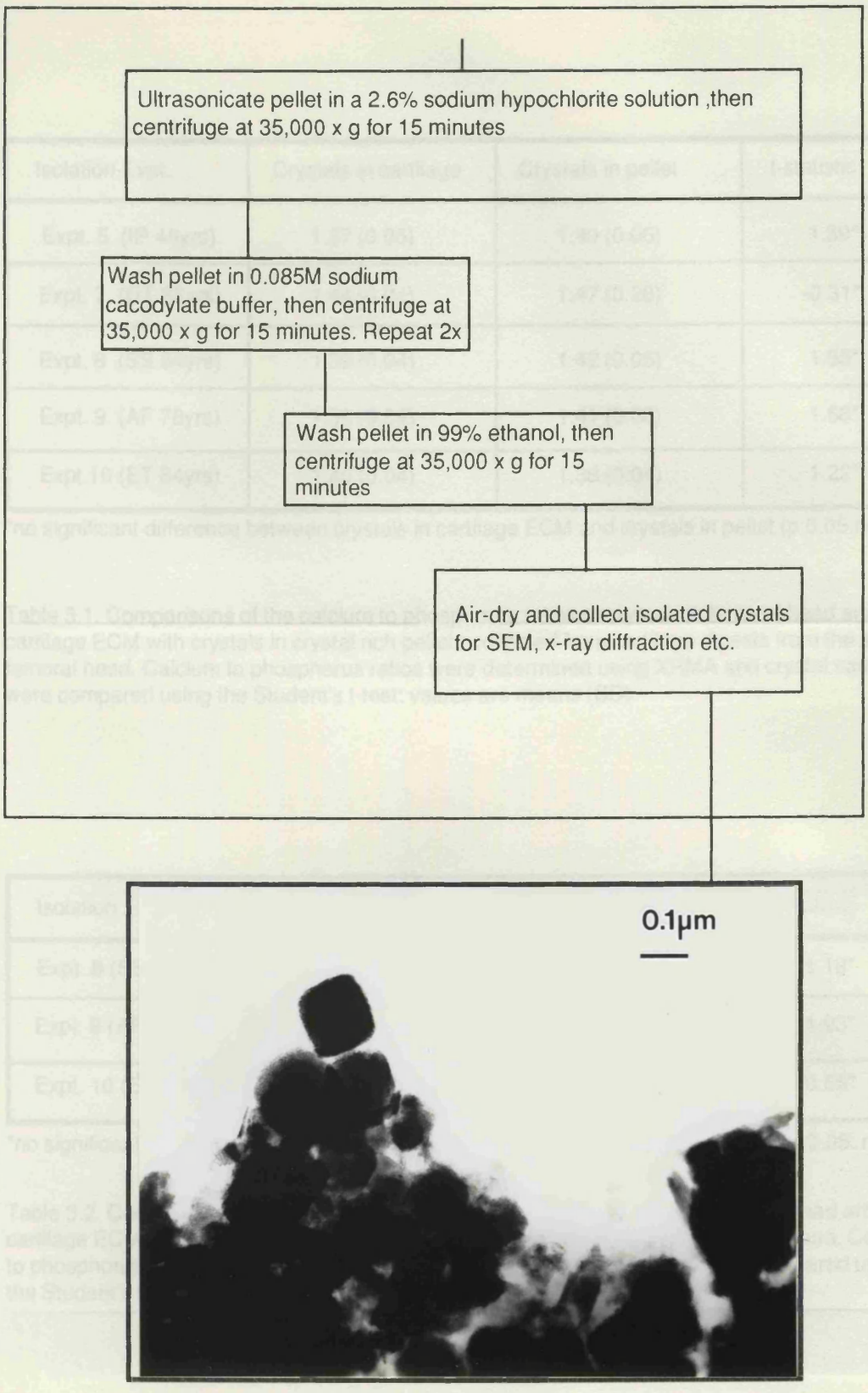

Fig. 3.4. Schematic representation of the protocol adopted to remove the remaining organic debris from crystal rich pellets derived from cartilage digests (see Fig. 3.2). The electron micrograph shows the edge of a clump of isolated crystals on a Piolform coated grid and imaged by TEM.

Isolation Expt.	Crystals in cartilage	Crystals in pellet	t-statistic
Expt. 5 (IP 46yrs)	1.37 (0.05)	1.40 (0.06)	1.39*
Expt. 7 (DT 87yrs)	1.44 (0.04)	1.47 (0.28)	-0.31*
Expt. 8 (SS 84yrs)	1.39 (0.04)	1.42 (0.05)	1.55*
Expt. 9 (AF 78yrs)	1.36 (0.04)	1.41 (0.08)	1.68*
Expt.10 (ET 84yrs)	1.40 (0.04)	1.38 (0.04)	1.22*

*no significant difference between crystals in cartilage ECM and crystals in pellet (p 0.05:n=10).

Table 3.1. Comparisons of the calcium to phosphorus ratios of crystals in femoral head articular cartilage ECM with crystals in crystal rich pellets collected from cartilage digests from the same femoral head. Calcium to phosphorus ratios were determined using XRMA and crystal samples were compared using the Student's t-test: values are means (SD).

Isolation Expt.	Crystals in cartilage	Isolated crystals	t-statistic
Expt. 8 (SS 84yrs)	1.39 (0.04)	1.41 (0.04)	1.18*
Expt. 9 (AF 78yrs)	1.36 (0.04)	1.41 (0.06)	1.93*
Expt. 10 (ET 84yrs)	1.40 (0.04)	1.39 (0.04)	0.55*

*no significant difference between crystals in cartilage ECM and isolated crystals (p 0.05: n=10)

Table 3.2. Comparisons of the calcium to phosphorus ratios of crystals in femoral head articular cartilage ECM with crystals isolated from cartilage digests from the same femoral head. Calcium to phosphorus ratios were determined using XRMA and crystal samples were compared using the Student's t-test: values are means.

Fig. 3.5

Fig. 3.5a. 'Cuboid' crystals, isolated from femoral head articular cartilage by collagenase digestion, centrifugation and treatment with sodium hypochlorite, imaged by SEM.

Fig. 3.5b Synthetic magnesium whitlockite crystals imaged by SEM for comparison with 3.5a; note the apparent cuboid or rhombohedral morpholgy (arrows).

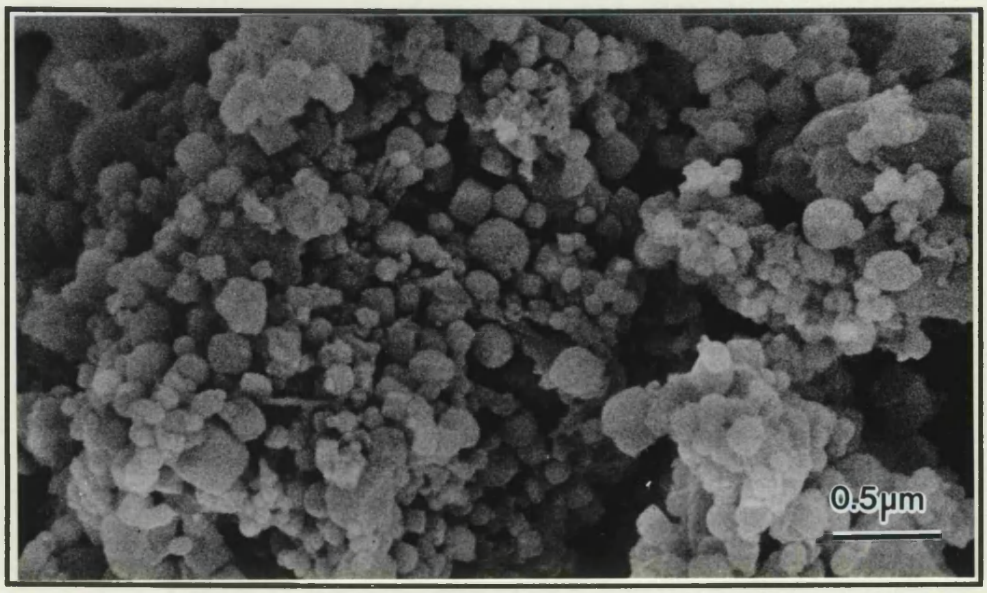

a

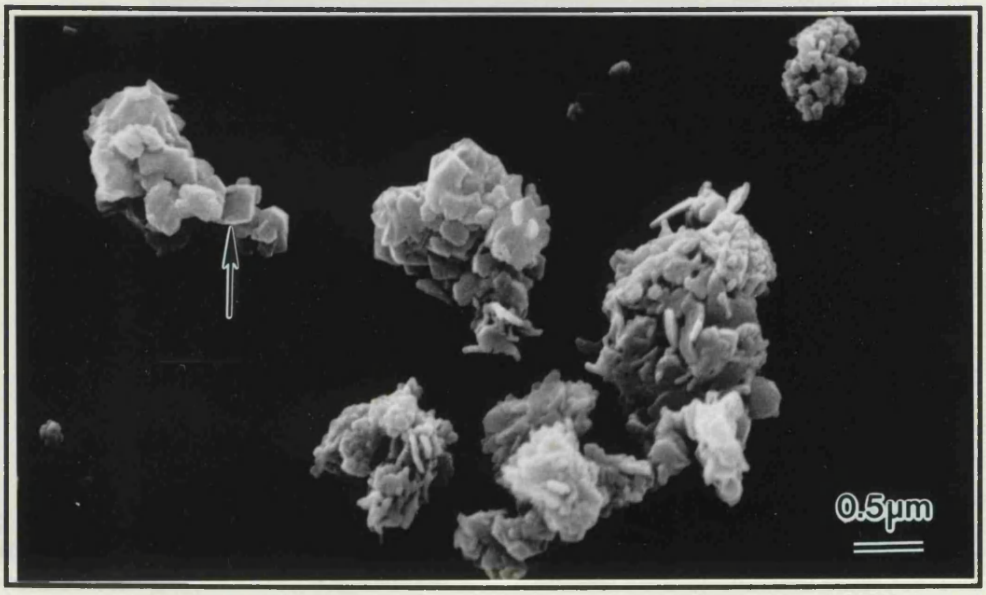

b

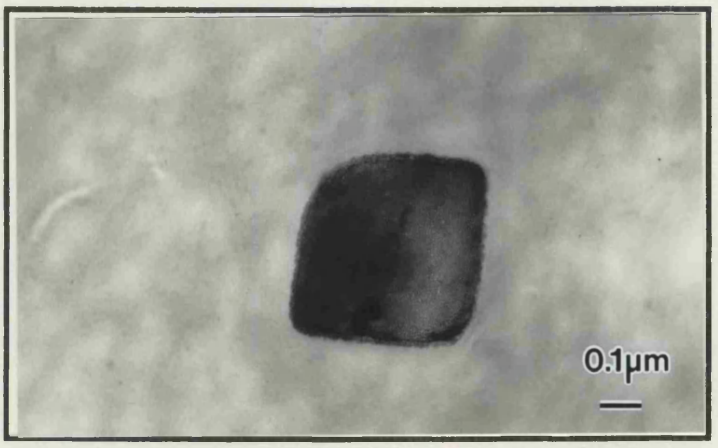

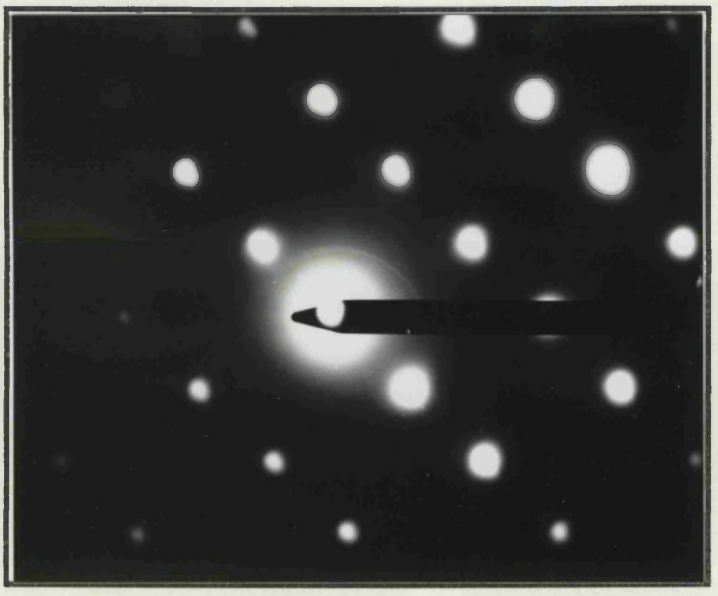

Fig. 3.6. Transmission electron micrograph of a 'cuboid crystal' in femoral head articular cartilage matrix (YA 16yrs.)and the corresponding selected area electron diffraction pattern generated from it.

Fig. 3.7

Fig. 3.7a. A selected area electron diffraction pattern from a 'cuboid' crystal preparation. Crystals were present in an ultrathin resin section (standard processing) of a crystal rich pellet produced by collagenase digestion and centrifugation as outlined in Fig. 3.2. Although diffraction rings were incomplete it was possible to measure d-spacings to clearly defined arcs. The 110 ring is indicated for reference (arrow).

Fig. 3.7b. Electron micrograph of the area from which the diffraction pattern in 3.7a was generated. 'Cuboid' crystals are present along the bottom edge of the pellet.

Fig. 3.7c. A selected area diffraction pattern from an area of the calcified zone of femoral head articular cartilage, close to the subchondral bone interface. The tissue was processed for TEM by the standard technique. The 002 ring is indicated for reference (arrow), evidence of preferred orientation of crystals within the tissue is apparent here .

Fig. 3.7d. Electron micrograph of the area of calcified zone articular cartilage from which the diffraction pattern in 3.7c was generated.

a

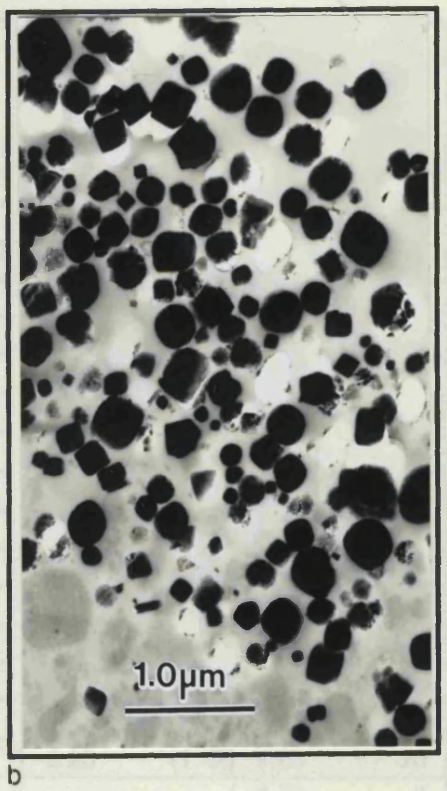

b

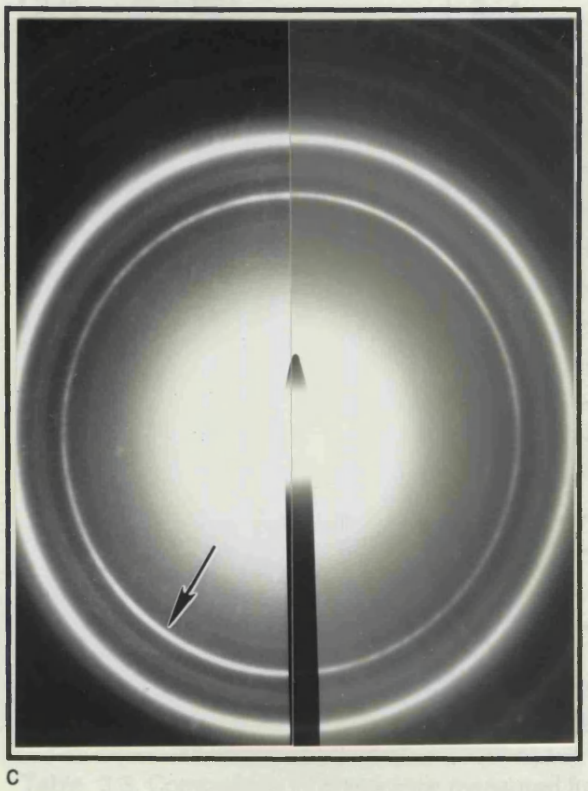

c

d

Crystal isolation specimen A.		Crystal isolation specimen B.		Mg whitlockite standard file.		Subchondral bone specimen.		Hydroxyapatite standard file.	
d-spacing	(n: SD)	d-spacing	(n: SD)	d-spacing	Int. %	d-spacing	(n: SD)	d-spacing	Int. %
8.06	(2: 0)	-	-	8.01	20	-	-	8.17	12
6.30	(2: 0.3)	6.47	(1: 0)	6.35	30	-	-	5.26	6
5.21	(10: 1.64)	5.21	(9: 2.4)	5.22	45	-	-	4.72	4
4.09	(4: 8.03)	4.07	(5: 2.6)	4.02	30	-	-	4.07	10
3.44	(7: 2.76)	3.44	(5: 2.3)	3.41	55	-	-	3.88	10
3.33	(2: 2.8)	3.31	(1:0)	3.3	10	-	-	3.51	2
3.16	(5:1.8)	3.16	(4: 1.4)	3.16	65	3.44	(4: 0)	3.44	40
2.97	(1: 0)	-	-	2.97	10	-	-	3.17	12
2.83	(6: 1.3)	2.86	(6:1.4)	2.84	100	-	-	3.08	18
-	-	2.73	(2: 0.7)	2.72	25				
-	-	-	-	2.67	10	2.77	(1: 0)	2.77	60
-	-	-	-	2.64	5	2.72	(1:0)	2.72	60
2.56	(9: 3.81)	2.56	(9: 2.5)	2.57	80	-	-	2.63	25
-	-	-	-	2.53	10	-	-	2.52	6
-	-	-	-	2.49	10	-	-	2.30	8
-	-	2.38	(2: 0.7)	2.38	20	2.28	(1: 0)	2.26	20
-	-	-	-	2.34	10	-	-	2.23	2
-	-	-	-	2.23	20	-	-	2.15	10
-	-	2.19	(1: 0)	2.17	20	-	-	2.13	4
2.15	(3: 1.52)	-	-	2.14	30	-	-	2.07	8
-	-	2.08	(1: 0)	2.08	10	-	-	2.04	2
-	-	-	-	2.05	10	-	-	2.0	6
-	-	-	-	2.01	30	1.95	(4: 0.5)	1.94	30
-	-	1.97	(3: 0.6)	1.98	10	-	-	1.89	16
1.93	(4: 3.56)	1.94	(1: 0)	1.91	50	-	-	1.87	6
-	-	-	-	1.88	30	1.85	(4: 0.5)	1.84	40
1.85	(2: 1.41)	1.87	(2: 6)	1.86	30	-	-	1.81	20
-	-	-	-	1.81	10	-	-	1.78	12
-	-	-	-	1.79	20	-	-	1.75	16
-	-	-	-	1.78	10	1.73	(4: 0.5)	1.72	12
-	-	-	-	1.75	20	-	-	1.68	4
1.69	(1: 0)	1.70	(8: 2.7)	1.70	80	-	-	1.64	10
-	-	-	-	1.69	15				

= measured d-spacings (Å) of frequently observed diffraction rings which closely match those of JCPDS standard files.

Table. 3.3. Comparison of d-spacings measured from electron diffraction patterns generated by two groups of isolated crystals with the 13.404 magnesium whitlockite standard file. The d-spacings measured from diffraction patterns generated by mineral at the calcified cartilage / subchondral bone interface are compared to the 9.432 hydroxyapatite standard file as a control. Experimental values are means (n: SD).

Fig. 3.8

Fig. 3.8a. An x-ray diffraction pattern generated from 'cuboid' crystals isolated from articular cartilage. Crystals were isolated using collagenase digestion, centrifugation and sodium hypochlorite treatment. The diffraction pattern (blue) is compared with a magnesium whitlockite standard file (13-404, JCPDS: green), showing an identifying match.

Fig. 3.8b. 'Cuboid' crystal pattern from 3.8a (blue) compared with a ß- TCP standard file (9-169, JCPDS: green); similarities are present, but the the two patterns do not clearly match.

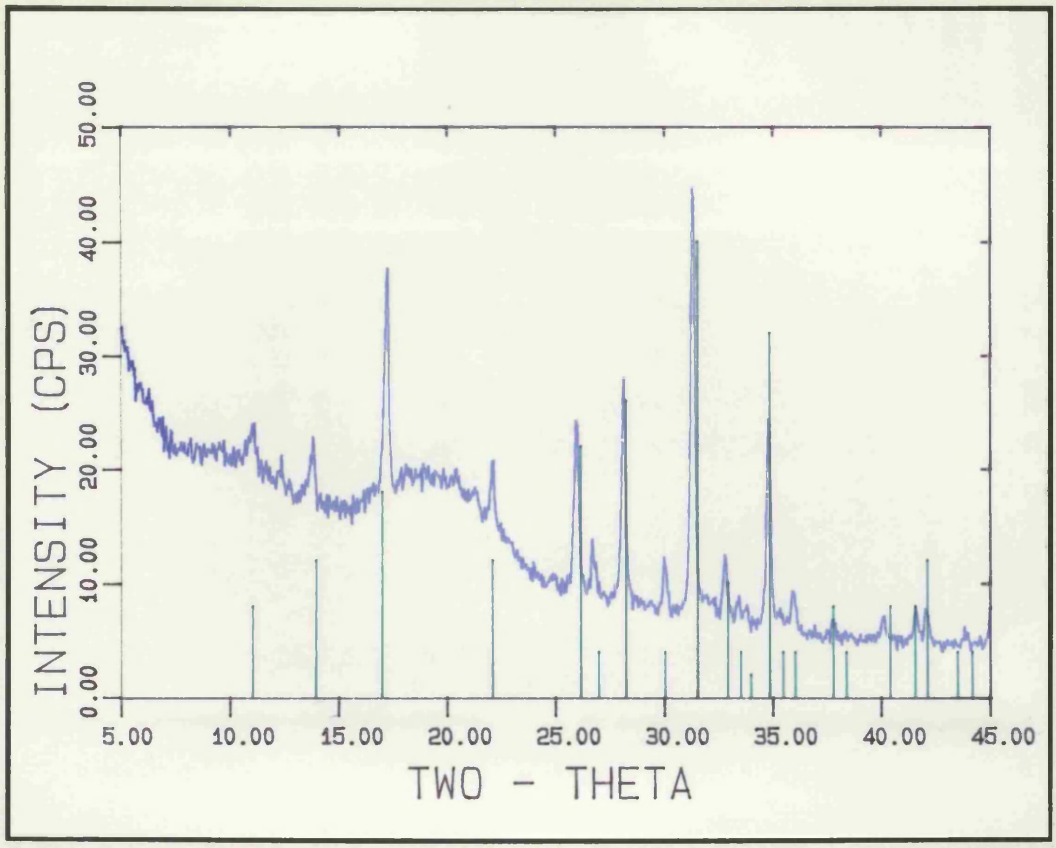
INTENSITY (CPS)
0.00
10.00
20.00
30.00
40.00
50.00
5.00
10.00
15.00
20.00
25.00
30.00
35.00
40.00
45.00
TWO - THETA

a

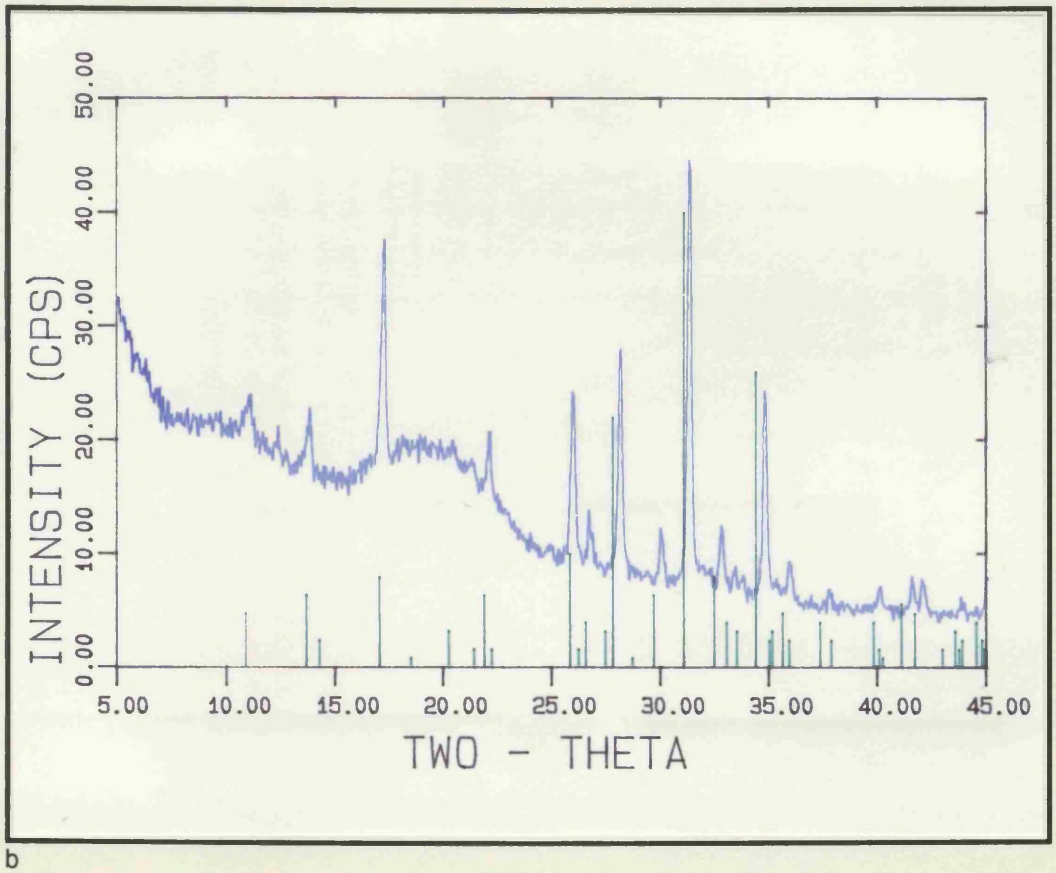
INTENSITY (CPS)
0.00
10.00
20.00
30.00
40.00
50.00
5.00
10.00
15.00
20.00
25.00
30.00
35.00
40.00
45.00
TWO - THETA

b

Fig. 3.8

Fig. 3.8c. 'Cuboid' crystal pattern from 3.8a (blue) compared with a hydroxyapatite standard file (9-432, JCPDS: green); the two patterns are clearly different.

Fig. 3.8d. An x-ray diffraction pattern generated from bone mineral isolated using the same technique employed for cuboid crystal isolation. The diffraction (blue) is compared with a hydroxyapatite standard file (9-432, JCPDS: green) showing a clear match, indicating no gross alteration of bone mineral phase during the isolation process.

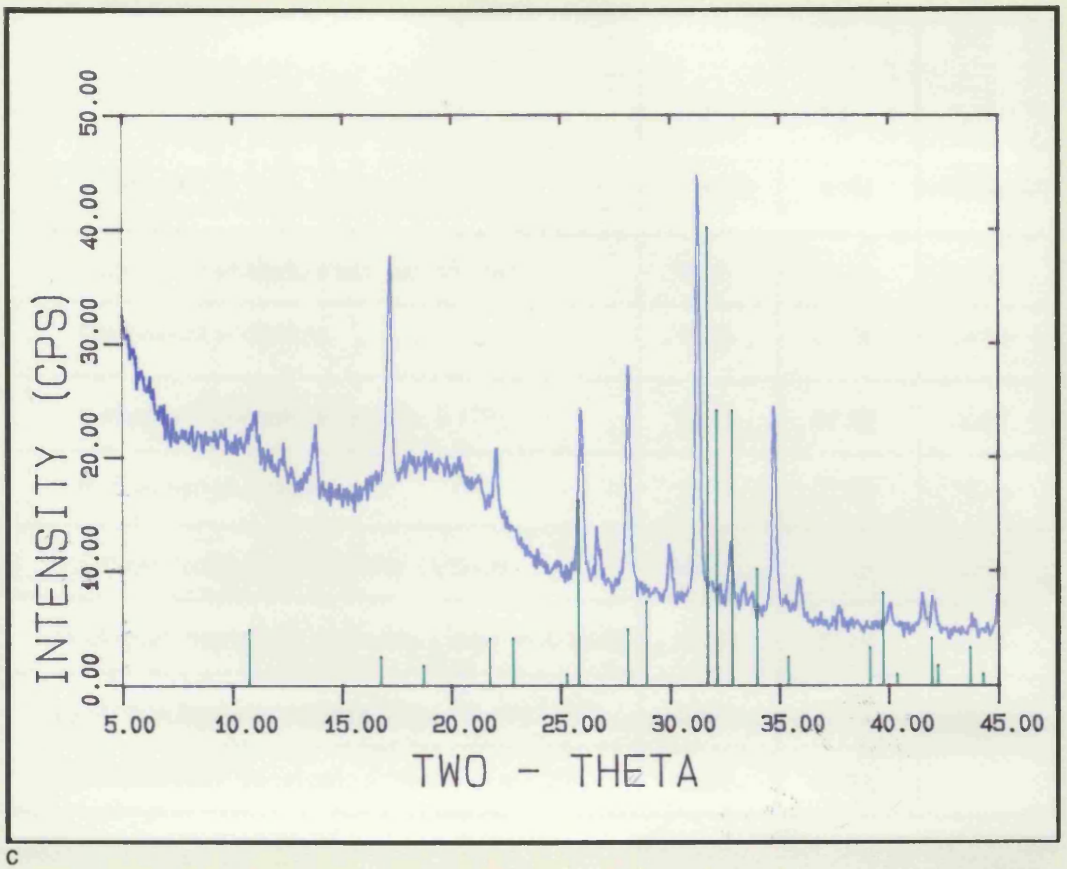
INTENSITY (CPS)
0.00
10.00
20.00
30.00
40.00
50.00
5.00
10.00
15.00
20.00
25.00
30.00
35.00
40.00
45.00
TWO - THETA

c

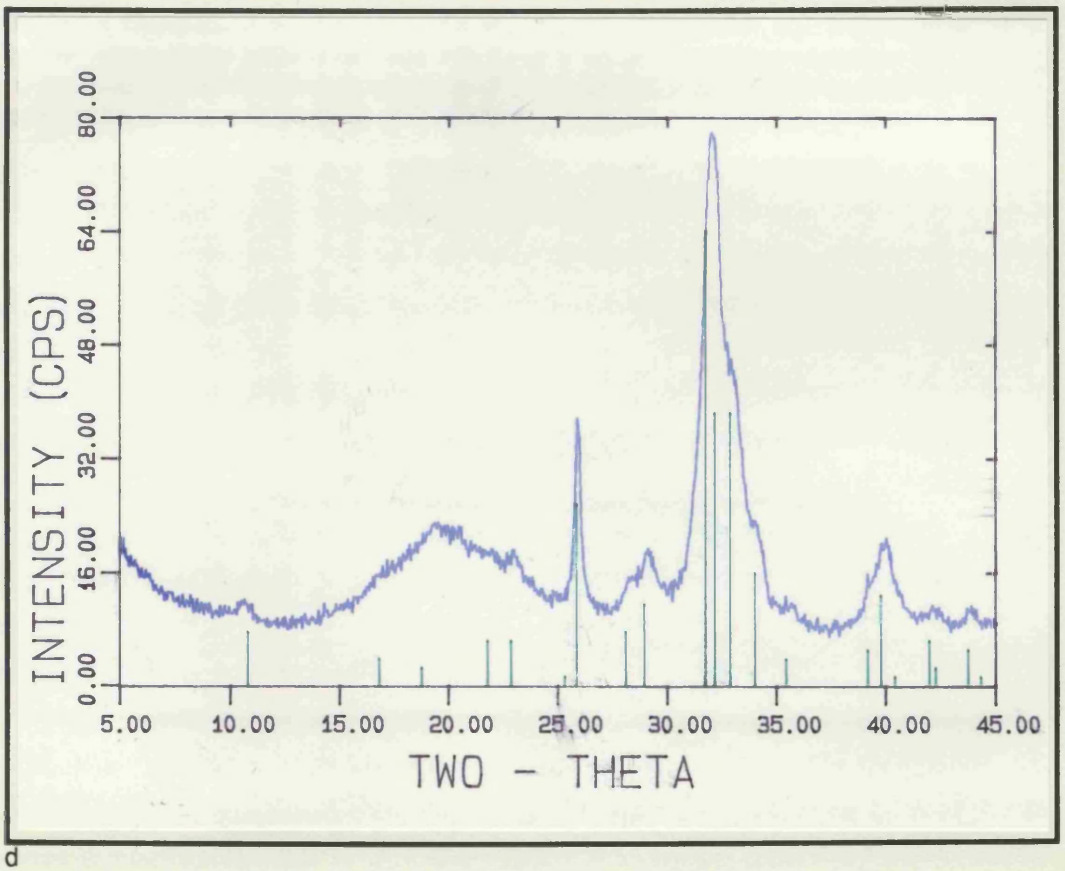
INTENSITY (CPS)
0.00
16.00
32.00
48.00
64.00
80.00
5.00
10.00
15.00
20.00
25.00
30.00
35.00
40.00
45.00
TWO - THETA

d

Mineral	Lattice constants		volume (Å³)
	a (Å)	b (Å)	
Magnesium whitlockite (std. file: 13.404)	10.37	37.19	3464
Magnesium whitlockite	10.35	37.09	3440
ß-tricalcium phosphate (std. file: 9.170)	10.43	37.38	3522
ß-tricalcium phosphate	10.43	37.31	3516
Crystals isolated from articular cartilage	10.31	37.19	3426
Geological magnesium whitlockite (Gopal *et al* 1975)	10.33	37.10	3428
Whitlockite from intervertebral disc (Rowles 1968)	10.31	37.19	-
Whitlockite from dental calculi (Sakae *et al* 1989)	10.35	37.24	-

Table 3.4. Comparison of lattice constants and unit cell volumes of crystals isolated from human femoral head articular cartilage with those of known magnesium whitlockite and ß-tricalcium phosphate mineral phases, geological and biological whitlockites reported previously and the corresponding JCPDS standard files.

Discussion

The identification of the 'cuboid crystals' mineral phase as magnesium whitlockite is only significant if the possibility of mineral phase changes due to the crystal isolation treatments can be eliminated.

The crystals used in this study were derived from cartilage that had been stored at -70°C. It could be speculated that freezing may cause or increase crystal deposition. Studies of storage of synovial fluid samples containing calcium pyrophosphate crystals (McGill *et al.* 1991) indicated that storage of crystals in their original mileau was optimised at -70°C, with no new crystal formation, existing crystal dissolution, or morphological change being detected. The dissolution of CPPD crystals had been reported previously within one week of storage at room temperature and 4°C (Kerolus *et al.* 1989), although such drastic changes were not detected in the subsequent study. McGill *et al.* (1991) suggested enzyme activity may be involved in crystal dissolution. Recent TEM, freeze/thaw studies, using rabbit femoral condyle articular cartilage, did not demonstrate any mineral formation in tissue that had been stored at -70°C (Tavakol *et al.* 1993). In the light of these studies and the observation of cartilage specimens from the same femoral head taken before and after freezing, storage of specimens at -70°C was considered.acceptable.

Although it has been demonstrated that crystal morphology, observed by SEM, as an indicator of calcium phosphate mineral phases in biological calcifications can be misleading, (Santos and Gonzalez-Diaz 1980, LeGeros *et al.* 1988, Sakae *et al.* 1989), the lack of change in either Ca/P ratio or crystal morphology suggests that the mineral phase of crystals is not altered due to any of the treatments to which they were subjected during crystal isolation. This conclusion is further supported by the control studies analysing bone mineral, processed using the same technique, by both electron and x-ray diffraction. On the basis of solubility studies, using synthetic calcium phosphate mineral phases, Driessens (1988) reports that magnesium whitlockite is less soluble than HAP under the same physico-chemical conditions. It would seem reasonable to accept therefore that the mineral phase identified using the two diffraction techniques is the same phase that may be observed in articular cartilage by TEM using the three processing techniques described in chapter one. Indeed treatments reported to convert other mineral phases to artefactual magnesium whitlockite are high temperature (900°C+) or radio frequency, ignition or ashing techniques in the presence of magnesium (Blatt *et al.* 1958, Ennever and Vogel 1980) The maximum temperature any of the crystals examined in this study have been exposed to is 60°C whilst those prepared for x-ray diffraction were subjected to temperatures not greater than 37°C.

The choice of TES-sucrose buffer for initial incubation and isolation was made to exclude any extraneous phosphate from the system that might interfere with later analyses. This has been used previously to isolate matrix vesicles from epiphyseal cartilage with the associated initial mineral phase intact (Ali *et al.* 1970). Disaggregation of bone using sodium hypochlorite solution has been shown not to grossly alter the mineral phase, crystal size or shape of the isolated crystals (Weiner and Price 1986, Moradian-Oldak *et al.* 1991). In the studies cited crystals were

washed in distilled water saturated with respect to hydroxyapatite. It was reported that in the hypochlorite treated crystals did not undergo 'ripening' in saturated solutions, in contrast to the behaviour of untreated crystals. Moradian-Oldak *et al.* (1991) attribute this phenomenon to the sodium hypochlorite affecting the crystal surface; this was not considered to significantly affect mineral phase and morphology studies (Moradian-Oldak *et al.* 1991). In the present study the hydroxyapatite-saturated water was replaced with 0.085M sodium cacodylate buffer (pH7.4), on the basis of earlier observations described in chapter one, to avoid introduction of extraneous calcium and phosphate into to the system. A very recent report (Swan *et al.* 1992) has described the development of a similar technique to the one used in this study, for extracting CPPD and HAP crystals from articular cartilage. This also involved enzyme digestion, centrifugation and sodium hypochlorite treatment, also control experiments exposing synthetic CPPD and HAP crystals to the extraction procedure were undertaken. These experiments indicated that the recovery of crystals was good and that, of those recovered, no alteration or addition of new material, as a result of the procedure, was detected; further supporting the validity of the technique developed in this study.

The standard isolation protocol developed for crystal analysis proved to be the most economical method of preparing the limited crystal yields for a variety of uses. The two step isolation provided the option of a crystal rich pellet for TEM processing and thin section analysis, or to completion of the schedule to produce a crystal preparation with associated debris which did not interfere with mineral phase analyses. To maximise the crystal yield, the second pellet, produced at higher speed, was also taken to this stage, the yields being combined upon completion of the process. Although not an immediate problem, the debris associated with the final crystal isolate would need to be considered if this protocol was extended to produce crystals for coincubation in tissue culture studies. The use of sterilised glass petri dishes during cartilage mincing may prove effective in reducing the amount of extraneous debris. Further washing with the possible introduction of a mild detergent may be investigated to eliminate lingering organic debris.

As the electron diffraction patterns of individual 'cuboid crystals' are characteristic of single crystals, the previous reports of these crystals, inferring such a structure, are justified (Ali and Griffiths 1981, 1983, Marante *et al.* 1983, Ali 1985, Stockwell 1990). This analysis is not consistent with observations of apparently similar structures from other sites, using SEM and TEM, described in the literature. Particles reported by Faure *et al.* (1980), from a subcutaneous calcification of a patient with scleroderma and described as ovoid and spherical of a similar size to the upper end of the 'cuboid' crystal range, were considered to be agglomerations of apatite microcrystals. Crystals identified as apatite reported by Pritzker and Luk (1976) from knee joint synovial fluid and a pulmonary nodule were described as ovoid or spheroidal and 100 to 1000nm in size with an electron dense shell surrounding an electron lucent core; these were suggested to represent crystal deposition about an electron lucent impurity. They interpretted these particles as being complex aggregations of hydroxyapatite crystallites combined with a more amorphous calcium phosphate. The TEM and SEM images of crystals,particularly from the pulmonary nodule

bore a strong resemblance to those from this study. The SEM images of isolated 'cuboid' crystals confirm the approximately cuboidal or spherical shape suggested from TEM studies, and support SEM observations of plasma-ashed thick sections of crystal containing articular cartilage by Rees *et al.* (1986).

This is the first report of magnesium whitlockite in articular cartilage and would account for the 'cuboid', or more precisely rhombohedral morphology (Frondel 1941) of crystals described in this study and elsewhere (Ali and Griffiths 1981,1983, Marante *et al.* 1983, Ali 1985, Stockwell 1990). The crystals are similar to those described for this mineral in synthetic (LeGeros *et al.* 1989), geological (Frondel 1941) and biological samples (Vahl *et al.* 1964, Schupbach *et al.* 1992); a more common observation than the variants described by Santos and Gonzalez-Diaz in human urinary calculi (1980) and Sakae *et al.* in dental calculi (1989).

Magnesium whitlockite deposition has been reported in a number of biological calcifications, both as calculi and in tissues and is reported to be a minor constituent of bone mineral (Driessens and Verbeeck 1986). On the basis of solubility studies of synthetic calcium phosphate mineral phases and experimental analyses of bone mineral from a number of species, Driessens and colleagues have attributed up to fifteen percent of the inorganic phase of bone to magnesium whitlockite, co-occurring with carbonated apatite phases as separate crystalline particles (Driessens 1980, 1988, Driessens and Verbeeck 1980, 1986). Identification of pathological depositions containing magnesium whitlockite has been reported from a diversity of sites. The most common of these are orally associated, with sites including dental calculi, particularly sub-gingival (Tovberg Jensen and Rowles 1957, Knuuttila *et al.* 1979, Kani *et al.* 1983, Sundberg and Friskopp 1984, LeGeros *et al.* 1988, Sakae *et al.* 1989), arrested carious dentine (Vahl *et al.* 1964, Rowles and Levine 1973, Daculsi *et al.* 1987, Schupbach *et al.* 1992), and sialoliths associated with submandibular and parotid salivary glands (Burstein *et al.* 1979). The occurrence of whitlockite has also been reported in urinary calculi (Santos and Gonzalez-Diaz 1980, Verplaetse *et al.* 1985), though it is considered a minor component in such situations. Deposition of whitlockite within tissues has been reported at various sites including, aortic valvular tophi (Gawoski *et al.* 1985), pulmonary calcifications (LeGeros *et al.* 1973, Bestetti-Bosisio 1984), though this was not conclusive, and in cartilage from the nasal septum, trachea, epiglottis and intervertebral disc (Rowles 1968). McCarty and colleagues (1983) have also identified whitlockite amongst crystal populations of synovial fluid from the shoulder joint of a patient exhibiting symptoms consistent with 'Milwaukee Shoulder syndrome', by fourier transform infra-red spectroscopic (FTIR) analysis. In a number of these reports the authors were unable to comment on the biological significance of the presence of whitlockite (McCarty *et al.* 1983, Gawoski *et al.* 1985).

Magnesium whitlockite was discovered by Frondel in1941; it was described as a geological mineral of hydrothermal origin, although subsequent reports of its presence in human dental calculi (Tovberg Jensen and Rowles 1957) showed that the formation was not exclusively a high temperature phenomenon. The calcium phosphate lattice of the mineral was shown to be stabilised by the substitution of other cations including magnesium, manganous and ferrous ions

(Rowles 1968). In biological calcifications this is restricted to magnesium (Rowles 1968), although traces of ferrous ions have been reported in whitlockite depositions from subgingival dental calculi (Sundberg and Friskopp 1984) . The x-ray diffraction pattern of whitlockite is similar to that of ß-TCP(Tovberg Jensen and Rowles 1957, Calvo and Gopal 1975). ß-TCP does not form from aqueous systems (LeGeros *et al.* 1989) and may only be formed at temperatures around 900°C (LeGeros and LeGeros 1984), however the use of these two terms has become confused. In this study magnesium whitlockite will be used for the mineral phase in which Mg^{2+}, H_20 and $HP0_4^{2-}$ play a structural role and ß-TCP for the mineral with the formula $Ca_3(PO_4)_2$ in which these three components are absent. A third variant is possible in which H_2O and HPO_4^{2-} are absent but Mg^{2+} have replaced some of the Ca^{2+} ions in the ß-TCP structure. However it seems reasonable to assume that ß-TCP-like substances made in aqueous systems in the presence of Mg^{2+} contain structural Mg^{2+}, H_2O and HPO_4^{2-} and hence be considered magnesium whitlockites (Dr JC Elliott, personal communication). In biological depositions the mineral exists in a solid solution series, with magnesium substituting for calcium in varying amounts. The smaller size of the magnesium ion relative to the calcium ion has been used to explain the observed contraction in lattice constants with increasing substitution of magnesium for calcium. Rowles (1968), from *in vitro* studies, and Knuuttila *et al.* (1980) from *in vivo* demonstration with dental calculi, noted that the a axis of the crystal structure contracts as the magnesium content increases to a maximum of fifteen percent of the cations, with a change in slope at ten percent, whilst the c axis also contracts with increasing magnesium content, but reaches a minimum at around ten percent sustitution, expanding again up to a maximum of about fifteen percent of the cation. This has been explained by structural work on preferred sites of cation substitution relative to the percentage of magnesium ions already present (Terpstra *et al.* 1983, Elliot personal communication). The relationship has been used to estimate the percentage of magnesium present in biological whitlockites (Rowles 1968, LeGeros and LeGeros 1984.). Marked differences have been reported between the lattice constants of whitlockites formed in calculi and those from cartilages (Rowles 1968). The lattice constants calculated for the whitlockite crystals in articular cartilage correspond with those of tracheal and intervertebral disc cartilage. This would correspond to a magnesium content of 4% by weight according to LeGeros and LeGeros (1984), and approximates to the 3.8% reported by LeGeros (1974) as the theoretical maximum magnesium substitution.

Studies designed to simulate the *in vivo* physico-chemical micro-environment of bone and other calcification sites in order to determine the effects of magnesium on the formation and transformations of various calcium phosphates known to occur in biological systems have enabled Cheng and co-workers (1983, 1988) to identify conditions in which magnesium whitlockite is the energetically favoured mineral phase. Initial studies showed that the presence of magnesium in, and the Ca/P ratios of, the solutions were important in determining whether whitlockite would precipitate or not. Subsequent work defined these conditions more specifically and showed that with low $[Ca^{2+}]$ (1nM), no *de novo* mineral precipitation occurred, though brushite was detected and transformed to HA. Whitlockite only precipitated at higher $[Ca^{2+}]$ (3mM) and was formed

directly from an initial amorphous phase from solutions with $[Ca^{2+}]$=3mM, $[Mg^{2+}]$ =1mM and [Pi] (10-30mM). When solutions contained $[Ca^{2+}]$=3mM, [Pi] (10-30mM) with a Mg/Ca ratio ≤1 an amorphous phase precipitated initially, transformed to hydroxyapatite, with a further transformation to whitlockite. Solutions containing $[Ca^{2+}]$=3mM, [Pi]> 30mM wih a Mg /Ca ratio ≤1 precipitated an initial amorphous phase which transformed to brushite then underwent a subsequent transformation to magnesium whitlockite.

In all these pathways the levels of [Ca], [Mg] and [Pi] were closer to those of saliva ([Ca]=1-3mM, [Mg] =0.1-0.5mM and [Pi] = 3-7mM) and urine ([Ca]=0.7-7.8mM, [Mg] =0.7-7.8mM and [Pi] = 7-45mM) than serum ([Ca ultrafiltrate]=1.5mM, [Mg] and [Pi] both close to 1) (Cheng et al 1988). *In vivo* observation of whitlockite deposition appears to support the *in vitro* studies. The observation of whitlockite crystals in arrested dentine caries but not enamel caries (Daculsi *et al.* 1979) has been suggested to be due to the higher Mg content of dentine (LeGeros 1981). Kani *et al.* (1983), from x-ray diffraction analyses of whitlockite and other phases in dental calculi propose a mechanism for whitlockite formation in subgingival calculi in conditions of 'low pH and high Ca/P ratio', whereby brushite is formed first and, in the presence of magnesium, is transformed to whitlockite.

The *in vitro* studies above were carried out at fixed pH; *in vivo* studies have suggested optimal pH conditions for whitlockite formation. LeGeros *et al.* (1988) suggest that the difference in oral pH between dogs (pH 8.5) and humans (pH 7) is responsible for the differences in mineral phases of dental calculi observed between the two species, with, in the presence of magnesium above about 0.1 (Mg/Ca) , whitlockite being one of the favoured phases at the lower pH whilst not occurring at the higher. Driessens *et al.* (1985) correlated mineral phase deposition in calculi from a number of species with salivary pH producing similar results.

The internal pH of articular cartilage is dependent on the negative fixed charge density of the tissue, a characteristic imparted to the tissue by the proteoglycan constituent of the ECM. It has been suggested that the pH of mid zone articular cartilage would be 0.3 units lower than the external solution; variation in pH throughout the matrix would be proportional to the proteoglycan concentration (Maroudas 1979). Regions of high proteoglycan concentration such as around cell lacunae (Ratcliffe *et al.* 1984) would be expected to have the lowest pH values. The concentrations of a number of ions in articular cartilage have been measured by a variety of techniques. Most recently Pritzker and colleagues (1987), using a technique of inductively coupled plasma emission spectroscopy, determined wet weight values of [Ca] = 52.6 mM/kg, (Mg] = 6.9 mM/kg and [Pi] =23.1 mM/kg for normal human articular cartilage. These values are consistent with *in vitro* experiments of Benderly and Maroudas (1975) in that the total [Ca] concentration of normal cartilage was 10 to 20 times that of unstructured interstitial fluid. The concentration of [Ca] in fluid expressed from articular cartilage under controlled pressure was determined by Sokaloff and Linn (1965) to be1.2mM/kg, similar to that for serum ionic calcium, indicating that the bulk of [Ca] in the tissue is firmly bound. Values for extractable [Ca] from cartilage comparable to those of interstitial fluid were determined by Howell *et al.* (1968) and Wuthier (1977). Much of the difference between extractable and total concentrations of [Ca] and

[Mg] is likely to be attributable to the strong negative fixed charge density of proteoglycans. The increase in [Pi] recorded by Pritzker and colleagues (1987) was shown to correlate strongly with calcium, suggesting [Ca] is not only bound to the organic matrix, but also has a binding relationship with extracellular [Pi]. These workers found no evidence of a mineral association, but calculated that if mineral (apatite) was present it must have been less than 0.4% of the cartilage wet weight. It is not clear whether any of the proteoglycan bound ions would be available for mineral formation. On the basis of the values determined for extractable [Ca] and [Pi] (Howell *et al.* 1968), both whitlockite and apatite mineral phases would be in equilibrium (Driessens 1988). Although the work of Cheung and colleagues (1988) suggests that neither whitlockite nor apatite would form de novo. Cheng *et al.* (1988) suggest that a slight elevation of pH from neutral, at which their studies were conducted, to 7.4 -7.6 consistent with that of bone and epiphyseal cartilage (Howell *et al.* 1968), would enhance the propensity for HAP formation. Conversely a slight reduction in pH would favour whitlockite formation, as the crystallinity of whitlockite and its propensity to form has been shown to be greater when obtained at low pH (pH 5) (LeGeros *et al.* 1989).

The above conditions are considered in the absence of the promotional and inhibitory factors associated with biological calcification described in the introduction. Tovberg Jensen and Rowles (1957) suggested some 'further factor' must determine the appearance of whitlockite in pathological calcifications. Knuuttila *et al.* (1980) suggested that zinc ions may act as nucleators in the formation of whitlockite; they detected a thirty fold greater concentration of these ions in sub gingival than supra gingival dental calculi. However zinc has not been detected in association with the crystals studied here. The possibility of nucleation of magnesium whitlockite formation by organic components has been suggested. Collagen fibrils have been repeatedly observed in association with whitlockite deposition in urinary calculi (Santos and Gonzalez-Diaz 1980), and dental calculi (Schupbach *et al.* 1992), although these authors considered crystal formation to be independent of collagen fibril presence. Pritzker and Luk (1976) suggested that glycosaminoglycans may be responsible for the electron lucent core of crystals from a pulmonary nodule, functioning as a nidus for crystal precipitation; this seems unlikely considering the inhibitory effects on mineral formation determined for proteoglycans (Chen *et al.* 1984, Chen and Boskey1985, 1986, Hunter *et al.* 1985). Whitlockite containing sialoliths from human submandibular and parotid salivary glands have been shown to contain calcium-acidic phospholipid-phosphate complexes predominantly of phosphatidylserine and phosphatidylinositol (Boskey *et al.* 1983). These membrane debris were suggested to nucleate calcium phosphate mineral formation.

Identification of the 'cuboid' crystal mineral phase allowed comparison of the physical conditions required for their deposition, with those expected within cartilage. The available data suggested that likely prevailing conditions within cartilage would not support *de novo* whitlockite formation. It would appear, therefore, that additional factors must be extant at sites of crystal deposition.

CHAPTER 4
ASSOCIATION OF CRYSTALS WITH MATRIX COMPONENTS

Introduction

Several organic components have been associated with the control of mineral formation in various calcified tissues, either as promotors or inhibitors. These include extracellular matrix vesicles, collagen fibrils, proteoglycans, phospholipids, proteolipids, phosphoproteins, enzymes, including alkaline phosphatase, and inorganic factors such as pyrophosphate.

Previous studies of 'cuboid' crystals and similar depositions have variously described crystal deposition to be associated with matrix vesicles, cell debris and intramatrical lipidic debris (Ali and Griffiths 1981, 1983, Ghadially and Lalonde 1981, Ali 1985, Stockwell 1990). Identification of the organic component in each case was based on TEM observations only and it has been suggested that such descriptions may be interchangable (Ghadially 1983). No study has been undertaken to determine the nature of such crystal associated debris and it remains unclear whether such structures are present at all sites of deposition.

Matrix vesicles have been implicated as sites of initial mineral formation in epiphyseal cartilage and osteoid (Anderson 1967, Morris *et al.* 1992). They are identifiable in their own right, using TEM, by size and morphological characteristics (Anderson *et al.* 1970), but also contain notable alkaline phosphatase activity, a feature that has been used as a biochemical marker (Ali *et al.* 1970, Ali 1976). Alkaline phosphatase, an isozymic membrane bound glycoprotein, has long been associated with mineralization (Robison 1923). It was originally proposed that mineralization was induced by raised inorganic phosphate levels mediated by the enzyme. Subsequently proposed modes of activity include destruction of inhibitors of crystal growth, specifically pyrophosphate (Fleisch and Neuman 1961), and function as an inorganic phosphate transport protein in plasma membranes of target tissues. These and other possible modes of action have been recently reviewed by Wuthier and Register (1985). Lipids have been associated with pathological mineral deposition in articular cartilage (Ohira and Ishikawa 1987, Ohira *et al.* 1988). Phospholipids, in particular the acidic phospholipids, phosphatidylserine and phosphatidylinositol have been implicated in initial mineral formation (Boskey 1989) and, more recently, also in the regulation of crystal growth (Boskey and Dick 1991). Proteoglycans have been shown to inhibit HAP formation and growth *in vitro* (Blumenthal *et al.* 1979, Chen *et al.*1984, Chen and Boskey 1985, 1986) and observations alluding to similar events occurring *in vivo* have been made (Franzen *et al.* 1982, Campo and Romano 1986, Buckwalter and Rosenberg 1988).

It was decided to screen articular cartilage specimens for the presence or absence and distribution of these tissue components in order to evaluate any association with magnesium whitlockite crystals. This was considered to be an initial step in the investigation of the mode of crystal formation. Standard TEM was used to examine the association of the intramatrical lipidic debris described above with crystals and the ultrastructural detail of this material. More specific methods employed for the identification of individual components are outlined here.

Safranin O is a cationic dye that binds to polyanions. In permanently mounted cartilage sections this activity is restricted to proteoglycan components in a semi-quatitative manner, dye molecules binding to negatively charged chondroitin and keratan sulphate molecules (Rosenberg

1971). This therefore provides a suitable simple technique for observing changes in the proteoglycan content of articular cartilage within and between specimens.

The Oil Red O method of Lillie and Ashburn (1943) provides an intense red positive stain for lipids and has been used on cartilage with favourable results in earlier studies (Meachim and Stockwell 1979). Although the Sudan Black B procedure provides a simple method of detecting all the main lipid classes, the Oil Red O technique has been recommended for detailed histology, localizing lipids more precisely (Bayliss High 1990).

Standard protocols of tissue preparation for TEM tend to leach out lipids (Ward and Gloster 1976). Recently fixation with glutaraldehyde and malachite green (a water soluble weakly basic diaminotriphenylmethane dye) has been proposed as a method of permitting retention of such lipids during fixation (Teichman *et al.* 1972). The mechanism of reaction between lipids and this fixative combination is not completely known. Teichman *et al.* (1972) suggest ionic attraction between the two malachite green tertiary amines and the anionic groups of the lipids; whatever the mechanism, malachite green appears to bind to hydrophilic phospholipids (Teichman *et al.* 1974, Boshier *et al.* 1984, Nefussi *et al.* 1992). Osmium tetroxide fixation is required for visualization of lipids preserved by this method, producing electron dense complexes apparent on examination by TEM. This method has been used to study malachite green retained material in several studies of cells and tissues including spermatozoa, dentin and bone nodules (Teichman *et al.* 1972, Goldberg and Septier 1985, Goldberg and Escaig 1987, Nefussi *et al.* 1992).

Alkaline phosphatase activity has been localized ultrastructurally in many tissues including growth plate and condylar cartilage (Matsuzawa and Anderson1971, Lewinson *et al.* 1982, Ralphs and Ali 1986). The method used involved the deposition of electron opaque lead phosphate at sites of enzyme activity. Reaction specificity has been shown to be retained if incubation is carried out at pH 9, eliminating confusion with the activity of other phosphatases (Doty 1980). This method is considered to show the precise localization of alkaline phosphatase activity in thin sections (Lewinson *et al.* 1982).

The above methods were used in this investigation with the aim of studying the presence and distribution of ECM components described, relative to crystal deposition.

Materials and Methods

Specimens.

Samples of articular cartilage were taken as described in chapter one. The specimens used were taken from normal femoral heads unless stated otherwise.

Histology.

Wax and frozen tissue sections prepared and cut as described in chapter one were subjected to the following staining techniques.

Safranin O staining

7µm wax sections were dewaxed with xylene (Merck, Poole, UK), rehydrated through a graded alcohol series (absolute, 96%, 70%) and washed in running tap water. Sections were stained with Mayer's haematoxylin (Smith and Bruton 1977) for 15 minutes, differentiated in acid alcohol (1% hydrochloric acid in 70% alcohol) and 'blued' in running tap water for about 5 minutes prior to staining with 0.1% Safranin O (Rosenberg 1971; Raymond A Lamb, London, UK), acidified with a few drops of glacial acetic acid, for 1 minute. Sections were taken directly to 96% alcohol then transferred to absolute alcohol to complete dehydration, cleared with xylene and mounted in DPX (Merck, Poole, UK).

Oil Red O staining

10µm frozen sections collected on uncoated slides were floated off the slides into distilled water prior to staining with freshly filtered oil red O (Raymond A Lamb, London, UK) in 60% isopropanol (Merck, Poole, UK) (Lillie and Ashburn 1943) for 15 minutes in a closed container. The unmounted sections were then taken through 60% isopropanol and washed in distilled water before counterstaining with Mayer's haematoxylin for 2 minutes followed by 'blueing' in tap water. Sections were picked up onto uncoated slides and mounted in glycerine jelly (Raymond A Lamb, London, UK).

All sections were examined and photographed using an Olympus BH2 photomicroscope.

Transmission Electron Microscopy.

Standard Processing.

Tissue samples were processed using the standard resin protocol for TEM as described in chapter one.

Alkaline Phosphatase Electron Microscopic Histochemistry.

A metal salt method modified from that described by Lewinson and colleagues (1982) and Rees and Ali (1988) was used. Blocks of full depth articular cartilage were fixed in 1.5% glutaraldehyde in 0.085M sodium cacodylate buffer for 2 hours at 4°C; during this period the tissue was cut into translucent full depth slices under a dissecting microscope, using a new razor blade. Samples were washed in sodium cacodylate buffer and incubated in 10ml of 40mM Tris/HCl buffer (pH 9.0) (Merck, Poole UK) containing 9mM sodium ß-glycerophosphate (Merck, Poole, UK), 5mM magnesium chloride (Merck, Poole, UK) and 3.6mM lead nitrate (Merck, Poole, UK), for 30 minutes at 37°C (Lewinson *et al.* 1982, Rees and Ali 1988). Control samples containing levamisole hydrochloride (Aldrich, Gillingham, UK), a potent uncompetitive inhibitor of liver, kidney and bone alkaline phosphatase (van Belle, 1976), at a concentration of 2mM were included in the incubation medium. Components of the incubation media were stored separately at -20°C in 2ml aliquots at concentrations that diluted to those given above when constituted to the10ml

incubation medium. Media were constituted immediately prior to tissue incubation in the order described above, to avert precipitation. Samples were then washed in 0.085M sodium cacodylate buffer (pH7.4), post fixed in 1% osmium tetroxide and processed as for the standard technique.

Glutaraldehyde-Malachite green-Osmium tetroxide fixation.

Blocks of full depth articular cartilage, approximately 1mm in 2 dimensions were taken from the superior region of freshly resected femoral heads and fixed in 2% glutaraldehyde-0.1% malachite green (Gurrs, London, UK) buffered in 0.085M sodium cacodylate (pH7.4) at 4°C for 12hours (Boshier *et al.*1984). Samples were buffer washed for 3 x 10 minutes then post fixed in 1% osmium tetroxide for 90 minutes; processing was completed as for the standard technique. Controls were processed normally without malachite green.

Ultrathin sections were cut, examined, stained and unstained, and recorded as described in chapter one. XRMA and elemental mapping was carried out as described in chapter two.

Results

Specimens used for histological investigation had also provided samples for the image analysis study in chapter one. The condition of these specimens has already been described in that chapter.

Safranin O staining.

Safranin O staining intensity varied within cartilage sections and between samples. The most intense stain was detected around chondrocytes, both within the lacunae and extending into the territorial matrix, especially in mid zone cartilage. More distant ECM demonstrated a moderately less intense positive stain in this region. A definite reduction in staining was noted in the superficial zone from the articular surface extending to the top of the intermediate zone (Fig. 4.1). In this region pericellular staining was restricted mainly to the territorial matrix, with sharp attenuation in the surrounding ECM. The depth to which the lack of, or poor staining, extended appeared greater in specimens from older patients (Fig. 4.1a,b). In this group the reduced staining intensity in inferior specimens appeared to extend deeper than superior specimens (Fig. 4.1). No similar reduction in staining was apparent at any of the cut edges of the specimens, indicating the reduced staining in the superficial zone was not an 'edge' effect.

Oil red O staining.

The bright red positive stain for lipid (Lillie and Ashburn 1943) was most clearly observed immediately below, and parallel to, the articular surface (Fig. 4.2). At low magnification, staining in some specimens appeared as a continuous band. Higher magnification revealed intra and extracellular staining. Intracellular staining was restricted to discrete, densely staining, lipid droplets within the cytoplasm and occurred in chondrocytes throughout the depth of the tissue (Fig. 4.2).The frequency of the droplets was greater in specimens from older patients. In the

ECM, staining was slightly less intense and extended to one or two cells' depth in the superficial zone. Within this region staining was observed as patches extending across interterritorial areas of ECM and pericellularly (Fig. 4.2). Focal areas of increased staining intensity were observed randomly within these patches and adjacent to the apices of superficial zone chondrocytes (Fig. 4.2c). Such areas contained structural features consistent with the location and extent of intramatrical debris observed by TEM. Positive staining was abundant in both superior and inferior sections of specimens from elderly patients in which crystal deposition had been demonstrated by TEM. In young specimens (12 years) positive staining was clearly observed in superior regions (Fig. 4.2e); however staining in the inferior regions was much less distinct, not being detected in sections from the specimen that registered the lowest crystal deposition density in the image analysis study (Fig. 4.2f).The extent and distribution of staining correlated well with the distribution of crystals, observed by TEM, in sections of tissue from adjacent sites of the same specimen (Fig. 4.2d,h). No staining was observed on any of the cut edges of tissue sections, indicating the staining was not an 'edge' effect artefact.

Standard TEM.

Crystal distribution within the ECM has been described in chapter one. Here the relationship between crystals and matrix components, observed by TEM is described in more detail. Descriptions are drawn from all patient groups and joint sites where crystal deposition was observed.

Crystals with a pericellular distribution, or those present at the sites of cell necrosis were frequently associated with, or scattered amongst, intramatrical lipidic debris of a membranous or amorphous nature (Fig. 4.3). Such structures, although variable in size particularly at sites of necrosis, frequently fell within a 100-500nm range (Fig. 4.3). Similar bodies were also observed in the ECM amongst the close packed tangential collagen fibrils between the articular surface and the initial superficial zone chondrocytes (Fig. 4.3), an area commonly associated with crystal deposition.

The association of crystals and intramatrical debris extended to deeper layers of cartilage, occurring in association with two recognisable matrix features: first, pericellularly to chondrocytes (Fig. 4.3) and second, associated with chondrocyte necrosis (Fig. 4.3f). Amorphous and membranous debris were commonly observed at both locations, surrounding deposited crystals in an environment of structures of variable size and electron density (Fig. 4.3). Crystals could not be attributed to any characteristic structure, although these areas were clearly delineated within the ECM and crystal deposition appeared similarly restricted (Fig. 4.3). Globular structures approximately 100nm in diameter, with evidence of a laminated structure and variable electron density in unstained sections were observed in three specimens (Fig. 4.4). The densest of the structures observed appeared crystalline with an XRMA spectrum and calcium to phosphorus ratio that was consistent with those of 'cuboid' crystals. At one site signals for calcium and phosphorus were detected in very small needle-like electron densities situated within and aligned with the apparent laminar structure of one deposit (Fig. 4.4).

Crystals were also observed in association with less common features within the ECM. In two specimens, crystals were observed in close proximity to large extracellular lipidic debris approximately 1μm in diameter (Fig. 4.3e). Giant collagen fibrils were also observed as focal disruptions within the ECM (Fig. 4.5). At one site these were associated with the type of lipid deposits described above (Fig. 4.5). These fibrils appeared to arise from the coalescence of numerous normal fibrils. In longitudinal section the periodic banding of the giant collagen fibrils was in register (Fig. 4.5). Such fibrils were randomly oriented and observed in the mid zone, away from the tidemark. 'Cuboid' crystal deposition was again observed at such sites with the extent of deposition restricted to the area of matrix abnormality (Fig. 4.5). Whorls of crystals appearing needle shaped in thin section were also observed in close proximity to 'cuboid' crystals. These aggregates appeared to centre upon amorphous structures within the matrix (Fig. 4.5) and contained calcium and phosphorus. Similar structures were also noted in the superficial zone of one specimen (YA 16 years).

Alkaline phosphatase localization.

The method described for alkaline phosphatase histochemical localization satisfied requirements. Incubation media constituted from the stored aliquots of the component parts remained clear throughout the incubation period and non-specific lead phosphate deposition, such as 'edge' effects, was not observed.

Hypertrophic chondrocytes in close proximity to the mineralizing front were used as positive controls. In younger specimens (12-20 years) the positive control sites described above demonstrated well defined areas of electron opaque lead phosphate deposition, indicative of alkaline phosphatase activity (Fig. 4.6a) and not apparent in levamisole treated controls (Fig. 4.6b). Alkaline phosphatase activity was localized in discrete distribution to chondrocyte membranes, at the end of cell processes, associated with vesicles on the internal side of the plasma membrane (Fig. 4.6a), and associated with vesicular structures in the surrounding matrix (Fig. 4.6c). Activity was detected up to 50μm from the mineralization front. No activity was detected within this region of tissue from elderly patients. Levamisole control sections contained sparse beading of lead salt deposition along the plasma membrane of a small number of chondrocytes immediately adjacent to the mineralization front (Fig. 4.6b,d). It was not possible to detect lead salt deposition in the superficial zone associated either with chondrocyte membranes (Fig. 4.6e), or in areas of the ECM where crystal deposition was observed in any specimens (Fig. 4.6g). Indeed there was no detectable difference between experimental and levamisole treated sections (Fig. 4.6g,h).

Glutaraldehyde-malachite green-osmium tetroxide fixation.

Tissue fixation by this method proved satisfactory, although chondrocyte ultrastructure was slightly less well preserved than that achieved with the standard processing technique. Ultrathin sections processed using the malachite green method demonstrated electron dense features not observed in sections from tissue processed by standard techniques (Fig. 4.7a-d). These were

most obvious in unstained sections, contrasting sharply with surrounding unstained tissue. The electron dense features interpreted as lipid deposits were present both intra-cellularly and within the ECM. Intra-cellular deposits were consistent with previous observations of lipid droplets, although not all droplets exhibited strong electron density, whilst some showed mixed density (Fig. 4.7e,f). Extracellularly the distribution of the lipidic bodies varied with depth in the tissue. In the superficial region, the bodies appeared globular or ovoid approximately 100nm in diameter and occurring at frequent intervals in the matrix amongst tangentially orientated collagen fibrils (Fig. 4.7i,j). Co-occurrence of crystals and the slightly less electron dense lipidic bodies was noted in approximately 10% of crystal observations (Fig. 4.7g,h); the observation of both crystals and lipid bodies occurring separately being more frequent. In the intermediate, mid and deep zones similar electron densities were apparent, although the distribution was different. The deposits were larger, up to ten fold and appeared multi-lobular (Fig. 4.7kl). The distribution within the matrix was clearly sparser, with orientations along collagen fibrils noted. That this was not a diffusion artefact was indicated by a similar distribution at the cut edges of mid and deep zone tissue. Elemental maps of ultrathin sections, processed using malachite green demonstrated strong phosphorus signals associated with the lipid deposits, no such signals were generated from comparable regions of ECM in sections of tissue from adjacent sites processed using the standard technique (Fig. 4.8).

Fig. 4.1

Fig. 4.1a. Elderly articular cartilage from the superior region of the femoral head, stained with Safranin O and Mayer's haematoxylin. A poorly stained band of tissue is observed extending from the articular surface to to the bottom of the superficial zone: (DT 87 years).

Fig. 4.1b. Elderly articular cartilage from the inferior region of the femoral head, stained with Safranin O and Mayer's haematoxylin. A broad, poorly stained band of tissue, extending from the articular surface to the intermediate zone is apparent; limited pericellular staining within this band is observed (arrows): (DT 87 years).

Fig. 4.1c. Young adult articular cartilage from the superior region of the femoral head, stained with Safranin O and Mayer's haematoxylin. A narrow, poorly stained band of tissue is present immediately below the articular surface, with a gradual increase in the staining intensity of the ECM from the superficial zone to the deep zone: (MC 12 years).

Fig. 4.1d. Young adult articular cartilage from the inferior region of the femoral head, stained with Safranin O and Mayer's haematoxylin. A poorly stained band of tissue is present immediately below the articular surface, with a gradual increase in the staining intensity of the ECM from the superficial zone to the deep zone: (MC 12 years).

a

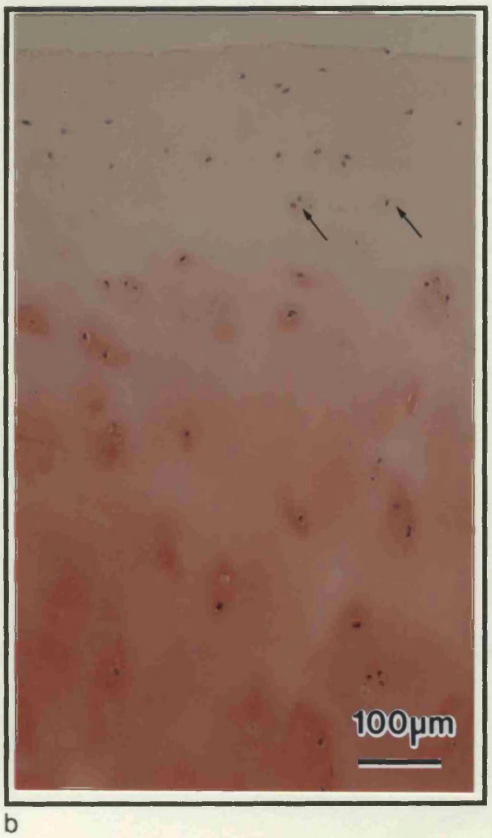

b

c

d

Fig. 4.2

Fig.4.2a. Elderly articular cartilage from the superior region of the femoral head, stained with Oil red O (counterstained with Mayer's haematoxylin). A strong positive stain can be seen immediately below the articular surface, whilst the ECM below remains clear: (DT 87 years).

Fig. 4.2b. Elderly articular cartilage from the inferior region of the femoral head, stained with Oil red O (counterstained with Mayer's haematoxylin). A strong positive stain can be seen immediately below the articular surface, whilst the ECM below remains clear: (DT 87 years).

Fig. 4.2c. Detail of the section shown in 4.2a; the positive Oil red O stain is seen as a narrow band below the articular surface, and with a close pericellular distribution. Intracellular lipid droplets are also observed with a positive stain (arrow).

Fig. 4.2d. Electron micrograph of superficial zone articular cartilage, from the same site as that shown in 4.2c. Crystals can be clearly observed in the ECM below the articular surface (A), and in a pericellular distribution. Unstained section.

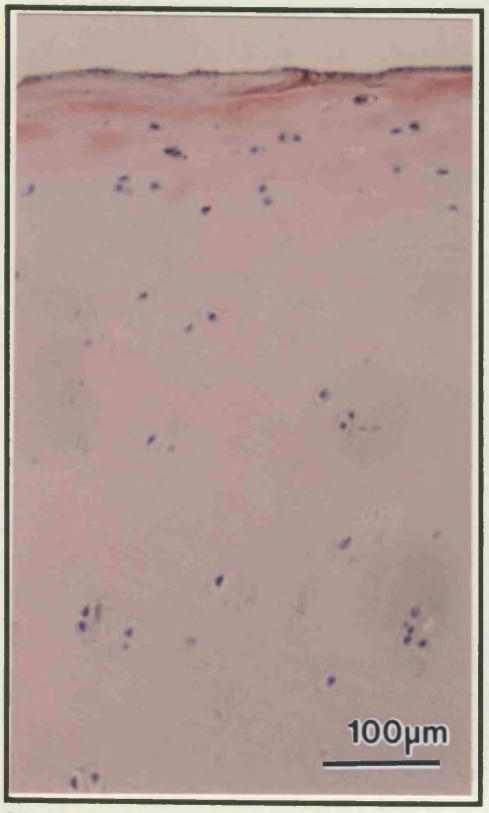

a

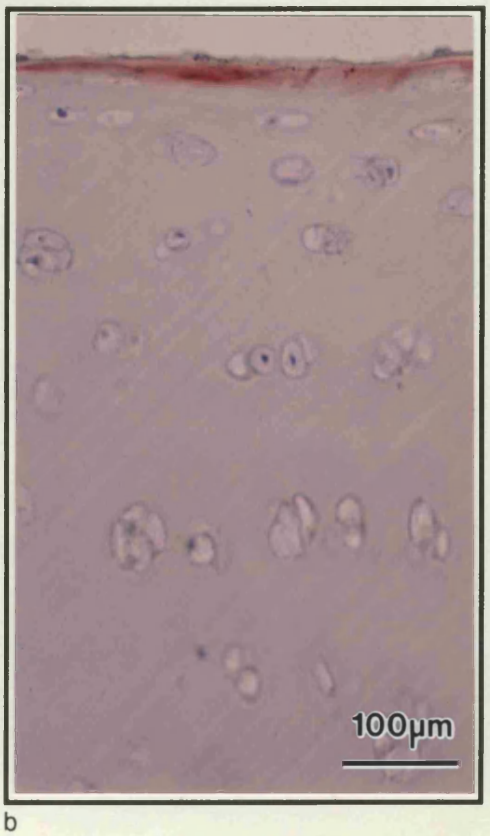

b

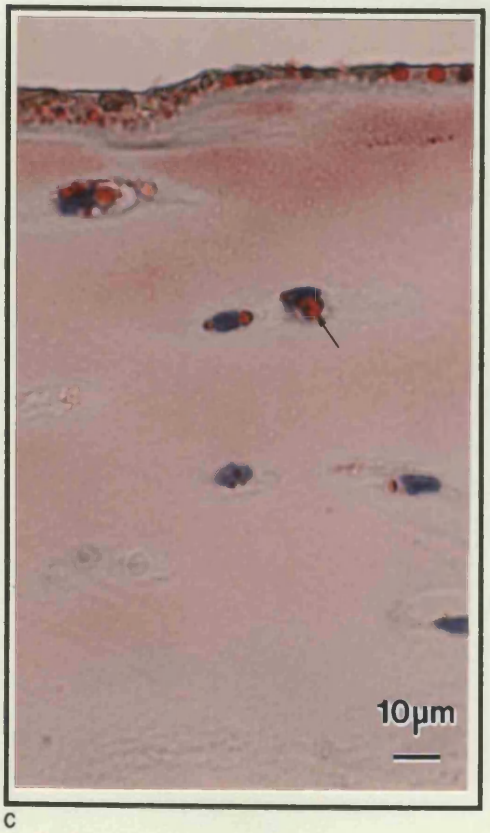

c

d

Fig. 4.2

Fig. 4.2e. Young adult articular cartilage from the superior region of the femoral head, stained with Oil red O (counterstained with Mayer's haematoxylin). A narrow, broken band of positive staining is present immediately below the articular surface, whilst the ECM below remains clear: (MI 12 years).

Fig. 4.2f. Young adult articular cartilage from the inferior region of the femoral head, stained with Oil red O (counterstained with Mayer's haematoxylin). No evidence of positive staining in the ECM is present (DF 10 years).

Fig. 4.2g. Detail of the section shown in 4.2e; the positive Oil red O stain forms a narrow patchy band below the articular surface. Intracellular lipid droplets are also observed with a positive stain (arrow).

Fig. 4.2h. Electron micrograph of superficial zone articular cartilage, from the same site as that shown in 4.2g. Crystals are present in the ECM, immediately below the articular surface (A).

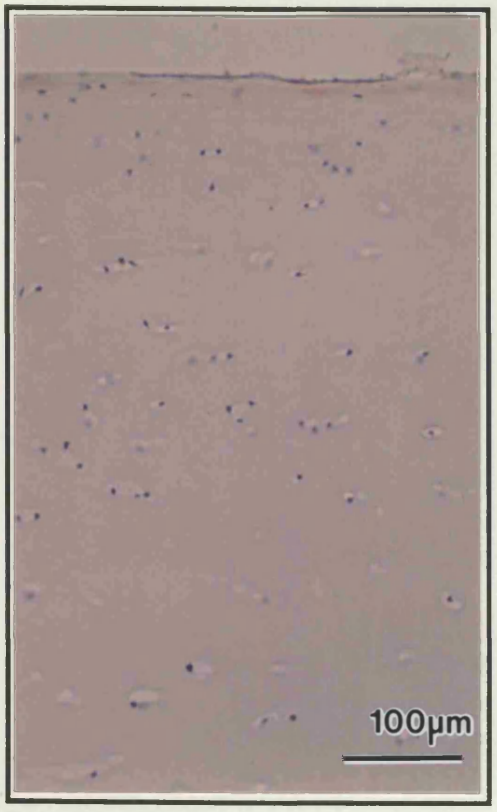

e

f

g

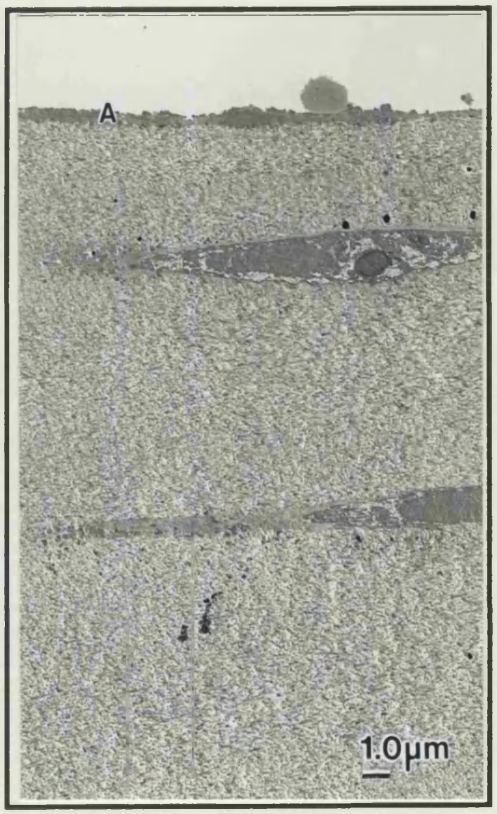

h

Fig. 4.3

Fig. 4.3a. Superficial zone chondrocyte with pericellular lipidic debris (D). Crystals (C) are present in close association with the debris as well as the ECM above the chondrocyte: (Femoral head, KM 43 years). Unstained section.

Fig. 4.3b. A focal area of intramatrical lipid debris (D), possiblely derived from chondrocyte necrosis, in superficial zone articular cartilage. Crystal deposition (C) is concentrated within this area. The surrounding ECM shows relatively sparse crystal deposition: (Metacarpal, 62 years). Unstained section.

Fig. 4.3c. Intramatrical lipid deposition (D) in superficial zone articular cartilage. Crystals present within this area are larger and at a higher density than in the surrounding ECM: (Carpal, IB 19 years). Unstained section.

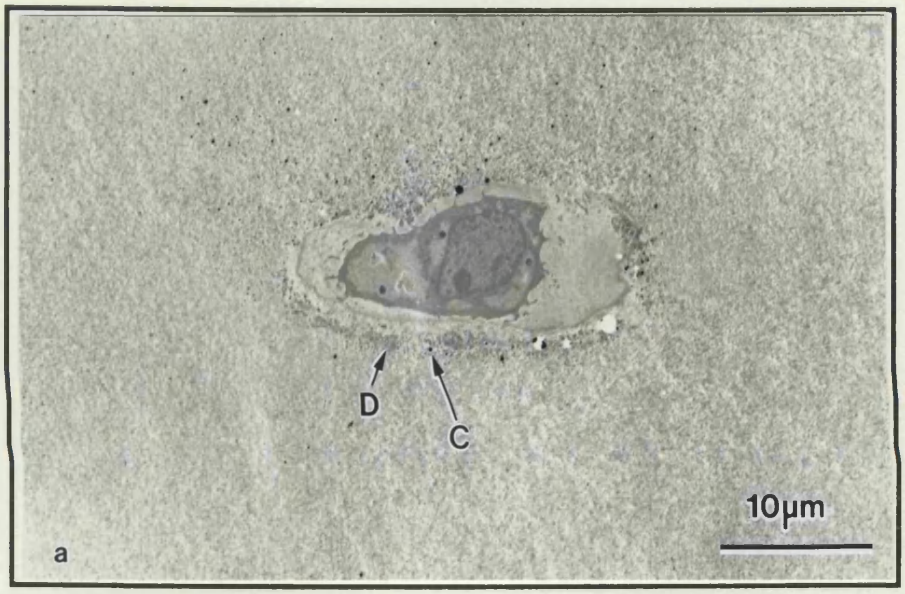
D
C
10µm
a

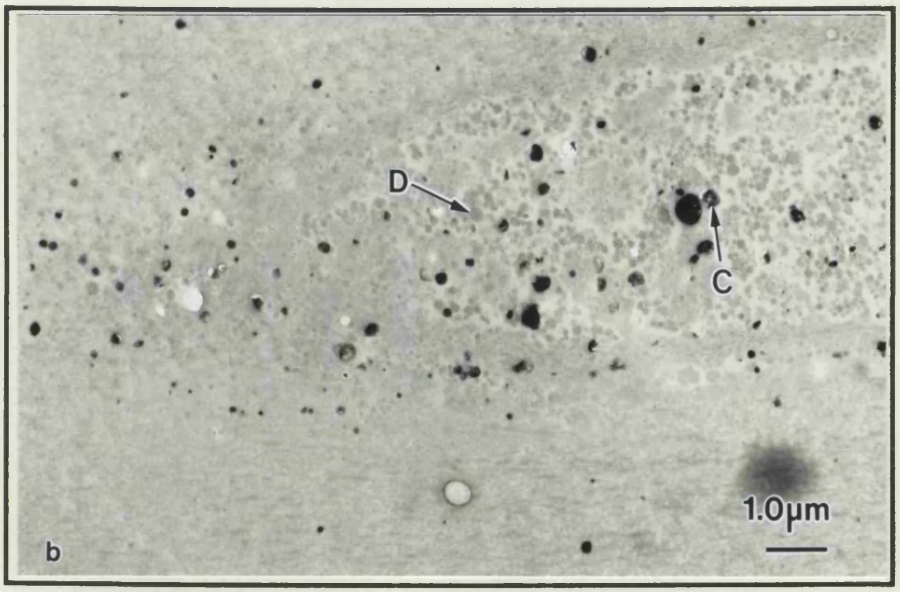
D
C
1.0µm
b

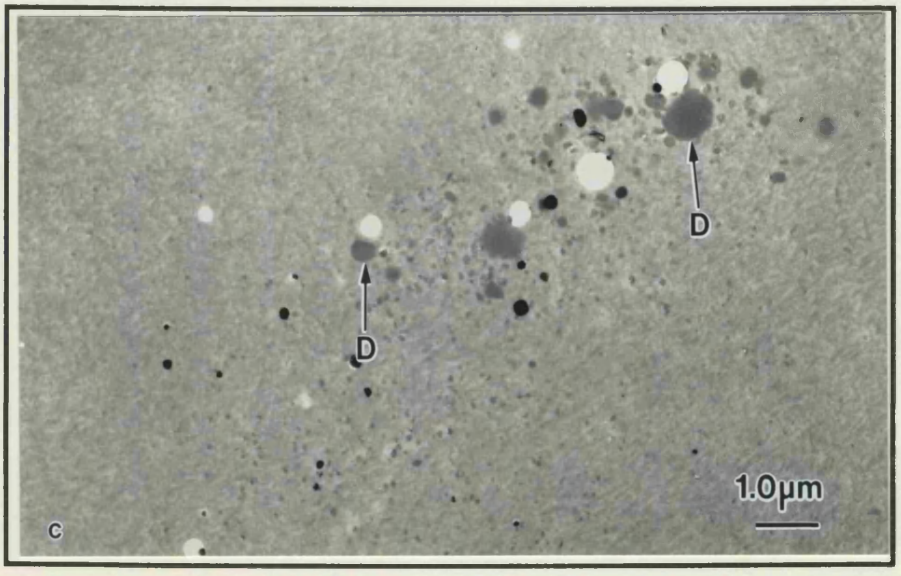
D
D
1.0µm
c

Fig. 4.3

Fig. 4.3d. Pericellular distribution of intramatrical lipidic debris (D) in deep zone articular cartilage. Crystal deposition (C) is present within the area of debris, but not in the surrounding ECM: (Femoral head, CL 81 years,). Section stained with uranyl acetate and lead citrate.

Fig. 4.3e. Crystal deposition associated with isolated, large, extracellular lipid deposits (D): (Radial head, IB 19 years). Unstained section.

Fig. 4.3f. Site of chondrocyte necrosis (N) in fibrillated, femoral head, articular cartilage. Crystal deposition (C) is present amongst the necrotic material: (RB 60 years). Section stained with uranyl acetate and lead citrate.

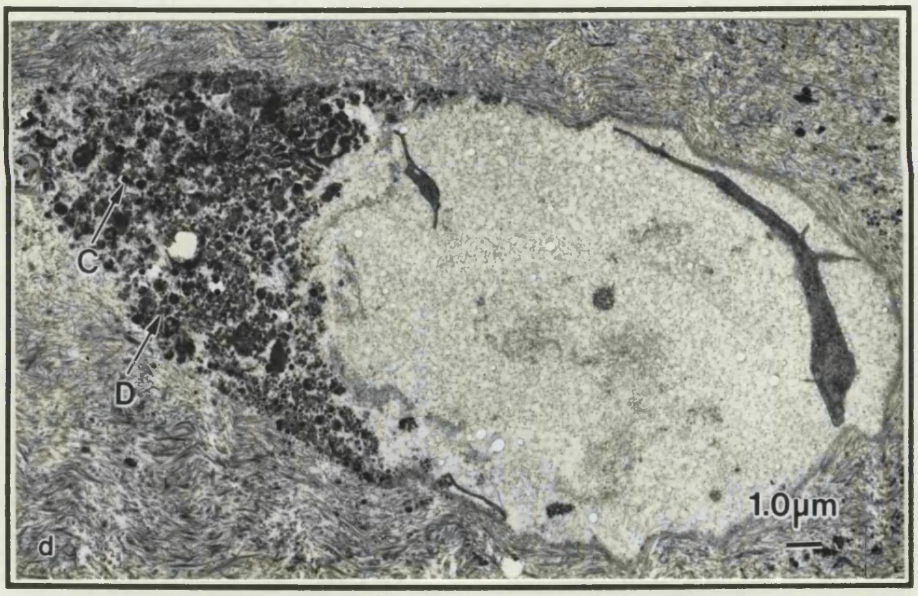
C
D
1.0μm
d

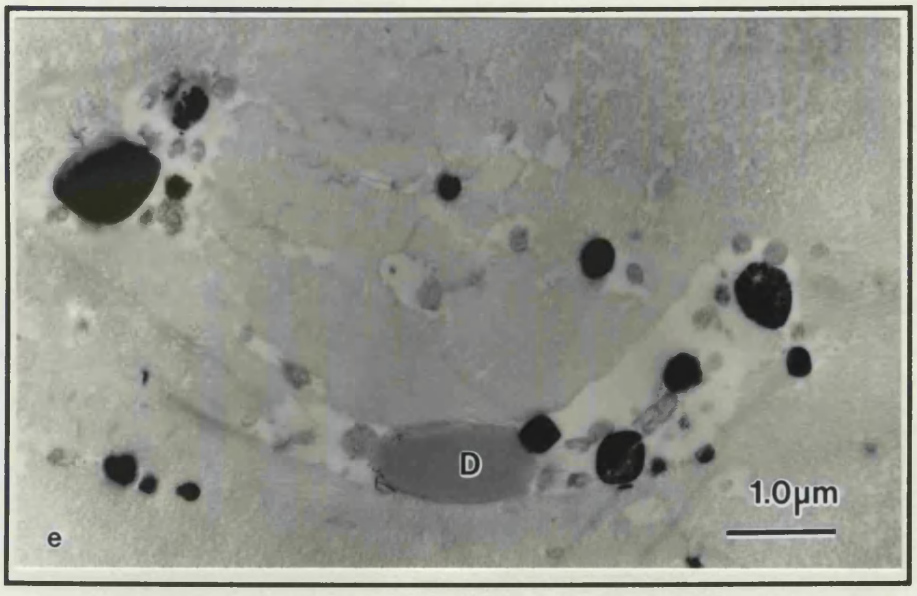
D
1.0μm
e

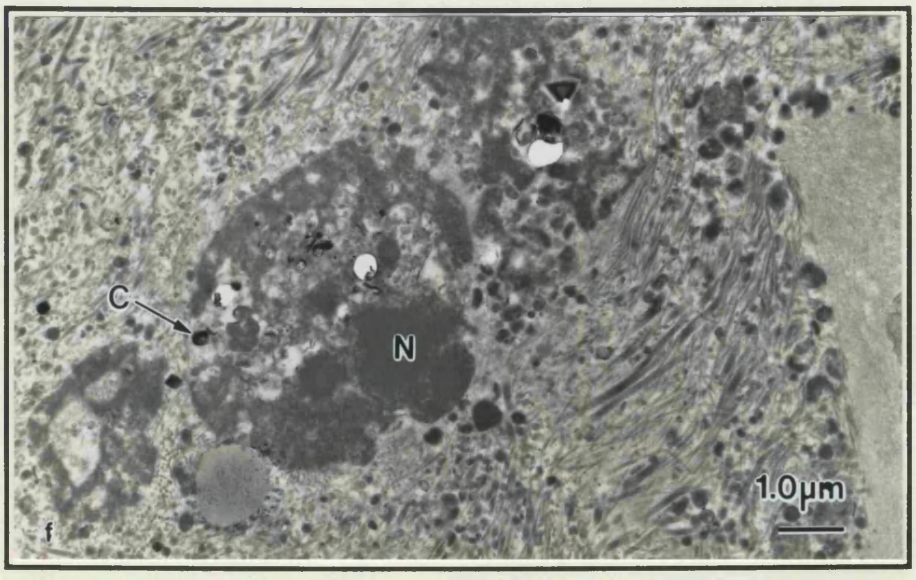
C
N
1.0μm
f

Fig. 4.4

Fig. 4.4a. Focal distribution of lipidic structures (L) in intermediate zone, articular cartilage ECM. Crystal deposition is apparent within this area (C) and fine mineral deposition is present within the outline of one lipid structure (arrow): (Femoral head, VO 85 years). Unstained section.

Fig. 4.4b. Detail of 4.4a; a lipidic body (L), adjacent to a crystalline deposit (C), shows an apparently laminated structure along which is aligned fine material with an electron density consistent with apatite or whitlockite mineral. Unstained section.

Fig. 4.4c. XRMA spectrum generated from the crystalline deposit shown in 4.4b. The spectrum is consistent with those generated from 'cuboid' crystals.

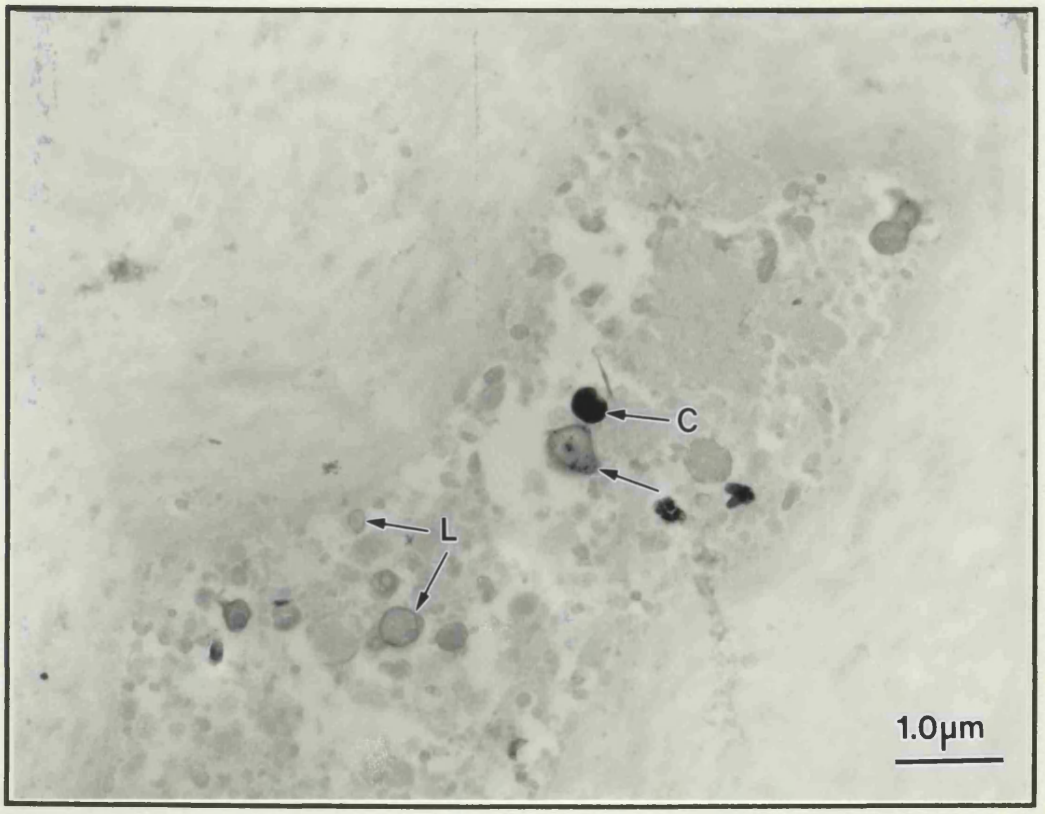

a

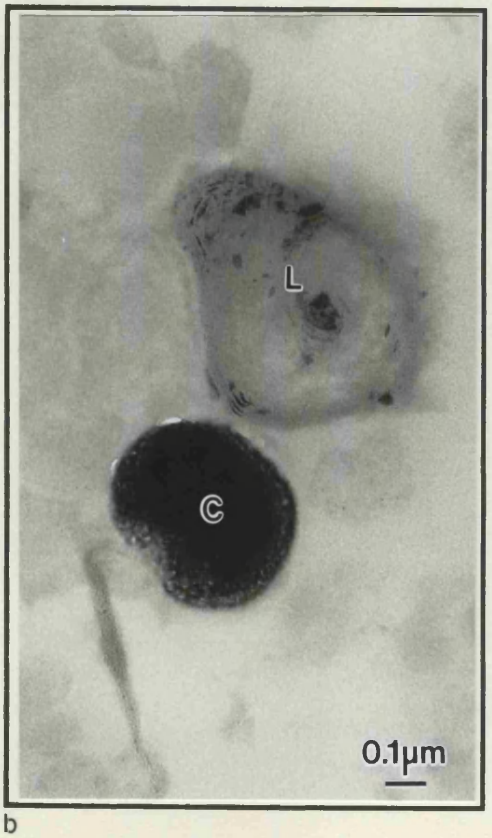

b

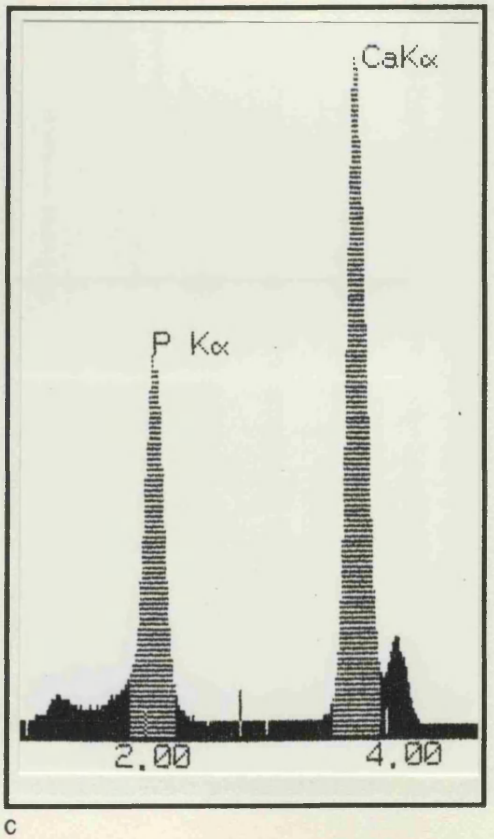

c

Fig. 4.5

Fig. 4.5a. A 'microscar' in deep zone articular cartilage. Crystal deposition (C) is focussed within this area, in association with lipid debris (L) and amianthoid fibres (A): (Radial head, IB 19 years). Unstained section.

Fig. 4.5b. Detail of 4.5a; 'cuboid' crystals and apatite-like needles (arrow) are present within the 'microscar' area. Unstained section.

Fig. 4.5c. Detail of 4.5a; Amianthoid fibres (A) within the microscar, adjacent to crystal deposition. Section stained with uranyl acetate and lead citrate.

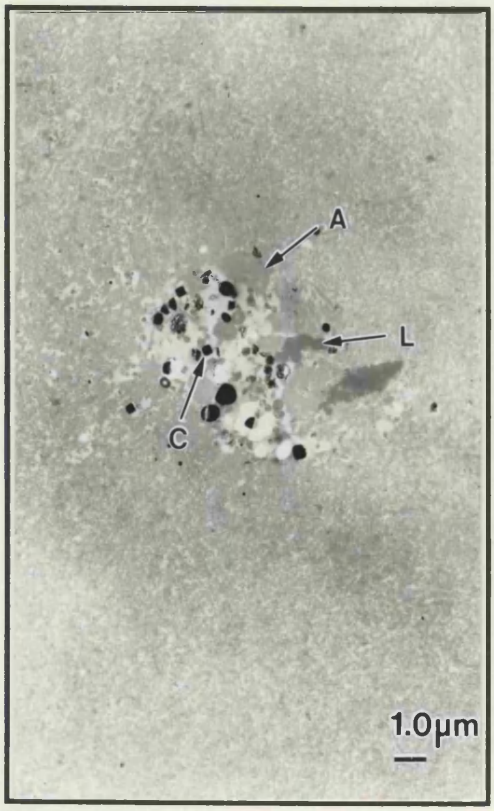

a

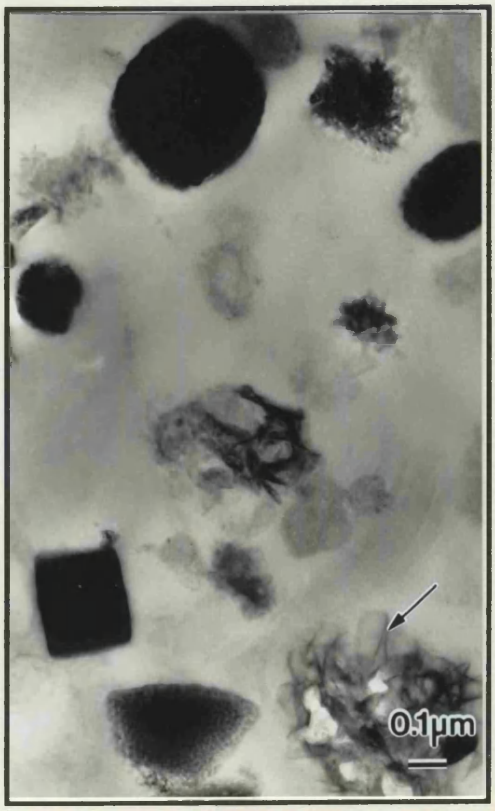

b

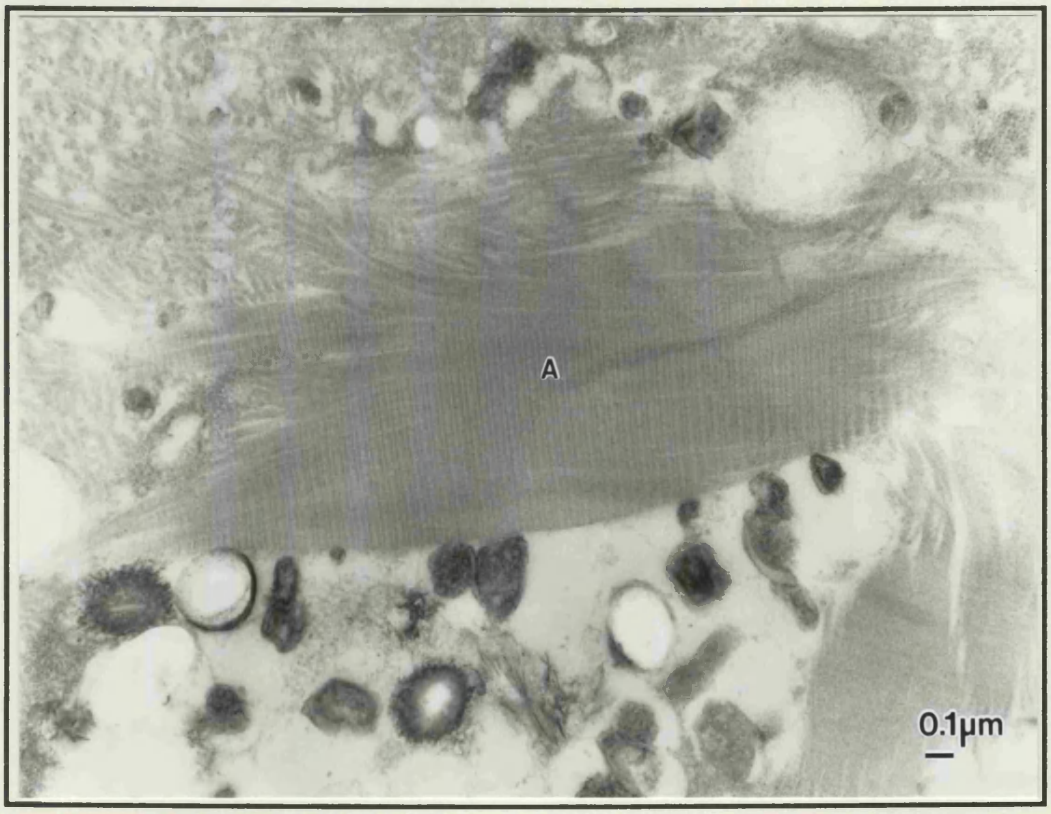

c

Fig. 4.6

Fig. 4.6a. Hypertrophic chondrocytes close to the calcification front in articular cartilage incubated to demonstrate alkaline phosphatase activity. Lead salt deposition (arrows) associated with cell membranes indicates activity of the enzyme: (Femoral head, CK 16 years).

Fig. 4.6b. Hypertrophic chondrocytes close to the calcification front in articular cartilage incubated as in 4.6a but in the presence of levamisole hydrochloride to provide a negative control. Lead salt deposition (arrow) is limited to fine beading close to the cell membrane: (Femoral head, CK 16 years).

Fig. 4.6c. ECM close to the calcification front in articular cartilage incubated to demonstrate alkaline phosphatase activity. Lead salt deposition is associated with matrix vesicles and initial mineral deposition (arrows): (Femoral head, MI 12 years).

Fig. 4.6d. ECM close to the calcification front in articular cartilage incubated as in 4.6c, but in the presence of levamisole hydrochloride to provide a negative control. Lead salt deposition is extremely limited (arrow): (Femoral head, CK 16 years).

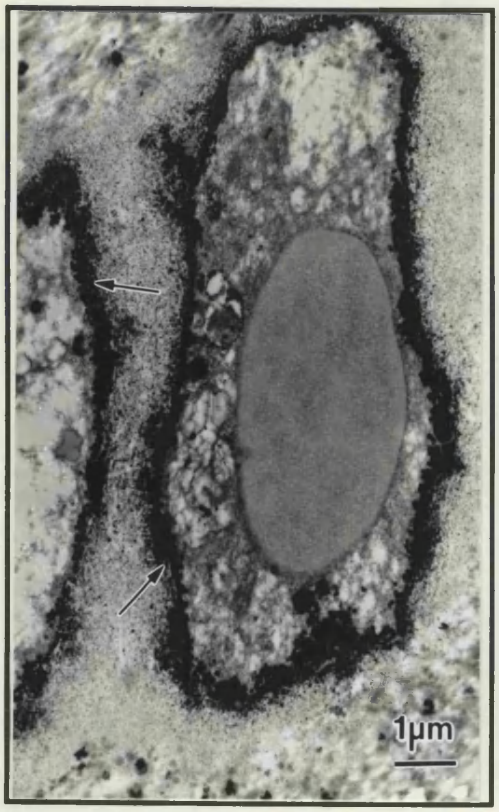

a

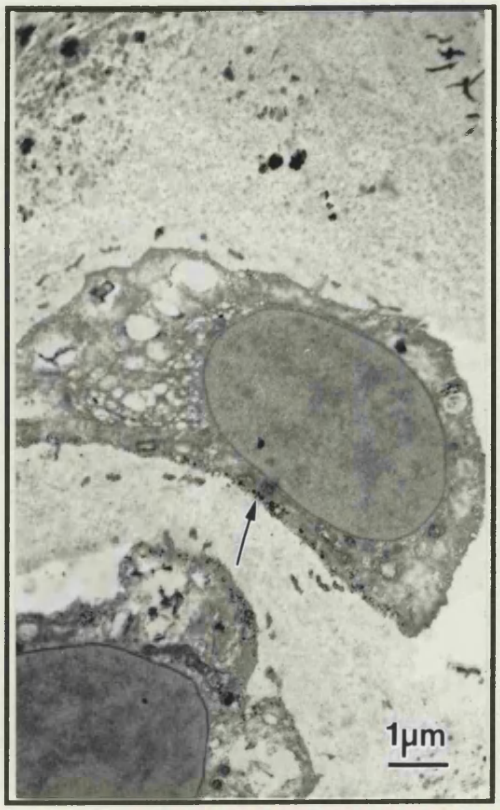

b

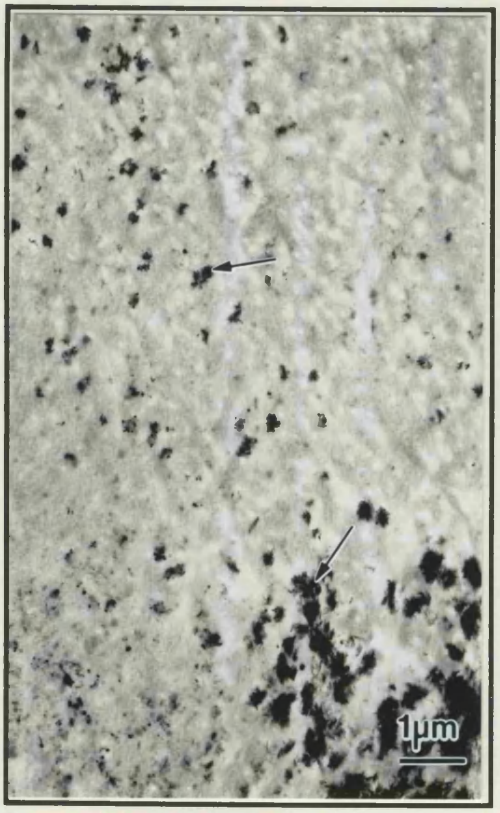

c

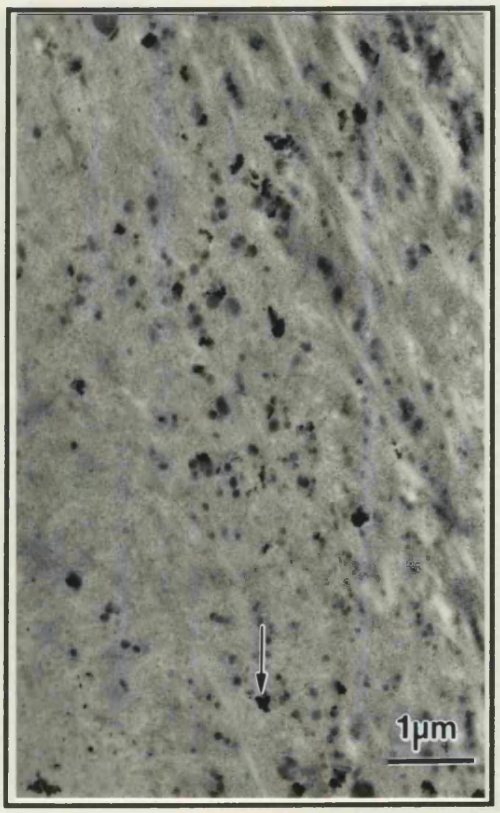

d

Fig. 4.6

Fig. 4.6e. Superficial zone chondrocyte with associated matrical debris (D) and crystal deposition (C), in articular cartilage incubated to demonstrate alkaline phosphatase activity. No lead salt deposition is apparent: (Femoral head, CK 16 years).

Fig. 4.6f. Superficial zone chondrocyte with associated matrical debris (D) and crystal deposition (C), in articular cartilage incubated as in 4.6e, but in the presence of levamisole hydrochloride to provide a negative control. No lead salt deposition is apparent: (Femoral head, MI 12 years).

Fig. 4.6g. Crystals in the ECM of superficial zone articular cartilage incubated to demonstrate alkaline phosphatase activity. No lead salt deposition is apparent: (Femoral head, MI 12 years).

Fig. 4.6h. Crystals in the ECM of superficial zone articular cartilage incubated as in 4.6g, but in the presence of levamisole hydrochloride to provide a negative control. No lead salt deposition is apparent: (Femoral Head MI 12 years).

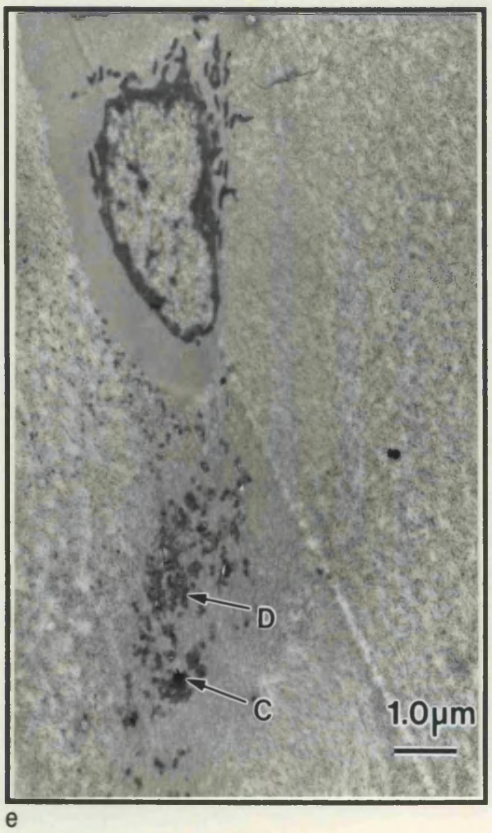

e

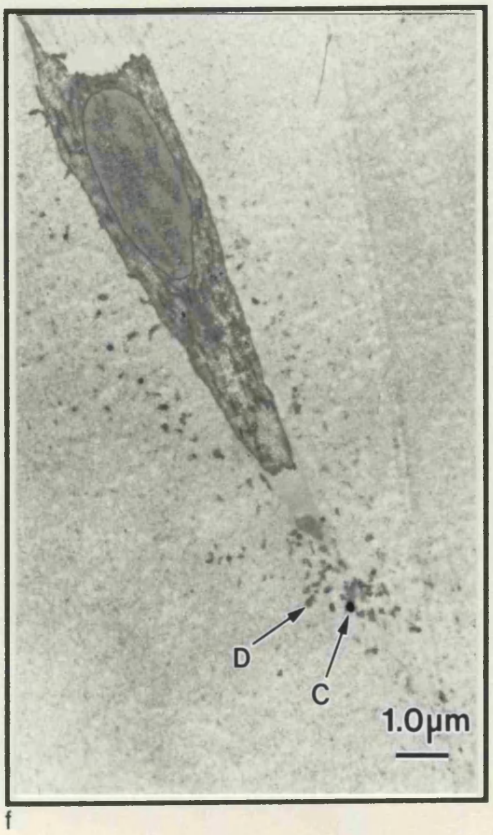

f

g

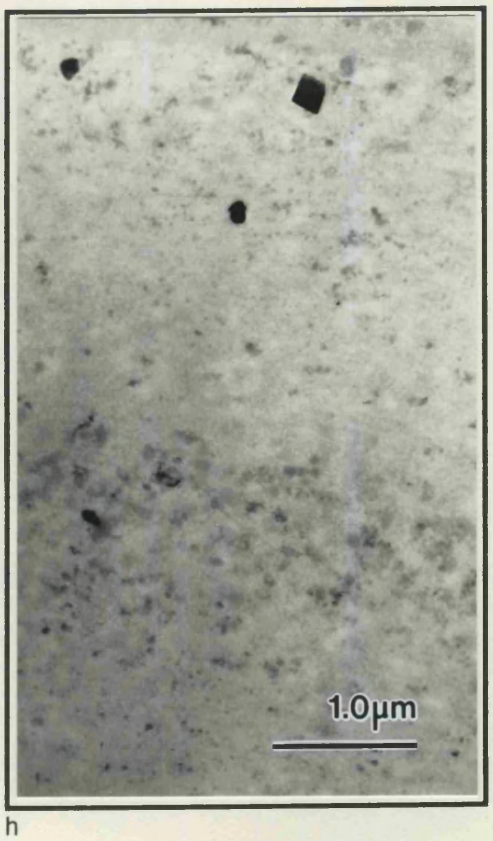

h

Fig. 4.7

Fig. 4.7a. Superficial zone ECM of articular cartilage, fixed using the malachite green method. Crystals (C) and electron dense lipidic debris (D) are apparent in the matrix: (Femoral head, CM 30 years). Unstained section.

Fig. 4.7b. Superfical zone of articular cartilage, fixed by the standard method. Crystals (C) are apparent in the matrix: (Femoral head, CM 30 years). Unstained section.

Fig. 4.7c. Superficial zone ECM of articular cartilage, fixed using the malachite green method. Electron dense lipidic debris (D) are apparent throughout the matrix : (Femoral head, CM 30 years). Unstained section.

Fig. 4.7d. Superficial zone ECM of articular cartilage, fixed using the standard method. No electron dense lipidic debris are present: (Femoral head, CM 30 years). Unstained section.

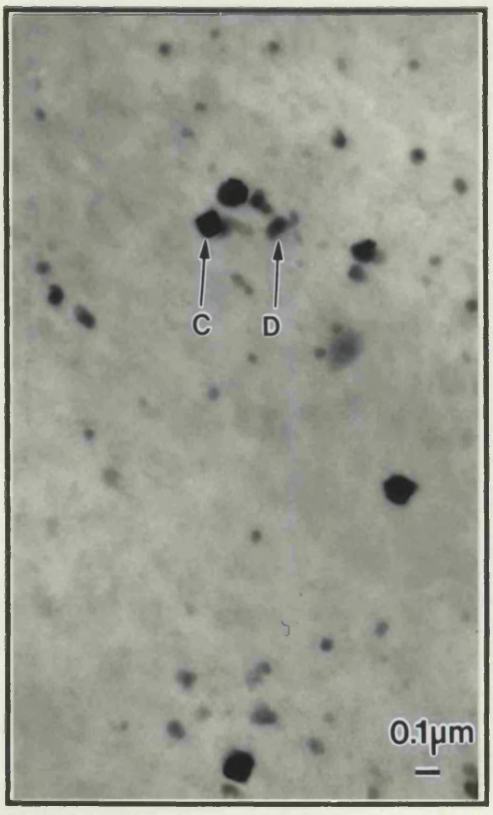

a

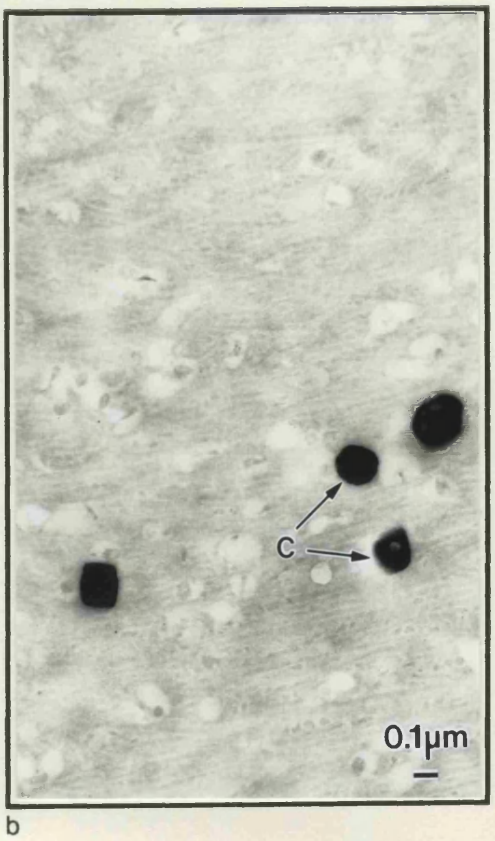

b

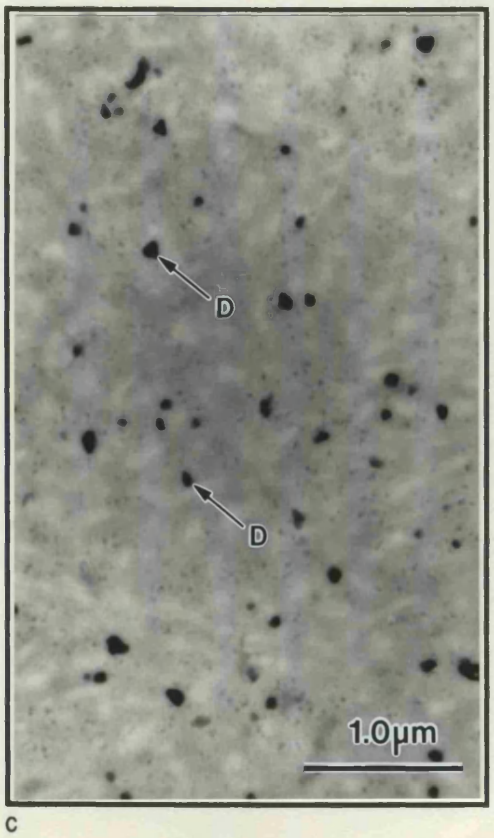

c

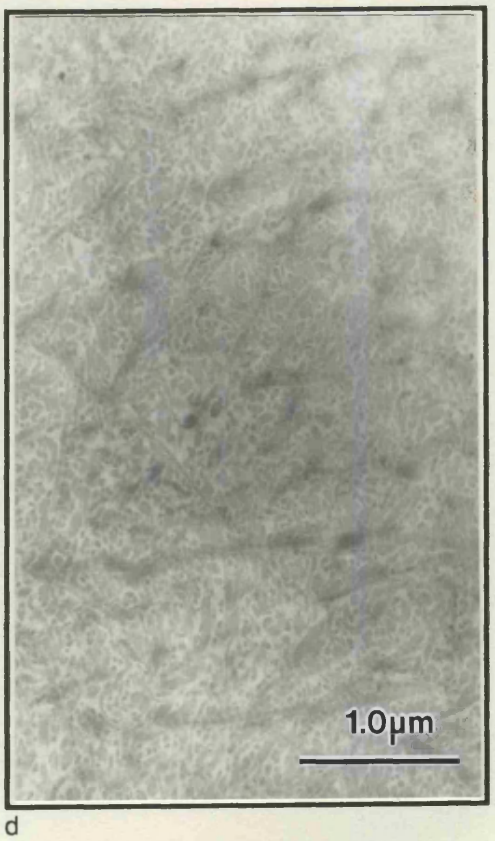

d

Fig. 4.7

Fig. 4.7e. Chondrocyte in the superficial zone of articular cartilage, fixed using the malachite green method. Pericellular, electron dense lipidic debris are present in the ECM: (Femoral head, CM 30 years). Section stained with uranyl acetate and lead citrate.

Fig. 4.7f. Chondrocyte in the superficial zone of articular cartilage, fixed using the malachite green method. Electron dense lipid is present intracellularly (L) and scattered through the ECM: (Femoral head, CM 30 years). Unstained section.

Fig. 4.7g. Superficial zone ECM of articular cartilage, fixed using the malachite green method. Crystals (C) are observed in close association with electron dense lipidic debris (D): (Femoral head, CM 30 years). Unstained section.

Fig. 4.7h. Superficial zone ECM of articular cartilage, fixed using the malachite green method. Crystal (C) observed in close association with electron dense lipidic debris (D): (Femoral head, CM 30 years). Unstained section.

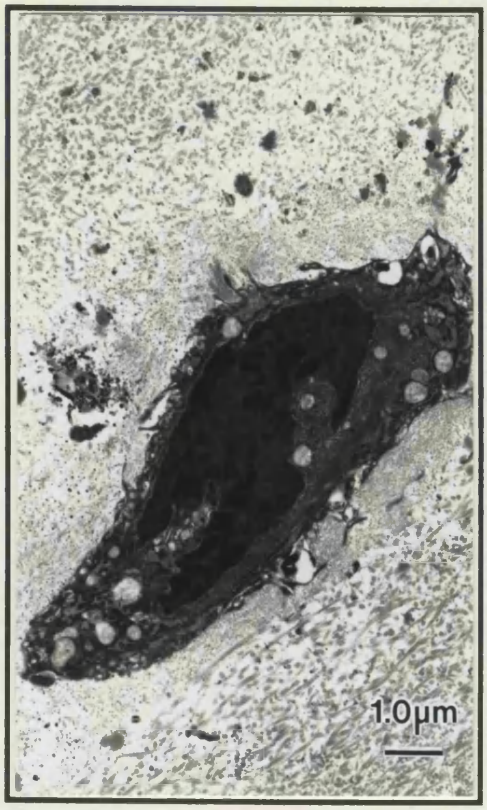

e

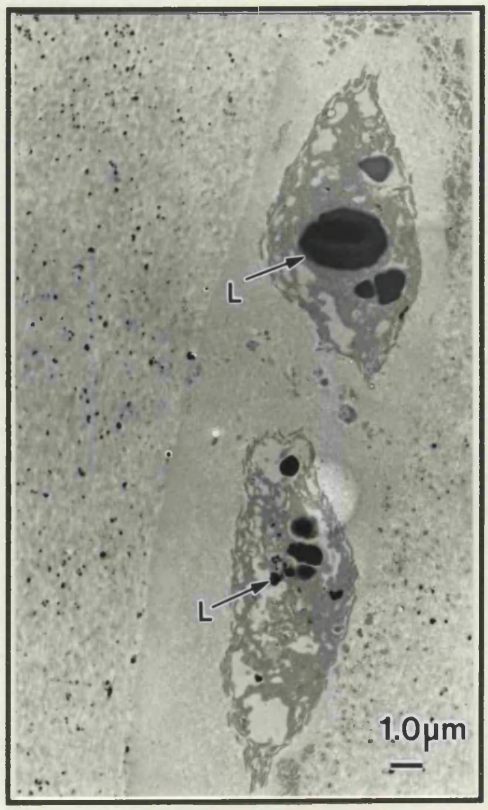

f

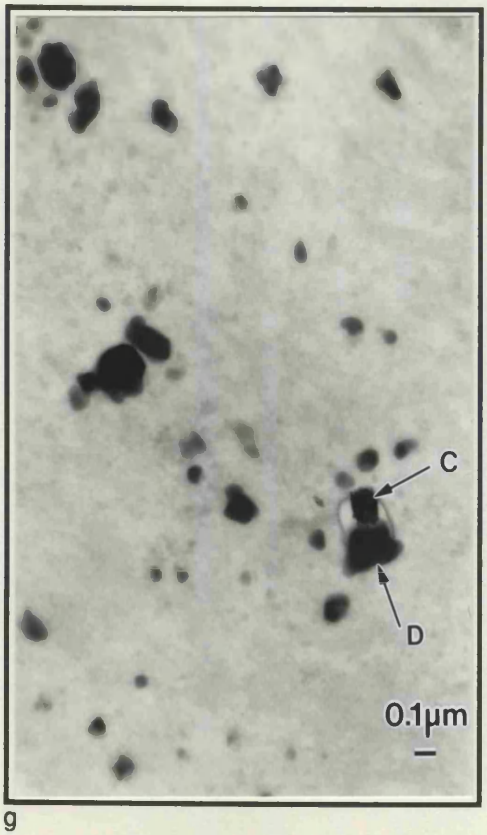

g

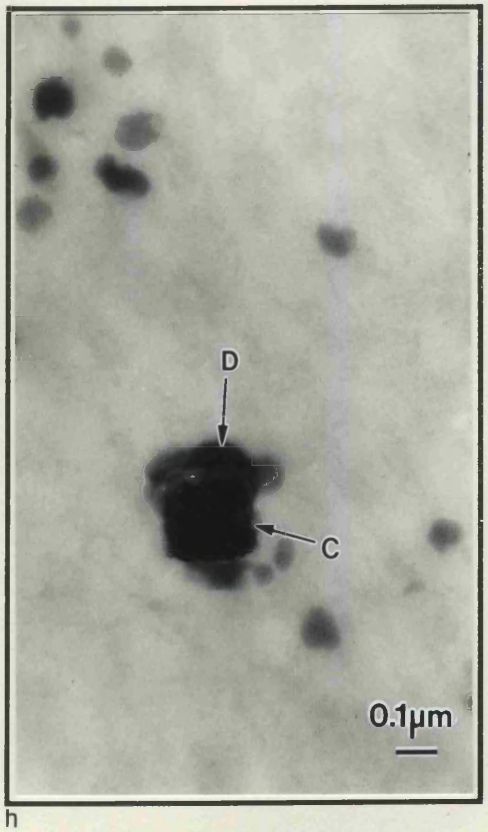

h

Fig. 4.7

Fig. 4.7i. Superficial zone ECM of articular cartilage, fixed using the malachite green method. Small electron dense lipidic debris are scattered throughout the matrix: (Femoral head, CM 30 years). Unstained section.

Fig. 4.7j. Detail of 4.7i, showing globular electron dense lipidic debris in the ECM. Unstained section.

Fig. 4.7k. Deep zone ECM of articular cartilage, Fixed using the malachite green method. Electron dense lipidic debris are sparsely distributed through the matrix in comparison with 4.7i: (Femoral head, CM 30 years). Unstained section.

Fig. 4.7l. Detail of 4.7k, showing multi-lobular, electron dense lipidic debris in the ECM. Unstained section.

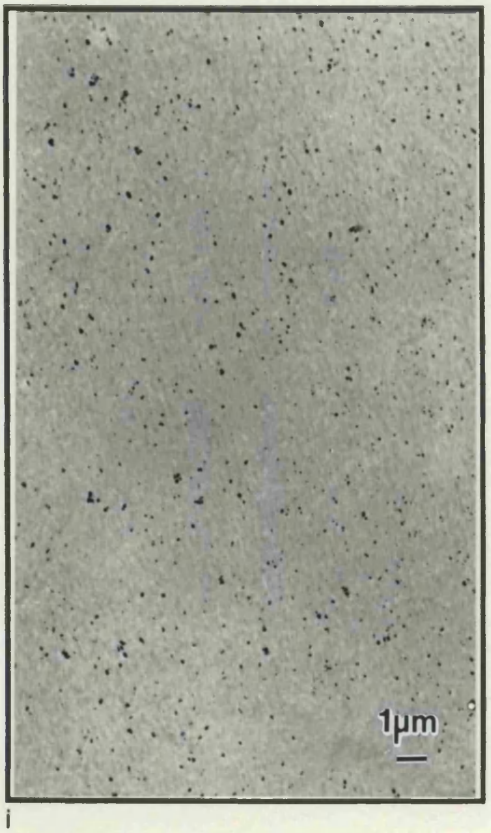

i

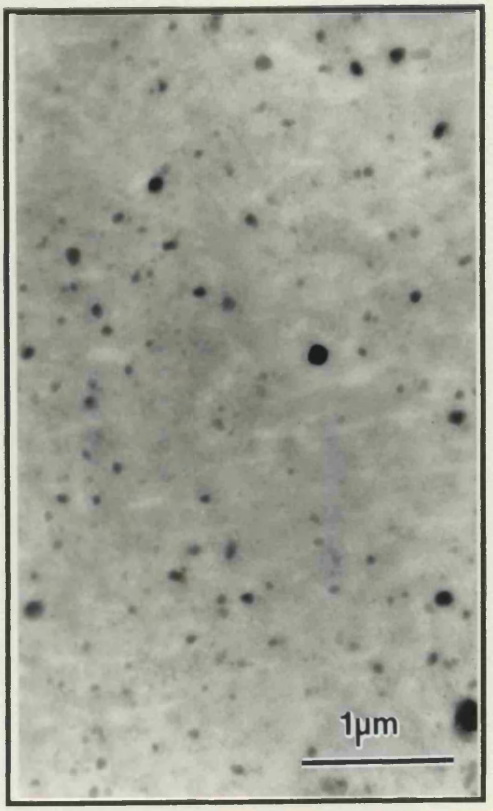

j

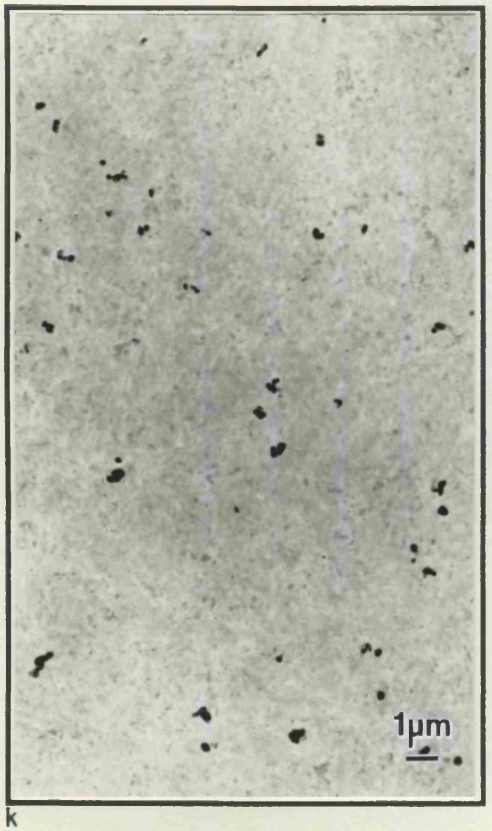

k

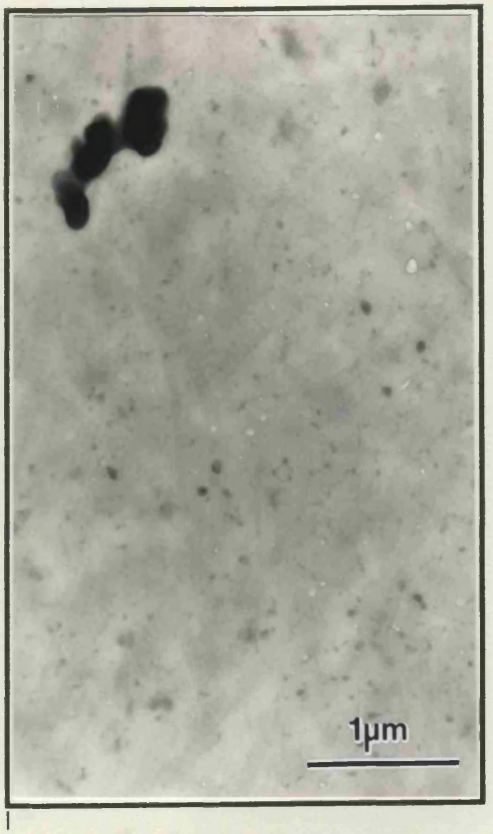

l

Fig. 4.8

Fig. 4.8a. Superficial zone articular cartilage, fixed using the malachite green method. Crystals (C) are present in the ECM and electron dense lipid is apparent in the territorial matrix and within the chondrocyte (D): (Femoral head, CM 30 years). Unstained section.

Fig. 4.8b. XRMA calcium map of the area shown in 4.8a, indicating the crystals (C).

Fig. 4.8c. XRMA phosphorus map of the area shown in 4.8a, indicating crystals (C) and lipid (D).

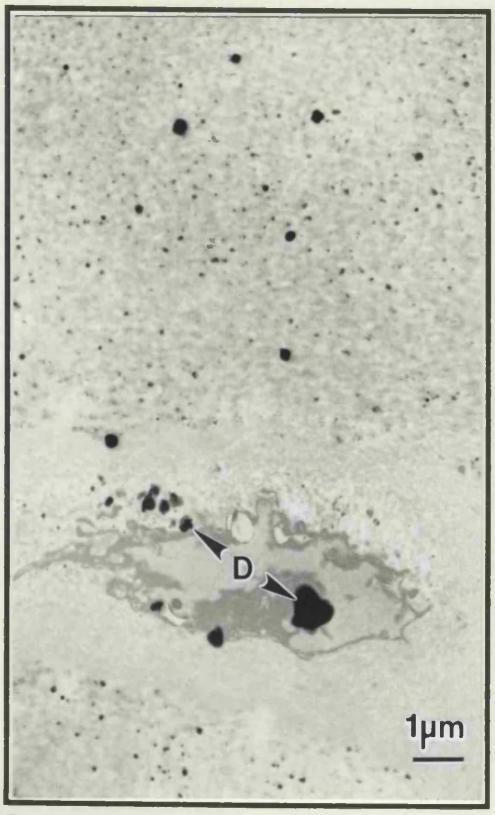

a

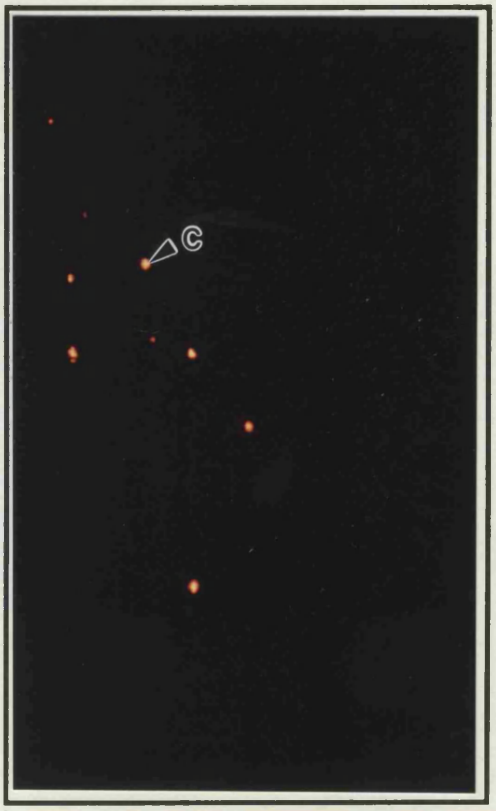

b

c

Fig. 4.8

Fig. 4.8d. Crystal (C) and associated electron dense lipid (D) in superficial zone articular cartilage, fixed using the malachite green method: (Femoral head, CM 30 years). Unstained section.

Fig. 4.8e. XRMA calcium map of the area shown in 4.8d, indicating the crystal (C).

Fig. 4.8f. XRMA phosphorus map of the area shown in 4.8d, indicating crystal (C) and lipid (D).

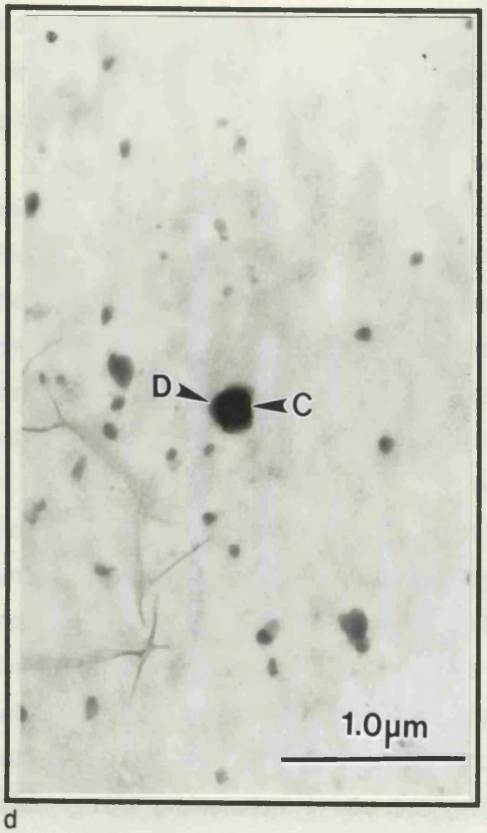

d

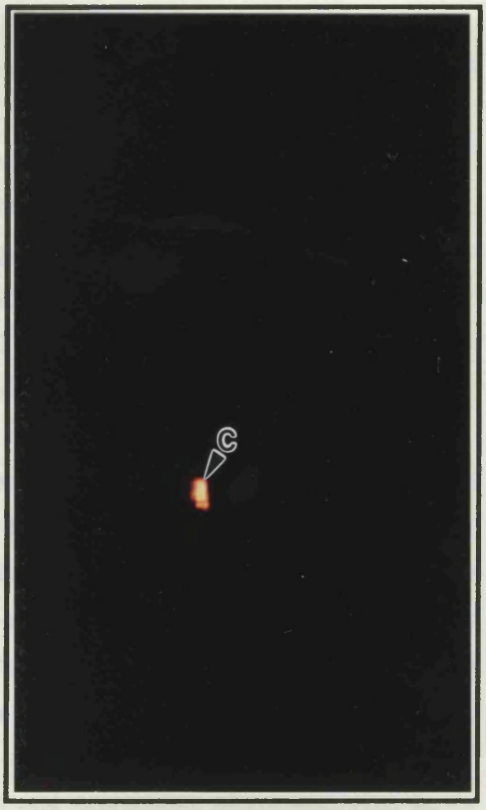

e

f

Discussion

Evidence of a role in whitlockite crystal nucleation for each of the ECM components examined will be assessed individually.

The distribution of safranin O staining observed is consistent with previous studies, which reported low proteoglycan concentrations in the superficial zone relative to deeper zones. These concentrations were determined by histological, biochemical and immunocytochemical methods (Stockwell and Scott 1967, Venn and Maroudas 1977, Maroudas 1979, Bayliss *et al.* 1983, Ratcliffe *et al.* 1984). Reduction in safranin O staining intensity in the superficial zone of cartilage sections may be of significance in relation to magnesium whitlockite crystal formation and patterns of deposition.

Aggregating proteoglycans have been shown to inhibit hydroxyapatite formation and growth *in vitro* (Blumenthal *et al.* 1979, Chen *et al.* 1984, Chen and Boskey 1985, 1986). This function has been attributed to both hydrodynamic size (aggregates were more active than monomers, which were more active than isolated side chains) and the fixed negative charge density of the aggregates. Both these factors are thought to interfere with the diffusion rates of calcium and phosphate ions, and the negatively charged groups, particularly chondroitin sulphates (Hunter *et al.* 1985), may interact with active growth sites on HAP nuclei further reducing HAP proliferation. *In vivo* disaggregation and degradation of proteoglycans at the mineralizing front of growth cartilage (Franzen *et al.* 1982, Campo and Romano 1986, Buckwalter and Rosenberg 1988) may make them less effective inhibitors, enabling mineral formation.

The effect of proteoglycans on whitlockite formation has not been reported. Magnesium is known to inhibit HAP formation, stabilizing precursor states (Blumenthal *et al.* 1979), whilst biolgical apatite has been shown to transform to magnesium-substituted ß-TCP (a mineral phase with close structural similarity to whitlockite as described in chapter three), in the presence of magnesium, at temperatures in excess of 900°C (Bigi *et al.* 1992). Considering the structural similarity between HAP and whitlockite suggested by these observations, it may be reasonable to speculate that proteoglycans would be inhibitive to magnesium whitlockite formation.

Given the above properties it may be expected that proteoglycans would arrest crystal growth in uncalcified cartilage, with regions of relatively low proteoglycan content having greater susceptibility to calcification.

On initial observation of specimens from elderly patients in this study, and those examined by Ali and colleagues (1981, 1983, 1985, 1986) and Stockwell (1990) this premise appears to be supported by a number of findings. First, electron microscopic observation has shown a rapid drop in the proportion of aggregated monomers, monomer length and side chain length, with age (Buckwalter and Rosenberg 1988). These authors observed the variation in monomer length to be related to variation in the length of the chondroitin sulphate rich region. Secondly,the superficial zone is also one of the first sites of proteoglycan loss in cartilage degeneration (Meachim *et al.* 1965). Thirdly, femoral head articular cartilage from cases of subcapital fracture have been shown to have reduced proteoglycan content (Roberts *et al.* 1986). A further site correlating low proteoglycan content and crystal deposition is human meniscus, with

a proteoglycan content of about one tenth that of articular cartilage, partly made up of small, non-aggregating proteoglycans (Buckwalter and Rosenberg 1988). Calcified bodies very similar to cuboid crystals have been reported at this location (Ghadially and Lalonde 1981).

On closer inspection, the association of crystal deposition with low proteoglycan concentrations is not fully consistent. It can be seen that the reduction in safranin O staining is more extensive than the depth of the band of crystal deposition, particularly in older specimens. Crystal deposition is also apparent in young specimens where proteoglycan aggregation is reportedly high (Buckwalter and Rosenberg 1988). In deeper tissue, crystals frequently occur in a pericellular distribution, an area rich in proteoglycan (Poole *et al.* 1980, Ratcliffe *et al.* 1984). Whilst proteoglycans are clearly potent inhibitors of HAP formation and growth and hence may be a factor in the regulation of whitlockite crystal formation they would not appear to be the prime determinant of crystal deposition.

The distribution of alkaline phosphatase activity was consistent with results of earlier studies of normal human articular cartilage (Ali and Bayliss 1974, Rees and Ali 1988). These authors reported, from biochemical and electron histochemical studies, that alkaline phosphatase activity was extremely low in articular cartilage from elderly individuals, the greatest reduction having occurred by the third decade of life. In such specimens the enzyme was restricted to hypertrophic chondrocytes and associated matrix vesicles within forty microns of the tidemark. Rees and Ali (1988) reported that chondrocytes and vesicles in the middle and superficial zones did not show alkaline phosphatase activity.

If it is assumed that crystal formation occurs, within or close to regions in which deposition was observed, and that variation in crystal size is indicative of recent crystal formation, detection of alkaline phosphatase activity in such areas may be taken to indicate an association between crystals and enzyme. The failure to detect alkaline phosphatase activity does not rule out the involvement of the enzyme in crystal formation, merely indicating that the enzyme was not active at the time the specimens were taken. It should also be noted that approximately 40% of the enzyme's activity is retained with the tissue fixation and processing technique employed in this study (Doty 1980). There is therefore the possibility that any weak enzyme activity may have remained undetected.

The formation of bone mineral has been associated with matrix components, with much supporting evidence from ultrastructural observation. The precise mechanism is subject to debate, but most workers agree that matrix vesicles and/or collagen fibrils, depending on tissue location, are integral in heterogenous nucleation of the initial mineral phase (Ali 1983, Landis 1986, Glimcher 1989, Anderson 1992, Arsenault 1992). No specific association with recognisable ultrastructural features was observed in this study. This differs from reports by Ali and colleagues (1981a,b, 1983, 1985), who describe matrix vesicles associated with crystals in OA cartilage, and Stockwell, who describes matrix vesicle-like structures amongst cell debris associated with crystals in normal articular cartilage from elderly patients. The report by Ghadially and Lalonde (1981), describing intramatrical lipidic debris associated with calcified bodies in human semilunar cartilages, is more consistent with the present study. The only apparent

common ultrastructural association was with mixed amorphous and membranous material described previously as intramatrical lipidic debris (chapter one and Ghadially 1983). This might be expected, as matrix vesicles are considered to be extracellular organelles generated, certainly in epiphyseal cartilage, by a controlled cellular process, feasibly by fluctuations in membrane fluidity (Boskey 1989) and charged with a variety of phospholipids and enzymes consistent with their proposed function of heterogenous mineral nucleation (Ali *et al.* 1970, Ali 1976, Peress *et al.* 1971, 1974, Wuthier 1973, Dean et al 1992). It would appear improbable that they would be present at the variety of crystal deposition sites; less specific membrane fragments and lipidic debris would be easier to envisage.

The association between intramatrical lipidic debris and crystal deposition is strengthened by observations of crystal deposition away from the superficial zone. In the intermediate and deep zones crystal deposition was restricted to necrotic cell debris, intramatrical lipidic debris both pericellular and in more remote matrix, and associated with the rare observation of giant collagen fibrils or amianthoid fibres (Ghadially 1983). Amianthoid fibres have been reported as rare occurrences in aged and fibrillated tissue, filling dead cell spaces and effectively forming microscars (Ghadially 1983); similar giant collagen fibres have also been reported in areas of matrix degeneration and HAP deposition in OA articular cartilage (Ohira and Ishikawa 1987). As intramatrical lipidic debris is also considered to be the product of chondrocyte necrosis (Ghadially 1983) it would appear that crystal deposition, at least away from the superficial zone, is associated with chondrocyte necrosis. This would suggest the co-occurrence of amianthoid fibres and crystals is not causally related, but a consequence of cellular degeneration.

Mixed crystal deposition, whorls of needle like crystals associated with a central lucent area, amongst cuboid deposition, both in the microscar and in superficial cartilage, was an extremely rare observation. Bone mineral crystals observed as needles in thin section have proved to exhibit a plate-like morphology (Weiner and Price 1986, Arsenault and Hunziker 1988, Landis *et al.* 1992). From the observed morphology it may be speculated that the needle-like crystals in this study were apatitic in nature. Similar fine needle-like crystal deposition close to the surface of intact full depth cartilage from OA specimens has been reported previously (Ali and Griffiths 1981a,b, 1983, Ali 1985). Clustering of the crystals around an electron lucent centre shares similarities with the report by Pritzker and Luk (1976) of spherical apatite crystals from a pulmonary nodule; however deposition observed in this study is much finer , individual needles forming a corona around the centre rather than dense crystal deposition. The lucent core was not identified, though the amorphous appearance suggests it may be lipidic. The rare observation of laminated lipidic structures amongst intramatrical lipidic debris requires comment. Micrographs would appear to suggest small lipidic bodies undergoing mineralization to produce crystals of similar size, if not morphology, to cuboid crystals. The lipidic bodies, whilst of a similar size to matrix vesicles, do not bear any structural similarities with these extracellular organelles (Bonucci 1967, Anderson 1967). The apparent mineralization of these rare structures was only observed on one occasion, in mid zone cartilage. Further observations would be necessary before a significant interpretation relating to crystal formation could be entertained.

Intramatrical lipid has been associated with pathological deposition of apatite and CPPD in previous ultrastructural studies of articular cartilage (Ohira and Ishikawa 1987, Ohira *et al.* 1988). The observation of oil red O staining for lipid in the the ECM, as a fine band immediately below the articular surface, is a documented feature of normal articular cartilage (Ghadially *et al.* 1965, Meachim and Stockwell 1979). Lipid forms about one percent wet weight of articular cartilage, although this varies between individuals (Meachim and Stockwell 1979). Diffuse lipid in the superficial zone ECM is commonly present by the third decade, although it is infrequent and minimal in childhood and adolescence (Stockwell 1965, Ghadially et al 1965). Bonner *et al.* (1975) showed that in the superficial 0.5-1mm layer, total lipid increases between the ages of fifteen and sixty six years to a far greater extent than in deeper cartilage. It has been shown that this superficial zone deposition reacts histochemically for phospholipid and neutral lipid (Stockwell 1965). The less intense matrix stain relative to that of intracellular lipid droplets may be indicative of a more diffuse distribution of lipid within the ECM or a reflection of the nature of the lipid. Some phospholipids are reported to appear pink when stained with Oil red O (Bayliss High 1990). The apparent co-localization of the Oil red O stain and crystal distribution, notable for both matrix location and differences in extent with age is interesting in that Ghadially (1983) suggested that components of the intramatrical lipidic debris, thought to be responsible for the staining in this study, become sites where calcium salts are deposited in menisci (Ghadially and Lalonde 1981) and deeper normal articular cartilage (Ali 1985, Rees and Ali 1988).

A probable identification of the Oil red O staining component and its association with crystal deposition has been provided by TEM examination and elemental mapping of tissue fixed using the glutaraldehyde-malachite green-osmium tetroxide fixation method. Teichman and colleagues (1974) report that phospholipids are preserved in tissue during TEM processing using this method and imparted with an electron dense character relative to surrounding unstained tissue. The dense globular bodies observed in sections from tissue processed by this method are considered to be phospholipid. This is supported by the phosphorus signal generated by them and observation of similar dense bodies found in cells including rabbit spermatozoa (Teichman *et al.* 1974) and bone nodules grown *in vitro* (Nefussi *et al.* 1992). Several electron micrographs show that intracellular lipids appear to be partly dislodged from their location during specimen processing (Fig. 4.8a), an observation similar to those made by Nefussi *et al.* (1992). These lipid droplets appear to remain in contact with the chondrocytes or at least within in the lacunae, remaining distinct from the smaller deposits within the ECM, which correspond with the distribution of intramatrical lipid debris described by Ghadially (1983) and are considered a component of these.

The acidic phospholipids phosphatidylserine and phosphatidylinositol have been closely associated with HA formation at a number of physiological sites, including matrix vesicles in the epiphyseal growth plate (Wuthier et al 1977, Boskey 1989), collagen fibres in dentine mineralization (Goldberg and Septier 1985) and type I collagen in other mineralizing tissues (Lelous 1982, Ennever et al 1984). That these phospholipids may be involved in whitlockite formation has been implied by Boskey et al (1983). Mineral and lipid associated with parotid gland

sialoliths were analysed; minerals present included HA and in one stone, whitlockite while phosphatidyl serine and phosphatidyl inositol made up almost all the calcium-acidic phospholipid-phosphate complexes. It was suggested that complexed acidic phospholipids form on membrane fragments providing a nidus for mineral formation. The mixture of lipids present was thought to be membrane fragments and cell debris derived from plasma membranes and bacterial cell walls.

Although malachite green does not have the specificity to characterize acidic phospholipids (Teichman *et al.* 1974) it has been used to investigate the role of phospholipid in the calcification of predentine and dentine (Goldberg and Septier 1985, Goldberg and Escaig 1987) and calcified matrix of bone nodules (Nefussi *et al.* 1992), with the aim of preserving phospholipids associated with early calcification. The technique revealed collagen-associated filaments and granules in the area of initial calcification of dentine and aggregates of 'crystal ghosts', crystal associated organic structures revealed by post-embedding decalcification and staining of tissue sections for TEM (Bonucci 1967, 1969), in bone nodules. Osmium removal and lipid solubilization studies on such sections suggested these structures did indeed have phospholipidic components. Whilst the presence of the large multilobed deposits in the deeper cartilage did not appear to be a diffusion artefact further causes of artefact cannot be eliminated as the efficacy of the malachite green dye with highly anionic and hydrophilic tissue such as mid zone cartilage matrix remains poorly characterized.

If the restriction of fine abundant globular bodies to the superficial zone is significant in relation to crystal formation, it may be expected that interaction of these matrix components would be observed. The problems associated with the interpretation of spatial relationships of small structures in thin sections in the TEM have been discussed in chapter one (Hunziker *et al.* 1989). From multiple observations of both features it was observed that they were commonly in excess of 100nm. Therefore apparent co-localization of one with another would suggest that physical interaction is a real observation. That such observations are limited to approximately 10% of crystal encounters would not rule out a role for such deposits in crystal formation. For example matrix vesicles are recognised as the site of initial mineral formation in epiphyseal cartilage and yet by TEM observation the proportion of uncalcified vesicles and mineral spherulites throughout the depth of the growth plate is far in excess of recognisable matrix vesicles containing identifiable crystals.

From this preliminary screening, lipid would appear to be the most likely component of the ECM to act as a nucleating agent for the formation of whitlockite crystals. Intramatrical lipidic debris are present in all areas of crystal deposition, this observation being enhanced in glutaraldehyde-malachite green-osmium tetroxide treated specimens. If it is accepted that this technique is specific for phospholipids (Teichman *et al.* 1974, Nefussi *et al.* 1992) the case for lipid mediated nucleation is strengthened further; however anomalies still remain in the form of the sparsely distributed large multilobed deposits in deeper cartilage of malachite green treated specimens and the paucity of evidence of definite crystal-phospholipid interaction. Although proteoglycan does not appear to be primarily associated with crystal deposition, in areas of low proteoglycan concentration and high lipid deposition the reduction in its inhibitory potential should not be

ignored. Whilst the failure to detect alkaline phosphatase activity does not rule out a role for the enzyme in crystal deposition, the known distribution of this enzyme in normal articular cartilage and the extent of crystal deposition amongst specimens in this study would point against it.

GENERAL DISCUSSION

The objects of the present study were, to establish the occurrence of 'cuboid' crystals in human femoral head articular cartilage, to describe their spatial distribution, to catalogue their occurrence in cartilage from various joint sites and other species, to identify ECM factors that may contribute to the formation of crystals and, through the development of a suitable isolation technique, to determine the crystals' mineral phase. This was achieved by applying electron microscopic and related techniques to fresh, human, normal and OA articular cartilage. Crystals were established as real, rather than artefactual, by the use of several fixation and processing techniques, including an anhydrous method. The presence of crystals in normal femoral head articular cartilage was found across a broad age range and the distribution within normal femoral head articular cartilage established both qualitatively and quantitatively. Cartilage specimens from other sites were screened for crystal presence or absence and relative deposition density. Samples of porcine, lapine and bovine articular cartilage were also examined for evidence of similar crystal deposition. The elemental composition of crystals was investigated principally by XRMA; spectra and Ca/P ratios from a diversity of specimens indicated a consistent elemental composition. These results vindicated the development of an isolation technique, based on collagenase digestion of cartilage and sequential centrifugation, to enable mineral phase analysis using electron and x-ray diffraction techniques. A number of matrix components with the potential to nucleate calcium phosphate crystal formation were screened for their spatial distribution with respect to crystal deposition using histological methods. Alkaline phosphatase, proteoglycans, matrix vesicles and collagen fibrils did not appear to be closely related to crystal formation. Lipid, as examined by light microscopy, standard TEM and observation of tissue processed in a manner to preserve and stain phospholipids for TEM, showed a close correlation with crystal distribution.

The results presented in this study confirm the presence of 'cuboid' crystals in articular cartilage, and provide the first recognition of magnesium whitlockite in articular cartilage supporting and broadening the more limited studies of Ali and colleagues (1981, 1983, 1985, 1986) and Stockwell (1983, 1990). With the exception of these authors, such crystal deposition in articular cartilage has not been previously reported although the report of the deposition of calcified bodies in human meniscus by Ghadially and Lalonde (1981) is most closely related. A number of points may be raised in an attempt to explain this apparent oversight. The ultrastructural study of normal, human, femoral head, articular cartilage, a site where deposition has been observed at its most dense, is limited. Ghadially (1983) commented that knowledge of the fine structure of normal articular cartilage is derived largely from a study of animal material, particularly rabbit, with the more limited studies of human cartilage from fibrillated and normal looking OA specimens, juvenile specimens taken at autopsy and young adult surgically obtained specimens. Many of these studies were based on specimens from the femoral condyle, a site which , in this study, exhibited a lower maximum crystal deposition density than superior region femoral head specimens. The commonly used thin section stain uranyl acetate, and distilled water, routinely used to float thin sections away from the ultratome knife edge, both showed a propensity to crystal loss . Uranyl acetate and lead citrate staining imparts greater electron density to matrix components in thin section, possibly concealing the presence of crystals in cases of sparse

deposition. With this in mind, examination of early studies of human articular cartilage (Ghadially *et al.* 1965) show electron densities amongst stained lipid debris bearing an arguable resemblance to 'cuboid' crystals.

It is necessary to try to discern how magnesium whitlockite crystal deposition is able to occur in normal articular cartilage as it is generally considered that crystal deposition is prevented in this tissue by in situ inhibitors of calcification including, proteoglycans, pyrophosphate and non-collagenous proteins. Fundamental to the understanding of crystal formation is an appreciation of the milieu at deposition sites. Crystals in this study showed a distribution which could be most closely related to one common factor, intramatrical lipidic debris, whether it be pericellular, in association with necrotic chondrocytes and microscars or within the initial depth of the superficial zone. Insight into whitlockite deposition may be gained by comparison of crystal distribution with the more extensively investigated depositions of HA and CPPD and their matrical associations in articular cartilage.

CPPD crystal deposition in articular cartilage characterisitcally shows a sharp demarcation of crystal bearing and non crystal bearing matrix, a feature also observed, especially below 50μm depth of crystal, in this study. CPPD crystal deposition has been observed to take two forms, firstly small deposits at the edge of the chondron and secondly, larger agglomerates which appear to replace both the chondrocyte and its territorial matrix. These two depositional forms have been sequentially linked (Pritzker *et al.* 1988). Although the pericellular distribution of small crystals has similarities with whitlockite crystal deposition in the present study, there is no parallel with the agglomeration stage; an aspect considered below. Pericellular CPPD crystal deposition has been reported to orient in the pericellular matrix, apposed to the articular and subarticular poles of the chondrocyte, this was speculated to be in relation to biomechanical pressures (Pritzker *et al.* 1988). Polarization of crystal deposition observed in this study may have similar origins. Pritzker and colleagues (1988) were unable to detect association or orientation between CPPD deposition and either matrix vesicles or collagen fibres. This is in contrast to descriptions of apatite formation in articular cartilage, reported to be associated with matrix vesicles (Ali 1985) and degenerate collagen fibrils (Ohira and Ishikawa 1987). In the present study, matrix associations were limited to lipidic debris and rare associations with abnormal collagen fibrils in microscars. Associations between CPPD crystal deposition and intramatical lipid have been reported(Ohira *et al.* 1988, Ohira and Ishikawa 1991). Despite the similar matrix component associations, CPPD crystal deposition was never observed in association with whitlockite in this study, although Ali (personal communcation) has observed one co-occurrence. Further, although CPPD crystal deposition has been reported thoroughout the cartilage depth (Hayes *et al.* 1992, Ohira and Ishikawa 1987) preference for the midzone (Schumacher 1988), rather than superficial zone has been described. The rare occurrences of mixed crystal deposition involving whitlockite was with apparently needle shaped, apatite-like crystals. CPPD crystal deposition has been associated with apatite deposition although this is also rare (Pritzker *et al.* 1988). The paucity of reports of such mixed deposition, combined with *in vitro* observations, has led investigators to conclude that the physico-chemical conditions for CPPD and apatite crystal deposition are mutually exclusive

(Cheng and Pritzker 1983, Pritzker *et al.* 1988). It seems unlikely that this is the case for whitlockite and apatite co-deposition; HA and whitlockite have been reported together at locations including root caries, sialoliths, dental plaques, aortic calcification and in renal stones. Also, *in vitro* studies have shown that changes in solute concentrations mediated a range of precipitated mineral phases in which both HA and whitlockite are represented (Cheng *et al.* 1988). The near absence of HA associated with whitlockite crystals in this study may be due to sub-optimal nucleation conditions combined with a prevalence of inhibitory factors. A suggestion as to why these do not prevent whitlockite formation is offered below. The mechanism of CPPD formation remains elusive; recent studies have focussed on enzyme defects in affected tissues (Howell *et al.* 1984, Ryan *et al.* 1985, Ryan *et al.* 1991) and ionic and matrix conditions that favour CPPD deposition *in vivo* (Pritzker *et al.* 1988, Ohira and Ishikawa 1991) and *in vitro* (Pritzker *et al.* 1985). Due to the ubiquity of crystal deposition in the present study it seems unlikely that enzyme defects are responsible for the observed whitlockite deposition. Therefore, in the proposal of any mechanism for whitlockite deposition, ionic and matrix conditions will be given primary consideration.

Free calcium ion and inorganic phosphate concentrations in cartilage are too low for *de novo* crystal formation (Cheng *et al.* 1988), particularly in the presence of inhibitors. The apparent association of intramatrical lipidic debris with crystal deposition provides the basis for the proposal of a mechanism of mineral formation. The origin of debris has been ascribed to chondrocyte necrosis or detachment of cell processes (Ghadially 1983). This cellular association is supported by the observation that cells are most numerous near the articular surface, one third of all cells lying beneath a given area of the articular surface within the superficial 0.22mm (Stockwell and Meachim 1979), corresponding to a high density of lipidic debris.

The concentration of calcium ions in the extracellular fluid is believed to be 10^2 to 10^5 fold higher than that of calcium in the chondrocyte cytoplasm (Rasmussen 1970, Farber 1981). This situation is known to result from calcium ions moving to the extracellular space by a pump mechanism in the cell membrane, calcium ions in the extracellular fluid entering cells by a passive process. Loss of calcium control in the cell membrane and the subsequent increase of intracellular calcium appear to be the final common pathway to cell death (Farber 1981). Intracytoplasmic lipid may play a role in the intracellular accumulation of this calcium influx. Ohira and Ishikawa (1991), demonstrated that intracytoplasmic lipid droplets of 'hypertrophic' chondrocytes in cartilage with CPPD deposition formed antimony-calcium complexes at their margins. Ohira *et al.* (1988) demonstrated that lipids are abundant not only in the hypertrophic chondrocytes around CPPD crystals but also in the degenerated matrix surrounding chondrocytes with a hypertrophic appearance. This material was also shown to contain a large amount of calcium (Ohira and Ishikawa 1991). A mechanism could be envisaged whereby, with the onset of chondrocyte necrosis, a calcium influx enables the formation of calcium-lipid complexes which, in the presence of appropriate inorganic phosphate concentrations and the lattice stabilizing effect of magnesium ions, form whitlockite.

At cell death lysosomal enzymes are released, including phosphatases and ATPases. Two effects related to mineral formation may arise from this: first, pyrophosphate and ATP, two known molecular inhibitors of mineral formation may be removed form the local milieu, and secondly, inorganic phosphate may be generated raising the calcium x phosphate product. In the epiphyseal growth plate a cell mediated increase in inorganic phosphate occurs in conjunction with initial mineral formation (Althoff *et al.* 1982). This is obviously a more controlled mechanism, but may have analogies with the mechanism proposed here.

Raised inorganic phosphate levels may also act to precipitate mineral formation by another method. Hunter (1987) proposed a role for proteoglycan in crystal formation rather than inhibition. Recognising that total calcium exists at high concentration in cartilage, being mainly bound to the anionic groups of protoglycans, the mechanism proposes that local increases in inorganic phosphate concentrations displace calcium ions from proteoglycan by an ion exchange effect raising the calcium x phosphate product above the threshold for precipitation of mineral. Ishikawa et al (1989) have linked an abundance in intracellular proteoglycans with intracellular accumulation of calcium in chondrocytes adjacent to CPPD crystal deposition sites in cartilage.

The second source of intramatrical lipidic debris is thought to be detachment of the tips of cellular processes (Ghadially 1983, Ghadially *et al.* 1965), a similar process to formation of matrix vesicles. If it is assumed that calcium pumps fail some time after detachment, a similar mechanism for mineral formation may be envisaged.

An alternative or complimentary explanation for the accumulation of crystals in a surface band may be considered. Movement of debris from sites of cellular necrosis to the articular surface has been suggested (Ghadially 1983). There are reasons to speculate that the superficial region may provide an optimal site for crystal deposition; first, aggregating proteoglycan concentration has been reported to be at a minimum and secondly, Ryan *et al.* (1991) have reported evidence to suggest synovial fluid ATP acts as a substrate for the production of inorganic pyrophosphate and phosphate formation in the process of CPPD and apatite crystal deposition. This marginal site would provide a prime location for an elevated inorganic phosphate concentration from such a source.

A combination of maximal stresses on superficial zone superior region femoral head cartilage (O'Connor *et al.* 1988), contributing to chondrocyte necrosis and detachment of tips of cell processes and high cell density, may contribute to the differences in crystal deposition density recorded between superior and inferior regions of the femoral head in this study.

Crystal sizes recorded in this study varied over a small range (50-500nm). At other sites, particularly in stone formation, whitlockite crystals attain greater size. Also CPPD crystals in cartilage form large agglomerates, ostensibly from small pericellular crystals. The growth rate, size and orientation of crystals,particularly apatite, in connective tissues are believed to be controlled by factors including proteoglycans and non collagenous proteins. It would seem reasonable to expect a similar mechanism to be in effect here, though less efficient at preventing whitlockite crystal formation.

Irrespective of their mode of formation, the presence of these crystals requires consideration of their role in articular cartilage, physiological or pathological. The demonstration of crystal deposition in articular cartilage from normal, adolescent to elderly, cartilage, in this study, suggesting that they do not *per se,* pose a pathological risk to the tissue.

It would be pejorative not to consider crystal deposition in a physiological context. The higher cell density in the superficial zone has been related to nutritional conditions and metabolic requirements and it was speculated that the superficial chondrocytes may act as a 'metabolic sink' , to ensure the proper environment for the deeper tissue (Stockwell and Meachim 1979). If this is so, crystal deposition in the superfical zone may serve to remove excess calcium ions from the extracellular cartilage fluid easing stresses on the chondrocytes and matrix components below. Tenuous as this is, it is difficult to anticipate an alternative physiological role. Failure to define such a role would tend to indicate that they were the result of opportunistic deposition, with no defined function. Their circumstantial association with intramatrical lipidic debris may relate crystal deposition to the removal of material generated from chondrocyte necrosis from the ECM to the synovial fluid; a function considered by Ghadially (1983). This would provide an opportunity for further speculation on crystal deposition; first, providing possible means of damping ion fluxes at cell necrosis, minimising the effects on the pericellular environment and secondly, raising the question do crystals stay at the site of formation, or is there a migration to the articular surface as suggested for necrotic debris. The existence of a crystal band in the superficial zone may support the latter.

The possibility of the involvement of sub articular matrical lipid in boundary lubrication, the formation of an adsorbed protective layer on articulating surfaces, has been raised (Swanson 1979). Little *et al.* (1969) demonstrated a large increase in the coefficient of friction of cartilage samples from which this extracellular lipid had been extracted, at least in the absence of synovial fluid. It was not clear whether this was solely attributable to lipid removal or whether hyaluronan at the surface was also interfered with. Of course, the absence of synovial fluid would detract from the boundary lubrication effect afforded by synovial fluid hyaluranon (Maroudas 1979). If lipid does act as a boundary lubricant, an involvement in crystal formation may reduce such activity. In the presence of synovial fluid, with the potential for boundary lubrication from hyaluranon, it would be hard to envisage a significant drop in the coefficient of friction due to a loss of lipid as suggested. An increase in the coefficient of friction of cartilage samples has been reported in conjunction with increased incidence of crystal deposition, nominally CPPD, and severity of tissue fibrillation, although the relative contribution of either factor was not determined (Clift *et al.* 1989).

The presence of crystals in articular cartilage may alter tissue compliance. It would seem unlikely that the crystal deposition observed in this study, being deposited primarily at the articular surface, would significantly alter the load spreading ability of the tissue. More pertinent may be the local differences in physical properties between cartilage matrix and crystals, providing potential for disruption of the articular surface integrity. A correlation between CPPD crystal deposition and severity of fibrillation has been reported by Clift *et al.* (1989); however no evidence of fibrillation associated with crystal deposition to support this premise was observed in this study.

In the presence of degenerative cartilage changes of non-crystalline origin, crystals in the surface may further the process of tissue degeneration, being released from the matrix. Crystals would be available to mediate tissue degeneration by mechanical and cellular means. Free crystals would have the potential to increase wear through scouring remaining articular surfaces. BCP and CPPD crystals have also been shown to stimulate release of proteases including collagenase, and PGE_2 from synovial membrane derived cells *in vitro* (Cheng *et al.* 1981, Borkowf *et al.* 1986). Chondrocytes have been shown to respond similarly (Cheung *et al.* 1983, Mitchell *et al.* 1992). McCarty (1981) has described patients with severely damaged joints where their synovial fluid contained hydroxyapatite crystals and high levels of activated collagenase, suggesting this system may operate in vivo. Despite lack of confirmation of this finding by Dieppe *et al.* (1988) the involvement of whitlockite crystals in such a system cannot be ruled out, whilst appreciating the dose dependency of such reactions. This scenario is essentially that of an amplification loop described by Dieppe and Calvert (1983) and outlined in the general introduction. To entertain this further it would be necessary to establish that crystals are released from cartilage and that they persist in the synovial fluid.

In conclusion, magnesium whitlockite crystal deposition has been demonstrated in articular cartilage across a broad age range at several joint sites. It seems possible that the formation of crystals is primarily associated with lipid, possibly phospholipid debris within the ECM, deposition occurring where the local milieu is favourable. Further investigation of the mode of formation could be provided by *in vitro* studies using a dynamic collagen gel system similar to that described by Boskey (1989a). If this apparently opportunistic mode of crystal deposition is accepted, the potential of a physiological role for magnesium whitlockite crystals seems minimal; a role as an aggravator of pathological degeneration would seem more plausible. The potential for such a role may be clarified by further study. First, establishing the presence of crystals in synovial fluids with accompanying clinical and biochemical correlations. Secondly , the crystal isolation technique developed in this study may be used to enable co-incubation of crystals with cells derived from articular tissues. It is important to recognise the limitations of this regarding alterations in the crystal surface during the isolation process, particularly with respect to adsorbed organic material. Biphasic finite element analysis, already applied to the investigation of CPPD crystal deposition in cartilage (Clift 1992), used in conjunction with the quantitative crystal depostion data obtained in this study, may provide insight to modifications of tissue compliance attributable to magnesium whitlockite deposition.

REFERENCES

Addadi L, Weiner S (1985). Interactions between acidic proteins and crystals: Stereochemical requirements in biomineralization. Proc. Natl. Acad. Sci. USA., 82: 4110-4114.

Afoke NYP, Byers PD, Hutton WC (1987). Contact pressures in the human hip joint. J. Bone Joint Surg., 69: 536-541.

Aherne WA, Dunnill MS (1982). *Morphometry*: London : Edward Arnold.

Aitkin JM (1982). The prevention of osteoporosis. In *Calcium Disorders* (eds. DA Heath & SJ Marx), London, Butterworth: pp. 47-68.

Alexander GJM, Dieppe PA, Doherty M, and Scott DGI (1982). Pyrophosphate arthropathy: a study of metabolic associations and laboratory parameters. Ann. Rheum. Dis., 41: 377-381.

Ali SY (1976). Analysis of matrix vesicles and their role in the calcification of epiphyseal cartilage. Fed. Proc. Fed. Am. Soc. Exp. Biol., 35: 135-142.

Ali SY, (1977). Matrix vesicles and apatite nodules in arthritc cartilage. In *Perspectives in inflammation* (eds. DA Willoughby, JP Giroud, GP Velo); Lancaster UK, MTP Press: pp. 211-223.

Ali SY (1983). Calcification of Cartilage. In *Cartilage vol. 1. Structure Function and Biochemistry* (ed. BK Hall); London, Academic Press: pp. 343-378.

Ali SY (1985). Apatite-type crystal deposition in articular cartilage. Scanning Electron Microscopy, IV: 1555-1566.

Ali SY, Sajdera SW, Anderson HC (1970). Isolation and characterization of calcifying matrix vesicles from epiphyseal cartilage. Proc. Nat. Acad. Sci., 67: 1513-1520.

Ali SY, Evans L (1973). The uptake of [^{45}Ca] calcium ions by matrix vesicles isolated from calcifying cartilage. Biochem J., 134: 647-650.

Ali SY, Bayliss MT (1974). Enzymic changes in human osteoarthritic cartilage. In *Normal and Osteoarthritic Articular Cartilage* (eds. SY Ali, MW Elves & DH Leaback);London: Institute of Orthopaedics, University of London: pp. 189-203.

Ali SY, Wisby A (1975). Mitochondrial granules of chondrocytes in cryosections of growth cartilage. Am. J. Anat., 144: 243-248.

Ali SY, Griffiths S (1981a) New types of calcium phosphate crystals in osteoarthritic cartilage. Sem. Arthritis Rheum., 11 (Suppl. 1): 124-126.

Ali SY, Griffiths S (1981b). Matrix vesicles and apatite deposition in osteoarthritis. In *Matrix vesicles: Proceedings of the Third International Conference on Matrix Vesicles*; Milan, Wichtig Editore: pp. 241-247.

Ali SY, Griffiths S (1983). Formation of calcium phosphate crystals in normal and osteoarthritic cartilage. Ann. Rheum. Dis., 42 (Suppl.): 45-48.

Ali SY, Griffiths S, Bayliss MT, Dieppe PA (1983). Ultrastructural studies of pyrophosphate crystal deposition in articular cartilage. Ann. Rheum. Dis., 42 (Suppl.): 97-98.

Althoff J, Quint P, Krefting E-R, Hohling HJ (1982). Morphological studies on the epiphyseal growth plate combined with biochemical and x-ray microprobe analyses. Histochemistry, 74: 541-552.

Anderson HC (1967). Electron microscopic studies of induced cartilage development and calcification. J. Cell Biol., 35: 81-101.

Anderson HC (1976). Matrix vesicle calcification. Fed. Proc. Fed. Am. Soc. Exp. Biol. USA, 35: 105-108.

Anderson HC (1980). Calcification processes. Pathol. Ann., 15: 45-75.

Anderson HC (1988). Mechanisms of pathologic calcification. Rheum. Dis. Clin. N. Am.,14 (2) (ed. McCarty DJ); Philadelphia, WB Saunders: 303-319.

Anderson HC (1992). Conference introduction and summary. Bone and Mineral, 17: 107-112.

Anderson HC, Matsuzawa T, Sajdera SW, Ali SY (1970) Membranous particles in calcifying cartilage matrix. Trans. NY Acad. Sci., 32: 619-630.

Anderson HC, Reynolds JJ (1973). Pyrophosphate stimulation of calcium uptake into cultured embryonic bones. Fine structure of matrix vesicles and their role in calcification. Dev. Biol., 34: 211-227.

Armstrong CG, Bahrani AS, Gardner DL (1977). Alteration with age in compliance of human femoral-head cartilage. Lancet, 1: 1103-1104.

Armstrong C, Mow VC (1982) Variations in the intrinsic mechanical properties of human articular cartilage with age degeneration and water content., J. Bone Joint Surg. 64A: 88-94.

Arsenault AL, Hunziker EB (1988). Electron microscopic analysis of mineral deposits in the calcifying epiphyseal growth plate. Calcif. Tissue Int., 42: 119-126.

Arsenault AL (1992). Structural and biochemical analyses of mineralization using the turkey leg tendon as a model tissue. Bone and Mineral, 17: 253-256.

Ayad S, Abedin MZ, Weiss JB, Grundy SM (1982). Characterization of another short-chain disulphide-bonded collagen from cartilage, vitreous and intervertebral disc. FEBS Lett., 139: 300-304.

Ayad S, Evans H, Weiss JB, Holt L (1984). Type VI collagen but not type V collagen is present in cartilage. Coll. Rel. Res., 4: 165-168.

Bader DL, Kempson GE, Egan J, Gilbey W, Barrett AJ (1992). The effects of selective matrix degradation on the short-term compressive properties of adult human articular cartilage. Biochim. Biophys. Acta, 1116: 147-154.

Bancroft JD, Stevens A (1990). Theory and Practice of Histological Techniques. London, Churchill Livingstone.

Barnett CH, Cochrane W, Palfrey AJ (1963). Age changes in articular cartilage of rabbits. Ann. Rheum. Dis., 22: 389-400.

Bayliss MT, Ali SY (1978). Age related changes in the composition and structure of human articular cartilage proteoglycans. Biochem. J., 176: 683-693.

Bayliss MT, Ali SY (1981). Age related changes in human articular cartilage proteoglycans. Semin. Arthritis Rheum.,11 (Suppl. 1): 20-21.

Bayliss MT, Venn M, Maroudas A, Ali SY (1983). Structure of proteoglycans from different layers of human articular cartilage. Biochem. J., 209: 387-400.

Bayliss High OB (1990). Lipids. In *Theory and Practice of Histological Techniques* (eds. JD Bancroft & A Stevens); London, Churchill Livingstone: pp. 215-244.

Benderly H, Maroudas A (1975). Equilibria of calcium and phosphate ions in human articular cartilage. Ann. Rheum. Dis., 34 (suupl.): 46-47.

Beninghoff A (1925). Form und Bau der Gelenkknorpel in ihren Beziehungen zur function. II. Der Aufbau des Gelenkknorpels in seinen Beziehungen zur Function. Z. Zellforsch. mikrosk. Anat., 2: 783.

Bernard GW (1969). The ultrastructural interface of bone crystals and organic matrix in woven and lamellar endochondral bone. J. Dent. Res., 48: 781-788.

Bernard GW, Pease DC (1969). An electron microscope study of initial intramembranous osteogenesis. Am. J. Anat., 125: 271-290.

Berry EE (1967). The structure and composition of some calcium-deficient apatites. J. Inorg. Nucl. Chem., 29: 317-327.

Berthet- Colominas C, Miller A, White SW (1979). Structural study of the calcifying collagen in turkey leg tendons. J. Mol. Biol., 134: 431-445.

Bestetti-Bosisio M, Cotelli F, Schiaffino E, Sorgato G, Schmid C (1984). Lung calcification in long-term dialysed patients: a light and electron microscopic study. Histopathology, 8: 69-79.

Bianco P, Hayashi G, Silvestrini G, Termine JD, Bonucci E (1984). Ultrastructural localisation of osteonectin and Gla-protein in calf bone. Calcif. Tissue Int., 36 (Suppl. 2): S2.

Bigi A, Foresti E, Gregorini R, Ripamonti A, Roveri N, Shah JS (1992). The role of magnesium on the structure of biological apatites. Calcif. Tissue Int., 50: 439-444.

Bishop MA , Warshawsky H (1982). Electron microscopic studies on the potential loss of crystallites from routinely processed sections of young enamel in the rat incisor. Anat. Rec., 202: 177-186.

Bjelle AO, Sundstrom BKG (1975). An ultrastructural study of the articular cartilage in calcium pyrophosphate dihydrate (CPPD) crystal deposition disease (chondocalcinosis articularis). Calcif. Tiss. Res., 41: 63-71.

Blatt M, Denning M, Zumberge H, Maxwell H (1958). Studies in sialoliths I. The structure and mineralogical composition of salivary gland calculi. Annals Otol., 67: 595-617.

Blumenthal NC, Betts F, Posner AS (1975). Nucleotide stabilization of amorphous calcium phosphate. Mat. Res. Bull., 10: 1055-1060.

Blumenthal NC, Betts F, Posner AS (1975a). Effect of carbonate and biological macromolecules on formation and properties of hydroxyapatite. Calcif. Tiss. Res., 18: 81-90.

Blumenthal NC, Posner AS, Silverman LD, Rosenberg LC (1979). Effects of proteoglycans on *in vitro* hydroxyapatite formation. Calcif. Tissue Int., 27: 75-82.

Blumenthal NC, Betts F, Posner AS (1981). Formation and structure of Ca-deficient hydroxyapatite. Calcif. Tissue Int., 33: 111-117.

Boggs J, Wood D, Moscarello M, Papahadjapolous, D (1977). Lipid phase separation induced by hydrophobic protein in phosphatidylserine-phosphatidylcholine vesicles. Biochem., 16: 2325-33.

Bonar LC, Grynpas MD, Roberts JE, Griffin RG, Glimcher MJ (1985). Physical and chemical characterisation of the development and maturation of bone mineral. In *The Chemistry and Biology of Mineralized Tissues* (ed. WT Butler); Alabama, Ebsco Media: pp. 226-233.

Bonar LC, Lees S, Mook HA (1985a). Neutron diffraction studies of collagen in fully mineralized bone. J. Mol. Biol., 181: 265- 270.

Bonner WM, Jonsson H, Malanos C, Bryant M (1975). Changes in the lipids of human articular cartilage with age. Arthritis Rheum., 18: 461-473.

Bonucci E (1967). Fine structure of early cartilage calcification. J. Ultrastruct. Res., 20: 33-50.

Bonucci E (1969). Further investigation of the organic /inorganic relationships in calcifying cartilage. Calcif. Tiss. Res., 3: 38-54.

Boothroyd BJ (1964). The problem of demineralisation in thin sections of fully calcified bone. J. Cell Biol., 20: 165-173.

Borkowf A, Cheung HS, McCarty DJ (1986). Effects of BCP crystals on specific protein synthesis. Arthritis Rheum., 29: S103.

Bornstein P, Sage H (1980). Structurally distinct collagen types. Ann. Rev. Biochem., 49: 957-1003.

Boshier DP, Holloway H, Kitchin LF (1984). A comparison of standard lipid staining techniques used in electron microscopic studies of mammalian tissues. Stain Technology, 59: 83-89.

Boskey AL (1989). Phospholipids and calcification. In *Calcified Tissue* (ed. DWL Hukins); London, MacMillan Press: pp. 215-243.

Boskey AL (1989a). Hydroxyapatite formation in a dynamic collagen gel system: effects of type I collagen lipids and proteoglycans. J. Phys. Chem., 93: 1628-1633.

Boskey AL, Posner AS (1974). Magnesium stabilization of amorphous calcium phosphate. A kinetic study. Mat. Res. Bull., 9: 907-916.

Boskey AL, Posner AS (1976). Extraction of a calcium-phospholipid-phosphate complex from bone. Calcif. Tiss. Res., 19: 273-283.

Boskey AL, Burstein LS, Mandel ID (1983). Phospholipids associated with human parotid gland sialoliths. Arch. Oral Biol., 28: 655-657.

Boskey AL, Bullough PG (1984). Cartilage calcification: normal and aberrant. Scanning Electron Microscopy, II: 943-952.

Boskey AL, Dick BL (1991). The effect of phosphatidylserine on *in vivo* hydroxyapatite growth and proliferation. Calcif. Tissue Int., 49: 193-196.

Boskey AL, Mearesca M, Butler WT, Prince C (1992). Osteopontin is an effective *in vitro* inhibitor of hydroxyapatite formation and growth. Trans. 38th Annual Meeting, Orthopaedic Research Society: p185.

Bowen-Pope DF, Rubin H (1983). Growth stimulatory precipitate of Ca++ and pyrophosphate. J. Cell Physiol., 117: 51-61.

Boyan-Salyers BD, Boskey AL (1981). Relationship between proteolipids and calcium-phospholipid-phosphate complexes in *Bacterionema matruchoti* calcification. Calcif. Tiss. Int., 30: 167-74.

Boyan BD, Boskey AL (1984) Co-isolation of proteolipids and calcium -phospholipid -phosphate complex. Calcif. Tiss. Int., 36: 214-18.

Boyan BD, Swain L, Renthal R (1986). Proton transport by calcifiable proteolipids. In *Cell Mediated Calcification and Matrix Vesicles* (ed. SY Ali); Amsterdam, Elsevier Bioscience BV: pp. 199-204.

Boyde A, Jones SJ (1970). Bone and other hard tissues. In *Principles and Techniques of Scanning Electron Microscopy* (ed. MA Hayat); New York, Van Nostrand Reinhold Company: pp. 123-149.

Bray BA, Lieberman R, Meyer K (1967). Structure of human skeletal keratosulfate. The linkage region. J. Biol. Chem., 242: 3373-3380.

Brighton CT, Heppenstall RB (1971). Oxygen tension in zones of the epiphyseal plate, the metaphysis and diaphysis. An *in vitro* and *in vivo* study in rats and rabbits. J. Bone Joint Surg., 53A: 719-728.

Brighton CT, Hunt RM (1978). The role of mitochondria in growth plate calcification as demonstrated in a rachitic model. J. Bone Joint Surg., 60A: 630-639.

Brodelius A (1961). Osteoarthrosis of the talar joints in footballers and ballet dancers. Acta Orthopaedica Scand., 30: 309-314.

Broom ND (1986). The collagenous architecture of articular cartilage - a synthesis of ultrastructure and mechanical functions. J. Rheumatol., 13: 142-152.

Brown RA, Jones K (1992). Fibronectin synthesis and release in normal and osteoarthritic human articular cartilage. Eur. J. Musculoskel. Res., 1: 25-32.

Brown WE (1966). Crystal growth of bone mineral. Clin. Orthop., 44: 205-220.

Brown WE, Smith JP, Lehr LR, Frazier WA (1962). Octocalcium phosphate and hydroxyapatite. Nature 196: 1048-1055.

Brown WE, Shroeder LW, Ferris JS (1979). Interlayering of crystalline OCP and HAP. J. Phys. Chem., 83: 1385-1388.

Buckley CJ, Foster GF, Burge RE, Ali SY, Scotchford CA (1992). Elemental mapping of biological tissue by x-ray absorption difference imaging in the STXM. In *X-ray Microscopy III. Springer Series in Optical Sciences 67* (ed. Michette, Morrison, Buckley); Berlin, Springer Verlag: pp. 432-6.

Buckwalter JA (1983). Proteoglycan structure in calcifying cartilage. Clin. Orthop., 172: 207-232.

Buckwalter JA, Roughley PJ (1987). Age related changes in human articular cartilage proteoglycans. Trans. 33rd Annual Meeting of the Orthopaedic Research Society, 12,151.

Buckwalter JA, Rosenberg LC (1988). Electron microscopic studies of cartilage proteoglycans. Electron Microsc. Rev., 1: 87-112.

Bullough P, Goodfellow J, O'Connor J (1973). The relationship between degenerative changes and load bearing in the human hip. J. Bone Joint Surg., 55B: 746-758.

Bullough PG, Vigorita VJ (1984). Atlas of Orthopaedic Pathology. With clinical and radiological correlations. London, Butterworth.

Burgeson RE, Hollister DW (1979). Heterogeneity in human cartilage: identification of several new collagen chains. Biochem. and Biophys. Res. Commun., 87: 1124-1131.

Burstein LS, Boskey AL, Tannenbaum PJ, Posner AS, Mandel IR (1979). The crystal chemistry of submandibular and parotid salivary gland stones. J. Oral Pathol., 8: 284-291.

Byers PD, Contepomi CA, Farkas TA (1970). A post-mortem study of the hip joint. Including the prevalence of the features of the right side. Ann. Rheum. Dis., 29: 15-31.

Byers PD, Hoaglund FT, Purawel GS, and Yau ACMC (1975). Articular cartilage changes in Caucasian and Asian hip joints. Ann. Rheum. Dis., 33: 157-161.

Calvo C, Gopal R (1975). The crystal structure of whitlockite from the Palermo Quarry. American Mineral., 60: 120-133.

Campo RD, Romano JE (1986). Changes in cartilage proteoglycans associated with calcification. Calcif. Tissue Int., 39: 175-184.

Carlisle EM (1970). Silicon: a possible factor in bone calcification. Science, 167: 279-280.

Carlstrom D, Glas JE (1959). The size and shape of apatite crystallites in bone as determined from line-broadening measurements on oriented specimens. Biochim. Biophys. Acta, 35: 46.

Carney SL, Muir H (1988). The structure and function of cartilage proteoglycans. Physiol. Rev., 68: 858-910.

Caswell AM, Guilland-Cumming DF, Hearn PR, McGuire MKB, Russel RGG (1983): Pathogenesis of chondrocalcinosis and pseudogout. Metabolism of inorganic pyrophosphate and production of calcium pyrophosphate dihydrate crystals. Ann. Rheum. Dis., 42 (suppl. 1): 27-37.

Chapman JA, Hulmes DJS (1984) Electron microscopy of the collagen fibril. In *Ultrastructure of the Connective Tissue Matrix* (eds. A Ruggeri, PM Motta); Boston, Martinus Nijhoff: pp.1-33.

Chen CC, Boskey AL, Rosenber g LC (1984). The inhibitory effect of cartilage proteoglycans on hydroxyapatite growth. Calcif.Tissue Int., 36: 285-290.

Chen CC and Boskey AL (1985). Mechanisms of proteoglycan inhibition of hydroxyapatite growth. Calcif. Tissue Int., 37: 395-400.

Chen CC, Boskey AL (1986). The effects of proteoglycans from different cartilage types on in vitro hydroxyapatite proliferation. Calcif. Tissue Int., 39: 324-327.

Chen Q, Fitch JM, Linsenmayer C, Linsenmayer TF (1992). Type X collagen: covalent crosslinking to hypertrophic cartilage-collagen fibrils. Bone and Mineral, 17: 223-227.

Cheng P-T, Pritzker KPH (1983). Solution Ca/P ratio affects calcium phosphate crystal phases. Calcif. Tissue Int., 35: 596-601.

Cheng P-T, Pritzker KPH (1983a). Pyrophosphate, phosphate ion interaction effects on calcium pyrophosphate and calcium hydroxyapatite crystal formation in aqueous solutions. J Rheumatol., 10: 769-777.

Cheng P-T, Grabher JJ, LeGeros RZ (1988). Effects of magnesium on calcium phosphate formation. Magnesium, 7: 123-132.

Cheung HS, Halverson PB, McCarty DJ (1983). Phagocytosis of hydroxyapatite or calcium pyrophosphate dihydrate crystals by rabbit articular chondrocytes stimulates release of collagenase , neutral protease and prostaglandin E2 and F2. Proc. Soc. Exp. Biol. Med., 173: 181-189.

Cheung HS, Story MT, McCarty DJ (1984). Mitogenic effects of hydroxyapatite and calcium pyrophosphate dihydrate crystals on cultured mammalian cells. Arthritis Rheum., 27: 668-674.

Cheung HS, Van Wyk JJ, Russel WE, McCarty DJ (1986). Mitogenic activity of hydroxyapatite: requirement for somatomedin C. J. Cell Physiol., 128: 143-148.

Cheung HS, McCarty DJ (1988). Mechanisms of connective tissue damage by crystals containing calcium. Rheum. Dis. Clin. N. Am.,14 (2) (ed. McCarty DJ); Philadelphia, WB Saunders: 365-377.

Clark JM (1990). The organisation of collagen fibrils in the superficial zones of articular cartilage. J. Anat., 171: 117-130.

Clift SE, Harris B, Dieppe PA, Hayes A (1989). Frictional response of articular cartilage containing crystals. Biomaterials, 10: 329-334.

Clift SE (1992). Finite-element analysis in cartilage biomechanics. J. Biomed. Eng., 14: 217-221.

Culty M, Miyake K, Kincade PW, Silorski E, Butcher EC, Underhill C (1990). The hyaluronate receptor is a member of the CD44 (H-CAM) family of cell surface glycoproteins. J. Cell. Biol., 111: 2765-2774.

Cunningham LW, Davies HA, Hammonds RD (1976). An analysis of the association of collagen based on structural models. Biopolymers, 15: 483-502.

Daculsi G, Kerebel B, Le Cabellec MT, Kerebel LM (1979). Qualitative and quantitative data on arrested caries in dentine. Caries Res., 13: 190-202.

Daculsi G, LeGeros RZ, Jean A, Kerebel B (1987). Possible physico-chemical processes in human dentin caries. J. Dent. Res., 66: 1356-1359.

Dean DD, Azzo W, Martel-Pelletier J, Pelletier JP, Woessner JF (1987). Levels of metalloproteases in human osteoarthritic cartilage. J. Rheumatol., 14: 43-44.

Dean DD, Schwartz Z, Muniz OE, Gomez R, Swain LD, Howell DS, and Boyan BD (1992). Matrix vesicles are enriched in metalloproteinases that degrade proteoglycans. Calcif. Tissue Int., 50: 342-349.

Dieppe PA, Huskisson EC, Crocker P, Willoughby DA (1976). Apatite deposition disease: a new arthropathy. Lancet, 1: 266-268.

Dieppe PA, Doherty M (1982). The role of particles in the pathogenesis of joint disease. In *Current Topics in Pathology, vol. 71, Bone and Joint Disease* (ed. CL Berry); Heidelberg, Springer: 199-233.

Dieppe PA, Alexander GJM, Jones HE, Doherty M, Scott DGI, Manhire A, Watt I (1982). Pyrophosphate arthropathy: a clinical and radiological study of 105 cases. Ann. Rheum. Dis., 41: 371-376.

Dieppe PA, Calvert P (1983). Crystals and Joint Disease. London, Chapman and Hall.

Dieppe PA, Doherty M, MacFarlane D (1983). Crystal related arthropathies. Ann. Rheum. Dis., 42 (Suppl): 1-3.

Dieppe PA, Doherty M, MacFarlane DG, Hutton CW, Bradfield JW, Watt I (1984). Apatite associated destructive arthritis. Br. J. Rheumatol., 23: 84-91.

Dieppe PA, Watt I (1985). Crystal deposition in osteoarthritis: an opportunistic event? Clin. Rheum. Dis., 11: 367-392.

Dieppe PA, Campion G, Doherty M (1988). Mixed crystal deposition. Rheum. Dis. Clin. N. Am.,14 (2) (ed. McCarty DJ); Philadelphia, WB Saunders:415-425.

Dieppe PA, Cawston T, Mercer E, Campion GV, Hornby J, Hutton CW, Doherty M, Watt I, Woolf AD, Hazleman B (1988). Synovial fluid collagenase in patients with destructive arthritis of the shoulder joint. Arthritis Rheum. 31: 882-890.

Di Giovine FS, Malawista SE, Nuki G, Duff GW (1987). Interleukin 1 (IL 1) as a mediator of crystal arthritis: stimulation of T cell and synovial fibroblast mitogenesis by urate crystal-induced IL 1. J. Immunol., 138: 3213-3218.

Dirksen TR (1969). The *in vitro* incorporation of acetate ^{14} C into the lipids of newborn rat calvaria. Arch. Biochem. Biophys., 134: 603-609.

Doherty M , Dieppe PA (1981) Acute pseudogout: crystal shedding or acute crystallisation. Arthritis Rheum., 24: 954- 957.

Doherty M, Watt I, Dieppe PA (1982). Localised chondrocalcinosis in post-meniscectomy knees. Lancet 1: 1207-1210.

Doherty M, Whicher JT, Dieppe PA (1983). Activation of the alternative pathway of complement by monosodium urate monohydrate crystals and other inflammatory particles. Ann. Rheum. Dis., 42: 285-291.

Dmitrovsky E, Lane LB, Bullough PG (1978). The characterization of the tidemark in human articular cartilage. Metab. Bone Dis. Rel. Res., 1: 115-135.

Doty SB (1980). Problems inherent in obtaining the alkaline phosphatase reaction. J. Histochem. Cytochem., 28: 66-68.

Driessens FCM (1980). Probable phase composition of the mineral in bone. Z. Naturforsch, 35c: 357-362.

Driessens FCM (1988). Physiology of hard tissues in comparison with the solubility of synthetic calcium phosphates. Ann. NY Acad. Sci., 523: 131-6.

Driessens FCM, Verbeeck RMH (1980). Evidence for intermediate metastable states during equilibration of bone and dental tissues. Z. Naturforsch, 35c: 262-267.

Driessens FCM, Borggreven JMPM, Verbeeck RMH, DijK WE van, Feagin FF (1985). On the physicochemistry of plaque calcification and the phase composition of dental calculus. J. Periodont. Res., 20: 329-336.

Driessens FCM, Verbeeck RMH (1986). The dynamics of bone mineral in some vertebrates. Z. Naturforsch., 41c: 468-471.

Duance VC, Shimokomaki M, Bailey AJ (1982). Immunofluorescence localisation of type-M collagen in articular cartilage. Biosci. Rep., 2: 223-227.

Eanes ED (1985). Dynamic aspects of apatite phases of mineralized tissues, model studies. The chemistry and biology of mnieralized tissues. In *The Chemistry and Biology of Mineralized Tissues* (ed. WT Butler); Alabama, Ebsco Media: pp. 213-220.

Eanes ED, Meyer JL (1977). The maturation of crystalline calcium phosphates in aqueous suspension at physiologic pH. Calcif. Tiss. Res., 23: 259-269.

Ehrlich MG, Houle PA, Vigliani G, Mankin HJ (1978). Correlation between articular cartilage collagenase activity and osteoarthritis. Arthritis Rheum., 21: 761-765.

Eisenburg BR, Kuda AM, Peter JB (1974). Stereological analysis of mammalian skeletal muscle. J. Cell Biol., 60: 732-754.

Elliot RJ, Gardner DL (1979). Changes with age in the glycosaminoglycans of human articular cartilage. Ann. Rheum. Dis., 38: 371-377.

Ellman MH, Brown NL, Porat AP (1980). Laboratory investigations in pseudogout patients and controls. J. Rheum., 7: 77- 81.

Ellman MH, Brown ML, Levin B (1981). Narrowing of the knee joint space in patients with pseudogout. Ann. Rheum. Dis., 40: 34-36.

Ennever J, Riggan LJ, Vogel JJ (1984). Proteolipid and collagen calcification *in vitro*. Cytobiol., 39: 155-6.

Ennever J, Vogel JJ (1980). Magnesium inhibition of apatite nucleation by proteolipid. J. Dent. Res., 60: 838-841.

Evans HB, Ayad S, Abedin MZ, Hopkins S, Morgan K, Walton KW, Weiss JB, Holt PJL (1983). Localisation of collagen types and fibronectin in cartilage by immunofluorescence. Ann. Rheum. Dis., 42: 575-581.

Evans RW, Cheung HS, McCarty DJ (1984a). Cultured human monocytes and fibroblasts solubilize calcium phosphate crystals. Calcif. Tissue Int., 36: 645-650.

Evans RW, Cheung HS, McCarty DJ (1984b). Cultured canine synovial cells solubilize ^{45} Ca-labelled hydroxyapatite crystals. Arthritis Rheum., 27: 829-831.

Eyre DR, Wu JJ, Apone S (1987). A growing family of collagens in articular cartilage: Identification of 5 genetically distinct types. J. Rheumatol., 14: 25-27.

Faure G, Netter P, Malaman B, Steinmetz J, Duheille J, Gaucher A (1980). Scanning electron microscopic study of microcrystals implicated in human rheumatic diseases. Scanning Electron Microscopy, III: 163-176.

Faure G, Daculsi G, Netter P, Gaucher A, Kerebel B (1982). Apatites in heterotopic calcifications. Scanning Electron Microscopy, IV: 1629-1634.

Faure G, Daculsi G (1983). Calcified tendinitis: a review. Ann. Rheum. Dis., 43: 49-53.

Farber JL (1981). The role of calcium in cell death. Life Science, 29: 1289-1293.

Feenstra TR, de Bruyn PL (1979). Formation of calcium phosphates in moderately supersaturated solutions. J. Phys. Chem., 83: 475-479.

Fleisch H, Neuman WF (1961). Mechanisms of calcification: Role of collagen, polyphosphates, and phosphatase. Am. J. Pysiol., 200: 1296-1300.

Font F, Goldman J, Toro R (1982). Monosodium urate crystals (MSUC) and spherulites (SP) in symptomatic metatarsophalangeal (MTP) joints. Arthritis Rheum., 25 (Suppl): 53.

Franzen A, Heinegard D, Reiland S, Olsson S-R (1982). Proteoglycans and calcification of cartilage in the femoral head epiphysis of the immature rat. J. Bone Joint Surg., 64A: 558-566.

Freeman MAR, Swanson SAV, Manley PT (1975). Stress-lowering function of articular cartilage. Med. Biol. Eng., 13: 245-251.

Frondel C (1941). Whitlockite a new calcium phosphate, $Ca_3(PO_4)_2$. Am. Mineral., 26: 145-152.

Garnett J, Dieppe P (1990). The effects of serum and human albumin on calcium hydroxyapatite crystal growth. Biochem. J., 266: 863-868.

Gatter RA, McCarty DJ. (1967) Pathological tissue calcifications in man. Arch. Path., 84: 346-353.

Gawoski JM, Balogh K, Landis WJ (1985). Aortic valvular tophus: identification by X-ray diffraction of urate and calcium phosphates. J. Clin. Pathol., 38: 873-876.

Genge B, Cao X, Wu LNY, Wuthier RE (1992). Establishment of the primary structure of two major matrix vesicle annexins by peptide and DNA sequencing. Bone and Mineral, 17: 202-208.

Ghadially FN, Meachim G, Collins DH (1965). Extra-cellular lipid in the matrix of human articular cartilage. Ann. Rheum. Dis., 24: 136-146.

Ghadially FN, Fuller JA, Kirkaldy-Willis WH (1971). Ultrastructure of full thickness defects in articular cartilage. Arch. Path., 92: 356-369.

Ghadially FN, Lalonde J-MA (1981) Intramatrical lipidic debris and calcified bodoies in human semilunar cartilages. J. Anat.,132: 481-490.

Ghadially FN (1983). Fine Structure of Synovial Joints. London, Butterworth and Co. Ltd.

Giclas PC, Ginsberg MH, Cooper NR (1979). Immunoglobulin G-independent activation of the classical complement pathway by monosodium urate crystals. J. Clin. Invest., 63: 759-765.

Ginsberg MH, Giclas P, Cooper N (1979). The mechanism of complement activation by monosodium urate crystals. Arthritis Rheum., 22: 612.

Ginsberg MH, Jaques B, Cochrane CG, Griffin JH (1980). Urate crystal-dependent cleavage of Hageman factor in human plasma and synovial fluid. J. Lab. Clin. Med., 95: 497-506.

Glimcher MJ (1976). Composition, structure and organisation of bone and other mineralised tissues and the mechanism of calcification. In *Handbook of Physiology 7: Endocrinology, Vol. BII* (eds. RO Greep, EB Astwood); Washington DC, American Physiological Society: pp. 25-116.

Glimcher MJ (1984). Recent studies of the mineral phase in bone and its possible linkage to the organic matrix by protein-bound phosphate bonds. Philos. Trans. R Soc. Lond. 304 [Biol]: 479-508.

Glimcher MJ (1985). The role of collagen and phosphoproteins in the calcification of bone and other collagenous tissues. In *Calcium in Biological Systems* (eds. RP Rubin, G Weiss, JW Putney Jr.); New York, Plenum: pp. 607-616.

Glimcher MJ (1989). Mechanisms of calcification: role of collagen fibrils and collagen -phosphoprotein complexes *in vitro* and *in vivo*. Anat. Rec., 224:139-153.

Glimcher MJ, Francois L, Richards L, Krane SM (1964). The presence of organic phosphorus in collagen and gelatins. Biochim. Biophys. Acta, 93: 585-602.

Goldberg M, Septier D (1985). Improved lipid preservation by malachite green glutaraldehyde fixation in rat incisor predentine and dentine. Arch. Oral Biol., 10: 717-726.

Goldberg M, Escaig F (1987). Rapid-freezing and malachite green-acrolein-osmium tetroxide freeze-substitution fixation improve visualization of extracellular lipids in rat incisor pre-dentin and dentin. J. Histochem. Cytochem., 35: 427-433.

Gordon GV, Villanueva T, Schumacher HR, Gohel V (1984) Autopsy study correlating degree of OA, synovitis and evidence of articular calcification. J. Rheumatol., 11: 681-686.

Grant ME, Ayad S, Kwan APL, Bates GP, Thomas JT, McClure J. 1988. The structure and function of cartilage collagens. In *The Control of Tissue Damage* (ed. AM Glauret); Amsterdam, Elsevier Science Publishers BV: pp. 3-28.

Griffiths G, McDowall A, Back R, Dubochet J (1984). On the preparation of cryosections for immunocytochemistry. J. Ultrastruct. Res., 89: 65-78.

Halverson PB, McCarty DJ (1979). Identification of hydroxyapatite crystals in synovial fluid. Arthritis Rheum., 22: 389-395.

Halverson PB, McCarty DJ, Cheung HS, Ryan LM (1984). Milwaukee shoulder syndrome: eleven additional cases with the involvement of the knee in seven (basic calcium phosphate crystal deposition disease). Sem. Arthritis Rheum., 14: 36-44.

Halverson PB McCarty DJ (1988). Clinical aspects of basic calcium phosphate crystal deposition. Rheum. Dis. Clin. N. Am.,14 (2) (ed. McCarty DJ); Philadelphia, WB Saunders: 427-439.

Hardingham TE (1979). The role of link protein in the structure of cartilage proteoglycan aggregates. Biochem. J.,177: 237-247.

Hardingham TE, Muir H (1974). Hyaluronic acid in cartilage and proteoglycan aggregation. Biochem. J., 139: 565-581.

Hardingham TE, Fosang AJ (1992). Proteoglycans: many forms and functions. FASEB J., 6: 861-870.

Hascall VC, Heinegard D (1974). Aggregation of cartilage proteoglycans. 1. The role of hyaluronic acid. J. Biol. Chem., 249: 4232-4241.

Hascall VC, Kimura JH (1982). Proteoglycans: isolation and characterization. Methods enzymol., 82A: 769-800.

Hasselbacher P (1979a). Monosodium urate urate monohydrate activates C3 by the classical pathway. Arthritis Rheum., 22: 620-621.

Hasselbacher P (1979b). C3 activation by monosodium urate monohydrate and other crystalline material. Arthritis Rheum., 22: 571-578.

Hasselbacher P (1982). Crystal-protein interactions in crystal-induced arthritis. In *Advances in Inflammation Research, 4*: (ed. G Weissmann); New York, Raven Press: pp. 25-44.

Hayes A, Turner IG, Powell KA, Dieppe PA (1992). Crystal aggregates in articular cartilage as observed in the SEM. J. Mat. Sci.: Materials in Medicine, 3: 75-78.

Hearn PR, Russell RGG (1980). Formation of calcium pyrophosphate crystals *in vitro*. Implications for calcium pyrophosphate crystal deposition disease (pseudogout). Ann. Rheum. Dis., 39: 222-227.

Heinegard D, Hascall VC (1974). Aggregation of cartilage proteoglycans .III. Characteristics of the proteins isolated from trypsin digests of aggregate. J. Biol. Chem., 249: 4250-4256.

Heughebaert JC, de Rooij JF, Nancolllas GH (1986). The growth of dicalcium phosphate dihyhydrate on octocalcium phosphate at 25^{o}C. J. Cryst. Growth, 77: 192-198.

Hewitt AT, Varner HH, Silver MH, Dessau W, Wilkes CM, Martin GR (1982). The isolation and partial characterisation of chondronectin, an attachment factor for chondrocytes. J. Biol. Chem., 257: 2330-2334.

Howell DS (1982). Crystal deposition disease. In *Topical reviews in rheumatic disorders, 2.* (ed. V Wright);Bristol: PSG Wright.

Howell DS (1984). Etiopathogenesis of osteoarthritis. In *Osteoarthritis: Diagnosis and Management* (eds. DS Howell, VM Goldberg, HJ Mankin); Philadelphia, Saunders: pp.129-146.

Howell DS, Pita JC, Marquez JF, Madruga JE (1968). Partition of calcium, phosphate and protein in the fluid phase aspirated by calcifying sites in epiphyseal cartilage. J. Clin. Invest., 47: 1121-1132.

Howell DS, Martell-Pelletier J, Pelletier JP, Morales S, Muniz O (1984). NTP pyrophosphohydrolase in human chondrocalcinotic and osteoarthritic cartilage. II. Further studies on histologic and subcellular distribution. Arthritis Rheum., 27: 193-199.

Huber S, van der Rest M, Bruckner P, Rodriguez, E. Winterhalter KH, Vaughan L (1986). Identification of the type IX collagen polypeptide chains. The α2 (IX) polypeptide carries chondroitin sulphate chain(s). J. Biol. Chem., 261: 5965-5968.

Hukins DWL (1989). Mineral deposits in tissues. In *Calcified Tissue* (ed. DWL Hukins); London, Macmillan: pp. 1-20.

Hulmes DJS, Miller A, Parry DAD, Pietz KA, Woodhead-Galloway J (1973). Analysis of the primary structure of collagen for the origin of molecular packing. J. Mol. Biol., 79: 137-148.

Humphrey CD, Pittman FE (1974). A simple methylene blue-azure II-basic fuchsin stain for epoxy - embedded tissue sections. Stain Technology, 49: 9-13.

Hunter GK (1987). An ion exchange mechanism of cartilage calcification. Conn. Tiss. Res., 16: 111-120.

Hunter GK, Allen BL, Grynpas MD, Cheng PT (1985). Inhibition of hydroxyapatite formation in collagen gels by chondroitin sulphate. Biochem. J., 228: 463-469.

Hunziker EB, Herrmann W, Cruz-Orive LM, Arsenault AL (1989). Image analysis of electron micrographs relating to mineralization of calcifying cartilage: Theoretical considerations. J. Electron Microsc. Technique, 11: 9-15.

Inerot S, Heinegard D (1983). Bovine tracheal cartilage proteoglycans. Variations in structure and composition with age. Collagen Relat. Res., 3: 245-262,

Irving JT. (1963). The sudanophil material at sites of calcification. Arch. Oral Biol., 8: 735-45.

Ishikawa K, Masuda I, Ohira T, Yokoyama M (1989). A histological study of calcium pyrophosphate dihydrate crystal-deposition disease. J. Bone Joint Surg., 71A: 875-886.

Jackson JP (1968). Degenerative changes in the knee after meniscectomy. Br. Med. J., 2: 525-527.

Jackson SA, Cartwright AG, Lewis D (1978). The morphology of bone mineral crystals. Calcif. Tiss. Res., 25: 217-222.

Jander R, Troyer D, Rauterberg J (1984). A collagen-like glycoprotein of the extracellular matrix is the undegraded form of type VI collagen. Biochemistry, 23: 3675-3681.

Jeffrey AK, Blunn GW, Archer CW, Bentley G (1991). Three-dimensional collagen architecture in bovine articular cartilage. J. Bone Joint Surg., 73B: 795-801.

Jones SJ, Boyde A (1983). Ultrastructure of dentin and dentinogenesis. In *Dentin and Dentinogenesis. Vol. 1* (ed. A Linde); Florida, CRC Press: pp. 81-134.

Joy D, Maher EM (1977). Sensitivity limits for thin specimen x-ray microanalysis. Scanning Electron Microscopy, 1: 325-334.

Kani T, Kani M, Moriwaki Y, Doi Y (1983). Microbeam x-ray diffraction analysis of dental calculus. J. Dent. Res., 62: 92-95.

Kempson GE (1979). Mechanical properties of articular cartilage. In *Adult Articular Cartilage* (ed. M.A.R. Freeman); Tunbridge Wells, Pitman Medical: pp. 333-414.

Kerolus G, Clayburne G, Schumacher HR (1989). Is it mandatory to examine synovial fluids promtly after arthrocentesis? Arthritis Rheum., 32: 271-8.

Kielty CM, Whittaker SP, Grant ME, Shuttleworth CA (1992). Type VI collagen microfibrils: evidence of a structural association with hyaluranon. J. Cell Biol., 118: 979-990.

Kim KM , Huang SN (1972). Ultrastructural study of dystrophic calcification of human aortic valve. Lab. Invest., 26: 481-490.

Klein CPAT, Patka P, den Hollander W (1988). A histological comparison between hydroxylapatite and ß-whitlockite macroporous ceramics implanted in dog femora. TheThird World Biomaterials Congress p67.

Knuuttila M, Lappalainen R, Kontturi-Narhi V (1979). Concentrations of Ca, Mg, Mn, Sr, and Zn, in supra- and subgingival calculus. Scand. J. Dent. Res., 87: 192-196.

Knuuttila M, Lappalainen R, Kontturi-Narhi V (1980). Effect of Zn and Mg on the formation of whitlockite in human subgingival calculus. Scand. J. Dent. Res., 88: 513-516.

Koutsoukos PG, Nancollas GH (1986). The adsorption of inorganic phosphate by collagen. Colloid Surfaces, 17: 81-90.

Kozin F, McCarty DJ (1977). Protein binding to monosodium urate monohydrate, calcium pyrophosphate and silicon dioxide crystals, I. physical characteristics. J. Lab. Clin. Med., 89: 314-325.

Kozin F, McCarty DJ (1980). Molecular orientation of immunoglobulin G adsorbed to microcrystalline monosodium urate monohydrate. J. Lab. Clin. Med., 95: 49-58.

Kwan APL, Freemont J, Grant ME (1986). Immunopperoxidase localisation of type X collagen in chick tibae. Biosci. Rep., 6: 155-162.

Landis WJ (1979). Application of electron probe x-ray microanalysis to calcification studies in bone and cartilage. Scanning Electron Microscopy, II: 555-570.

Landis WJ (1986). A study of calcification in the leg tendons from the domestic turkey. J. Ultrastruct. Mol. Struct. Res., 94: 217-23.

Landis WJ, Paine MC, Glimcher MJ (1977). Electron microscopic observations of bone tissue prepared anhydrously in organic solvents. J. Ultrastruct. Res., 59: 1-30.

Landis WJ, Glimcher MJ (1978). Electron diffraction and electron probe microanalysis of the mineral phase of bone tissue prepared by anhydrous techniques. J Ultrastruct. Res., 63: 188-223.

Landis WJ, Glimcher MJ (1982). Electron optical and analytical observations of rat growth plate cartilage prepared by ultracryomicrotomy: the failure to detect a mineral phase in matrix vesicles and the

identification of heterodispersed particles as the initial solid phase of calcium phosphate deposited in the extracellular matrix. J. Ultrastruct. Res., 78: 227-268.

Landis WJ, Paine MC, Hodgens KJ, Glimcher MJ (1986). Matrix vesicles in embryonic chick bone: Considerations of their identification, number, distribution and possible effects on calcification of extracellular matrices. J. Ultrastruct. Res., 95: 142-163.

Landis WJ, Hodgens KJ, McKee MD, Nanci A, Song MJ, Kiyonaga S, Arena J, McEwen B (1992). Extra cellular vesicles of calcifying turkey leg tendon characterised by immunocytochemistry and high voltage electron microscopic tomography and 3-D graphic image reconstruction. Bone and Mineral, 17: 237-41.

Lee DD, Landis WJ, Bonar LC, Glimcher MJ (1984). Mineral phase of embryonic chick bone studied by high voltage electron microscopy. Calcif. Tissue Int., 36: 486.

LeGeros RZ (1981). Apatites in biological systems. Prog. Cryst. Growth. Charact., 4: 1-45.

LeGeros RZ, Trautz, OR, LeGeros JP, Klein E (1968). Carbonate substitution in the apatite structure. Bull. Soc. Chim . Fr., (n^{o} special) 2^{e} trimestre: 1712-1718.

LeGeros RZ, Contiguglia SR, Alfrey AC (1973). Pathological calcifications associated with uremia. Two types of calcium phosphate deposits. Calcif. Tiss. Res., 13: 173-185.

LeGeros RZ (1974). Variations in the crystallographic components of human dental calculus: I. crystallographic and spectroscopic methods of analysis. J. Dent. Res., 53: 45-50.

LeGeros RZ, LeGeros JP (1984). Phosphate minerals in human tissues. In *Phosphate Minerals* (eds. JO Nriagu PB Moore); Heidelberg, Springer-Verlag: pp. 351-385.

LeGeros RZ, Orly I, LeGeros JP, Gomez C, Kazimiroff J, Tarpley T, Kerebel B (1988). Scanning electron microscopy and electron probe microanalyses of the crystalline components of human and animal dental calculi. Scanning Microscopy, 2: 345-356.

LeGeros RZ, Daculsi G, Kijowska R, Kerebel B (1989). The effect of magnesium on the formation of apatites and whitlockites. In *Magnesium in Health and Disease* (eds. Y Itokawa, J Durlach,); London, John Libbey & Co: pp. 11-19.

Lehninger AL (1970). Mitochondria and calcium ion transport. Biochem. J., 119: 129-138.

Lelous M, Boudin D, Salomon S, Polonvski J (1982). The affinity of type I collagen for lipid *in vivo*. Biochem. Biophys. acta, 708: 26-32.

Lewinson D, Toister Z, Silberman M (1982). Quantitative and distributional changes in the activity of alkaline phosphatase during the maturation of cartilage. J. Histochem. Cytochem., 30: 261-269.

Lillie RD, Ashburn LL (1943). Supersaturated solutions of fat stains in dilute isopropanol for demonstration of acute fatty degeneration not shown by Herxheimers technic. Arch. Pathol., 36: 432.

Linsenmayer TF, Eavey RD, Schmid TM 1988. Type X Collagen: A hypertrophic cartilage-specific molecule. Pathol. Immunopathol. Res., 7: 14-19.

Little T, Freeman MAR, Swanson SAV (1969). Experiments on friction in the human hip joint. In: *Lubrication and Wear in Joints* (ed. V. Wright); London, Sector: pp. 110-114.

Low MG, Zilversmit DB (1980). Role of phosphatidylinositol in attachment of alkaline phosphatase to membranes. Biochem., 19: 390-5.

McCarty DJ, Hollander JL (1961). Identification of urate crystals in gouty synovial fluid. Ann. Intern. Med., 54: 542-546.

McCarty DJ, Kohn NN, Faires JS (1962). The significance of phosphate crystals in the synovial fluid of articular patients: The Pseudogout Syndrome. Ann. Intern. Med., 56: 711-737.

McCarty DJ, Gatter RA (1966). Recurrent acute inflammation associated with focal apatite crystal deposition. Arthritis Rheum., 9: 804-819.

McCarty DJ, Silcox DC, Coe F, Jacobelli S, Reiss E, Genant A, Ellman M (1974). Diseases associated with calcium pyrophosphate dihydrate crystal deposition: a controlled study. Am. J. Med., 56: 704- 714.

McCarty DJ, Halverson PB, Carrera GF (1981). Milwaukee shoulder: association of microspheroids containing hydroxyapatite crystals, active collagenase and neutral protease with rotator cuff defects. I. Clinical aspects. Arthritis Rheum., 24: 464-473.

McCarty DJ, Lehr JR, Halverson PB (1983). Crystal populations in human synovial fluid. Arthritis Rheum., 26: 1220-1224.

McCarty DJ, Cheung HS (1985). Prostaglandin (PG) E2 generation by cultured canine synovial fibroblasts exposed to microcrystals containing calcium. Ann. Rheum. Dis., 44: 316-320.

McGee-Russell SM (1958). Histochemical methods for calcium. J. Histochem. Cytochem., 6: 22-41.

McGill N, Swan A, Dieppe PA (1991). Survival of calcium pyrophosphate crystals in stored synovial fluids. Ann. Rheum. Dis. 50: 939-941.

McGill NW, Dieppe PA (1991). The effect of biological crystals and human serum on the rate of formation of crystals of monosodium urate monohydrate *in vitro*. Br. J. Rheum., 30: 107-111.

McKee MD, Nanci A, Landis WJ, Gerstenfield LC, Gotoh Y, Glimcher MJ (1989). Ultrastructural immunolocalization of a major phosphoprotein in embryonic chick bone. Connect. Tiss. Res., 21: 21-29.

McKibbin B, Maroudas A (1979). Nutrition and Metabolism. In Adult articular cartilage (ed. MAR Freeman); Tunbridge Wells, Pitman Medical: pp. 461-486.

Malawista SE, Duff G, Atkins E, Cheung HS, McCarty DJ (1985). Crystal-induced endogenous pyrogen production. A further look at gouty inflammation. Arthritis Rheum., 28: 1039-1046.

Mann S (1986). The study of biominerals by high resolution transmission electron microscopy. Scanning Electron Microscopy, II: 393-413.

Mandel NS (1976). The structural basis of crystal-induced membranolysis. Arthritis Rheum., 19: 439-455.

Marante I, MacDougall R, Ross A, Stockwell RA (1983). Ultrastructural observations of crystals in articular cartilages of aged human hip joints. Ann. Rheum. Dis., 42 (Suppl): 96-97.

Maroudas A (1976). A balance between swelling pressure and collagen tension in normal and degenerate cartilage. Nature, 260: 808-809.

Maroudas A (1979). Physicochemical properties of articular cartilage. In *Adult Articular Cartilage* (ed. MAR Freeman); Tunbridge Wells, Pitman Medical: pp. 215-290.

Maroudas A, Bullough PJ (1968). Permeability in articular cartilage. Nature, 219: 1260-1261.

Matsuzawa T, Anderson HC (1971). Phosphates of epiphyseal cartilage studied by electron microscopic cytochemical methods. J. Histochem. Cytochem.,19: 801-808.

Matthews JL, Martin JH, Carson FL (1978). Ultrastructure of calciphalaxis in skin. Metab. Bone Dis. Rel. Res., 1: 219-226.

Mayne R (1989). Cartilage collagens. Arthritis Rheum. 32, 241-246.

Meachim G, Ghadially FN, Collins DH (1965). Regressive changes in the superficial layer of human articular cartilage. Ann. Rheum. Dis., 24: 23-30.

Meachim G, Stockwell RA (1979). The Matrix. In *Adult Articular Cartilage* (ed. MAR Freeman); Tunbridge Wells, Pitman Medical: pp. 1-68.

Mechanic GL, Banes AJ, Henmi M , Yamauchi M (1985). Possible collagen structural control of mineralization. In *The Chemistry and Biology of Mineralized Tissues* (Ed. WT Butler) Alabama, Ebsco Media: pp. 98-102.

Meyer JL (1984). Can biological calcification occur in the presence of pyrophosphate. Arch. Biochem. Biophys., 231: 1-8.

Mitchell P, Pledger WP, Cheung HS (1989). Molecular mechanism of basic calcium phosphate crystal-induced mitogenesis: role of protein kinase C. J. Biol. Chem., 264: 14071-14077.

Mitchell PG, Struve JA, McCarty GM , Cheung HS (1992). Basic calcium phosphate crystals stimulate cell proliferation and collagenase message accumulation in cultured adult articular chondrocytes. Arthritis Rheum., 35: 343-350.

Mitrovic DR (1983). Pathology of articular deposition of calcium salts and their relationship to osteoarthritis. Ann. Rheum. Dis., 42 (Suppl): 19.

Mollenhauer J, Bee JA, Lizarbe MA, Von der Mark K(1984). Role of anchorin CII a 31,000-mol-wt membrane protein, in the interaction of chondrocytes with type II collagen. J. Cell Biol., 98: 1572-1579.

Moradian-Oldak J, Weiner S, Addadi L, Landis WJ, Traub W (1991). Electron imaging and diffraction study of individual crystals of bone , mineralized tendon and synthetic carbonate apatite. Connective Tiss. Res., 25: 219-228.

Morgan AJ, Davies TW, Erasmus DA (1975). Changes in the concentration and distribution of elements during electron microscope preparative procedures. Micron, 6: 11-23.

Morris DC, Vaananen HK, Anderson HC (1983). Matrix vesicle calcification in rat epiphyseal growth plate cartilage prepared anhydrously for electron microscopy. Metab. Bone Dis. Rel. Res., 5: 131-137.

Morris DC, Masuhara K, Takaoka K, Ono K, Anderson HC (1992). ImmunolocAlization of alkaline phosphatase in osteoblasts and matrix vesicles of human foetal bone. Bone and Mineral, 19: 287-298.

Mow VC, Holmes MH, Lai WM (1984). Fluid transport and mechanical properties of articular cartilage: a review. J.Biomech., 17: 377-394.

Muir H (1977). Molecular approach to the understanding of osteoarthritis. Ann. Rheum. Dis., 36: 199-208.

Muir IHM (1979). Biochemistry. In *Adult Articular Cartilage* (ed. MAR Freeman); Tunbridge Wells, Pitman Medical: pp.145-214,

Muir H (1986). Current and future trends in articular cartilage research and osteoarthritis. In *Articular Cartilage Biochemistry.* (eds. KE Kuettner, R Scleyerbach, VC Hascall); New York, Raven Press: pp. 423-440.

Muller-Glauser W, Humbel B, Glatt M, Strauli P, Winterhalter KH, Bruckner P (1986). On the role of type IX collagen in the extracellular matrix of cartilage: type IX is localised to intersections of collagen fibrils. J. Cell Biol., 102: 1931-1939.

Muniz O, Pelletier J-P, Martel-Pelletier J, Morales S, Howell DS (1984). NTP pyrophosphohydrolase in human chondrocalcinotic and osteoarthritic cartilage 1. Some biochemical characteristics. Arthritis Rheum., 27: 186-192.

Murata K, Bjelle AO (1979). Age dependent constitution of chondroitin sulphate isomers in cartilage proteoglycans under associative conditions. J. Biochem., 86: 371-376.

Myers ER, Armstrong CG, Mow VC (1984). Swelling pressure and collagen tension. In *Connective Tissue Matrix* (ed. DWL Hukins); London, Macmillan: pp.161-168.

Nanci A, Bai P, Warshawsky H (1983). The effect of osmium postfixation and uranyl and lead staining on the ultrastructure of young enamel in rat incisor. Anat. Rec., 207: 1-16.

Nancollas GH (1982). Phase transformation during precipitation of calcium salts. In *Biological Mineralization and Demineralization* (ed. GH Nancollas); New York, Springer Verlag: pp. 77-99.

Nancollas GH, Lore M, Perez L, Richardson C, Zawacki SJ (1989). Mineral phases of calcium phosphate. Anat. Rec., 224: 234-241.

Nefussi J-R, Septier D, Sautier J-M, Forest N, Goldberg M (1992). Localization of malachite green positive lipids in the matrix of bone nodules formed *in vitro*. Calcif. Tiss. Int., 50: 273-282.

Nelson DGA, Salimi MH, Nancollas GH (1986). Octocalcium phosphate and apatite overgrowths: A crystallographic and kinetic study. J. Colloid. Int. Sci., 110: 32-39.

Neuman WF (1980). Bone material and calcification mechanisms. In *Fundamental and Clinical Bone Physiology* (ed. MR Urist); Philadelphia, Lipincott: pp. 83-107.

Neuman WF, Mulryan BJ (1971). Synthetic hydroxyapatite crystals IV. Magnesium incorporation. Calcif. Tiss. Res., 7: 133-138.

O'Connor P, Orford CR, Gardner DL (1988). Differential response to compressive loads of zones of canine hyaline articular cartilage: micromechanical, light and electron microscopic studies. Ann. Rheum. Dis., 47: 414-420.

Ohira T, Ishikawa K (1987). Hydroxyapatite deposition in osteoarthritic articular cartilage of the proximal femoral head. Arthritis Rheum., 30: 651-660.

Ohira T, Ishikawa K, Masuda I, Yokoyama M, Honda I (1988). Histologic localization of lipid in the articular tissues in calcium pyrophosphate dihydrate crystal deposition disease. Arthritis Rheum., 31: 1057-1062.

Ohira T, Ishikawa K (1991). Histochemical localization of calcium with potassium pyroantimonate in the articular tissues in calcium pyrophosphate dihydrate crystal deposition disease. Clin. Orthop. Rel. Res., 264: 286-294.

Okazaki M, Takahashi J, Kimura H (1986). Unstable behaviour of magnesium containing hydroxyapatites. Caries Res., 20: 324-331.

Omar SA, Cheng P-T, Nyburg SC, Pritzker KPH (1979). Application of scanning and transmisson electron microscopy, x-ray energy spectroscopy , and x-ray diffraction to calcium pyrophosphate crystal formation *in vitro*. Scanning Electron Microscopy, II: 745-749.

Oppenheim FG, Hay DI, Franzblou C (1971). Proline rich proteins from human parotid saliva. I. Isolation and partial characterisation. Biochemistry, 10: 4233-4238.

Orford CR, Gardner DL (1984). Proteoglycan association with collagen d-band in articular cartilage. Connect. Tissue Res., 12: 345-348.

Oryschak AF, Ghadially FN, Bhatnager R (1974) Nuclear fibrous lamina in chondrocytes of articular cartilage. J. Anat., 118: 511-515.

Owens JL, Cheung HS, McCarty DJ (1986). Endocytosis precedes dissolution of basic calcium phosphate crystals by murine macrophages. Calcif. Tissue Int., 38: 170-174.

Ozawa H, Yamamoto T (1983). An application of energy-dspersive x-ray microanalysis for the study of biological calcification. J. Histochem. Cytochem., 1983: 210-213.

Pappas PW (1971). The use of a chrome allum-gelatin (subbing solution) as a general adhesive for parafin sections. Stain Technology, 46: 121-124.

Paul H, Reginato AJ, Schumacher HR (1983). Alizarin red S-staining as a screening test to detect calcium compounds in synovial fluid. Arthritis Rheum., 26: 191-200.

Paul JP (1976). Approaches to design. Force actions transmitted by joints in the human body. Proc. R. Soc. Lond. [Biol.], 192: 163-172.

Peress N, Sajdera SW, Anderson HC (1971). Lipid analysis of vesicles isolated from the matrix of calcifying cartilage. Fed. Proc., 30: 1244.

Peress NS, Anderson HC, Sajdera SW (1974). The lipids of matirx vesicles from bovine fetal epiphyseal cartilage. Calcif. Tiss. Res., 14: 275-281.

Perl-Treves D, Addadi L (1988). A structural approach to pathological crystallizations. Gout: the possible role of albulmin in sodium urate crystallization. Proc. R. Soc. Lond. B., 235: 145-159.

Phelps P, McCarty DJ (1966). Crystal induced inflammation in canine joints. II. Importance of polymorphonuclear leukocytes. J. Exp. Med., 124: 150-166.

Phelps P, Andrews R, Rosenbloom J (1981). Demonstration of chemotactic factor in human gout. J. Rheumatol., 8: 889-894.

Poole AR, Pidoux I, Reiner A, Tang L-H, Choi H, Rosenberg L (1980). Localization of proteoglycan monomer and link protein in the matrix of bovine articular cartilage. J Histochem. Cytochem., 28: 621-635.

Poole AR, Pidoux I (1989). Immunoelectron microscopic studies of type X collagen in endochondral ossification. J. Cell Biol., 109: 2547-2554.

Poole CA, Flint MH, Beaumont BW (1984): Morphological and functional inter-relationships of articular cartilage matrices. J. Anat., 138: 113-138.

Poole CA, Flint MH, Beaumont BW (1987). Chondrons in cartilage: Ultrastructural analysis of the pericellular microenvironment in adult human cartilages. J. Orthopaedic Res., 5: 509-522.

Poole CA, Ayad S, and Schofield, JR (1988). Chondron from articular cartilage. I. Immunolocalization of type VI collagen in the pericellular capsule of isolated canine tibial chondrons. J. Cell Sci., 90: 635-643.

Posner AS (1969). Crystal chemistry of bone mineral. Physiol. Rev., 49: 760-791.

Posner AS, Betts F (1975). Synthetic amorphous calcium phosphate and its relation to bone mineral structure. Accounts Chem. Res., 8: 273-281.

Pritchard MH, Jessop JD (1977). Chondrocalcinosis in primary hyperparathyroidism. Ann. Rheum. Dis., 36: 146-151.

Pritzker KPH (1980). Crystal associated arthropathies: what's new in old joints? J. Am. Geriatr. Soc., 28: 439-445.

Pritzker KPH (1986). Calcium pyrpphosphate crystal arthropathy: a biomineralization disorder. Human Pathol.,17: 543-545.

Pritzker KPH, Luk SC (1976). Apatite associated arthropathies: preliminary ultrastructural studies. Scanning Electron Microscopy, III: 493-499.

Pritzker KPH, Cheng P-T, Hunter GK, Grynpas MD, Kessler MJ, Renlund RC (1985). *In vitro* and *In vivo* models of calcium pyrophosphate crystal formation. In *Chemistry and Biology of Mineralised Tissues* (ed. WT Butler); Alabama, Ebsco Media: pp. 381-384.

Pritzker KPH, Chateauvert JMB, Grynpas MD (1987). Osteoarthritic cartilage contains increased calcium, magnesium and phosphorus. J. Rheumatol., 14: 806-810.

Pritzker KPH, Cheng P-T, Renlund RC (1988). Calcium pyrophosphate crystal deposition in hyaline cartilage. Ultrastructural analysis and implications for pathogenesis. J. Rheumatol. 15, 828-835.

Prockop DJ, Williams CJ (1982). Structure of the organic matrix: collagen structure (chemical). In *Biological Mineralization and Demineralization* (ed. GH Nancollas); New York, Springer Verlag: pp.161-177.

Puranen J, Ala-Ketola L, Peltokallio and Saarela J (1975). Running and primary osteoarthritis of the hip. Br. Med. J., 2: 424-425.

Ralphs JR, Ali SY (1986). Histochemical localization of alkaline phosphatase in rabbit distal ulnar growth plate. In *Cell Mediated Calcification and Matrix Vesicles* (ed. SY Ali); Amsterdam: Elsevier Science Pubishers BV: pp. 69-74.

Radin EL, Paul IL, Rose RM (1972). Role of mechanical factors in pathogenesis of primary osteoarthritis. Lancet, 1: 519-522.

Radin EL, Rose RM (1986). Role of subchondral bone in the initiation and progression of cartilage damage. Clin. Orthop. Rel. Res., 213: 34-40.

Rasmussen H (1970). Cell communication, calcium ion and cyclic adensine monophosphate. Science, 170: 404-411.

Ratcliffe A, Fryer PR, Hardingham TE (1984). The distribution of aggregating proteoglycans in articular cartilage: comparison of quantitative immunoelectron microscopy with radioimmunoassay and biochemical analysis. J. Histochem. Cytochem., 32: 193-201.

Rees JA, Ali SY, Mason AZ (1986). Scanning electron microscopy and microanalysis of 'cuboid' crystals in human articular cartilage. In Cell Mediated Calcification and Matrix Vesicles (ed. SY Ali); Amsterdam, Elsevier Science Pubishers BV: pp. 365-371.

Rees JA, Ali SY (1988). Ultrastructural localization of alkaline phosphatase activity in osteoarthritic human articular cartilage. Ann. Rheum. Dis., 47: 747-753.

Resnik D, Niwayama G (1981). Diagnosis of Bone and Joint Diseases. Philadelphia: WB Saunders.

Reynolds ES (1963). The use of lead citrate at high pH as an electron-opaque stain in electron microscopy. J. Cell Biol., 17: 208-212.

Ricard-Blum S, Hartman DJ, Herbage D, Payen-Meyran C, Ville, G (1982). Biochemical properties and immunolocalization of minor collagens in foetal calf cartilage. FEBS Lett., 146: 343-347.

Richards AJ, Hamilton EBD (1974). Destructive arthropathy in chondrocalcinosis articularis. Ann. Rheum. Dis. 33: 196-203.

Richardson KC, Jarrett L, Finke EH (1960). Embedding in epoxy resins for ultrathin sectioning in electron microscopy. Stain Technology, 35: 313-323.

Roberts S, Weightman B, Urban J, Chappell D (1986). Mechanical and biochemical properties of human articular cartilage from the femoral head after subcapital fracture. J. Bone Joint Surg., 68: 418-422.

Robinson RA, Watson ML (1952). Collagen-crystal relationships in bone as seen in the electron microscope. Anat. Rec., 114: 383-392.

Robison R (1923). The possible significance of hexosophosphoric esters in ossification. IX. Calcification in vitro. Biochem J. 24, 1927-1941.

Romberg RW, Werness PG, Riggs BL, Mann KG (1986). Inhibition of hydroxyapatite crystal growth by bone specific and other calcium binding proteins. Biochemistry, 25: 1176-80.

Rosenberg L (1971). Chemical basis for the histological use of safranin O in the study of articular cartilage. J. Bone Joint Surg., 53A: 69-82.

Rothenberg RJ (1987). Modulation of prostaglandin E2 synthesis in rabbit synoviocytes. Arthritis Rheum., 30: 266-274.

Rothwell WP, Waugh JS, Yesinowski JP (1980). High-resolution variable temperature ^{31}P NMR of solid calcium phosphates. J. Am. Chem. Soc. 102, 2637-2643.

Rouffose AH, Landis WJ, Sabine WK, Glimcher MJ (1979). Identification of brushite in newly deposited bone mineral from embryonic chicks. J. Ultrastruct. Res., 68: 235-255.

Roughley PJ, White RJ (1980). Age related changes in the structure of the proteoglycan subunits from human articular cartilage. J. Biol. Chem., 255: 217-224.

Rowles SL (1968). The precipitation of Whitlockite from aqueous solutions. Bulletin Societ Chim. France, 1797-1802.

Rowles SL, Levine RS (1973). The inorganic composition of arrested carious dentine. Caries Res., 7: 360-367.

Russ JC (1974). The direct element ratio model for quantitative analysis of thin sections, In *Microprobe Analysis as Applied to Cells and Tissues* (eds. TA Hall, P Echlin, R Kaufmann); London, Academic Press: pp. 269-76.

Ryan LM, Wortmann RL, Karas B, McCarty DJ (1985). Cartilage nucleoside triphosphate phosphohydrolase. II. Role in extracellular pyrophosphate generation and nucleoside metabolism. Arthritis Rheum., 28: 413-417.

Ryan LM, Rachow JW, McCarty DJ (1991). Synovial fluid ATP: a potential substrate for the production of inorganic pyrophosphate. J. Rheumatol., 18: 716-720.

Sah RLY, Kim YJ, Doong JY, Grodzinsky AJ, Plaas AH, Sandy JD (1989). Biosynthetic response of cartilage explants to dynamic compression. J. Orthopaedic Res., 7: 619-636.

Sakae T, Yamamoto H, Mishima H, Matsumoto T, Kozawa Y (1989). Morphology and chemical composition of dental calculi mainly composed of whitlockite. Scanning Microscopy, 3: 855-860.

Salimi MH, Heughebaert JC, Nancollas GH (1985). Crystal growth of calcium phosphates in the presence of magnesium ions. Langmuir, 1:119-122.

Santos M, Gonzalez-Diaz PF (1980). Ultrastructural study of apatites in human urinary calculi. Calcif. Tissue Int., 31: 93-108.

Sayegh FS, Solomon GC, Davis RW (1974). Ultrastructure of intracellular mineralization of deers antlers. Clin. Orthop. Rel. Res., 99: 267-284.

Schenk RK, Eggli PS, Hunziker EB (1986). Articular cartilage morphology. In *Articular Cartilage Biochemistry* (eds. KE Kuettner, R Scleyerbach, VC Hascall); New York, Raven Press: pp3-22.

Schlesinger DH, Hay DI, (1977). Complete covalent structure of statherin , a tyrosine-rich acidic peptide which inhibits calcium phosphate precipitation from human parotid saliva. J. Biol. Chem., 252: 1689-1695.

Schmid TM , Linsenmayer TF (1983). A short chain (pro) collagen from aged endochondral chondrocytes: biochemical characterisation. J. Biol. Chem., 258: 9504-9509.

Schmid TM, Linsenmayer TF (1984). Denaturation-renaturation properties of two molecular forms of short chain (SC) cartilage collagen. Biochemistry, 23: 553-558.

Schmid TM , Linsenmayer TF (1985). Immunohistochemical localisation of short chain cartilage collagen (type X) in avian tissues. J. Cell Biol., 100: 598-605.

Schmid TM, Popp RG, Linsenmayer TF (1990). Hypertrophic cartilage matrix. Type X collagen supramolecular assembly, and calcification. Ann. NY Acad. Sci., 580: 64-73.

Schroeder LW, Dickens B, Brown WE (1977). Crystallographic studies of the role of Mg as a stabilizing impurity in ß -$Ca_3(PO_4)_2$: II . refinement of Mg-containing ß-$Ca_3(PO_4)_2$. J. Solid state Chem., 22: 253-262.

Schumacher HR (1977). Pathogenesis of crystal-induced synovitis. Clin. Rheum. Dis., 3: 105-131.

Schumacher HR (1988). Pathology of crystal deposition diseases. In Rheumatic Disease Clinics of North America, 14 (2) (ed. DJ McCarty); Philadelphia, Saunders: 269-288.

Schumacher HR, Phelps P, Agudelo CA (1974). Urate crystal induced inflammation in dog joints: sequence of synovial changes. J. Rheumatol., 1: 102-13.

Schumacher HR, Smolyo AP, Tse RL, Maurer K (1979). Arthritis associated with apatite crystals. Ann. Int. Med., 87: 411-416.

Schumacher HR, Miller JL, Ludvico C, Jessar JA (1981). Erosive arthritis associated with apatite crystal deposition. Arthritis Rheum., 24: 31-37.

Schumacher HR, Cherian PV, Reginato AJ, Bardin T, Rothfuss S (1983). Intra-articular apatite crystal deposition. Ann. Rheum. Dis., 42 (Suppl.): 54-59.

Schupbach P, Lutz F, Guggenheim B (1992). Human root caries: histopathology of arrested lesions. Caries Res., 26: 153-164.

Shah JS (1983). Application of physical methods in the investigations of crystal-related arthropathies. Ann. Rheum. Dis., 42 (suppl.): 68-72.

Shapiro IM (1970). The association of phospholipids with inorganic bone. Calcif. Tiss. Res., 5: 13-20.

Smith A, Bruton J (1977). A colour atlas of histological staining techniques. London, Wolfe Medical Publications.

Smith GN, Williams JM , Brandt KD (1985). Interaction of proteoglycans with the cellular (1α, 2α, 3α) collagens of cartilage. J. Biol. Chem. 260: 10761-10767.

Sokoloff L (1983). Aging and degenerative diseases affecting cartilage. In *Cartilage 3* (ed. BK Hall); New York, Academic Press: pp. 109-114.

Sokoloff L, Linn FC (1965). Movement and composition of interstitial fluid of cartilage. Arthritis Rheum., 8: 481-494.

Solomons CC, Neuman WF (1960). On the mechanisms of calcification: the remineralization of dentin. J. Biol. Chem., 235: 2502-2506.

Spillberg I, Mandel B (1982). Crystal-induced chemotactic factor. In *Advances in Inflammation Research* (ed. G Weissman); New York, Raven Press: pp. 57-65.

Stockwell RA (1965). Lipid in the matrix of ageing articular cartilage. Nature, 207: 427-428

Stockwell RA (1971). Cell density cell size and cartilage thickness in adult mammalian articular cartilage. J. Anat., 108: 584-585.

Stockwell RA (1979). Biology of Cartilage Cells. Cambridge, Cambridge University Press.

Stockwell RA (1987). Structure and function of the chondrocyte under mechanical stress. In *Joint Loading* (eds. HJ Helminen, I Kiviranta, M Tammi, A-M Saamanen, K Paukkonen, J Jurvelin); Bristol, Wright Brothers: pp. 126-148.

Stockwell RA (1990). Distribution of crystals in the superficial zone of elderly human articular cartilage of the femoral head in subcapital fracture. Ann. Rheum. Dis., 49: 231-235.

Stockwell RA, Scott JE (1967). Distribution of acid glycosaminoglycans in human articular cartilage. Nature, 215: 1376-1317.

Stockwell RA, Meachim G (1979). The Chondrocytes. In *Adult articular cartilage* (ed. MAR Freeman); Tunbridge Wells, Pitman Medical: pp. 69-144.

Sundberg M, Friskopp J (1984). Crystallography of supragingival and subgingival dental calculus. Scand. J. Dent. Res., 93: 30-8.

Swan AJ, Heywood BR, Dieppe PA (1992). Extraction of calcium containing crystals from synovial fluids and articular cartilage. J. Rheumatol., 19: 1764-1773.

Swanson SAV (1979). Friction wear and lubrication. In: *Adult Articular Cartilage* (ed. MAR Freeman); Tunbridge Wells, Pitman Medical: pp. 415-460.

Swanson SAV, Freeman MAR, Day WH (1971). The fatigue properties of human cortical bone. Med. Biol. Engg., 9: 23-32.

Tavakol K, Miller RG, Bazett-Jones DP, Hwang WS, McGann LE, Schacher NS (1993). Ultrastructural changes in articular cartilage chondrocytes associated with freeze thawing. J. Orthopaedic Res., 11: 1-9.

Teichman RJ, Fujimoto M, Yanagimachi R (1972). A previously unrecognised material in mammalian spermatozoa as revealed by malachite green and pyronine. Biol. Reprod., 7: 73-81.

Teichman RJ, Cummins JM, Takei GH (1974). The characterization of a malachite green stainable, glutaraldehyde extractable phospholpid in rabbit spermatozoa. Biol. Reprod., 10: 565-577.

Tenenbaum J, Muniz O, Schumacher HR, Good AE, Howell DS (1981). Comparison of phosphohydrolase activities from articular cartilage in calcium pyrophosphate deposition disease and primary osteoarthritis. Arthritis Rheum., 24: 492- 500.

Terkeltaub R, Curtiss LK, Tenner AJ, Ginsberg MH (1984). Lipoproteins containing apoprotein B are a major regulator of neutrophil responses to monosodium urate crystals. J. Clin. Invest., 73: 1719-1730.

Terkeltaub RA, Ginsberg MH (1988). The inflammatory reaction to crystals. In Rheum. Dis. Clin. N. Am. 14 (2) (ed. DJ McCarty); Philadelphia, Saunders: 353-364.

Termine JD, Posner AS (1967). Amorphous/crystalline interrelationships in bone mineral. Calcif. Tiss. Res., 1: 8-23.

Termine JD, Eanes ED (1972). Comparative chemistry of amorphous and apatitic calcium phosphate preparations. Calcif. Tiss. Res., 10: 171-197.

Termine JD, Eanes ED, Greenfield DJ, Nylen MU (1973). Hydrazine-deproteinated bone mineral. Calcif. Tiss. Res., 12: 73-90.

Termine JD, Kleinman HK, Whitson SW, Conn KM, McGarvey ML, Martin GR (1981). Osteonectin, a bone specific protein linking mineral to collagen. Cell, 26: 99-105.

Terpstra RA, Driessens FCM, Schaeken HG (1983). The whitlockite phase in the system CaO-P_2O_5-MgO at 1000^oC. Z. anorg. allg. Chem., 507: 206-212.

Thorogood PV, Craig Gray J (1975). Demineralization of bone matrix: observations from electron microscope and electron probe analysis. Calcif. Tiss. Res., 19: 17-26

Thorogood PV, Hinchliffe JR (1975). An analysis of the condensation process during chondrogenesis in the embryonic chick hind limb. J. Embryol. Exp. Morphol., 33: 581-606.

Tokuyasu KT (1986). Application of cryo-ultramicrotomy to immunocytochemistry. J. Microscopy, 143: 139-149.

Tovberg Jensen A, Rowles SL (1957). Magnesian whitlockite, a major constituent of dental calculus. Acta odontol. Scand., 16: 121-139.

Vahl von J, Hohling HJ, Frank RM (1964). Elektronenstrahlbeugung an rhombohedrisch aussehendwn mineralbilungen in kariosem dentin. Arch. Oral Biol., 9: 315-320.

van Belle H (1976). Alkaline phosphatase. 1. Kinetics and inhibition by levamisole of isoenzymes from humans. Clin. Chem., 22: 972-976.

Van Campen GPJ, Van de Stadt RJ (1987). Cartilage and chondrocyte responses to mechanical loading *in vitro*. In *Joint Loading* ((eds. HJ Helminen, I Kiviranta, M Tammi, A-M Saamanen, K Paukkonen, J Jurvelin)); Bristol, Wright Brothers: pp. 112-125.

Vaughan L, Mendler M, Huber S, Bruckner P, Winterhalter K, Irwin MH, Mayne R (1988). D-periodic distribution of collagen type IX along cartilage fibrils. J.Cell Biol., 106: 991-997.

Venn M, Maroudas A (1977). Chemical composition and swelling of normal and osteoarthritic femoral head cartilage. 1. Chemical composition. Ann. Rheum. Dis., 36: 121-129.

Verplaetse H, Verbeeck RMH, Minnaert H, Oosterlinck W (1985). Solubility of inorganic kidney stone components in the presence of acid-base sensitive complexing agents. Eur. Urol., 11: 44-51.

Von der Mark H, Aumailley M , Wick G, Fleischmajer R, Timpl R (1984). Immunochemistry, genuine size and tissue localisation of Collagen VI. Eur. J. Biochem., 142: 493-502.

Ward BJ, Gloster JA (1976). Lipid losses during processing of cardiac muscle for electron microscopy. J. Microsc., 108: 41-50.

Warley A , Gupta BL (1992). Quantitative biological x-ray microanalysis. In: *Electron Microscopy in Biology, a Practical Approach* (ed. JR Harris); IRL Press: pp. 243-281.

Watson ML (1958). Staining of tissue sections for electron microscopy with heavy metals. J. Biophys. Biochem. Cytol., 4: 475-478.

Weibel ER, Staubli W, Gnagi HR, Hess F (1969). Correlated morphometric and biochemical studies on the liver cell. J. Cell Biol., 42: 68- 91.

Weightman B, Kempson GE (1979). Load carriage. In *Adult Articular Cartilage* (ed. MAR Freeman); Tunbridge Wells, Pitman Medical: pp. 291-331.

Weiner S (1986). Organization of extracellularly mineralized tissues: a comparative study of biological crystal growth. CRC Critical Reviews in Biochemistry: pp. 365-408.

Weiner S, Price PA (1986). Disaggregation of bone into crystals. Calcif. Tissue Int., 39: 265-375.

Weiss C, Rosenberg L, Helfet AJ (1968). An ultrastructural study of normal young adult human articular cartilage. J. Bone Joint Surg., 50A: 663-674.

Weiss RE, Reddi AH (1981). Appearance of fibronectin during the differentiation of cartilage, bone and bone marrow. J. Cell Biol., 88: 630-636.

Werdegal JE, Baylink DJ (1974). Electron microprobe measurements of bone mineralization rate *in vivo*. Amer. J. Physiol., 226: 345-352.

White SW, Hulmes DJS, Miller A, Timmins PA (1977). Collagen-mineral axial relationship in calcified turkey leg tendin by x-ray and neutron diffraction. Nature, 266: 421-425.

Wilkins E, Dieppe P, Maddison P, Evison G (1983). Osteoarthritis and articular chondrocalcinosis in the elderly. Ann. Rheum. Dis. 42: 280-284.

Williams JB, Irvine JW (1954). Preparation of the inorganic matrix of bone. Science, 119: 771-772.

Winand L (1965). Physico-chemical study of some apatitic calcium phosphates. In *Tooth Enamel* (eds. MV Stack, RS Fernhead); Bristol, John Wright and Sons: pp. 15-19.

Wotton SF, Duance VC, Fryer PR (1988). Type IX collagen: a possible function in articular cartilage. FEBS Lett., 234: 79-82.

Wuthier RE (1968). Lipids of mineralising epiphyseal tissues in the bovine fetus. J. Lipid Res., 9: 68-78.

Wuthier RE (1973). The role of phospholipids in biological calcification. Clin. Orthop. Rel. Res., 90: 191-200.

Wuthier RE (1975). Lipid composition of isolated epiphyseal cartilage cells, membranes and matrix vesicles. Biochim. Biophys. Acta, 409: 128-143.

Wuthier RE (1977). Electrolytes of isolated epiphyseal chondrocytes, matrix vesicles and extracellular fluid. Calcif. Tiss. Res., 23: 125-133.

Wuthier RE, Majeska RJ, Collins GM (1977). Biosynthesis of matrix vesicles in epiphyseal cartilage. I. *In vivo* incorporation of ^{32}P phosphate into phospholipids of chondrocyte membrane and matrix vesicle fractions. Calcif. Tiss. Res., 23: 135-139

Wuthier RE, Register TC (1985). Role of alkaline phosphatase, a polyfunctional enzyme, in mineralising tissues. In *The Chemistry and Biology of Mineralised Tissues* (ed. WT Butler); Alabama, Ebsco Media: pp. 113-124.

Yamada H, Nakagawa T, Stephens RW, Nagai Y (1987). Proteinases and their inhibitors in normal and osteoarthritic articular cartilage. Biomed. Res., 8: 289-300.

Yosipovitch ZH, Glimcher MJ (1972). Articular chondrocalcinosis, hydroxyapatite depostion disease in adult mature rabbits. J, Bone Joint Surg., 54A: 841-853.

Zitnan D, Sitaj S (1976). Natural causes of articular chondrocalcinosis. Arthritis Rheum., 19: 363-390.

Appendix 1. Patient details relevent to tissue specimens used for quantitative analysis of crystal distribution.

Patient Initials	Age : Sex	Specimen	Reason for surgery	Serum ion concn. Ca	P	Other relevent information
DF	10 : M	Femoral head	Osteosarcoma: femur			*Notes unavailable*
NC	12 : F	Femoral head	Viable pleomorphic osteosarcoma: femur	**	**	Radiotherapy. Restricted hip and knee movement up to two years prior to resection.
YA	16 : M	Femoral head	Ewings sarcoma: femur	**	**	Chemotherapy, radiotherapy. No restriction of range of movement prior to resection.
YH	20 : F	Femoral head	Grade 1 chondrosarcoma: distal femur	**	**	No restriction of range of movement prior to resection.
TB	23 : F	Femoral head	Osteosarcoma: femur	2.46	1.29	No restriction of range of movement prior to resection.
KM	43 : M	Femoral head	Osteosarcoma: femur	2.26	**	Chemotherapy (Methotrexate, cis platin with adrianycin). No restriction of movement prior to resection.
MK	54 : F	Femoral head	Osteosarcoma: femur	**	**	*Notes unavailable*
EB	78 : F	Femoral head	Fractured neck of femur	**	**	*Notes unavailable*
CL	81 : M	Femoral head	Fractured neck of femur	**	**	*Notes unavailable*
MS	84 : F	Femoral head	Fractured neck of femur	**	**	*Notes unavailable*
DT	87 : F	Femoral head	Fractured neck of femur	**	**	*Notes unavailable*
**	89 : F	Femoral head	Fractured neck of femur	**	**	*Notes unavailable*

** Information unavailable. Normal serum total calcium range, 2.25-2.65mmol/l: normal serum phosphorus range, 0.8-1.4mmol/l.

APPENDIX II.

To determine the size of a representative sample for a morphometric study equation (1) has been recommended, assuming the desired level of precision is less than 5% of the mean. (Aherne and Dunnill 1982).

$$s / \sqrt{n} < 0.05\ X \qquad (1)$$

Where s= standard deviation , n= number of unit area samples , and X= mean

For the purpose of determining a required sample size from pilot study data may be represented as (2).

$$n=(s / 0.05\ X)^2 \qquad (2)$$

This equation remains valid for data approximating to a normal distribution (Aherne and Dunnill 1982). Due to the patchiness and overdistribution of the crystals the sample data did not appear to approach a normal distribution.

To overcome sampling problems caused by the crystal band running parallel to the surface withiin the sampling region a transect comprising 5 fields running perpendicluar from the surface to 50 μm depth was considered one sample area (Fig. 1.1). The results of a pilot study using this sampling structure were then subjected to a more empirical method of sample size determination based on a summation of averages graph. The result of this exercise is illustrated below.

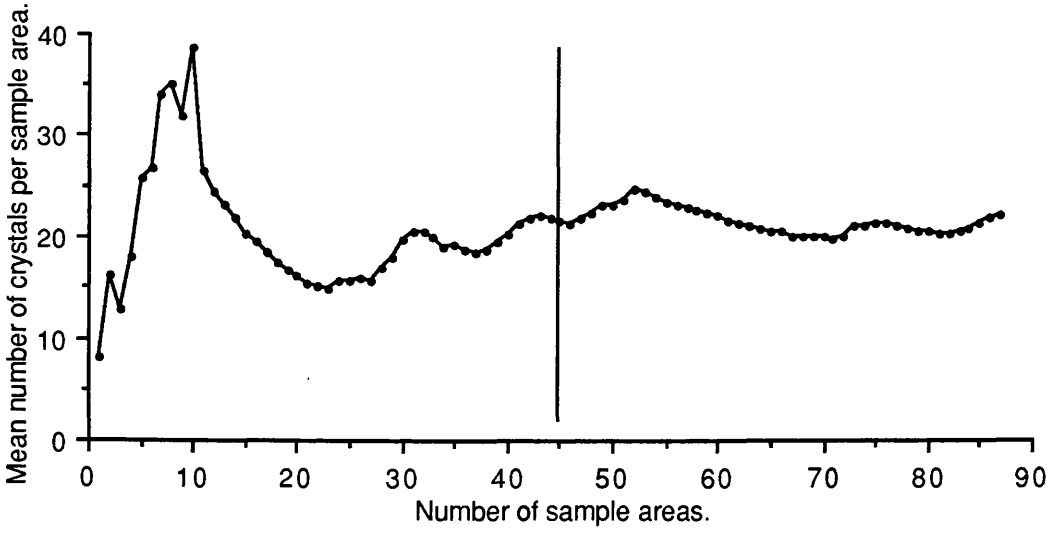

From this it was determined that 45 sample areas,comprising 225 fields (individual micrographs taken at 10000x magnification would be required for each cartilage site. It was reassuring to note that the number of fields indicated by this method were in excess of those indicated by (2) when applied to the pilot study data.

APPENDIX III.

Outline of the tasklist used in Genias image analysis software system (Joyce Loebl, Magiscan) for quantitative analysis of crystal distribution.

CAPTURE
QUIT AND PHOTO
GREY OPS.
NON LINEAR
SHARPEN EDGES
QUIT
QUIT
THRESHOLD
MANUAL
HIGH (255) return
LOW (110) return
QUIT
QUIT
BINARY OPS.
OBJECT BASED OPS.
ERASE 1 PIXEL OBJECTS
DELETE OBJECTS
AREA > MIN 0
>MAX 600
INCLUSIVE
QUIT
QUIT
IMAGE BASED OPS.
CLOSE (1 PASS)
QUIT
OBJECT BASED OPS.
FILL OBJECTS
QUIT
MEASURE.

Appendix IV. Patient details relevent to all tissue specimens used in this study.

Patient Initials	Age	Sex	Specimen	Reason for surgery	Other relevent information
KM	43	M	Femoral head	Osteosarcoma	Chemotherapy. No restriction of movement prior to resection
CL	81	M	Femoral head	Fractured neck of femur	
GM	72	M	Femoral head	OA	
TB	23	F	Femoral head	Osteosarcoma	No restriction of range of movement prior to resection
YH	20	F	Femoral head	Grade 1 chondrosarcoma distal femur	No restriction of range of movement prior to resection
MS	84	F	Femoral head	Fractured neck of femur	
IC	70	M	Femoral head	OA	
AT	72	M	Femoral head	OA	
YA	16	M	Femoral head	Ewings sarcoma femur	Chemo &, radiotherapy, no restriction of movement prior to resection
MB	53	M	Femoral head	OA	
NC	12	F	Femoral head	Viable pleomorphic osteosarcoma	Radiotherapy, restricted hip and knee movement 2 years prior to resection
CB	68	F	Femoral head	OA	
RL	73	F	Femoral head	OA	
DT	?	F	Femoral head	OA	
RR	74	M	Femoral head	OA	
RH	47	M	Femoral head	Chondrosarcoma grade I- II	Restriction of movement six months prior to resection
EN	80	M	Femoral head	OA	
LW	69	F	Femoral head	OA	
TD	19	M	Tibial plateau	Osteosarcoma	No restriction of movement prior to resection. [Ca 2.48]
?	?	?	Femoral head	Osteosarcoma	
CD	60	F	Femoral head	OA	
MG	48	F	Femoral head	OA	
NS	18	M	Distal femur	Osteosarcoma	Chemotherapy, no retsriction of movement prior to resection. [Ca 2.3] [P 1.2]

Patient Initials	Age	Sex	Specimen	Reason for surgery	Other relevent information
DW	71	F	Femoral head	OA	
SW	?	F	Femoral head	OA	
JO'C	?	F	Femoral head	OA	
EB	70	M	Femoral head	OA	
?C	69	F	Femoral head	OA	
RB	60	F	Femoral head	OA	
DH	75	F	Femoral head	OA	
DJ	83	F	Femoral head	OA	
MB	53	M	Femoral head	OA	
RR	?	F	Femoral head	OA	
IP	46	F	Femoral head	OA	
CT	64	F	Femoral head	OA	
HT	64	F	Femoral head	OA	
MG	48	F	Femoral head	OA	
MK	54	F	Femoral head	Osteosarcoma	
EB	78	F	Femoral head	Fracture of femoral neck	
VB	17	F	First metatarsal Phalanges	High grade malignant osteosarc. in ankle	
DT	87	F	Femoral head	Fracture of femoral neck	
?	89	F	Femoral head	Fracture of femoral neck	
DF	10	M	Femoral head	Ewings sarcoma	
?	62	M	2nd metacarpal and lunate	Tumour	
ET	84	F	Femoral head	Fracture of femoral neck	
SS	84	M	Femoral head	Fracture of femoral neck	

Patient Initials	Age	Sex	Specimen	Reason for surgery	Other relevent information
SW	8	M	Epiphyseal growth plate		
JO'B	26	F	Femoral head	Chondrosarcoma	
SR	13	M	Femoral head	Ewings Sarcoma	IVAD3 Chemotherapy,Discomfort 1year prior to resection
AF	78	M	Femoral head	Fractured neck of femur	
?	61	M	Femoral head 1st metatarsal	Tumour	
?	93	F	Femoral head	Fractured neck of femur	
?	78	F	Femoral head	Fractured neck of femur	
?	62	M	Femoral head	Fractured neck of femur	
VD	?	F	Femoral head	Fractured neck of femur	[Ca 2.26] [P 1.21].
IB	19	M	Radial head, prox. ulna dist. radius, carpal metacarpal, lunatel	Tumour	
VO	85	F	Femoral head	Fractured neck of femur	
MM	75	F	Femoral head	Fractured neck of femur	
?	69	F	Femoral head	Fractured neck of femur	
PH	20	M	Distal femur	Tumour	
RB	61	M	Femoral head	Chondrosarcoma, pelvis	Some pain 6 months prior to resection
MI	12	M	Femoral head	Osteosarcoma	Restricted movement 6 months prior to resection [Ca 2.38] [P1.13]
CK	16	M	Femoral head	Ewings sarcoma	
KM	20	F	Tibial plateau	Tumour	
?	12	?	Distal femur	Tumour	
?	72	F	Femoral head	OA	
JY	55	M	Femoral head	Tumour	
CM	30	F	Femoral head	OA	
AW	81	F	Femoral head	Fractured neck of femur	
?	60	M	Femoral head	Tumour	

Breakdown of patients from which cartilage specimens were taken by age and sex.

Age (years)	Male	Female	Sex unknown	Total
0 - 10	2	0		2
11 - 20	8	4	1	13
21 - 30	0	3		3
31 - 40	0	0		0
41 - 50	2	3		5
51 - 60	4	3		7
61 - 70	7	6		13
71 - 80	4	7		11
81 - 90	2	7		9
91 - 100	0	1	1	6
Unknown	0	5	1	6
Totals	29	39	2	70

Appendix V. A discussion of selection bias within this study at three sampling levels.

Specimens

All normal specimens, those obtained due to surgery for tumour or femoral neck fracture, were accepted. OA femoral head specimens were accepted if they contained areas of cartilage appearing intact (full depth) at a gross level (Type IV, Ali and Bayliss 1974).

Sample site

From the experience gained sampling initial specimens, sample site selection was refined to optimise the chances of encountering areas of crystal deposition.

Normal femoral head cartilage samples were taken from superior, inferior, posterior and anterior regions in many cases. If sampling was restricted to one area (due to competing demands for samples from a specimen), the superior region was the preferred site. Samples of articular cartilage from other joints were taken from the region of the joint considered to be exposed to maximal stresses, this being dependent upon specific joint morphology and conformation. Samples from the OA femoral heads selected were taken as illustrated below.

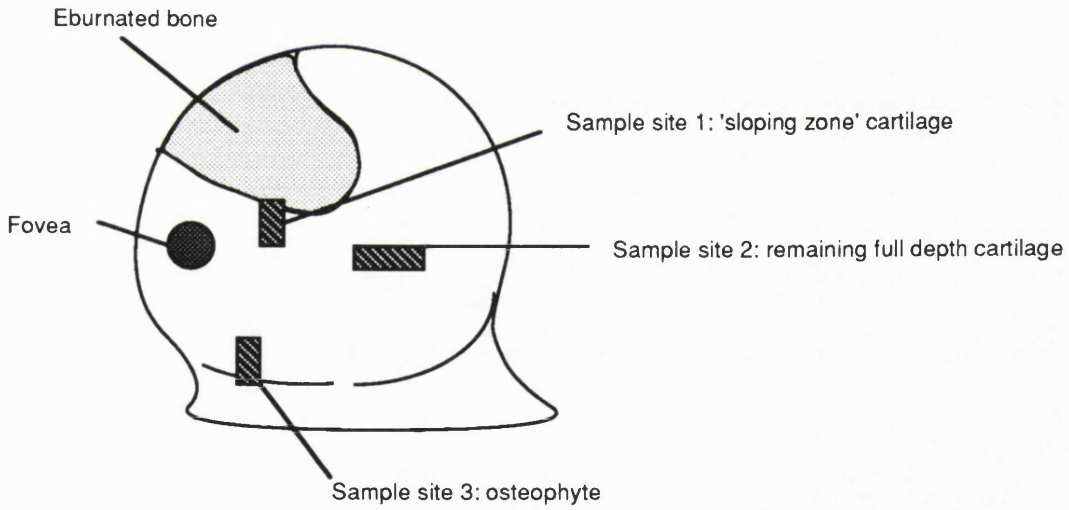

Diagram of OA femoral head illustrating the sites from which cartilage samples were taken.

Such specimen selection may be interpretted as introducing bias into the study of OA articular cartilage. The aim of the study was to determine crystal presence and therefore full depth tissue was required to maximise the chances of encountering crystal deposition. With the difficulty in observing crystals in 'sloping zone' cartilage from osteoarthritic femoral heads where crystal deposition was observed in adjacent full depth tissue, it is reasonable to speculate that crystals had been present in the superficial zone cartilage of more degenerate specimens.

In all samples, full depth cartilage with intact subchondral bone was taken; however the first area of each specimen to be screened by TEM included the superficial zone.

Crystals

Electron micrographs of crystals were selected on two criteria; first , to provide a comprehensive record of crystal deposition in any one specimen and second, to record specific observations from a specimen. Micrographs for quantitative analysis were selected as described in chapter one. The smallest crystals recorded in this study were between 30 and 50nm along one axis. This apparent lower limit of crystal size may be influenced by experimental procedure. There may be an increased tendency for crystals below this size to drop out of sections, or even if they remain in section may provide too slight contrast to be clearly imaged. It has been suggested that bone mineral crystals, having a plate-like morphology, exhibit a needle shaped appearance in the TEM as only those aligned in the direction of the electron beam provide sufficient contrast to be imaged (Weiner 1986). It is necessary to remember therefore, that the results of the crystal deposition quantification study relate the population of crystals apparent using the methods described.

Attempts were made to maintain objectivity when selecting crystals for XRMA. With the exception of studies to look for variation in Ca/P ratios of crystals with respect to size or shape, an average crystal Ca/P ratio for a specimen was achieved using standard criteria. A crystal closest to the TEM screen centre after random turns of the stage drives was measured along one axis, if the crystal was between 100-300nm a spectrum was recorded for it. Spectra were only discarded if the 200 live second count time was not fulfilled (due to section damage or specimen drift). A mean crystal Ca/P ratio was determined from the first 10 spectra to be generated.

As described in chapter three, the centrifugation stages introduced a variation in size between the two pellets selected as the final protocol. From observation of early centrifugation regimes it is suggested that crystals lost in lower speed fractions are largely within undigested cartilage fragments, whilst a small number of very small crystals (30nm approximately) are left in the supernatent. As the aim of this process was to achieve a high crystal/organic debris ratio, and as both pellets were pooled for x-ray diffraction analyses, presenting a full crystal size range, the loss of a low percentage of very small crystals was not considered to bias the results.

J. Anat. (1992) 181, pp. 293-300, with 5 figures Printed in Great Britain

Calcium phosphate crystal distribution in the superficial zone of human femoral head articular cartilage

C. A. SCOTCHFORD[1], S. GREENWALD[2] AND S. Y. ALI[1]

[1] *Institute of Orthopaedics (UCMSM), Royal National Orthopaedic Hospital, Stanmore and* [2] *Institute of Pathology, Royal London Hospital, London, UK*

(*Accepted 28 July 1992*)

ABSTRACT

The distribution of cuboid crystals in articular cartilage was examined by image analysis of electron micrographs. The specimens were considered to be functionally normal articular cartilage from femoral heads resected either because of femoral neck fracture or tumour in the distal femur. The study was restricted to the superficial region between 0 and 50 μm depth. Crystals were present in all specimens regardless of the age of the patient. The crystal profile area density was significantly greater in superior region samples than inferior region samples and this difference was less in older specimens. A band of microcrystals 10–20 μm below the articular surface was observed in superior samples. A significant correlation between mean individual crystal profile area and age was observed. It is noted that crystals are present in regions of cartilage subject to high mechanical stress.

INTRODUCTION

In normal articular cartilage, it has been accepted that crystal formation is restricted to the calcifying region, adjacent to the subchondral bone. Such crystal deposition is associated with extracellular matrix vesicles and the crystals are hydroxyapatite (Ali, 1977, 1978). Abnormal mineral deposition in human articular cartilage is a phenomenon frequently associated with ageing (Pritzker, 1980). In osteoarthritic cartilage, advancement of the calcification front extends such crystal deposition into the mid-zone of the cartilage (Ali, 1985). In other pathological states massive deposits of sodium urate, calcium pyrophosphate dihydrate and hydroxyapatite may be deposited in articular cartilage with deleterious effects on joint function due to cartilage degeneration (Dieppe et al. 1976; Ali, 1978; Pritzker, 1986; Halverson & Ryan, 1988; Schumacher, 1988). Microcrystals have also been reported in articular cartilage and a role in cartilage pathology has been suggested (Faure et al. 1980; Ali, 1985; Rees et al. 1986). Of these, cuboid calcium phosphate crystals were first reported in osteoarthritic cartilage (Ali & Griffiths, 1981*a*, *b*, 1983; Ali, 1985) and elderly articular cartilage (Marante et al. 1983). Due to their size (50–800 nm) they are not detectable by radiography or light microscopy but can be investigated by electron microscopy. In femoral heads resected following femoral neck fracture, electron microscopy has shown that cuboid crystals are located almost exclusively in the superficial zone of structurally normal cartilage (Stockwell, 1990). Further investigation of such specimens (Stockwell, 1990) suggested no orientation of crystal deposition and no primary role for chondrocytes in the deposition process. The factors influencing crystal deposition have yet to be elucidated. Three conditions whose co-occurrence may result in crystal formation are the occurrence of matrix vesicle-like structures, the presence of low proteoglycan concentrations and an extra-articular source of calcium and phosphate ions (Ali, 1985). To investigate their mode of formation and function further, the distribution of cuboid crystals within the superficial zone of normal femoral head articular cartilage was quantified by image analysis of electron micrographs. The effect of patient age on crystal presence and distribution was also assessed.

Correspondence to Mr C. A. Scotchford, Institute of Orthopaedics, Royal National Orthopaedic Hospital Trust, Brockley Hill, Stanmore, Middx HA7 4LP, UK.

MATERIALS AND METHODS

Femoral heads, resected for prosthetic replacement due to fracture of the femoral neck, or distal femoral tumour, were obtained from 12 patients within 20 min of resection. The patients (4 male, 8 female) ranged in age from 10 to 89 y. Blocks of articular cartilage a few millimetres long in each dimension were removed from the superior and inferior regions of each femoral head (Fig. 1). These blocks were then subdivided into 6 full-depth tissue blocks, which were fixed in 1.5% glutaraldehyde in 0.085 M sodium cacodylate buffer. After washing, the blocks were dehydrated through a graded alcohol series (70, 90, 96, 100%) and then transferred to propylene oxide prior to infiltration with, and embedding in, Araldite CY212 resin at 60 °C for 48 h.

A stratified systematic random sampling procedure was employed. Three resin-embedded blocks were selected at random and 2 nonserial, 100 nm sections were cut from each block, mounted on copper grids and examined unstained using a Philips CM12 transmission electron microscope operating at 80 kV. Seventy-five fields per block were recorded in a defined systematic manner. Fields were photographed at ×10000 magnification. The sampling area comprised a band delineated by the articular surface and a parallel line 50 μm below this. The depth was determined from preliminary studies which consistently indicated that over 90% of crystals occurred within this band. This supports observations by Stockwell (1990). An 18.3 μm^2 area of each micrograph was systematically examined using a Joyce Loebl Magiscan image analyser to record the number of crystals, the area of each crystal profile and the total crystal profile area. In total over 2500 negatives were analysed. Sample sizes were established from a preliminary study using criteria outlined by Aherne & Dunnill (1982). The Mann–Whitney U test was employed as a test for significance ($P < 0.05$) unless otherwise stated.

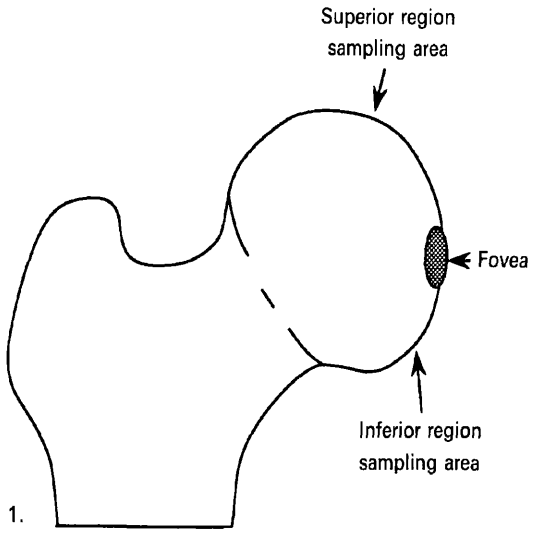

Fig. 1. Diagram of proximal femur, indicating femoral head articular cartilage sampling sites.

RESULTS

No abnormality of cartilage was observed at a gross or light microscope level. All specimens had intact superficial zone cartilage with a nonfibrillated articular surface. Surface roughening at the electron microscopic level was observed in some inferior specimens. This was not considered to be degenerative. All normal cartilage samples analysed were classified as either type I or type II (Ali & Bayliss, 1974). A substantial loss of crystals from resin sections cut onto distilled water was observed. It was possible to achieve a negligible loss by cutting sections onto 0.085 M sodium cacodylate buffer. In ultrathin sections the crystals were seen in sharp contrast to the surrounding tissue due to their high electron density relative to the unstained organic matrix (Figs 2*b*, 3*a*, *b*). This facilitated simple automated selection of crystal profiles for analysis. The characteristic electron density, morphology and size range allowed for any contaminant or artefact to be removed from the analysis at an optional editing step in the procedure. Within the sampling depth of cartilage, crystals frequently formed a denser band of variable thickness, with more sparsely distributed crystals above and below, apparently randomly distributed, or associated pericellularly with chondrocytes (Fig. 3*a*, *b*). Pericellular crystals were frequently associated with membranous structures or lipid debris (Fig. 2*c*, *d*). No intracellular crystals were observed; however, crystals were observed within necrotic chondrocyte debris (Fig. 3*a*). Crystal profile area ranges were similar in all patients. Samples from both sites of all patients contained crystals but there was great variation in crystal numbers and area densities between sites and patients (see Table 1). The greatest area density of crystals for a complete sample area was 0.39%; within the crystal band itself this rose to a maximum of 1.02%. The highest density recorded for a single unit area (18.2 μm^2) was 6%.

Crystal profile area

In all samples the crystal area profile frequency distributions were skewed to the lower end of the range. For statistical comparisons log transformations

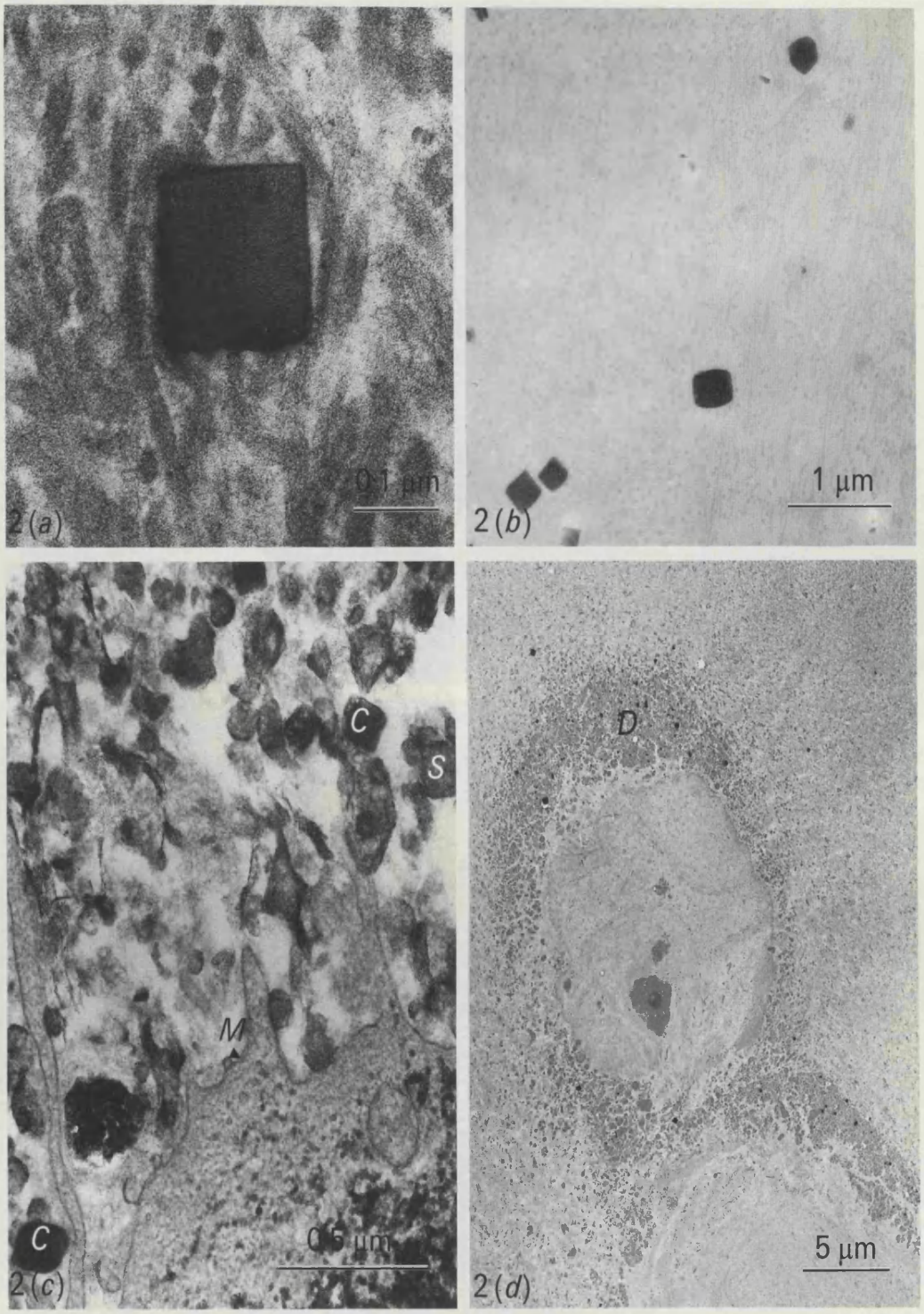

Fig. 2. 'Cuboid' crystals in articular cartilage showing (*a*) typical crystal morphology; (*b*) contrast between crystals and unstained matrix in an 18.2 μm² sample unit area; (*c*) crystals (*C*) associated with membranous structures (*S*) in close proximity to the chondrocyte membrane (*M*); (*d*) crystals distributed amid pericellular membranous and lipid debris (*D*).

of these data enabled parametric analysis. In superior region samples a significant correlation ($r = 0.7$; $P < 0.05$) between mean crystal area and age was observed (Fig. 4*a*) with crystal areas ranging from 0.0001 μm² to 0.6 μm². Crystal areas in inferior region samples ranged from 0.0001 μm² to 0.4 μm². No correlation with age was observed (Fig. 4*b*).

Crystal numbers and area density (% area of section occupied by crystal profiles)

For statistical analysis, to establish any age-related trends in crystal deposition, specimens were divided into 3 groups. These were 'juvenile to young adult' (10–25 y), 'adult' (40–55 y) and 'elderly' (75–90 y).

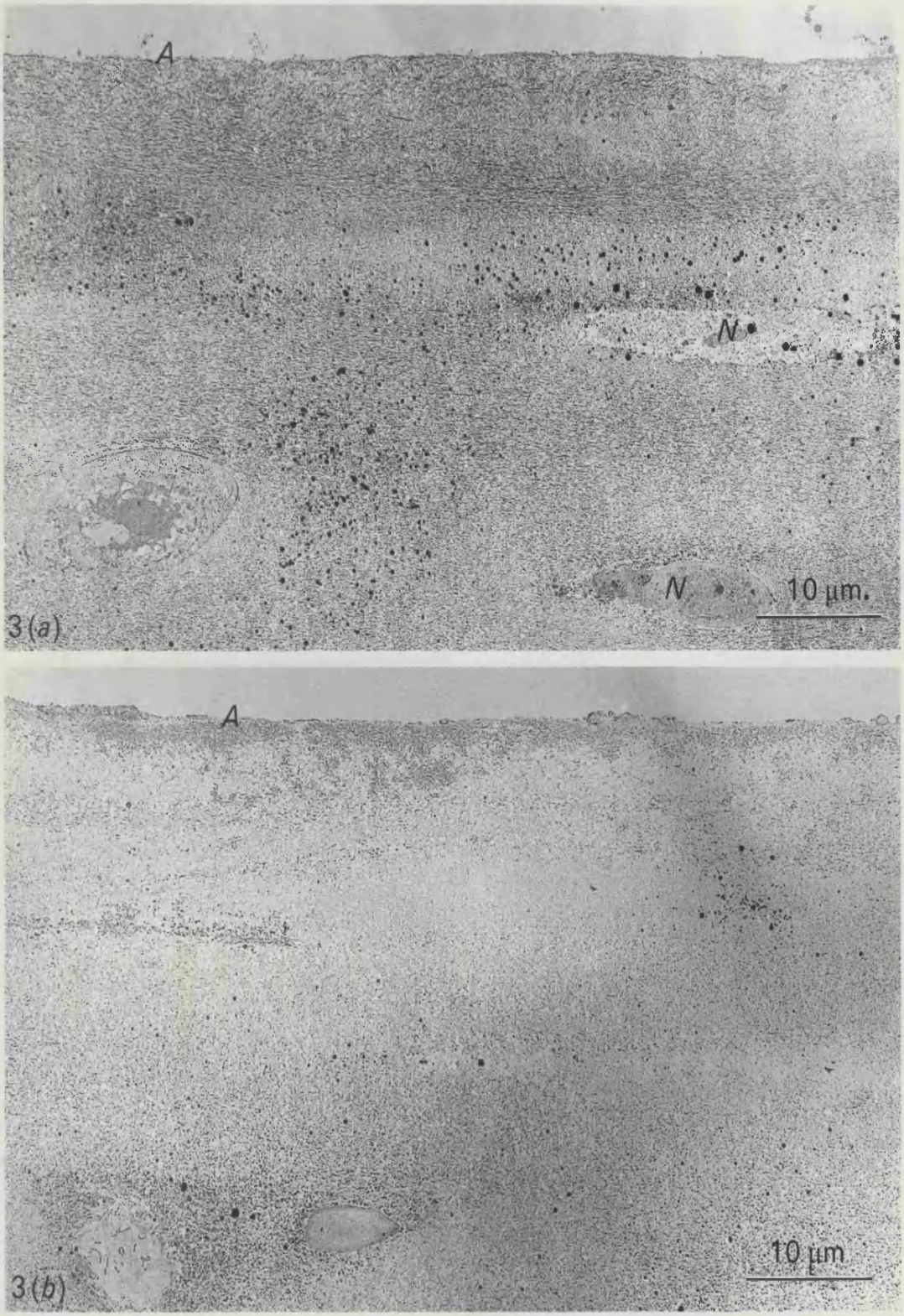

Fig. 3. Superficial zone articular cartilage demonstrating a crystal band in the superior region sample (*a*) with further crystal deposits both pericellularly and within necrotic chondrocyte debris (*N*). The inferior region sample (*b*) shows a sparser crystal distribution. Note smooth articular surface (*A*) in both regions.

Groupings were dictated to an extent by specimen availability, with the consequence that the 40–55 y group was very small. In the superior samples great variation between patients was observed in both variables ranging from 38 or 0.02 % to 1202 or 0.39 % (Table 1). This variation did not appear to be age related. Inferior samples also demonstrated great variation in both parameters ranging from 2 or 0.008 % to 541 or 0.11 %. The area density in the 10–25 y age group for inferior samples was signifi-

Table 1. *Mean number and area density (percentage area of section occupied by crystal profiles) of crystals in different regions of femoral head articular cartilage with age**

	10–25 y	40–55 y	75–90 y
Superior			
Crystal number	644 (475.1)[a]	885 (202.23)[c]	524.6 (155.2)[e]
Area density	0.186 (0.134)[b]	0.335 (0.007)[d]	0.308 (0.075)[f]
Inferior			
Crystal number	17.6 (13.54)[a]	336 (289.2)[c]	203.6 (155.03)[e]
Area density	0.012 (0.01)[b]	0.085 (0.35)[d]	0.116 (0.107)[f]

* Values are means (S.E.M.).
[a] U = 0; [b] U = 0; [c] U = 0; [d] U = 0; [f] U = 0; significant difference, $P < 0.05$. [e] U = 2 no significant difference $P > 0.05$.

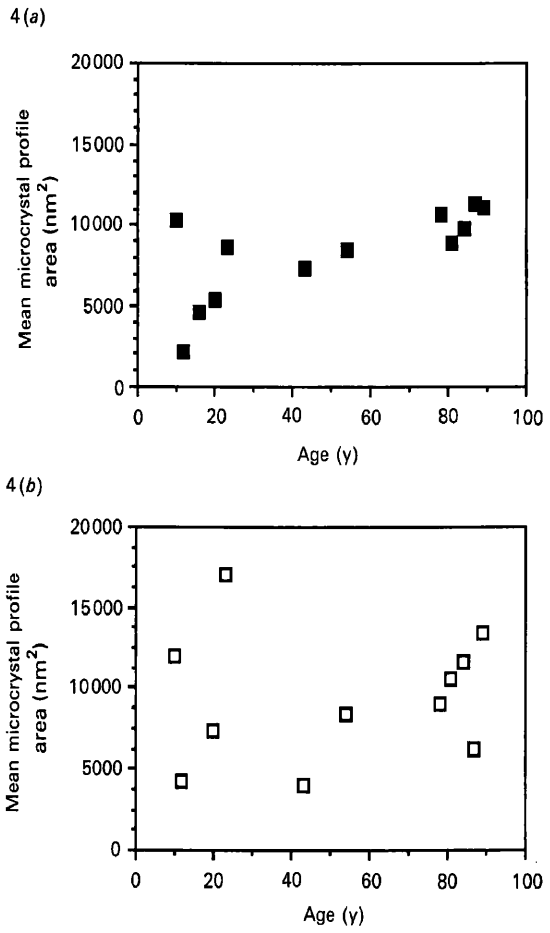

Fig. 4. Mean area of microcrystal profiles (size) in (*a*) superior region ($r = 0.7$) and (*b*) inferior region ($r = 0.3$) femoral head articular cartilage with age. (S.E.M. values are too close to the mean values to register on this scale.)

cantly lower than the 2 older inferior region groups (U = 2). In this region there appeared to be a trend for an increase in crystal number and area density with age. There were, however, significant differences in area density between the superior and inferior regions in each of the 3 age groups (Table 1).

Distribution of crystals with depth in cartilage

The banding of crystals below the articular surface as described above was confirmed quantitatively by subdividing the data for crystal number and area density into 5 sampling layers, each 10 μm in depth and parallel to the articular surface. In the superior samples this band was well defined, extending from the surface to between 20 and 30 μm depth (Fig. 5). Crystal area densities ranged from 1.02% within the band to 0% below this. This trend became less apparent with increasing age; in the oldest group area densities ranged from 0.59 to 0.02%. The inferior region samples demonstrated low crystal numbers throughout the depth profile in the younger specimens, the maximum area density being 0.04%. There was a slight increase in crystal area density with age throughout the depth profile, to a maximum of 0.45% (Fig. 5).

DISCUSSION

It was initially suggested that the deposition of cuboid crystals is related to ageing of normal cartilage or osteoarthritis (Ali & Griffiths, 1981*a*, 1983; Marante et al. 1983; Stockwell, 1990). All the specimens examined in this study were considered to be functionally normal articular cartilage, yet crystals were present in all cases, 5 of which were aged under 25 y. Indeed the youngest was 10 and a 16-y-old specimen had the second highest crystal area density recorded in the study. Such specimens demonstrated high levels of crystal deposition below smooth articular surfaces. It is acknowledged that the specimens were taken from patients with osteosarcomas or possible osteoporotic conditions (frequently associated with fracture of the femoral neck), both of which may alter cartilage metabolism (Roberts et al. 1986), allowing for the possibility of an increase in calcium ion concentrations. However, serum calcium levels were found to be within the normal range in cases where data were available.

The distribution of crystals in the superficial zone

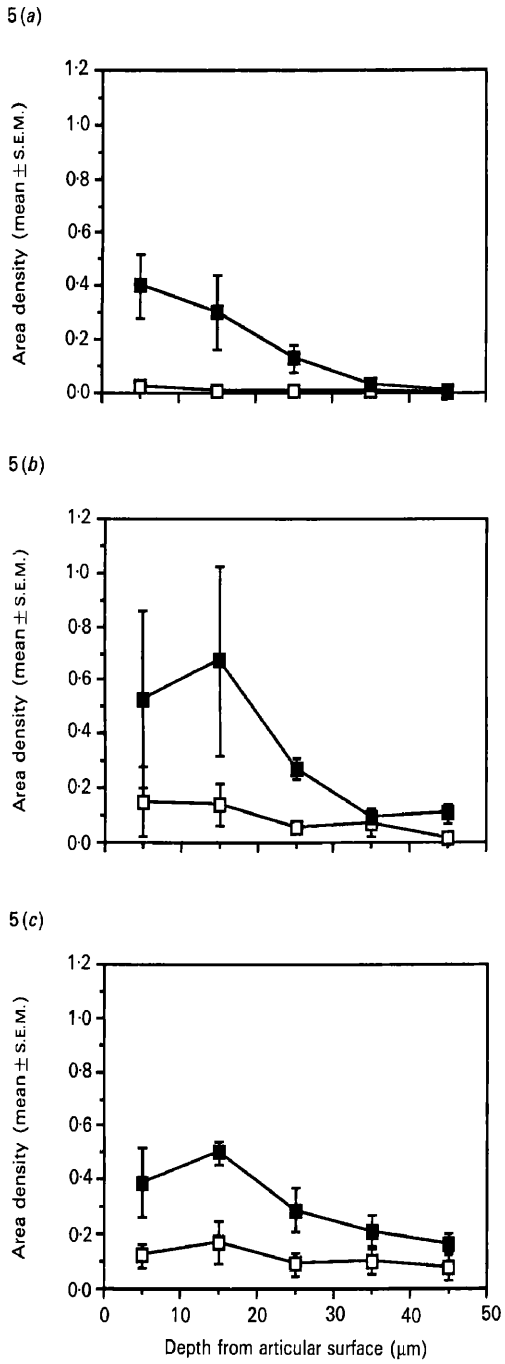

Fig. 5. Depth profile of microcrystal area density in the superficial zone, superior region (■) and inferior region (□), femoral head articular cartilage for three age groups: (*a*) 10–25 y, (*b*) 40–55 y, (*c*) 75–90 y.

(0–50 μm) was examined in detail in this study. The presence of the crystal band appearing within this zone may be considered in relation to the organisation and distribution of the major matrix components: collagens and proteoglycans. In the 3-dimensional architecture of collagen in articular cartilage, proposed independently by Clark (1990) and Jeffery et al. (1991), collagen in the intermediate and superficial zones is organised in a layered or leaf-like manner. The orientation changes from vertical in the intermediate zone to become tangential to the surface in the superficial zone (Jeffery et al. 1991). At the articular surface the tangential fibres are covered by a dense separate layer of small fibrils (Clark, 1990). The superficial zone also has a lower concentration of proteoglycan compared with the deeper tissue (Stockwell & Scott, 1967; Venn & Maroudas, 1977). Proteoglycans are known to inhibit hydroxyapatite growth (Blumenthal et al. 1979; Chen et al. 1984; Chen & Boskey, 1985, 1986). Hence a reduction of the proteoglycan concentration may produce favourable conditions for crystal formation. One or both of the above distributional factors may contribute to the co-occurring crystal deposition in the superficial zone.

The small sample size and large variability in crystal number and area density between patients precludes any definite associations between crystal deposition, patient age and cartilage site. However, it is possible to describe trends and from these to suggest further factors influencing the formation and distribution of these crystals. The results for crystal profile number and for crystal area density show a similar pattern, but it is difficult to estimate the absolute number of objects within an area or volume of tissue for a number of reasons (Aherne & Dunnill, 1982). These relate to the fact that sections will contain whole crystals and segments of crystals. A number of methods have been developed to overcome problems arising from this, but these have limitations in their use. For the purpose of comparison, estimates of area density (the percentage area of crystal profiles in the plane of the tissue section) are both simpler to obtain and more reliable. We therefore believe that area density rather than crystal number is a more useful variable. The most striking result of this study is the difference in crystal deposition between the superior and inferior regions of articular cartilage, coupled with the trend for this difference to lessen with increasing specimen age. This may explain the lack of such a difference recorded by Stockwell (1990) whose study was restricted to elderly femoral fracture patients.

One factor known to exert a major influence on articular cartilage is mechanical loading (Van Kampen & Van de Stadt, 1987; Sah et al. 1989). It has been suggested that mechanical stress is involved in the regulation of chondrocyte metabolism (Stockwell, 1987). The femoral head is part of one of the most heavily loaded joints in the body (Bullough et al. 1973; Paul, 1976). The distribution of weight-bearing stresses around this joint corresponds to the observed differences in crystal loading between the superior and inferior surfaces (Bullough et al. 1973; Paul, 1976).

The only recorded observation of calcified bodies similar to cuboid crystals outside femoral head articular cartilage was in the meniscus of the knee joint (Ghadially & Lalonde, 1981), which is also a load-bearing joint (Paul, 1976). Also the maximum strain during compressive loading of articular cartilage is exerted in the superficial zone (O'Connor et al. 1988). Any response of articular cartilage to mechanical load or strain is likely to be attributable to changes in chondrocyte metabolism, which may implicate the chondrocyte with an indirect role in crystal formation. In this study crystals have been observed in association with pericellular membranous vesicles and lipid material, and other cell debris away from pericellular regions, supporting previous observations (Ali & Griffiths, 1981*a*, *b*, 1983; Ali, 1985; Stockwell, 1990). The observed distribution is suggestive of an opportunistic mineralisation process rather than a specific system. It has been suggested that cellular debris and lipid in the matrix may be involved in the mineral formation process in hydroxyapatite deposition within osteoarthritic articular cartilage (Ohira & Ishikawa, 1987) and calcium pyrophosphate dihydrate crystal deposition disease (Ohira et al. 1988). The evidence presented would support the co-occurrence of matrix vesicle-like structures (of low specificity), reduced concentration of proteoglycan and an extra-articular source of calcium and phosphate ions as favourable conditions for cuboid crystal deposition. However, the cuboid crystals demonstrate a greater ubiquity in relation to cartilage age and a more specific distribution than was previously apparent. A further factor, mechanical load, is suggested for crystal formation, with this and the fibrillar architecture of the matrix contributing to their observed distribution.

ACKNOWLEDGEMENTS

We are grateful to Dr P. Ravell for the use of the Joyce Loebl image analysis system, Mr G. B. Newman, Department of Statistical Science, University College London, for his guidance, and Action Research for electron microscope facilities. This work was generously funded by the Arthritis and Rheumatism Research Council, UK.

REFERENCES

AHERNE WA, DUNNILL MS (1982) *Morphometry*. London: Edward Arnold.

ALI SY (1977) Matrix vesicles and apatite nodules in arthritic cartilage. In *Perspectives in Inflammation* (ed. D. A. Willoughby, J. P. Giroud & G. P. Velo), pp. 21–23. Lancaster: MTP Press.

ALI SY (1978) New knowledge of osteoarthrosis. *Journal of Clinical Pathology* **12** (Suppl.), 191–199.

ALI SY (1985) Apatite-type crystal deposition in articular cartilage. *Scanning Electron Microscopy* **4**, 1555–1566.

ALI SY, BAYLISS MT (1974) Enzymic changes in human osteoarthrotic cartilage. In *Normal and Osteoarthrotic Articular Cartilage* (ed. S. Y. Ali, M. W. Elves & D. H. Leaback), pp. 189–205. London: Institute of Orthopaedics, University of London.

ALI SY, GRIFFITHS S (1981*a*) New types of calcium phosphate crystals in osteoarthritic cartilage. *Seminars in Arthritis and Rheumatism* **11** (Suppl. 1), 124–126.

ALI SY, GRIFFITHS S (1981*b*) Matrix vesicles and apatite deposition in osteoarthritis. In *Matrix Vesicles: Proceedings of the Third International Conference on Matrix Vesicles*, pp. 241–247. Milan: Wichtig.

ALI SY, GRIFFITHS S (1983) Formation of calcium phosphate crystals in normal and osteoarthritic cartilage. *Annals of Rheumatic Diseases* **42** (Suppl.), 45–48.

BLUMENTHAL NC, POSNER AS, SILVERMAN LD, ROSENBERG LC (1979) Effects of proteoglycans on *in vitro* hydroxyapatite formation. *Calcified Tissue International* **27**, 75–82.

BULLOUGH P, GOODFELLOW J, O'CONNOR J. (1973) The relationship between degenerative changes and load-bearing in the human hip. *Journal of Bone and Joint Surgery* **55B**, 746–758.

CHEN CC, BOSKEY AL, ROSENBURG LC (1984) The inhibitory effect of cartilage proteoglycans on hydroxyapatite growth. *Calcified Tissue International* **36**, 285–290.

CHEN CC, BOSKEY AL (1985) Mechanisms of proteoglycan inhibition of hydroxyapatite growth. *Calcified Tissue International* **37**, 395–400.

CHEN CC, BOSKEY AL (1986) The effects of proteoglycans from different cartilage types on *in vitro* hydroxyapatite proliferation. *Calcified Tissue International* **39**, 324–327.

CLARK JM (1990) The organisation of collagen fibrils in the superficial zones of articular cartilage. *Journal of Anatomy* **171**, 117–130.

DIEPPE PA, CROCKER P, HUSKISSON EC, WILLOUGHBY DA (1976) Apatite deposition disease; a new arthropathy. *Lancet* **i**, 266–269.

FAURE G, NETTER P, MALAMAN B, STEINMETZ J, DUHEILLE J et al. (1980) Scanning electron microscopic study of microcrystals implicated in human rheumatic diseases. *Scanning Electron Microscopy* **3**, 163–176.

GHADIALLY FN, LALONDE J-MA (1981) Intramatrical lipidic debris and calcified bodies in human semilunar cartilages. *Journal of Anatomy* **132**, 481–490.

HALVERSON PB, RYAN LM (1988) Triple crystal disease: monosodium urate monohydrate, calcium pyrophosphate dihydrate, and basic calcium phosphate in a single joint. *Annals of Rheumatic Diseases* **47**, 864–865.

JEFFERY AK, BLUNN GW, ARCHER CW, BENTLEY G (1991) Three-dimensional collagen architecture in bovine articular cartilage. *Journal of Bone and Joint Surgery* **73B**, 795–801.

MARANTE I, MACDOUGALL R, ROSS A, STOCKWELL RA (1983) Ultrastructural observations of crystals in articular cartilage of aged human hip joints. *Annals of Rheumatic Diseases* **42** (Suppl.), 96–97.

O'CONNOR P, ORFORD CR, GARDNER DL (1988) Differential response to compressive loads of zones of canine hyaline articular cartilage: micromechanical, light and electron microscopic studies. *Annals of Rheumatic Diseases* **47**, 414–420.

OHIRA T, ISHIKAWA K (1987) Hydroxyapatite deposition in osteoarthritic articular cartilage of the proximal femoral head. *Arthritis and Rheumatism* **30**, 651–660.

OHIRA T, ISHIKAWA K, MASUDA I, YOKOYAMA M, HONDA I (1988) Histologic localization of lipid in the articular tissues in calcium pyrophosphate dihydrate crystal deposition disease. *Arthritis and Rheumatism* **31**, 1057–1062.

PAUL JP (1976) Approaches to design. Force actions transmitted by joints in the human body. *Proceedings of the Royal Society of London* (B) **192**, 163–172.

PRITZKER KPH (1980) Crystal-associated arthopathies: what's new in old joints. *Journal of the American Geriatrics Society* **28**, 439–445.

PRITZKER KPH (1986) Calcium pyrophosphate crystal arthropathy. *Human Pathology* **17**, 543–545.

REES JA, ALI SY, MASON AZ (1986) Scanning electron microscopy and microanalysis of 'cuboid' crystals in human articular cartilage. In *Cell Mediated Calcification and Matrix Vesicles* (ed. S. Y. Ali), pp. 365–371. Amsterdam: Elsevier Science.

ROBERTS S, WEIGHTMAN B, URBAN J, CHAPPELL D (1986) Mechanical and biochemical properties of human articular cartilage from the femoral head after subcapital fracture. *Journal of Bone and Joint Surgery* **68**, 418–422.

SAH RLY, KIM YJ, DOONG JY, GRODZINSKY AJ, PLAAS AH et al (1989) Biosynthesis response of cartilage explants to dynamic compression. *Journal of Orthopaedic Research* **7**, 619.

SCHUMACHER HR (1988) Pathology of crystal deposition diseases. *Rheumatic Disease Clinics of North America* **14**, 269–288.

STOCKWELL RA (1987) Structure and function of the chondrocyte under mechanical stress. In *Joint Loading* (ed. H. J. Helminen, I. Kiviranta, M. Tammi, A.-M. Säämanen, K. Paukkonen & J. Jurvelin), pp. 126–148. Bristol: Wright Brothers.

STOCKWELL RA (1990) Distribution of crystals in the superficial zone of elderly human articular cartilage of the femoral head in subcapital fracture. *Annals of Rheumatic Diseases* **49**, 231–235.

STOCKWELL RA, SCOTT JE (1967) Distribution of acid glycosaminoglycans in human articular cartilage. *Nature* **215**, 1316–1317.

VAN KAMPEN GPJ, VAN DE STADT RJ (1987) Cartilage and chondrocyte responses to mechanical loading *in vitro*. In *Joint Loading* (ed. H. J. Helminen, I. Kiviranta, M. Tammi, A.-M. Säämanen, K. Paukkonen & J. Jurvelin), pp. 112–125. Bristol: Wright Brothers.

VENN M, MAROUDAS A (1977) Chemical composition and swelling of normal and osteoarthritic femoral head cartilage. 1. Chemical composition. *Annals of Rheumatic Diseases* **36**, 121–129.

Micron and Microscopica Acta, Vol. 23, No. 3, pp. 383–384, 1992
Printed in Great Britain.

0739-6260/92 $5.00+0.00
Pergamon Press Ltd.

CALCIUM PHOSPHATE MICROCRYSTAL DEPOSITION IN ARTICULAR CARTILAGE: CHARACTERISATION BY XRMA.

Colin Scotchford and S Yousuf Ali
Institute of Orthopaedics, UCMSM, London, UK

INTRODUCTION

Deposition of calcium phosphate mineral phases, such as calcium pyrophosphate dihydrate(CPPD) and hydroxyapatite (HAP), in articular cartilage is associated with cartilage degeneration and ensuing arthropathies. Such pathological mineral depositions differ from normal biological mineral with respect to size, morphology and chemical composition. These massive mineral depositions may be detected by radiological imaging or light microscopy. Calcium phosphate microcrystals have been described in normal and osteoarthritic (OA) human articular cartilage using electron microscopy. Of these, "cuboid" crystals (size range 50 -500nm) are being further investigated (Fig.1). The present XRMA study aims to characterise the chemical composition of the cuboid crystals in relation to their role in the physiology and pathology of articular cartilage.

MATERIALS AND METHODS

Articular cartilage from freshly resected normal and OA human femoral heads was fixed in 1.5% glutaraldehyde in 0.085M sodium cacodylate buffer (pH 7.4) for 4 hours. After buffer washing, specimens were dehydrated through a graded alcohol series, then transferred to propylene oxide prior to overnight infiltration with araldite CY212 resin, under vacuum, and polymerisation at 60° C for 48 hours. 100nm sections were cut and collected on piolform coated, copper grids. XRMA was carried out using a Philips CM12 transmission electron microscope with an EDAX 9800 XRMA system.Spectra were recorded at 100kV for 200 live seconds, with a tilt angle of 20°. Ca/P ratios were calculated using a measured standard of sintered HAP, which was processed as described above. Samples of known calcium phosphate mineral phases were analysed to produce a standard curve. Samples of bone mineral were also analysed.

RESULTS AND DISCUSSION

Typically the crystals examined produced spectra comprising two major peaks with a low background. The major peaks were identified as corresponding to Ca (Ka at 3.69keV) and P (Ka at 2.01keV) . A small Mg peak (Ka 1.25 keV) was identified when an adjacent matrix spectrum was subtracted from a crystal spectrum. This procedure removed any interference due to As (La 1.28keV) from the buffer. Mg has been reported to stabilize amorphous calcium phosphate, inhibiting the progression to HAP (Blumenthal et al. 1977. Calcif. Tiss. Res. 23.245-250). Mg has also been reported as a stabilizing impurity in ß-tricalcium orthophosphate (Schroeder et al. 1977. J. Solid State Chem. 22, 253-262), and is integral in the Ca salt Mg-whitlockite. Mean Ca/P ratios of crystals for specimens ranged from 1.37 to 1.47, which were close to values recorded for synthetic tricalcium phosphate (TCP) (Fig.2).These values were significantly lower than those recorded for bone mineral. This difference does not rule out an apatitic nature to the crystals, as calcium deficient apatites have been described and synthesised (Blumenthal et al. 1981. Calcif. Tissue Int. 33, 111-117). Investigation of crystals from one specimen indicated that there was no significant change in the Ca/P ratio of crystals with respect to increases in crystal size (Fig.3). Similarly there was no significant change in the Ca/P ratio of crystals with increasing specimen age (Fig.2). This suggests that the crystals are in a

stable state and not functioning as intermediaries in a mineral "maturation" process. No significant difference in the Ca/P ratio was observed between crystals from normal and OA cartilage (Fig.2). The results described do not directly implicate these crystals in a degenerative role; however their occurrence in functionally normal cartilage requires further investigation.

Fig.1.

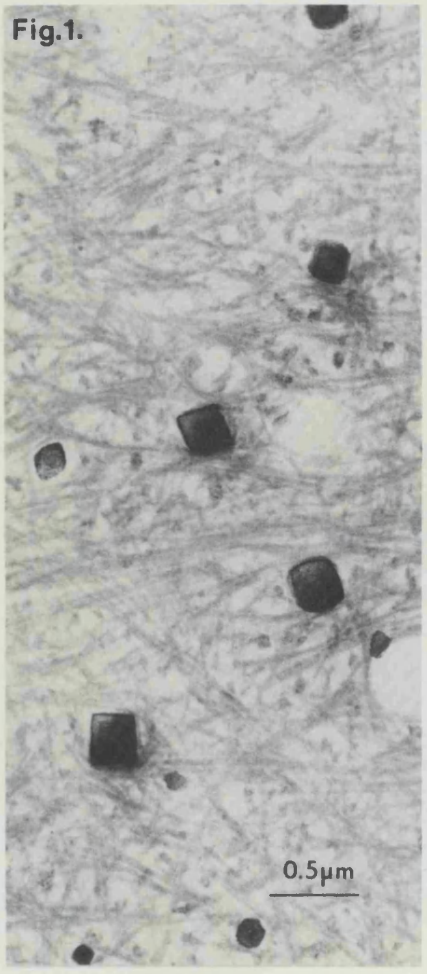

Fig. 2.

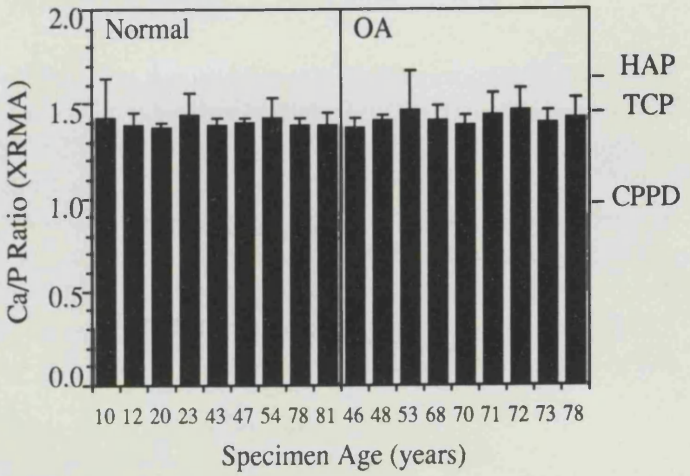

Fig. 3.

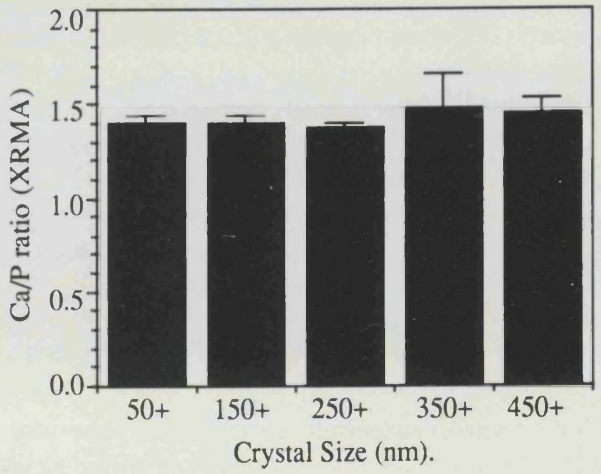

Fig. 1. Cuboid crystals in articular cartilage matrix.

Fig. 2. Variation in mean Ca/P ratio (+SD: n=10) with age, for crystals from normal and OA specimens. Mean values for HAP, TCP and CPPD are indicated.

Fig. 3. Variation in mean Ca/P ratio (n=10) with crystal size.

Electron microscopy and X-ray analysis of calcium phosphate microcrystals in human articular cartilage

Yousuf-Ali S and Scotchford C

Institute of Orthopaedics (University of London) Royal National Orthopaedic Hospital, Stanmore, Middlesex HA74LP,England.

Electron microscopy of human articular cartilage (from normal joints and from patients with osteoarthritis) has revealed the presence of 'cuboid' microcrystals of calcium phosphate in the surface zone[1]. The majority of these microcrystals range in size from 50 to 250nm and cannot normally be seen by x-ray radiography or by light microscopy. These cuboid microcrystals are quite different in composition, size,and distribution to sodium urate and calcium pyrophosphate crystals which are closely associated with joint degeneration in osteoarthritis[1]. A detailed study of these cuboid microcrystals is underway to determine occurrence, composition, mode of formation and function in articular cartilage.

Articular cartilage specimens from specific areas of normal and osteoarthritic femoral heads were processed for electron microscopy by conventional methods. Sections were examined in Philips CM12 electron microscope and a histomorphometric study of the micro-crystal distribution was carried out from electron micrographs. Glutaraldehyde fixed specimens were processed, sectioned and examined unstained by x-ray microanalysis with EDAX 9800 system.

The cuboid microcrystals were found predominately forming a band between 5 and 50 micrometers below the articular surface where they have an area density of 0.8%. There was a significant difference in crystal area density between cartilage samples from superior and inferior regions of the femoral head. A variation in distribution, and an increase in mean crystal size was apparent with age of patients. Electron probe x-ray microanalysis indicates that the micro crystals had a Ca/p ratio between 1.4 and 1.5 and had traces of magnesium associated with them. The Ca/p ratio was different from that for hydroxyapatite and may imply that these microcrystals are similar to β tricalcium phosphate or whitlockite. The mechanism of formation of these cuboid microcrystals is not known but they frequently occur either pericellularly amidst membranous matrix vesicles or are seen to occupy an oval area where there is membranous debris indicative of a profile of a dead chondrocyte in the matrix. Various new techniques are being applied to a study of these cuboid microcrystals to determine their role in physiology and pathology of articular cartilage.

REFERENCES

(1) Ali, S.Y. Apatite-type crystal deposition in arthritic cartilage. Scanning Electron Microscopy 4, 1555-1566 (1985).

Fig.1 Human articular cartilage surface region showing microcrystals in the matrix forming a band or distributed pericellularly around chondrocytes. Bar = 10um.

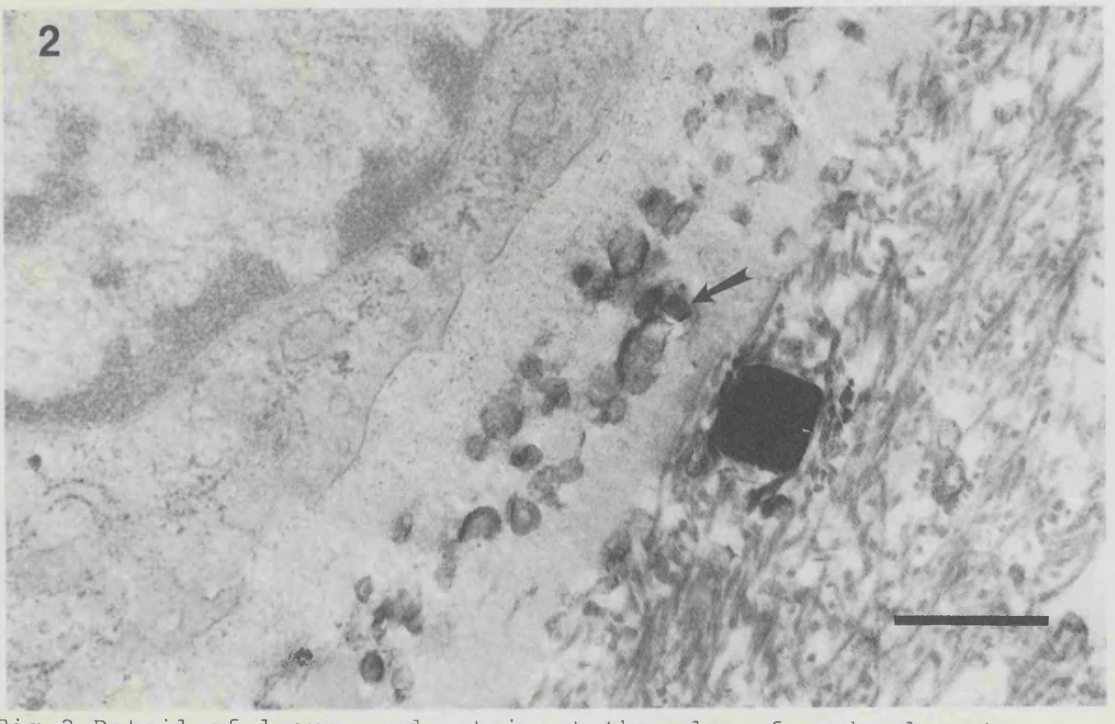

Fig.2 Detail of lacuna and matrix at the edge of a chondrocyte showing a cuboid microcrystal and the formation of another in a membranous vesicle (arrow). Bar = 0.5um.

Bone and Mineral, 17 (1992) 115–118
Elsevier

This paper was presented at the Fifth International Conference on Cell-Mediated Calcification and Matrix Vesicles, held November 16–20, 1991, Hilton Head, South Carolina.

Microcrystal deposition in cartilage and in osteoarthritis

S. Yousuf Ali, J.A. Rees and C.A. Scotchford

Department of Experimental Pathology, Institute of Orthopaedics, (University of London), R.N.O.H., Stanmore, Middx. HA7 4LP, UK

The destructive joint degeneration caused by the deposition of sodium urate crystals in gout has been known for a long time and is amenable to treatment in patients [1]. There is a strong association between calcium pyrophosphate deposition in joints and degenerative osteoarthritis and terms such as 'Crystal Deposition Disease' and 'Crystal Associated Arthritis' have been coined [1]. The role of hydroxyapatite and other calcium phosphate crystals in arthritis has yet to be elucidated [2,3]. We have made a detailed study of these various crystals by using the electron microscope and electron probe analysis. We have demonstrated the presence of at least three different types of calcium phosphate crystals in different sites of human articular cartilage from the femoral head [4]. Most of these microcrystals cannot be detected by either x-ray radiography or light microscopy [5].

With age and in arthritic conditions there is a continuous remodelling of the tide mark at the chondro-osseous junction. The calcified cartilage appears to advance into the non-calcified articular cartilage. The initial calcification occurs in extracellular matrix vesicles where fine needles of hydroxyapatite can be seen associated with the membranes of the vesicles and subsequently growing to form nodules of mineral. These nodules were described and characterised by us as being formed from hydroxyapatite crystals originating in matrix vesicles distributed pericellularly around the chondrocytes in the deep zone of articular cartilage [3,6]. A separate study had confirmed the presence of matrix vesicles in this region by the use of alkaline phosphatase as a marker enzyme biochemically [3] and by using enzyme histochemistry at the electron microscopic level [8]. The increase in alkaline activity seen in human osteoarthritic cartilage as compared with age-matched normal cartilage is probably derived from this region [3,8]. Thus there is increase in alkaline phosphatase, matrix vesicles and calcification in this zone of articular cartilage in osteoarthritis [2].

A second type of apatite-type calcium phosphate crystals were observed on the

surface of fibrillated or arthritic cartilage. These were in the form of fine needle-shaped crystals in clusters [4,5,6]. The mechanism of formation of those surface crystals is not known but they are probably formed subsequent to the disease process possibly by the process of bone rubbing against bone in the late stages of osteoarthritis [5,6].

A most interesting discovery was the observation of a third type of calcium phosphate crystal which appeared to be 'cuboid' in shape. These crystals were present in large numbers just under the surface of articular cartilage up to a depth of approximately 50 μm [4] (Fig. 1). Most of our original work was on osteoarthritic cartilage and the presence of these crystals in areas where cartilage degeneration occurs implied to us that they may be involved in the disease process [4,5]. Recently we have established their presence in normal cartilage with a smooth surface. They are usually present as a band of crystals but have a high frequency either pericellularly around chondrocytes in the surface zone or can be seen occupying an oval area where there is membranous debris indicative of a profile of a dead chondrocyte. On the basis of our long-term study we feel there is strong evidence indicative of the formation of these 'cuboid' crystals from membranous bodies. Pericellularly these membranous bodies resemble matrix vesicles in size and distribution (Fig. 2). Electron histochemistry did not indicate much alkaline phosphatase in this region and we have to turn to immunolocalisation to establish if alkaline phosphatase is present in an inactive form [8].

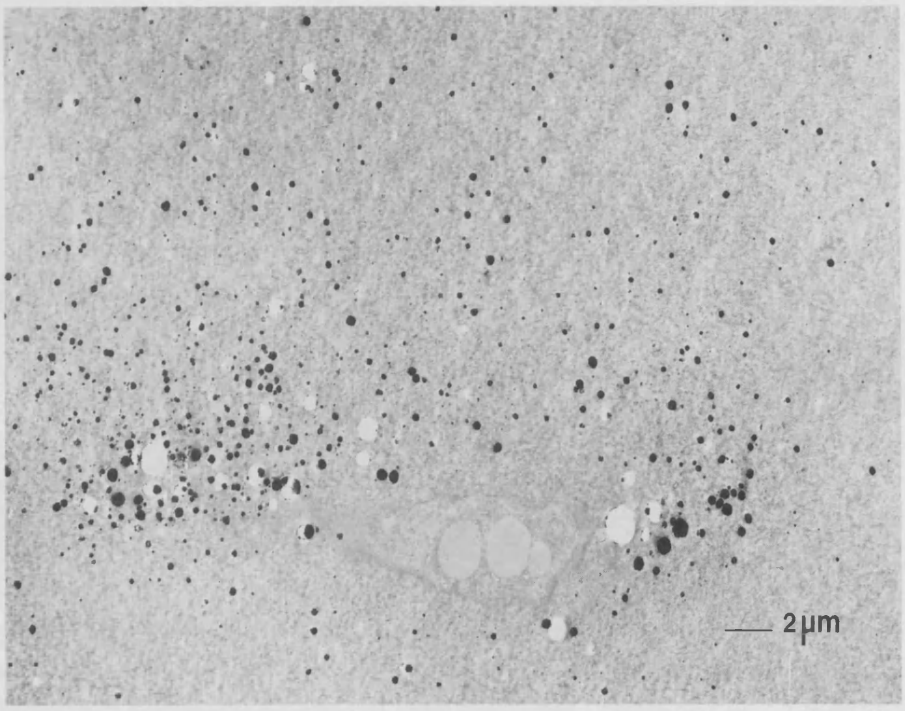

Fig. 1. Unstained section of human articular cartilage showing a dense band of 'cuboid' crystals. Note high density of crystals around the chondrocyte.

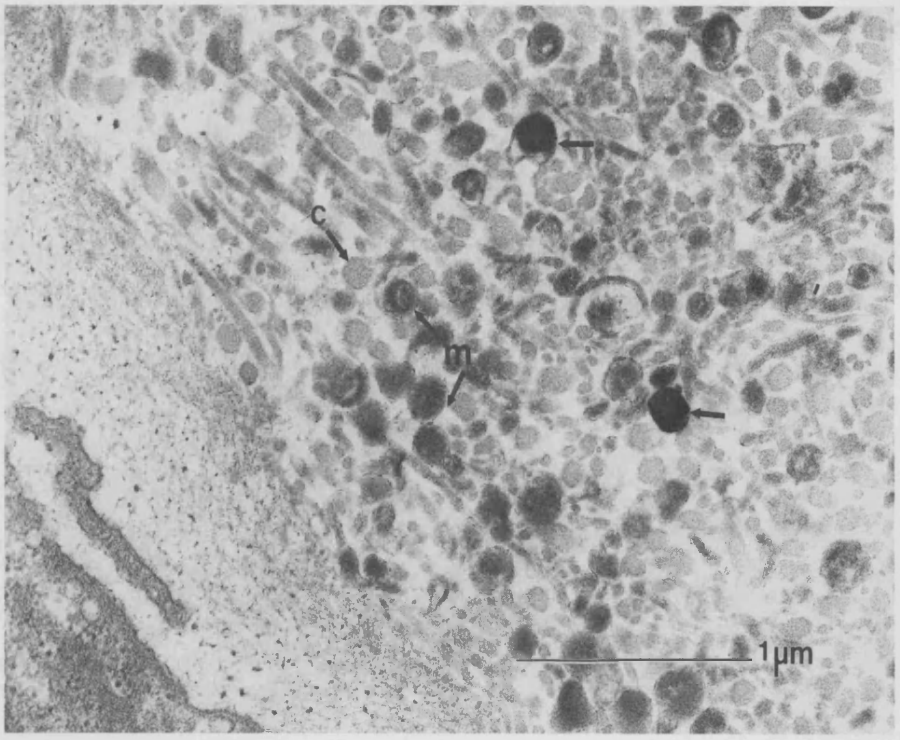

Fig. 2. Pericellular area of an articular chondrocyte, showing profiles of collagen fibrils (C), matrix vesicle type membranous bodies (m) and two 'cuboid' crystals (←), one with a membrane envelope.

Electron probe analysis clearly indicated that the 'cuboid' crystals were composed of calcium phosphate. Initial measurements of the Ca/P ratio appeared similar to hydroxyapatite but quite different to calcium pyrophosphate. In addition there appeared a small trace of magnesium also present. Because of their 'cuboid' shape and the presence of small amounts of magnesium we postulated that these crystals may be a form of 'Whitlockite' [4,5,6]. Recent more accurate analysis is beginning to indicate that the mean Ca/P ratio is well below that of hydroxyapatite and this study will be published in detail elsewhere.

These 'cuboid' crystals in human articular cartilage are also being studied by a recently developed new technique of elemental mapping by x-ray absorption difference imaging in the scanning transmission x-ray microscope with very high resolution [9]. The distribution of calcium containing crystals in articular cartilage by this technique has completely confirmed our findings by transmission and scanning electron microscopy and electron probe analysis [5,6,7,9].

Our original discovery of these calcium phosphate 'cuboid' crystals in human articular cartilage has subsequently been confirmed by the observation by Stockwell and colleagues [10,11]. We are occupied in the study of their distributon, with age and in different sites of the femoral head. A new crystal isolation procedure has been developed by the use of collagenase and ultracentrifugation and it is intended

that a detailed study of these isolated 'cuboid' crystals will facilitate a better understanding of their role in physiology and pathology.

Acknowledgements

We are grateful to the Arthritis and Rheumatism Council and to Action Research for continued support of our projects.

References

1 Dieppe PA, Calvert PT. Crystals and Joint Disease. Chapman and Hall, London, 1983.
2 Ali SY. New knowledge of osteoarthirits. J Clin Path 178:205–213.
3 Ali SY, Baylis MT. Enzymic changes in human osteoarthritic cartilage. In: Ali SY ed. Normal and Osteoarthritic Cartilage. Institute of Orthopaedics publication. London; 1974:189–205.
4 Aly SY, Griffiths S. New types of Calcium phosphate crystals in arthritic cartilage. Sem Arthritis and Rheumat 1981, XI (Suppl. 1) 124–126.
5 Ali SY, Griffiths S. Formation of calcium phosphate crystals in normal and osteoarthritic cartilage. Annals of Rheumatic Dis 1983;42:45–48.
6 Aly SY. Apatite-type crystal deposition in arthritic cartilage. Scanning Electron Microscopy 1985;4:1555–1566.
7 Rees JA, Ali SY, Mason AZ. Scanning electron microscopy and microcrystal analysis of 'cuboid' crystals in human articular cartilage. In: Ali SY ed. Cell mediated calcification and matrix vesicles. Amsterdam, Elsevier; 1986:365–371.
8 Rees JA, Ali SY. Ultrastructural localisation of alkaline phosphatase activity in osteoarthritic human articular cartilage. Ann Rheumat Dis 1988;47:747–753.
9 Buckley CJ, Foster GF, Burge RE, Ali SY, Scotchford CA. Elemental mapping of biological tissues by x-ray absorption difference imaging in the STXM. J. Microscopy 1991, in press.
10 Marente I, Macdougall R, Ross A, Stockwell RA. Ultrastructural observations of crystals in articular cartilage of aged human hip joints. Ann Rheum Dis 1983;42 (Suppl. 1) 96–97.
11 Stockwell RA. Distribution of crystals in the superficial zone of elderly human articular cartilage of the femoral head in subcapital fracture. Ann Rheum Dis 1990;49:231–235.